

**A SELF REPLICATING REACTION
AND A NEW APPROACH TO
IONOPHORE SELECTION**

A thesis submitted in accordance with the requirements of The University
of Liverpool for the Degree of Doctor of Philosophy

By

Bing Wang

Department of Chemistry

December 1996

To My Family

Acknowledgements

I wish to extend my sincere thanks to Professor I. O. Sutherland for his constant advice, encouragement, kind help and his enthusiasm throughout the time of my studying in Liverpool.

I record my deep appreciation for the love and support from my wife, Weiping, and my son, Minmin. Particularly, I wish to express my indebtedness to Weiping for her help and encouragement throughout the arduous preparation of this thesis.

I would also like to thank the British Government for the financial support and all the members of the technical staff in the Department of Chemistry who helped me, in particular, Alan Mills for his tireless work on the mass spectrometer and Steve Apter for his time, patience and skill in the help weighing hundreds of samples at milligram level for my experiments.

My thanks are also to my friends and colleagues at Liverpool, especially those in labs 247/249, who have made the past years so enjoyable.

Definitions and Abbreviations

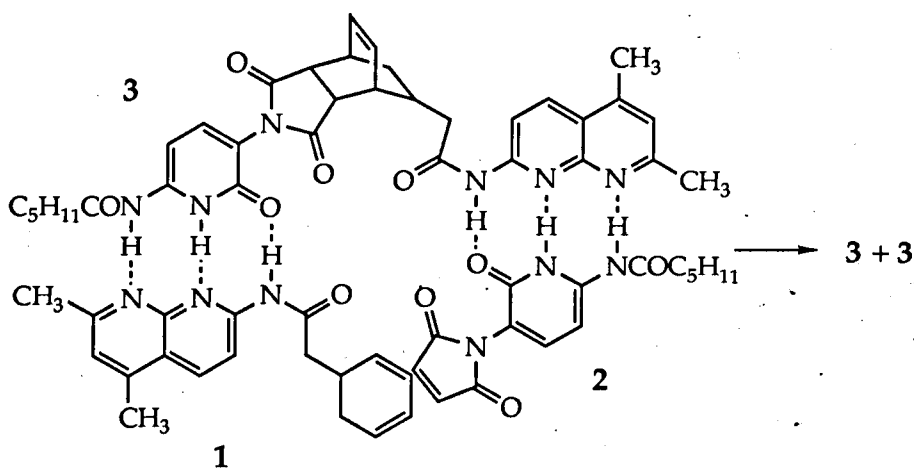
DCM	DiChloroMethane
DMF	DiMethylFormamide
DMSO	DiMethylSulfoxide
EI	Electron Ionization
ESI	ElectroSpra Ionization
FAB	Fast Atom Bombardment
HRMS	High Resolution Mass Spectroscopy
IR	InfraRed
MALDI	Matrix Assisted Laser Desorption/Ionization
m.p.	Melting Point
MS	Mass Spectrometry
NMR	Nuclear Magnetic Resonance Spectroscopy
3-NOBA	3-NitroBenzyl Alcohol (matrix for FAB MS)
Nujol	Liquid Paraffin
THF	TetraHydroFuran
Tof	Time Of Flight
UV	Ultra Violet

ABSTRACTS

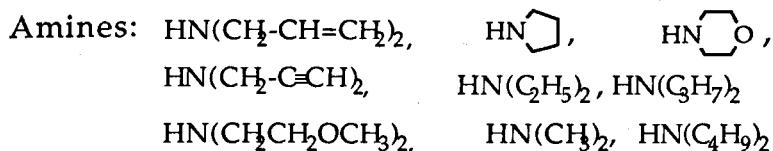
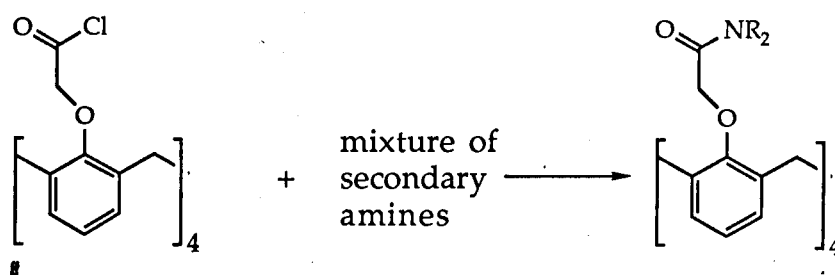
A molecular replicating system has been designed and made (1, 2 and 3) and the Diels-Alder reaction between 1 and 2 has been investigated in DCM at 23 °C and 40 °C. The phenomenon of autocatalysis of the reaction has been clearly observed from the experiments. A significant induction time of the reaction at both 23 ° and 40 ° was observed when only one equivalent of each 1 and 2 were in the reaction, so very clear sigmoidal curves (S shape) of product concentration vs time have been obtained. The experiments also showed that the reaction rate increased with the increase of the concentration of product added into the reaction. All this evidence strongly suggest that the product 3 did act as a template to 'hold reactants together' by the hydrogen bonds and the reaction was catalysed by the proximity.

The experimental results have also been evaluated by computer simulation based upon a full reaction scheme and a simple reaction scheme. The calculated results from full reaction scheme show that the 'effective molarity' is 119 M for the reaction at 23 °. The calculated results from simple reaction scheme show that the reaction rate is proportional to the 0.8 exponent of the concentration of product. Both results suggest that the template 3 have only a little inhibition by its dimerization.

The NMR investigation of stereochemistry shows that the reaction is diastereoselective and the template has also had some stereoselectivity in the binding process.



In the second project a combinatorial method was used to select good sodium ionophores based upon the calixa[4]arene compounds. Using a mixture of up to 4 amines out of 9 amines listed below, libraries containing up to 55 compounds were generated by following method. The libraries were screened by FAB MS, MALDI-TOF MS and ESI MS. The results show that calixa[4]arene-amides containing ethyl or propyl side chains are the best ionophores. The result was confirmed by extraction experiments. By comparing three MS techniques, ESI MS is the best screen method if the sodium level in the spectrometer can be totally controlled, because ESI MS can precisely present the composition of solution. FAB MS may cause serious error because the surface effect. MALDI MS is in between.



CONTENTS

Chapter One:	An Introduction to Molecular Replicating Systems	1
1.1	Where does the Idea Come from?	2
1.2	What has been Achieved in Biochemistry	4
1.3	Approaches by Organic Chemists	11
Chapter Two:	Objective	23
2.1	Theoretical Background	24
2.2	The Basic Requirements for a Replicating system	37
2.3	Binding Sites	40
2.4	The Reactants	52
Chapter Three:	Synthesis	64
3.1	Pyridone Compound	65
3.2	The Naphthyridine Component	80
Chapter Four:	Results and Discussion	96
4.1 _g	The Kinetic Results from Experiments and Computer Simulations	97
4.2	Discussion	122
4.3	The Stereochemistry of the System	128
4.4	More Stable Transition State?	131
4.5	Future Work	137
Chapter Five:	A New Approach to Optimise Ionophores	140
5.1	An Introduction to Combinatorial Chemistry	141
5.2	An Introduction to Calixarenes	147
5.3	A Unique Screening Method	154
5.4	Library Generating	158
5.5	The Study of Calixarene Libraries by FAB Mass Spectroscopy	162
5.6	The Study of Calixarene Libraries by MALDI and ESI Mass Spectroscopy	182
5.7	Conclusions and Discussion	194

Chapter Six:	Experiments	198
6.1	General	199
6.1.1	Procedures and Instruments	199
6.1.2	Solvents and Reagents	201
6.2	Synthetic Work for the Replicating System	202
6.2.1	2-Amino-6-hydroxypyridine (55)	202
6.2.2	2-Hexanoylamido-6-hydroxypyridine (76)	202
6.2.3	2-Hexanoylamido-5-nitro-6-hydroxypyridine (77)	203
6.2.4	5-Amino-2-hexanoylamido-6-hydroxypyridine (78)	204
6.2.5	5-Maleoylamido-2-hexanoylamido-6 -hydroxypyridine (79)	204
6.2.6	5-Maleimido-2-hexanoylamido-6 -acetoxypyridine (80)	205
6.2.7	5-Maleimido-2-hexanoylamido-6 -hydroxypyridine (81)	205
6.2.8	cis-1-Acetoxy-4-chloro-2-cyclohexene (94)	206
6.2.9	cis-1-Acetoxy-4-(dicarbomethoxymethyl) -2-cyclohexene (95)	207
6.2.10	5-(Dicarbomethoxymethyl)-1,3-cyclohexadiene (91)	208
6.2.11	5-Carbomethoxymethyl-1,3-cyclohexadiene (92)	208
6.2.12	2,4-Cyclohexadiene-1-acetic acid (5-carboxymethyl-1,3-cyclohexadiene) (90)	209
6.2.13	2-(2,4-Cyclohexadienylacetamido) -5,7-dimethyl-1,8-naphthyridine (114)	209
6.2.14	N-Phenylmaleimide (120)	210
6.2.15	2,4 -Cyclohexadienyl-acetyl-N-phenyl-amide (121)	211
6.2.16	2,4 -Dimethyl -7-phenylacetamido- 1, 8-naphthyridine (123)	211
6.2.17	2-Amino-5-nitropyridine (67)	212

6.2.18	2-Acetamido-5-nitropyridine (68)	212
6.2.19	2-Acetamido-5-nitropyridine-N-oxide (69)	213
6.2.20	2-Acetamido-5-nitro-6-acetoxypyridine (70)	213
6.2.21	2-Acetamido-5-nitro-6-hydroxypyridine (71)	213
6.2.22	2-Hexanoylamido-5-nitropyridine (73)	214
6.2.23	2-Hexanoylamido-5-nitropyridine-N-oxide (74)	214
6.3	Kinetic Studies of Diels-Alder Reaction of Replicating System by ^1H NMR	215
6.3.1	Diels-Alder Reaction Conditions	216
6.3.2	Characterization of the Product 116 of the Replication Reaction	217
6.3.3	Characterization of the Product 122 from the Model Diels-Alder Reaction	217
6.4	Measurement of Binding Constant	217
6.5	Computer Modelling of the Kinetics of a Self-Replication Process	221
6.6	Synthetic Work for Calixarenes	223
6.6.1	5,11,17,23-Tetra- <i>tert</i> -butyl-25,26,27,28- tetrahydrocalix[4]arene	223
6.6.2	25, 26, 27, 28-Tetrahydrocalix[4]arene (138)	223
6.6.3	25,26,27,28-Tetrakis[(ethoxycarbonyl)- methoxy]calix[4]arene (128)	224
6.6.4	25,26,27,28-Tetrakis[(<i>tert</i> --butoxycarbonyl)- methoxy]calix[4]arene (140)	225
6.6.5	25,26,27,28-Tetrakis[(carboxy)methoxy]- calix[4]arene (141)	226
6.6.6	25,26,27,28-Tetrakis[(chlorocarbonyl)- methoxy]calix[4]arene (139)	226
6.6.7	Library of methyl-, ethyl-, propyl- and butyl-	

carbamoyl methoxy-calix[4]arenes (142)	227
6.6.8 Library of methyl-, ethyl- and propyl- carbamoyl methoxycalix[4]arenes (143)	227
6.6.9 Library of methyl-, ethyl- and n-butyl- carbamoyl methoxycalix[4]arenes (144)	228
6.6.10 Library of methyl-, propyl- and n-butyl- carbamoyl methoxycalix[4]arenes (145)	228
6.6.11 Library of ethyl-, propyl and n-butyl- carbamoyl methoxycalix[4]arenes (146)	229
6.6.12 Library of ethyl- and propyl-carbamoyl methoxycalix[4]arenes (147)	229
6.6.13 25,26,27,28-Tetrakis(dimethylcarbamoyl methoxy)calix[4]arene (148)	229
6.6.14 25,26,27,28-Tetrakis(diethylcarbamoyl methoxy)calix[4]arene (149)	230
6.6.15 25,26,27,28-Tetrakis(dipropylcarbamoyl methoxy)calix[4]arene (150)	231
6.6.16 25,26,27,28-Tetrakis(dibutylcarbamoyl methoxy)calix[4]arene (151)	231
6.6.17 Library of ethyl- and morphlinyl-carbamoyl methoxycalix[4]arenes (153)	232
6.6.18 Library of morphlinyl-, propyl- and pyrrolidyl- carbamoyl methoxycalix[4]arenes (152)	232
6.6.19 25,26,27,28-Tetrakis(morphlinylcarbamoyl methoxy)calix[4]arene (157)	233
6.6.20 25,26,27,28-Tetrakis(pyrrolidinylcarbamoyl methoxy)calix[4]arene (156)	233
6.6.21 25,26,27,28-Tetrakis(dipropargylcarbamoyl methoxy)calix[4]arene (155)	234

6.6.22	25,26,27,28-Tetrakis(diallylcarbamoyl methoxy)calix[4]arene (154)	234
6.6.23	25, 26, 27, 28-Tetrakis[bis(methoxyethyl) carbamoyl methoxy]calix[4]arene (158)	235
6.7	Two Phase Extraction Experiment to Assess Complexation of Sodium by Calix[4]arene Ionophores	236
6.8	FAB MS Studies of Combinatorial Libraries	236
6.9	MALDI - TOF MS Studies of Libraries	237
6.10	Electrospray Ionization (ESI) MS Studies of Libraries	238
	Bibliography	240
Appendix 1	The Equations of Rate Law Used in the Computer Modelling	254
Appendix 2	Raw Data of Kinetic Studies of the Diels-Alder Reaction at 40 °C	255
Appendix 3	Raw Data of Kinetic Studies of the Diels-Alder Reaction at 23 °C	256

CHAPTER ONE

AN INTRODUCTION TO MOLECULAR REPLICATING SYSTEMS

1.1 Where does the idea come from?

Life is replicating. The mystery of replicating processes in living systems was not uncovered until 1953, when Watson and Crick proposed a double helix structure for deoxyribonucleic acid (DNA) by collecting the experimental evidences from others' work.¹ They suggested that two strands of DNA are associated together by hydrogen bonds between pairs of the four purine and pyrimidine bases which are attached to the deoxyribose-phosphate back bone of DNA. Based on the knowledge that it had been found experimentally that the ratio of the amounts of adenine to thymine, and the ratio of guanine to cytosine, are always very close to unity, they assumed that these four bases are specifically paired, that is adenine (A) with thymine (T) and guanine (G) with cytosine (C) (Figure 1.1). In other words, these bases have the ability of molecular recognition.

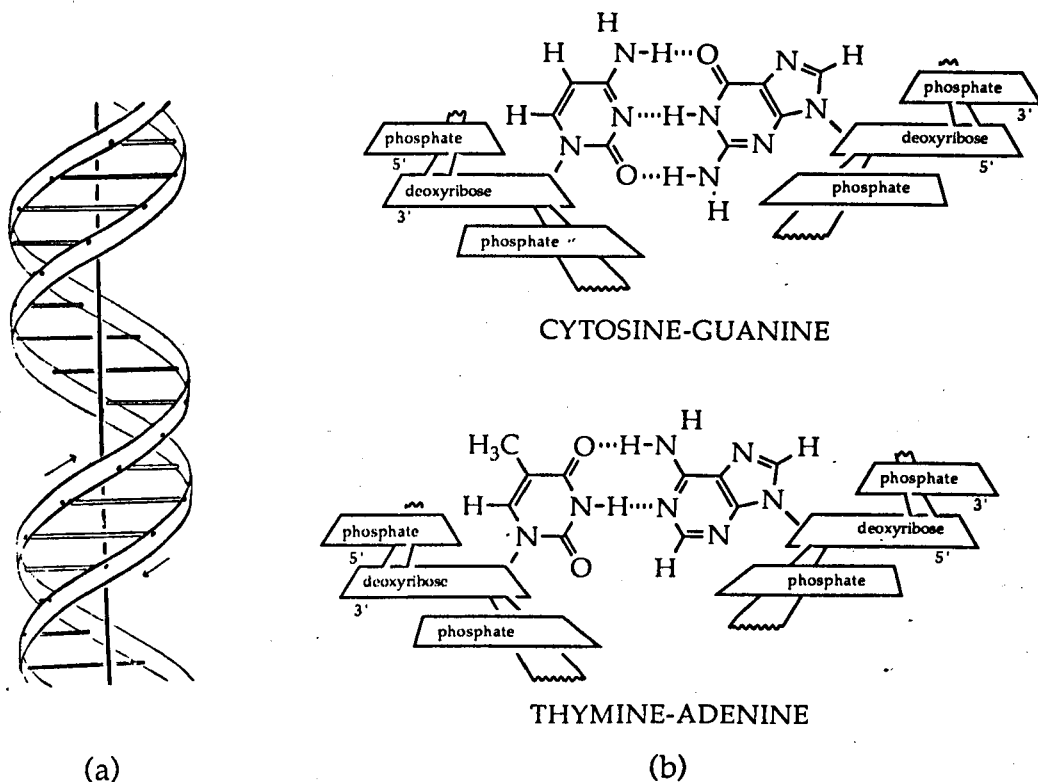


Figure 1.1 (a) Double strands of DNA. (b) Base pairs in DNA.

If the base sequence on one strand of DNA is given, then the sequence on the other chain is automatically determined. As a consequence of this assumption, a copying mechanism for the genetic material was further suggested by these two scientists.² They postulated that at the molecular level, the genetic information is stored in DNA in the terms of the sequence of the four bases along its back bone; when double strand DNA starts to replicate itself, the two strands are initially separated and then each strand serves as a template to 'pick up' mononucleotides aligned on them by the hydrogen bonds between the bases of the template and the monomers. Because the bases have the capability of molecular recognition, the sequence of monomers is determined by the template; so when the new strand is formed by the coupling reaction between the monomers, the information on the template in terms of the sequence of

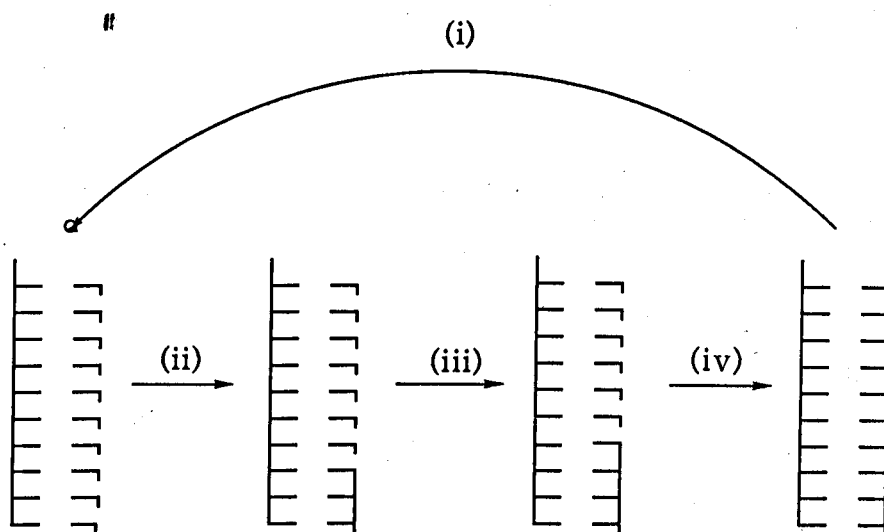


Figure 1.2 Idealized scheme for replication process *via* a double-strand intermediate.

(i) The double-strand product formed in the previous round of replication dissociates into single strands and the monomers line up upon a single strand; (ii) Start, (iii) Development, and (iv) Completion of the formation of the new strand.

A, C, G and T is transferred to the new strand as T, G, C and A. The new strand is not identical with the mother strand, but is complementary. In total, one double helix of DNA produces two identical double helices. Figure 1.2. is an idealized replication process.

Modern research in molecular biology shows that during the DNA replication in a biological system, the mother strand does serve as a template, but the reaction between nucleotides needs to be catalysed by enzymes. However, more recent researches demonstrate that RNA (Ribonucleic acid), an analog of DNA, does catalyse some processes without enzymes.³

1.2 What has been achieved in biochemistry?

The origin of life is always an interesting topic for human discussion. When people began to understand the replicating process in biological systems, the chicken-egg question was raised: "How did those molecules replicate themselves in the prebiotic time when there were no complicated protein enzymes on the Earth? Could simple compound like DNA or RNA catalyse the replication of themselves?"

The first non-enzymatic catalytic synthesis of polynucleotides *in vitro* was reported by Schramm's group in 1962, although it was analyzed by hybridization methods.⁴ They studied the polymerization of uridylic acid, activated by polyphosphate ester, in the presence and absence of its complementary species, polyadenylic acid (Figure 1.3). They found that the polymerization of uridylic acid was accelerated more than 10-fold in the presence of polyadenylic acid, whereas polyuridylic acid had no such effect. This meant that polymerization of nucleotides was favoured by the complementary strand. This result made them suggest that this kind of nonenzymatic formation of oligonucleotides could be involved in the self-

replicating cycle on the prebiotic Earth, in which the formation of nucleotide strands carried certain selective advantages, they favoured the formation of the complementary strand by a templating effect, and the complementary strand in turn speeded up the formation of the original strand.

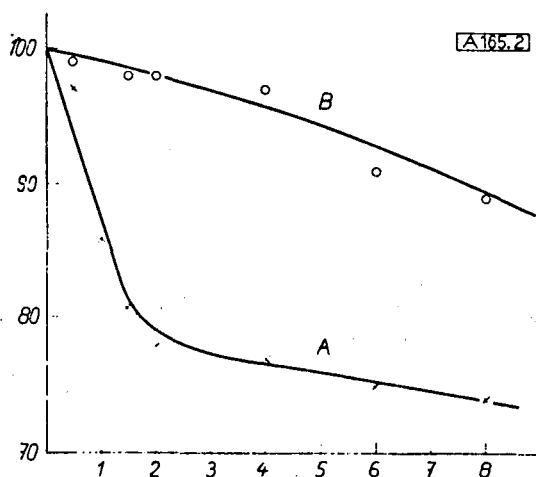
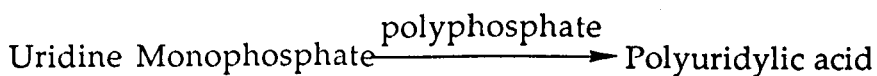


Figure 1.3 Polymerization of Uridine Monophosphate in the presence (A) and in the absence (B), of polyadenylic acid. (The decrease of free uridine monophosphate was measured chromatographically).

Abscissa: Time (hours). Ordinate: % Free uridine monophosphate (referred to the amount of starting material)

A more definitive experiment was done by the Gilham group in 1966 when they were studying the interaction and reaction of oligonucleotides in aqueous solution⁵. By using a mixture of thymidine hexanucleotide and polyadenylic acid with an activating diimide in aqueous solution, they achieved a synthesis of thymidine

dodecanucleotide in 5% yield, but when polyadenylic acid was omitted, no dodecanucleotide was produced. The result demonstrated that hexanucleotides bound to polyadenylic acid gave a head-to-tail 'Watson - Crick' arrangement which results in close proximity between 5'-phosphate and the 3'-hydroxyl groups of adjacent residues. (Figure 1.4)

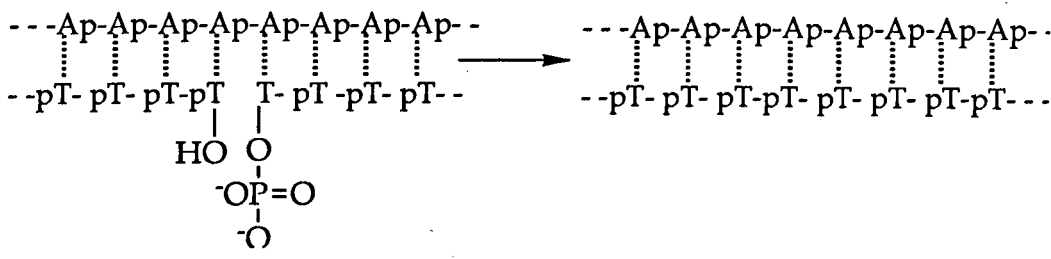


Figure 1.4 Templating reaction of oligonucleotide.

#

Similar nonenzymatic syntheses of oligonucleotides by using templates were intensively studied by the L. E. Orgel group in the 1970s and the 1980s.⁶ In 1984, Orgel's group reported a case of information transfer: starting with a mixture of two activated mononucleotides, guanosine 5'-phospho-2-methylimidazolid and cytidine 5'-phospho-2-methylimidazolid, and the pentanucleotide C-C-G-C-C as a template, the major pentameric product had the sequence pG-G-C-G-G in up to 17% yield.⁷ This was the first demonstration that a template with definite sequence can catalyse the formation of its complementary (-) - strand under nonenzymatic conditions.

Although all these work showed how nucleotide templates facilitate synthesis of their complementary strands, a true replicating system had not been made until 1986 when the G. von Kiedrowski's group reported the first replicating system⁸ (Figure 1.5). They used a hexamer of a

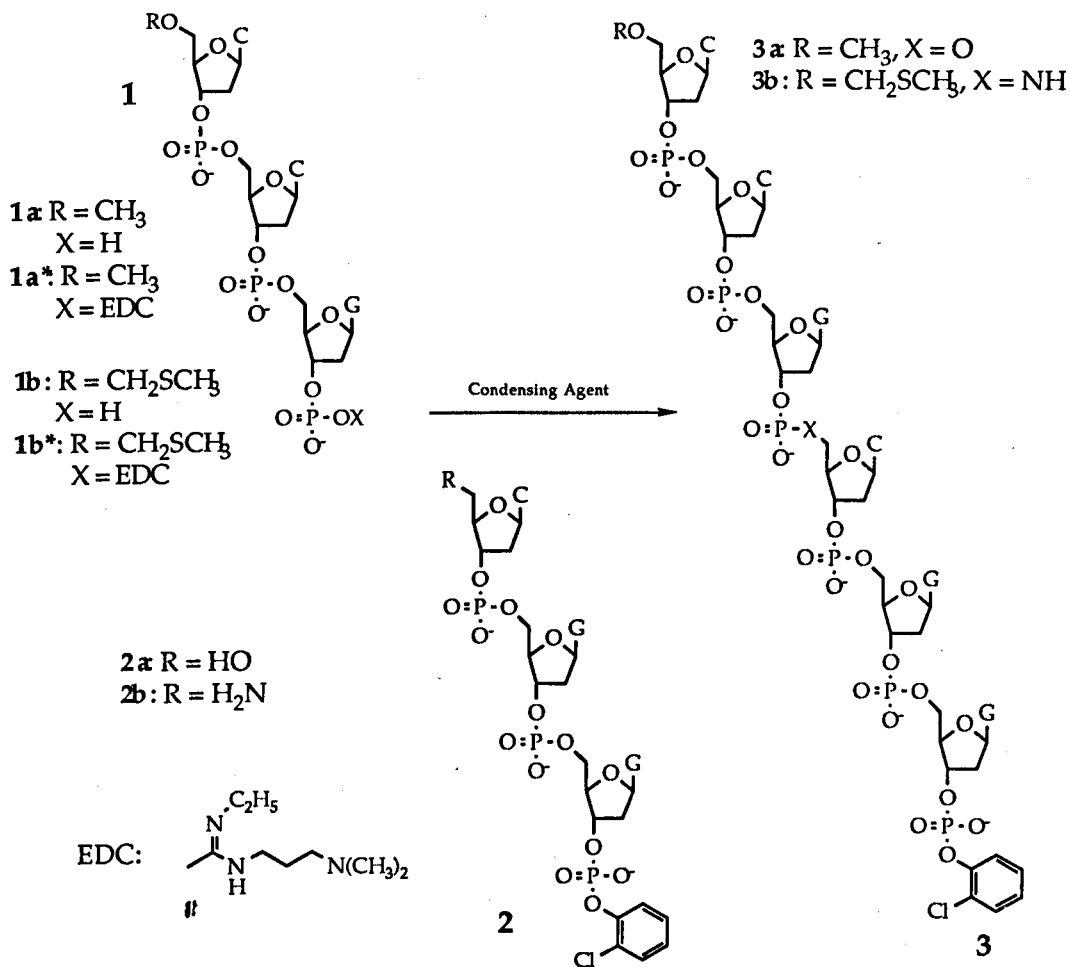


Figure 1.5 The first replication system of oligonucleotide analogues built *in vitro*.

C — cytosine, G — guanine.

deoxyribonucleotide analog as a template, which was protected with a methyl group at its 5'- end and an *o*-chlorophenyl group at its 3'- end (MeO-C-C-G-C-G-Gp-*o*-chl) **3a**. A complementary trideoxynucleotide 3'- phosphate with its 5'- terminus protected as its methyl ether (MeO-C-C-Gp) **1a**, and another complementary trideoxynucleotide 3'- phosphate with its 3'- terminus protected with an *o*-chlorophenyl group (HO-C-G-Gp-*o*-chl) **2a** were used as the two substrates. When the condensation between the two trimers was activated by carbodiimide in the presence of the template, the newly-formed hexamer was not only a complementary

strand of template, but also a template itself. By this clever choice of the base sequence of template and substrates, one step of the (+)-strand–(-)-strand–(+)-strand replicating cycle, which is happening *in vivo*, was omitted and a replicating cycle is completed *in vitro*. So the complexity of a biological replication experiment was simplified to a kinetic study of the formation of identical template components. Because the product of the reaction is also a template for its formation, obviously this reaction should have auto-catalytic character. Their results did show that the initial reaction rate was increased by increasing the initial template concentration. A square root law was proposed to describe the effect of added template upon initial reaction rate:

$$[dc(T)/dt]_{\text{initial}} = k_a c_0(T)^{1/2} + k_b \quad (1.1)$$

where $c_0(T)$ is the template concentration. The first term of the equation containing k_a (value of $9.48 \times 10^{-8} \text{ M}^{1/2} \text{ s}^{-1}$) is for the auto-catalytic reaction and k_b is for the non-autocatalytic process (value of $3.83 \times 10^{-9} \text{ M s}^{-1}$). Why is the increase in the rate of formation of template 3a proportional to the square root of the concentration of 3a, rather than first order in the concentration of 3a? The explanation is that most template molecules present in the solution are deactivated due to the formation of a double helix, only a small fraction are present as single-stranded species which can act as templates. A simple mechanism was also proposed for this replication process, which is shown in Figure 1.6. From this mechanism, it can be seen that there are three constants in the whole process: K_1 and K_2 are two equilibrium constants and k^* is the rate constant for the catalytic reaction, in which reactants are bound on the product template to form new product. According to this mechanism, the rate law of product dimer (T : T) should be as follows,

$$d[T : T] / dt = k^* [A^* : T : B] = k^* K_1 K_2^{-1/2} [A^*][B][T : T]^{1/2} \quad (1.2)$$

Since K_2 is very big, the equilibrium concentration, $[T : T]$, is supposed to be only slightly different from half of the total template concentration, $c(T)$, this equation gives an approximate solution for k_a in the autocatalytic term of the empirical rate law, equation (1.1).

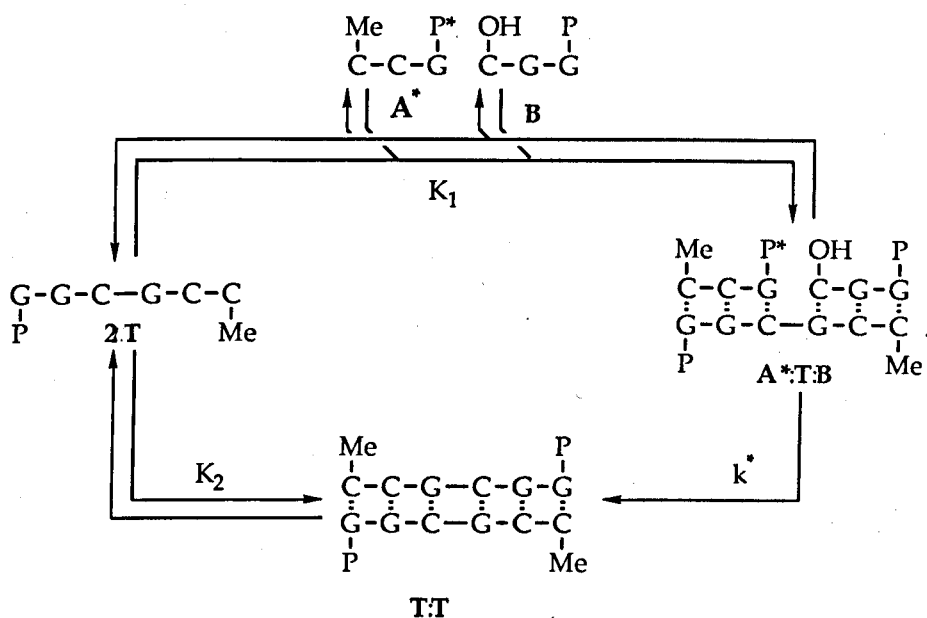


Figure 1.6 A mechanism for oligonucleotide replication system

Slightly later, these results were confirmed by the Orgel group. Instead of hexamers and trimers, they used a tetramer 6 of an RNA analog as template and two dimers (4 and 5) as substrates. Phosphate amidation was chosen instead of esterification. Their result also showed a roughly square-root dependence of the coupling reaction rate on the total concentration of tetramer.⁹ (Figure 1.7).

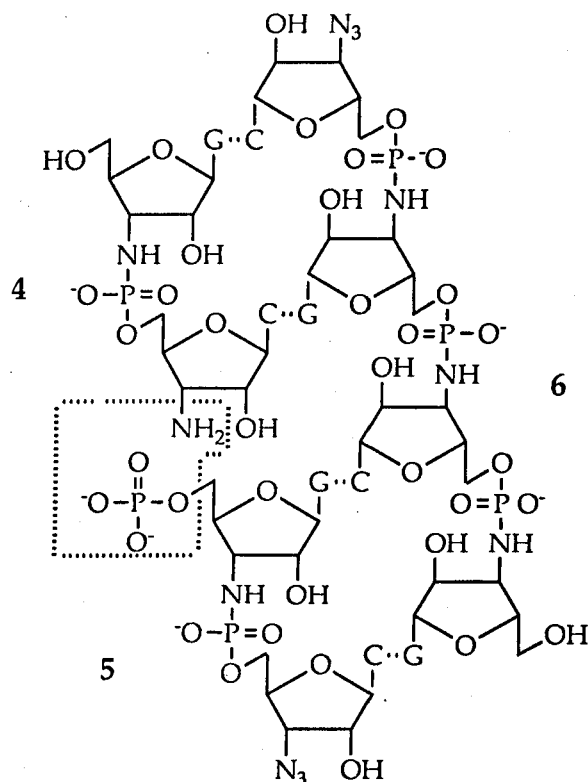


Figure 1.7 A self-replicating system with tetranucleotide as template.

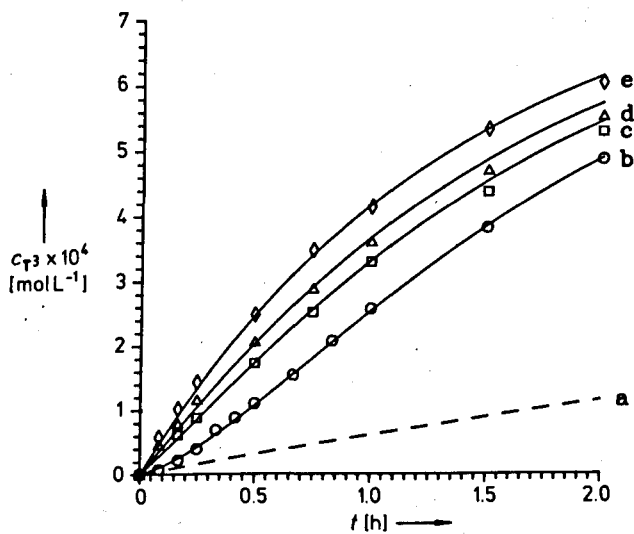


Figure 1.8 Sigmoidal curve (b) of reaction course for the replicating system. composed by compounds $1b^*$, $2b$ and $3b$ in Figure 1.5. a: Background reaction; b: without addition of template; c, d, and e: with addition of various concentration of template.

At the same time, von Kiedrowski's group investigated refinements of their original reaction. A more efficient system using **1b*** and **2b** as reactants and **3b** as template (see Figure 1.5) was set up. Because the amide is more stable than the ester, hydrolysis was avoided, so that the sigmoidal growth behaviour was observed¹⁰ (Figure 1.8), which should be seen for all autocatalytic reactions. The auto-catalytic rate constant k_α and non-catalytic rate constant k_β for equation (1.3) were calculated from the equation (1.1) by further consideration of the mass balance between reactants and template,

$$dc/dt = (c_A - c)(c_B - c)[k_\alpha(c + c_T)^{1/2} + k_\beta] \quad (1.3)$$

where c_A , c_B and c_T are the initial concentration of **1b**, **2b** and **3b**, c is the concentration of the product **3b**, k_α and k_β are the apparent rate constants for catalytic and non-catalytic reactions respectively. The reported results showed that k_α is $7.43 \text{ M}^{-2/3} \text{ s}^{-1}$ and k_β is $1.77 \text{ M}^{-1} \text{ s}^{-1}$. So the quotient k_α/k_β , which was named as "the autocatalytic excess factor ϵ ", is 420. Although their results still obeyed the square root law, they indicated that a first order reaction is possible.

1.3 Approaches by organic chemists

The approach to molecular replication from organic chemistry did not really start until the middle 1960s, although shortly after the discovery of the double helix structure of DNA, an organic chemist, Alexander Todd made a landmark proposal: "The use of one molecule as a template to guide and facilitate the synthesis of another...has not hitherto been attempted in laboratory synthesis, although it seems probable that it is common in living systems. It represents a challenge which must, and

surely can, be met by organic chemistry"¹¹. As we can see in the DNA replicating process, molecular recognition plays a key role when mother strand is templating the synthesis of son strand. Without the molecular recognition ability of nucleotide bases, the information on the template could not be transferred accurately to the product strands. Molecular recognition also exists in many other biological processes such as enzymic catalysis, membrane transport, hormonal signal transduction, metabolic regulation and friend-foe recognition in the immune response. So, to understand molecular recognition is essential for studying all those processes. This was why the attention of many chemists was attracted when the first cyclic polyether compound, which was later called a crown ether, was made together with the discovery of its capability of capturing cations by C. Pederson in 1967.¹² This kind of compound shows potential ability for molecular recognition. Since then a new branch of organic chemistry has been developed called host-guest chemistry or supramolecular chemistry and a new era for the study of molecular recognition by synthetic compounds has begun. Thousands of such macrocyclic compounds, with different shape, structure and selectivity towards cation or anion binding by non-covalent forces have since been made. In 1973, Lehn's group reported the first double-binding-site crown ether **7**, called a cryptand, which can capture two cations simultaneously.¹³ (Figure 1.9) Molecules of this type show that novel synthetic molecules could be used to store information and suitable modification could yield co-catalysts or co-carriers which would perform a reaction on the bound substrates. Obviously, to achieve these functions, molecules which can only capture cations or anions, or in other words, only have the capability of 'spherical recognition', are not enough. So at the same time, some chemists began to search for compounds which have the ability to recognise complex organic molecules.

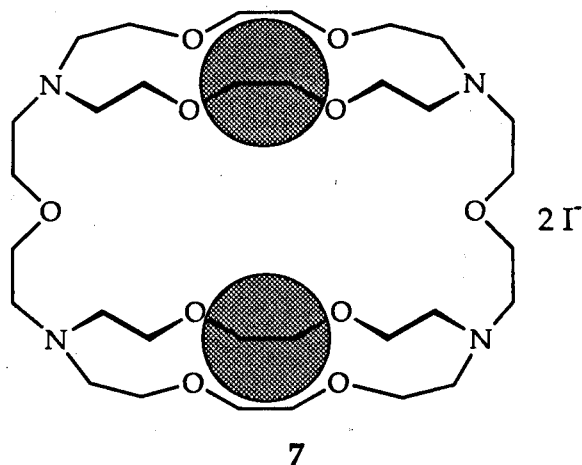


Figure 1.9 A cryptand which captures two sodium cation.

In 1973, D. J. Cram's group in Los Angeles made a crown ether analogue 8 and its enantiomer based upon α, α' -binaphthol.¹⁴ They found that this kind of chiral macrocyclic compound can not only bind amino acids by hydrogen bonding between host and guest, but can also show selectivity for one enantiomer. For example, the R, R compound 8 shows a preference to bind D-enantiomers of amino acids to form complex 9, while the S, S - enantiomer does vice versa. That means that they have chiral

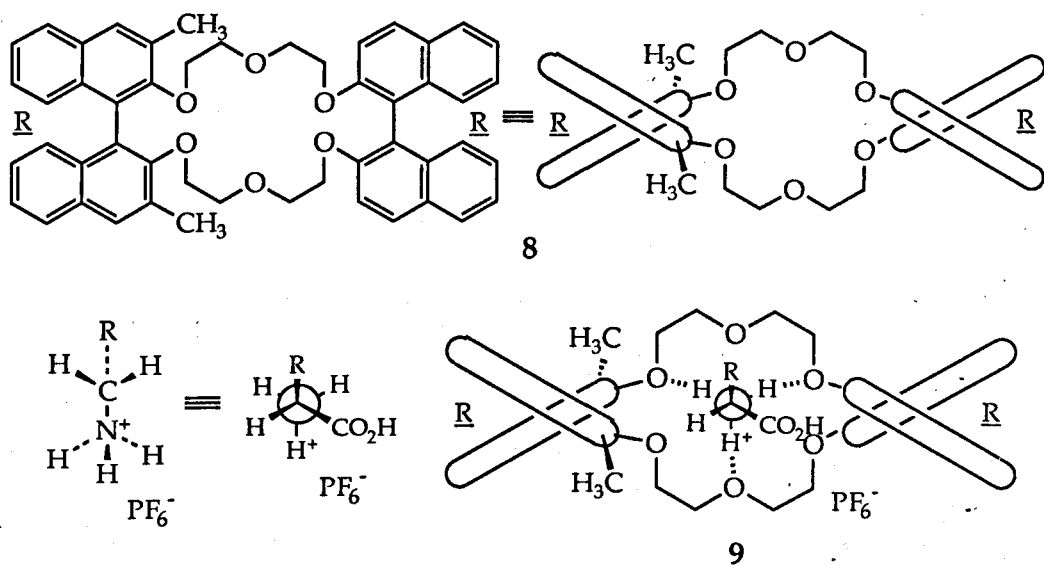


Figure 1.10 A chiral selective host compound based on binaphthol.

recognition ability (Figure 1.10). This is because of the chirality of the α,α' -binaphthol group. Based on this experiment, they made an enantiomer resolving machine. After that, many other synthetic molecular receptors for various substrate compounds have been reported.

But the development of molecules that recognize and bind to specific nucleotides or nucleotide base pairs has always provided an important goal for organic chemistry because of their important biological role. A key element in the design of such specific receptors concerns the incorporation of several recognition features (e.g., hydrogen bonding, hydrophobic or electrostatic forces) that complement the chemical characteristics of the target guest. A. D. Hamilton's group in 1987 designed a macrocyclic compound **10**, which possesses two binding sites for thymine derivatives **11**.¹⁵ A diacyl-pyridine unit provides a hydrogen bonding site while a naphthalene unit provides a π -stack site (Figure 1.11). X-ray crystallography showed that in complex **12**, three hydrogen bonds are

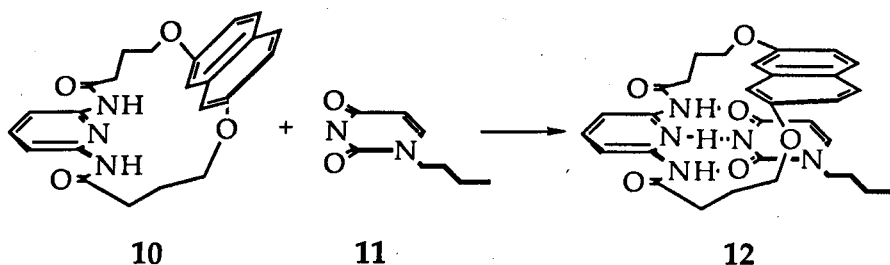


Figure 1.11 A receptor for thymine

formed between the pyridine and thymine rings and that the naphthalene unit lies nearly parallel (14°) to the plane of the thymine substrate at a closest inter-plane contact of 3.37 Å. The more interesting molecule **13** was also made by connecting two molecules **10** through an oxidative coupling reaction¹⁶. This double receptor **13** showed the ability to bind a bisthymine

derivative 14 which was made by a similar coupling reaction to that used for the synthesis of host 13 (Figure 1.12). The association constant for complex 15 is $2.03 \times 10^4 \text{ M}^{-1}$, which is a 13 - fold increase over that for the monomer complex 12.

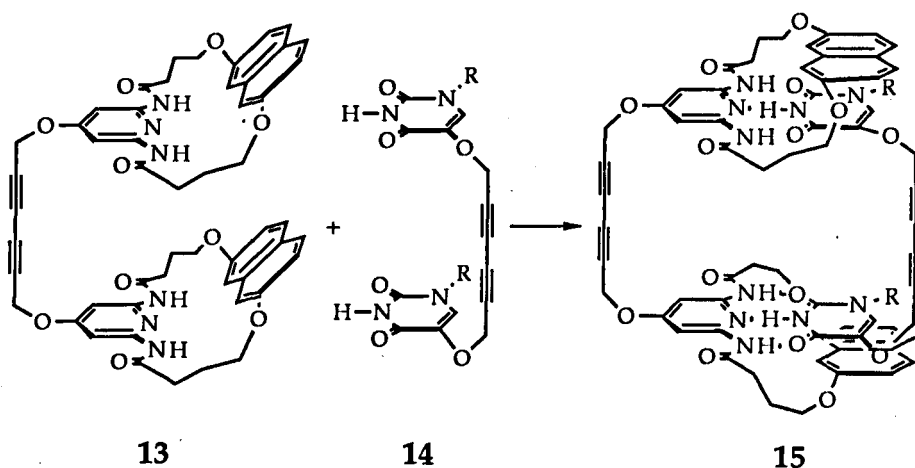
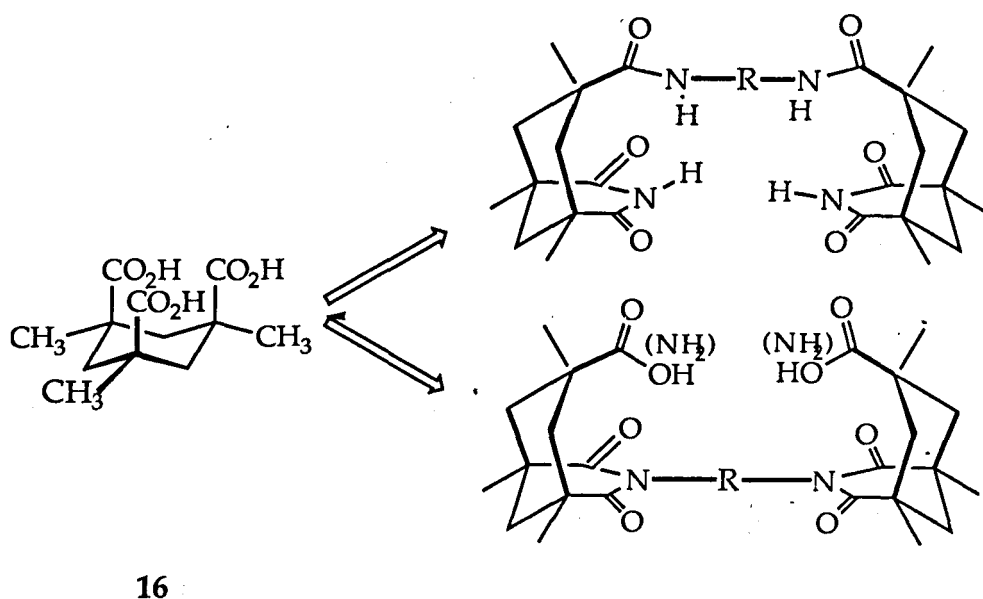


Figure 1.12 A two - binding - sited receptor for two connected thymine molecules

"

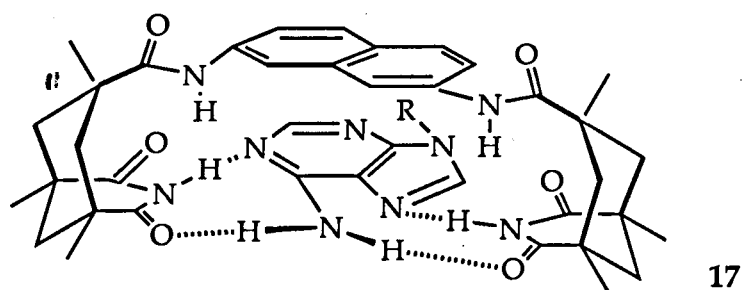
Instead of using a macrocyclic compound as the host receptor, J. Rebek's group made an open chain compound as a receptor for various substrates.¹⁷ Two U-shaped Kemp's triacid units 16 were used in the host



16

Figure 1.13 Molecular receptor based on Kemp's triacid.

molecule by converting two of the three carboxyl groups in each molecule to an imide and then linking them together by a spacer, or linking the two carboxylic groups on each triacid and leaving the imine groups as binding sites. The remaining two carboxyl groups or the two imine groups point towards each other to form a binding cleft (Figure 1.13). These two kinds of binding sites can provide hydrogen bonding, while a suitably selected aromatic spacer can provide a π -stack site. Many kinds of compounds with different spacer were investigated and results show that they are good hosts for a variety of DNA bases and amino acids.¹⁸ When a naphthalene group was employed as the spacer, the product **17** formed a very strong complex with adenine both thermodynamically ($K_a = 11,000 \text{ M}^{-1}$) and kinetically (activation energy for substrate exchange, $12.4 \text{ kcal mol}^{-1}$).^{18c}



The second key role of templating is to introduce selectivity into a chemical reaction as we have seen in a replicating process. That is to force the reaction partners into spatial and temporal proximity in their ground states prior to any chemical conversion event. This principle, ubiquitous in all processes of living systems, has been discussed previously. With knowledge of the molecular recognition properties of synthetic molecules, the next question is whether it is possible to introduce novel selectivity into a chemical reaction of a similar type to that observed in biological systems. To answer this challenge, chemists embarked on the exploration of the reaction between the substrates and synthetic receptors or templates.

Cram's group in 1983 reported an example of using a macrocyclic compound to mimic the function of serine proteases which catalyse acyl transfer¹⁹. They designed and made a compound **18**, which has binding sites and a hydroxy group on the rim of the basket like receptor (Figure 1.14). They found that the rate factor for acyl transfer from L-alanyl p-nitrophenyl ester perchlorate to the hydroxyl group of the host compound **18** was 10^{11} times greater than that of a acyl transfer to the model compound 3-phenylbenzyl alcohol **20** ($k_a/k_b = 10^{11}$). They supposed that this is because the host compound binds the substrate p-nitrophenyl ester perchlorate close to the hydroxyl group on the host to form a complex **19**, this proximity facilitated the acyl transfer.

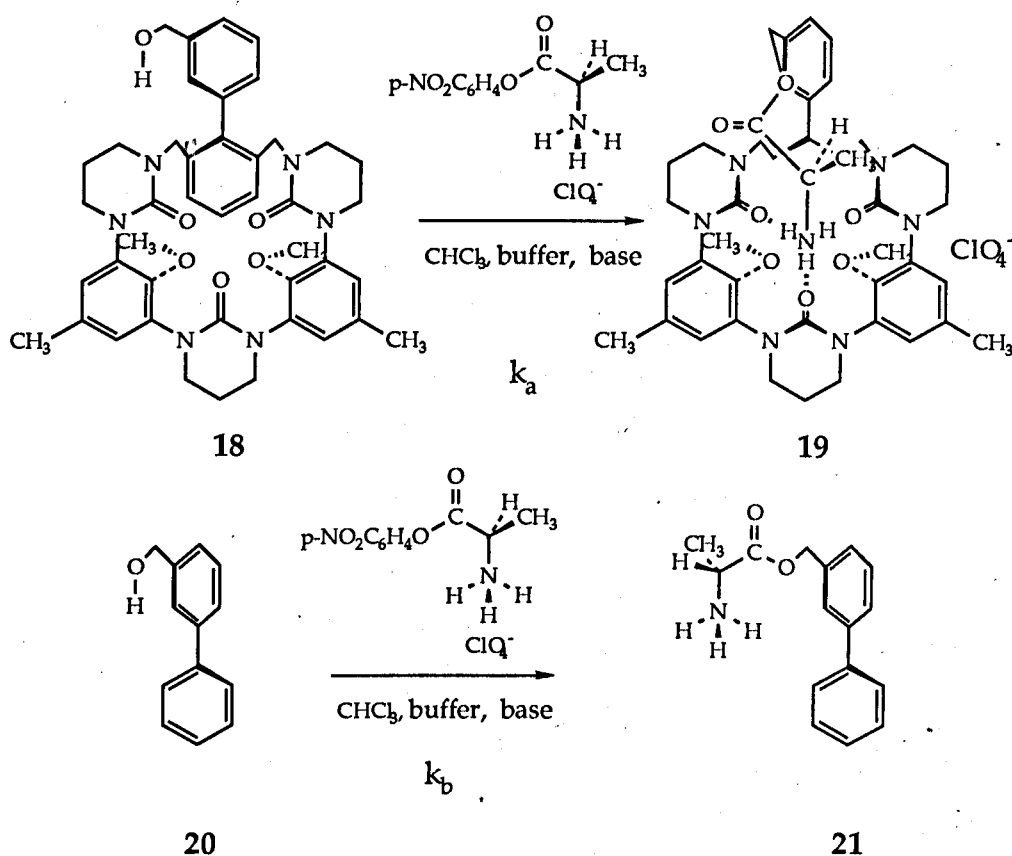


Figure 1.14 A Serine Proteases mimic reaction of acyl-transfer. Compound **20** is a model molecule used for comparing with the enzyme analogue **18**.

There are also some other reports of enzyme mimic reactions, but most of them are limited to the reactions of acyl transfer and hydrogen transfer from guest compounds to host compounds. In other words, only one substrate is involved in these reactions.²⁰

The first bimolecular reaction catalysed by a synthetic template was reported by Kelly et al.²¹ In their example, two pyridone molecules were linked together as template **22**. Each of two complementary naphthyridine derivatives, were used separately to generate two reaction sites, a primary amine **23** and a primary bromide **24** (Figure 1.15). In chloroform solvent at room temperature, the S_N2 reaction between **23** and **24** was monitored by ¹H NMR. The results showed that in the presence of 1 equivalent template **22** (all concentration are 0.0040 M), the reaction rate increased 6-fold. The NMR results supported the hypothesis that the rate acceleration results from the transient intermediacy of the ternary complex **25**. The turnover of the template, which is another characteristic of enzyme catalysed and auto-catalytic reactions, was also discussed. They believed that the turnover of **22** did occur because (1) Only average spectra were observed rather than superimposed spectra of bound and unbound species. (2) The product **27** precipitated from the reaction solution as its hydrobromide salt. The precipitation of **27**·HBr prevented what might otherwise be serious product inhibition.

One year later, Rebek's group reported the first example of a designed, hybrid synthetic replicating system.^{22a,b} Based on their early work on molecular receptors derived from Kemp's triacid, a triacid imide with a naphthalene spacer which bears a pentafluorophenyl ester was designed as a reaction site **29a** and an aminoadenosine was used as another component **28**, which contains both binding site and reaction site. The template **30a** was formed by an amidation reaction between the two components and the template in turn catalysed reaction between the

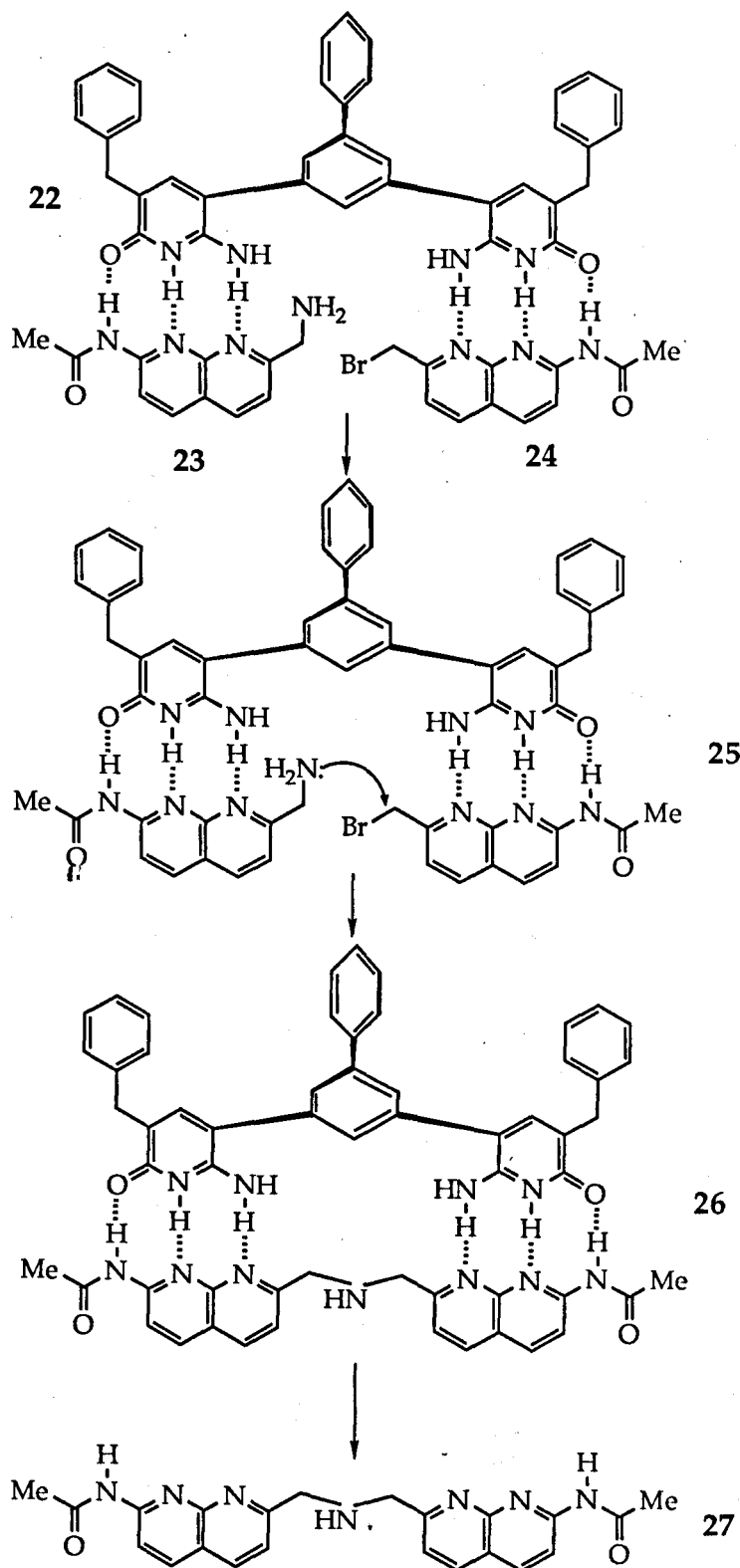


Figure 1.15 A mimic reaction of bimolecular-reaction catalysing enzyme.

unreacted reactants in the solution by binding them together.(Figure 1.16). This system showed several features. (1) The autocatalysis phenomenon was shown by addition of the product 30a to the reaction mixture which results in an increase in the initial coupling rate by 40%. (2) The dimerization of template does occur and the dimerization constant $K_d = 630 \text{ M}^{-1}$ was measured by an NMR dilution study, although it is not as big as it was expected from the association constant between the two reactants $K_a = 60 \text{ M}^{-1}$. The explanation is that there is some attenuation by steric effects in the middle of the structure. (3) When one binding site of template, acid imide, was inhibited by an alkyl group 30b, the reaction was 10 times slower than when it was not blocked and the reaction could also be slowed down by adding some bis(acylamino)-pyridine as an inhibitor.

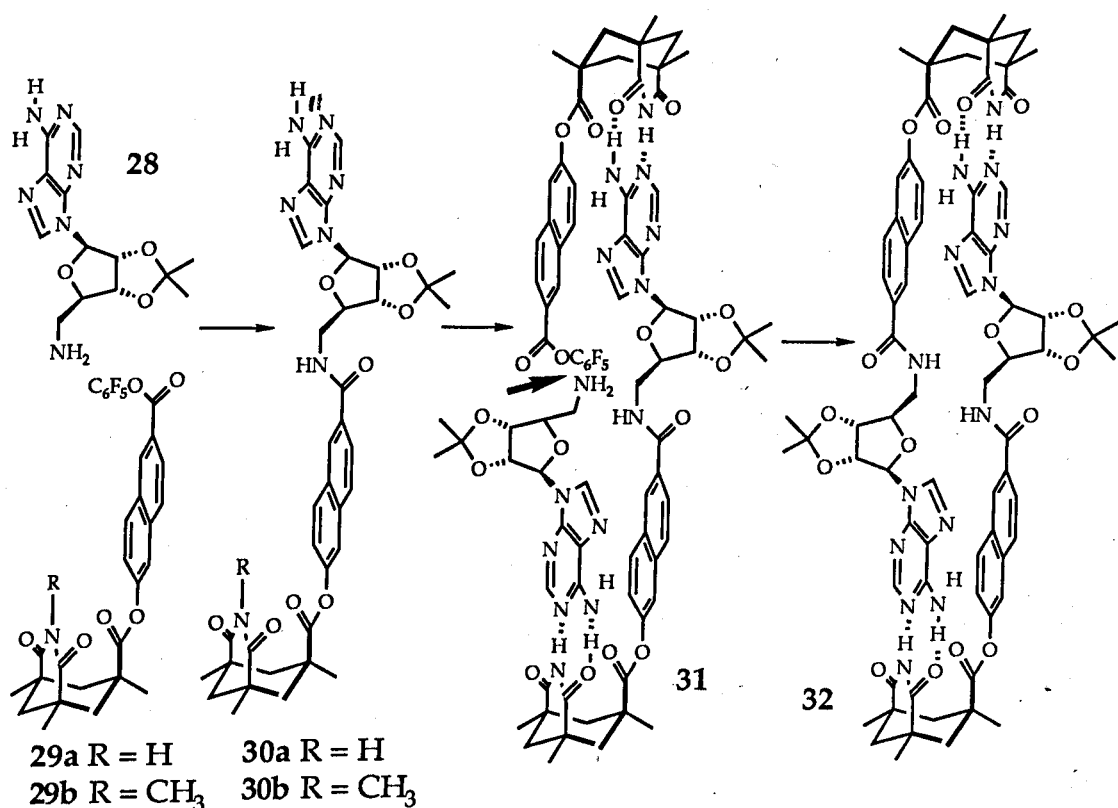
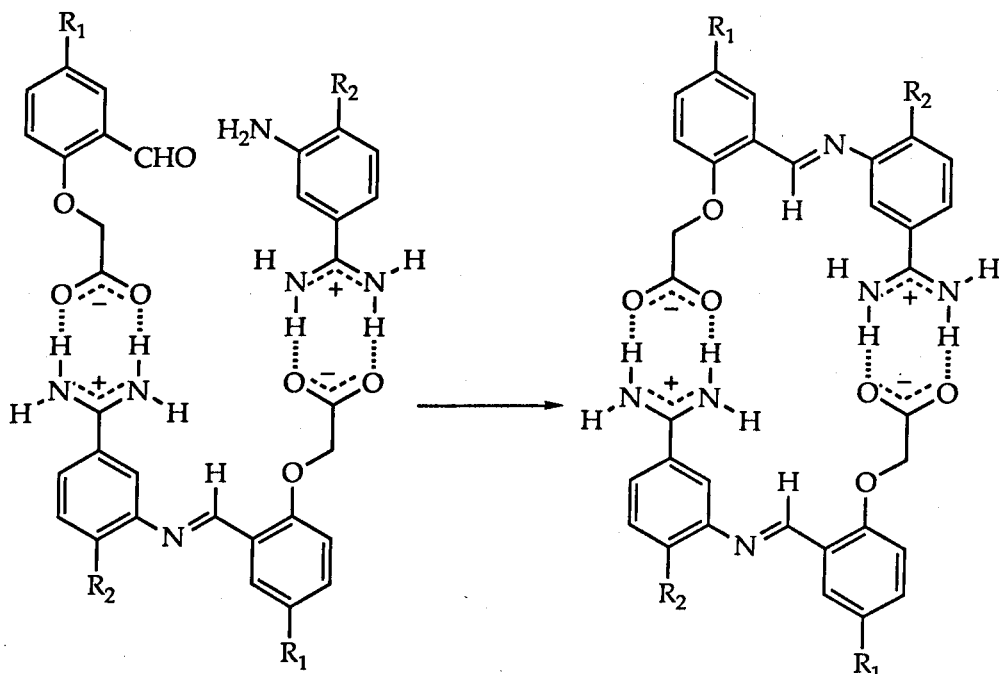


Figure 1.16 The first replicating system based on non-nucleotide molecules.

Having the results from replicating systems based on nucleotide compounds and understanding more about this kind of reaction, von Kiedrowki's group attempted to design a completely novel replicating system which contains no nucleoside at all for molecular recognition.²³ An amidinium-carboxylate salt bridge was adopted as a substitute for base pairing because NMR titration showed that this kind of bridge is sufficiently stable in d_6 -DMSO with an association constant of about 350 M^{-1} at 35°C . The reaction between an aromatic amine and a benzaldehyde is chosen because the rigid product anil can exist in conformations in which the recognition sites are aligned roughly parallel to each other. (Figure 1.17). Their results show that when compounds 33a and 34a were used to form product 35a, the reaction rate growth was approximately proportional to the square root of the initial concentration of the product, which is similar to the results they obtained previously from nucleotide replicating systems,¹¹ and the autocatalytic efficiency ϵ is about $16.4 \text{ M}^{-1/2}$, which is also similar to results which have been obtained by their group and other groups. But an unexpected result was obtained, when compounds 33a and 34b were employed as reactants and compound 35c, which is a structural analogue of the reaction product 35a, was used as the template. Anil 35c accelerated the synthesis of 35b by a factor as big as 370 M^{-1} , and the rate increase roughly corresponds to the initial concentration of 35c, rather than the square root of the concentration of 35c. They supposed that this first-order catalysis is because the ternary complex 33a:34b:35c is more stable than that of product duplex for some reason. This existence of first-order catalysis by a self-complementary template molecule suggested that self-replication with exponential autocatalysis (in the terms of time) should be feasible if the proper model system is used.

33a : $R_1 = \text{NO}_2$
33b : $R_1 = \text{H}$

34a : $R_2 = \text{t-Bu}$
34b : $R_2 = \text{Me}$



#

Figure 1.17 A self-replicating system involving anil formation.

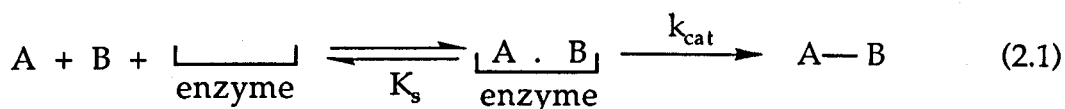
CHAPTER TWO

OBJECTIVE

2.1 Theoretical Background

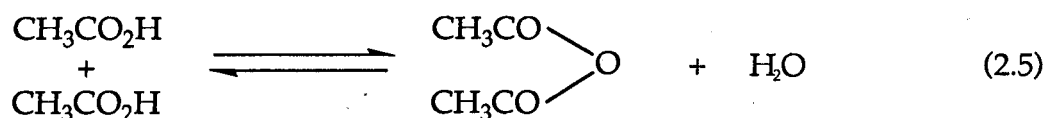
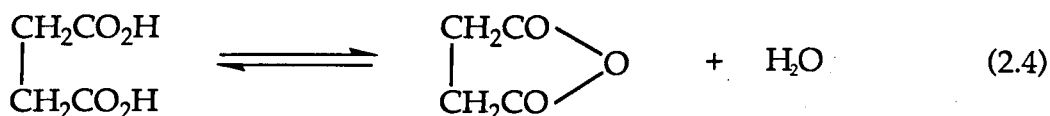
The molecular replication process is similar to the enzymatic reaction. In both processes the catalytic effect is brought about by holding the reactants together in an appropriate orientation at the binding site of templates or the active sites of enzymes, this is referred to as approximation or proximity. The only difference between these two processes is that in the replication process the product is the template itself. The theory which applies to the enzymatic catalytic process can be used to explain the replication process.

It has long been known that intramolecular reactions, (equation 2.2) in which the reactants are covalently bonded to one another, often proceed at very much faster rates than those of the analogous intermolecular reactions between two independent molecules. (equation 2.3) These intramolecular reactions are frequently taken as models for enzyme-catalysed reactions where the reactants are held close together in the enzyme-substrates complex (equation 2.1). Here it is supposed that catalysis is due only to the proximity effect, but the problem is then to express the



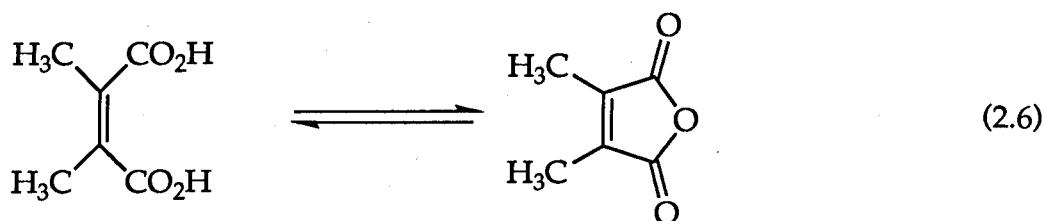
difference between the rate constants k_{cat} or k_{intra} with k_{uncat} , because they are expressed in different units. The reactions (2.1) and (2.2) are kinetically

first order, while the intermolecular reaction (2.3) is second order. Therefore, if k_{intra} is compared with k_{unecat} , the rate enhancement is expressed in units of concentration because a unimolecular reaction is being compared with a bimolecular one. What does the value of $k_{\text{intra}}/k_{\text{unecat}}$ actually mean? If one of the two reactants in the intermolecular reaction (2.3) is present in great excess over the other reactant, so that the process is effectively first order, the value of $k_{\text{intra}}/k_{\text{unecat}}$ is then actually the concentration of the more abundant species required to make the intermolecular reaction proceed at the same rate as that of the intramolecular one. So it is called "effective concentration" or "effective molarity". For example, the cyclization of succinic acid to form succinic anhydride (equation 2.4) is much more rapid than the formation of acetic anhydride from two molecules of acetic acid. (equation 2.5) The rate constant for reaction (2.4) is 3×10^5 M more



favourable than that for reaction (2.5).²⁴ Thus, we may say that in order to achieve the same reaction rate as for the intramolecular reaction (2.4), the concentration of acetic acid has to be as high as 3×10^5 M in reaction (2.5). Actually this is far above any concentration that could be obtained, even if the intermolecular reaction were carried out in pure acetic acid, (the concentration of glacial acetic acid is only 17.5 M). In many related reactions the results are even more dramatic, for example the rate constant

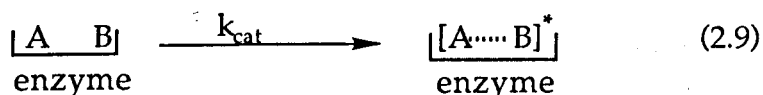
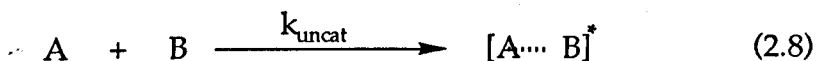
for the dehydration of dimethyl maleic acid to give the 5-membered ring acid anhydride (equation 2.6) is about 10^{12} M times more favourable than that for the formation of acetic anhydride from acetic acid^{24a, 25} (equation 2.5).



These examples from organic chemistry show that tying two reactants together in a single molecule can have an enormous effect on the rate of a reaction. This effect can be explained theoretically by using transition state theory. According to transition state theory, the rate constant of any reaction in which two molecules react to form a transition-state complex can be represented as equation (2.7),

$$k = \frac{k T}{h} e^{\Delta S^*/R} \cdot e^{-\Delta H^*/RT} \quad (2.7)$$

where k is the Boltzman constant, h is the Planck's constant, and ΔS^* and ΔH^* are the entropy and enthalpy of activation. Consider a reaction between two molecules A and B to give a transition state $[A \cdots B]^*$ and compare this with the same reaction occurring at the surface of an enzyme (equation 2.8 and 2.9). The contributions of enthalpy in both k_{uncat} and k_{cat}

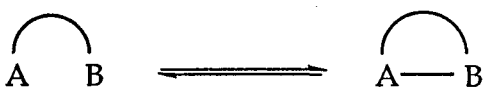


are very similar because the strengths of forming bonds and breaking bonds are very similar for the two reactions. So the high effective molarity or rate enhancement of the catalysed reaction ($k_{\text{cat}} / k_{\text{uncat}}$) must be from the entropy component $e^{\Delta S^*/R}$. Entropy is a measure of the degree of randomness or disorder of a system. The greater the disorder of the system, the more it is favoured and higher is its entropy. Obviously there is more entropy loss in reaction (2.8) than in reaction (2.9) because in reaction (2.8) two free starting molecules form a more ordered transition state while in reaction (2.9) the randomness is very similar in both starting complex and the transition state complex. Here the absolute value of entropy change of each reaction is not important, the important thing is the difference in the entropy change for the two reactions. The effective molarities of intramolecular reactions do not show a constant value but cover a very wide range from about 1 to 10^{15} moles/l.^{35b} It is easy to set an upper limit to the rate enhancement, in the absence of enthalpy effects, by considering the different entropy changes that occur in bimolecular and unimolecular reactions.

The different degrees of freedom lost in intramolecular and the analogous intermolecular reactions give rise to large differences in the entropy changes for the two systems. For a non-linear molecule containing n atoms there are 3 degrees of translational freedom (i.e. freedom to move along the 3 axes in space) and 3 degrees of rotational freedom representing the freedom of the whole molecule to rotate about its centre of gravity. This leaves $3n - 6$ degrees of freedom associated with internal motion in the molecule, i.e. vibrations and internal rotations. On forming the product of a bimolecular association reaction there is a loss of 3 degrees of translational freedom and a loss of 3 degrees of rotational freedom and there is a corresponding gain of 6 new vibrational modes in

	$A + B \rightleftharpoons A-B$	(2.10)
Translation	3 3 3	
Rotation	3 3 3	
Vibration	$3n - 6$ $3n' - 6$ $3n + 3n' - 6$	

the product (equation 2.10). However, in the uni- and intramolecular reaction there is no net change in the number of degrees of freedom of translation, rotation, and vibration upon forming the product (equation 2.11).

		(2.11)
Translation	3 3	
Rotation	3 3	
Vibration	$3n - 6$ $3n - 6$	

The entropy associated with these motions may easily be calculated from the partition functions, which are simply an indication of the number of quantum states that the molecule may occupy for each type of movement.

In Table 2.1^{35a} are shown some typical values of these entropy terms. For a standard state of 1 mole/l the translational entropy is normally about 120-150 J/K/mole and this value is not very dependent upon the molecular weight. For the majority of medium-sized molecules the entropy of rotation is about 85-115 J/K/mole and is also not normally very dependent upon the size and structure of the molecule. The entropy of internal rotation makes a comparatively small contribution to the total entropy of the molecule and the vibrational contribution is even smaller except for the very low vibrational frequencies.

So, in the gas phase, for the standard state of 1 mole/l and at 298 K the total loss of translational and rotational entropy for a bimolecular

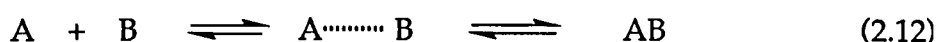
Motion	S° (J/K/mole)
Three degrees of translational freedom; molecular weight 20-200; standard state 1 mol/l	120-148
Three degrees of rotational freedom	
water	44
n-propane	90
endo-dicyclopentadiene C ₁₀ H ₁₂	114
Internal rotation	13-21
Vibration $\omega = 1000$ (cm ⁻¹)	0.4
800	0.8
400	4.2
200	9.2
100	14.2

Table 2.1 Typical entropy contributions from translational, rotational, and vibrational motions at 298 K.

association reaction is about -220 J/K/mole and this value has only a small dependence upon the masses, sizes and structures of the molecules involved. However, this loss is often compensated to varying extents by low frequency vibrations in the product or transition state. For reactions having "tight" transition states or covalently bonded products the change in internal entropy is about +50 J/K/mole so that total entropy change is predicted to be about -170 J/K/mole, which is similar to the value observed experimentally for many bimolecular gas phase reactions. In solution, the entropy change for a bimolecular reaction is estimated to be

only about 20 J/K/mole less than that in the gas phase, at the same standard state of 1 mole/l and 298K.

Since this large loss of entropy for a bimolecular reaction is avoided if the reactants are bound to an enzyme active site (equation 2.1) or converted to an intramolecular reaction (equation 2.2), the maximum entropic advantage from proximity may now be estimated (equation 2.12, Table 2.2).³⁵



	"loose" transition state or product	"tight" transition state or product	Maximum
ΔS (J/K/mole)	-40	-150	-200
Effective concentration (mole/l)	10^2	10^8	10^{11}

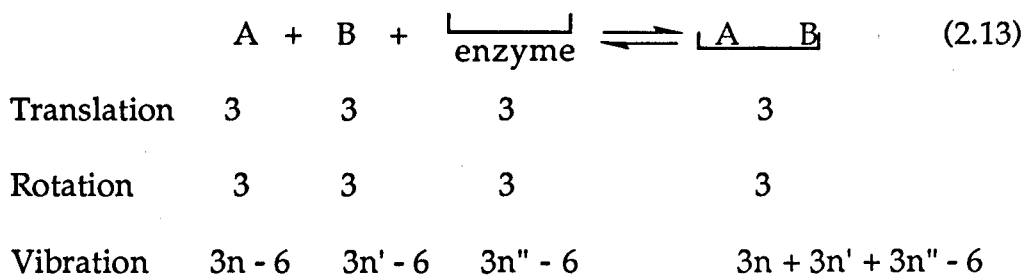
Table 2.2

The theoretical most negative entropy change for a bimolecular reaction is about -200 J/K/mole which is equivalent to 60 kJ/mole at 298 K and makes such a reaction unfavourable by antilog ($60/2.303 /RT$), a factor of 10^{11} moles/l. However, this is very rare and a more general situation is that this large loss of translational and rotational entropy is compensated for by an entropy change of about +50 J/K/mole, resulting from changes in internal motions on going from the reactants to the product or transition state and from differences in entropies of vaporisation of reactants and products giving bimolecular reactions a total entropy change of about -150 J/K/mole. Since this loss of entropy does not take place for a reaction in

which the reactants are bound to the active site of an enzyme or for an intramolecular reaction, the approximate maximum effective concentration or rate enhancement for these reactions from entropic factors alone is about 10^8 moles/l. In the comparatively rare situation of a bimolecular reaction having very "loose" transition state or product then association will be even less entropically unfavourable since the entropy of the low frequency vibrations in the "loose" complex will counterbalance the large loss of translational and rotational entropy. The rate enhancement for the analogous intramolecular reaction will, therefore, be smaller, perhaps in the range of 100 moles/l or less.

In summary, one of most important effects of proximity in enzyme catalysis is a more favourable entropy of activation. However, initial binding of the reactants A and B to the enzyme is, of course, entropically unfavourable. This means the entropy decrease associated with the formation of the transition state has been shifted to an early step in the reaction, the binding of the substrate to form the enzyme-substrate complex. This step is often driven by the binding energy (enthalpy decrease) associated with electrostatic interactions, such as hydrogen-bonding between polar or charged groups of the substrates and the enzyme. So any increase in the rate of reaction brought about by the enzyme is given by the energy of binding the enzyme and substrates, A and B, less the entropy of association of the transition state and enzyme.

The entropy loss of a template-substrate binding reaction is more than for a bimolecular reaction because it is a termolecular process. It can also be estimated roughly in a similar way to that is used for a bimolecular reaction. The total loss of translational and rotational freedom for a termolecular association reaction is double of that of a bimolecular reaction ($18 - 6 = 12$, see equation 2.13). So the entropy loss is doubled



($2 \times -220 = -440$ J/K/mole). The gain of vibrational modes in a termolecular reaction is also double that of a bimolecular one. The gain of entropy is +100 J/K/mol for a tight transition state or covalently bound product. Considering the solution factor of about 20 J/K/mole entropy gain, the maximum entropy loss for an enzyme-substrate binding reaction is -320 J/K/mole, which equivalent to 95 kJ/mole energy at 298 K. However, for most cases of enzyme-substrate complex, the entropy loss could be much less than -320 J/K/mole because the gain of entropy from vibration is much higher than +100 J/K/mole, as enzyme and substrates are loosely bound by non-covalent binding.

The complexation between enzyme and substrates can provide enormous binding energy to overcome the entropy loss during the process. For instance, the binding energy of a single hydrogen bond, which is a common non-covalent bond in enzyme substrate binding, is about 40 kJ/mole. So the multiple hydrogen-bonding, which is common in enzyme-substrate association, will provide enough energy to cover the entropy loss. The total binding energy less the unfavourable entropy loss give the free energy change in the complexation process, which will be reflected by the association constant or dissociation constant K_s by equation 2.14.

$$\Delta G = - RT \ln (1/K_s) \quad (2.14)$$

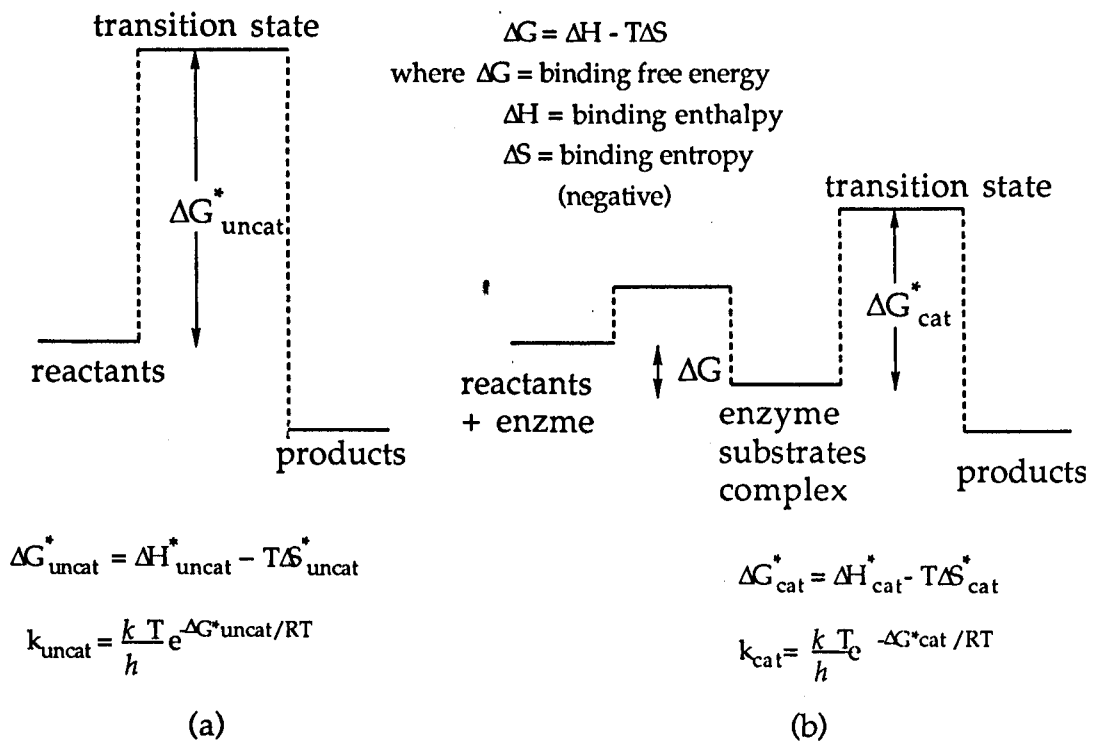


Figure 2.1 Energy profile for (a) uncatyalsed reaction and (b) enzyme catalysed reaction

Figure 2.1 shows the energy profile for a normal bimolecular reaction (equation 2.3) and an enzyme catalysed reaction (equation 2.1). According to transition state theory, the reaction rate constant is given by equation 2.7. In a bimolecular reaction, the entropy of activation, ΔS^* , has a large negative value as described above, and the enthalpy of activation ΔH^* results from new-bonds forming and old-bonds breaking. The energy provided by this to overcome the entropy loss is limited. As a consequence, a large free energy of activation, ΔG^* , is expected. Although there is also a big entropy loss in the transition state (a big minus figure for ΔS^*) of the first complexation step of an enzyme catalysed reaction, a large binding energy of the transition state (a large negative ΔH^* figure)

provided by multiple non-covalent binding will compensate for the entropy loss so that only a small activation energy ΔG^* is required. In the second step of a catalytic reaction, the change of enthalpy of activation is similar that of the bimolecular reaction, but the unfavourable entropy of activation is much smaller as discussed above. This results in a smaller activation energy ΔG^* .

In generally, enzymes separate a process with high activation energy, in which bond forming, bond breaking and entropy loss are happening at the same time, into two consecutive steps with low activation energy, in which the entropy loss is overcome by the binding energy of enzyme / substrates complexation in the first step and only bond forming and breaking are of importance in the second step. The step with the lower reaction rate will determine the rate of the whole reaction and in most cases, the second step is the rate determining step.

In the reaction within an enzyme substrate complex, besides the more favourable entropy, there is another effect which is similar to a solvation effect. The polar groups in enzymes can stabilise the charges developed in the transition state, which will make ΔG^* smaller and the reaction faster. However this kind of effect is unlikely to exist in simple molecular replicating systems because there are not likely to be many polar binding sites available around the reaction sites.

However, even though an enzyme or template may bind substrates, or stabilise the substrates there may be no catalysis. For catalysis, enzyme or template must bind the substrates in a way that favours the formation of the transition state of the reaction. In other words, they must stabilise the transition state of the reaction. An example can show this factor clearly.²⁶ Figure.2.2 shows an intramolecular Diels-Alder reaction, the two terminal substituents move from $\sim 6.0 \text{ \AA}$ apart in the required s-cis starting

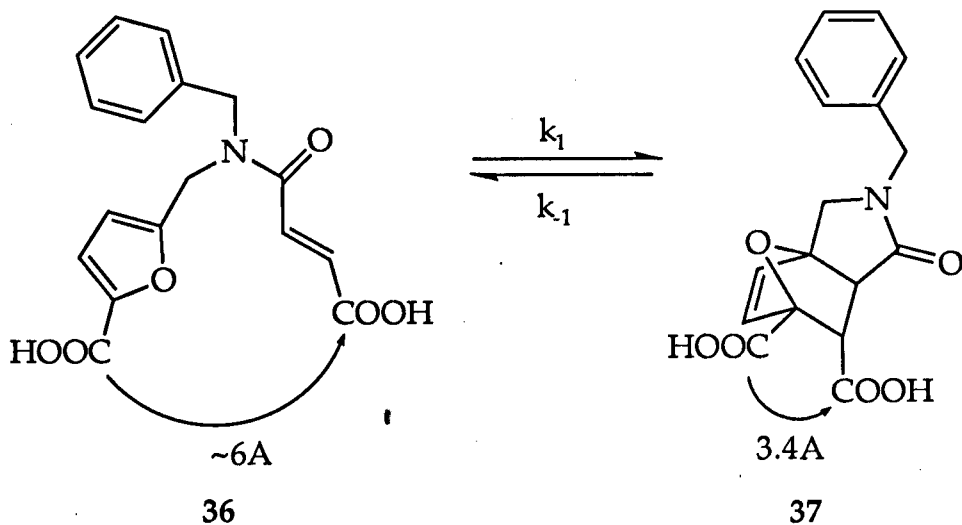
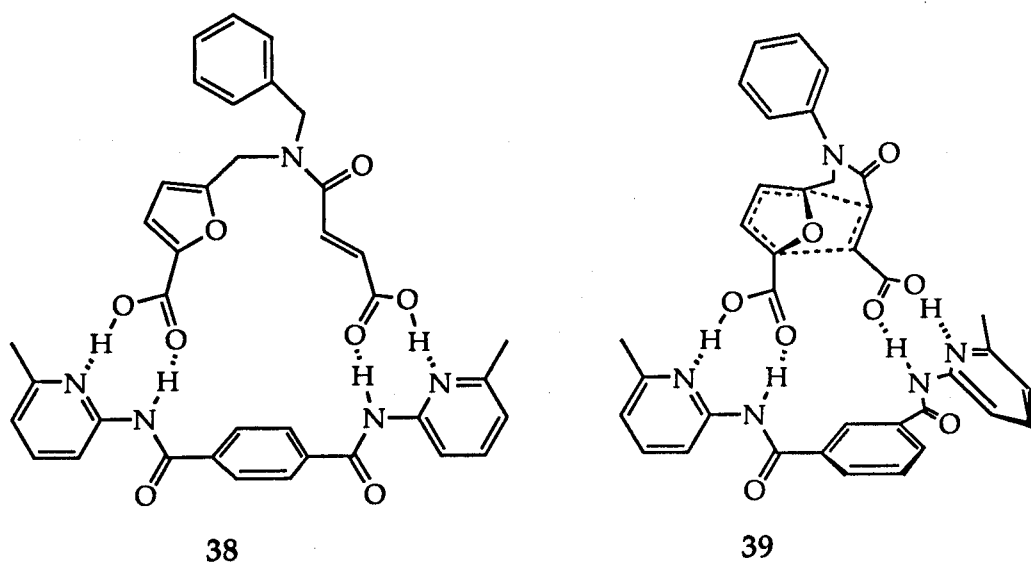


Figure 2.2 The distance between terminal carboxyl groups is changed after an intramolecular reaction.

material **36** to about 3.4 Å apart in the product **37**. If a simple terephthaloyl receptor is used to bind the starting material to form complex **38**, the reaction rate dropped by 10-fold as compared with the reaction of the unbound substrates. Because the receptor is only complementary to the *cis* ground state, it is necessary to break hydrogen bonds to reach the



transition state for the intramolecular reaction. In contrast, the analogous isophthaloyl based receptor gives a 3.5-fold increase in the rate of the intramolecular Diels-Alder reaction as compared with the reaction of the unbound substrates. The reason is that in this case the receptor binds to more closely spaced carboxylates as in the putative transition state complex 39. The energy profile for these three reaction conditions are shown in Figure 2.3. The non-templated reaction is used as a standard (i), (ii) shows

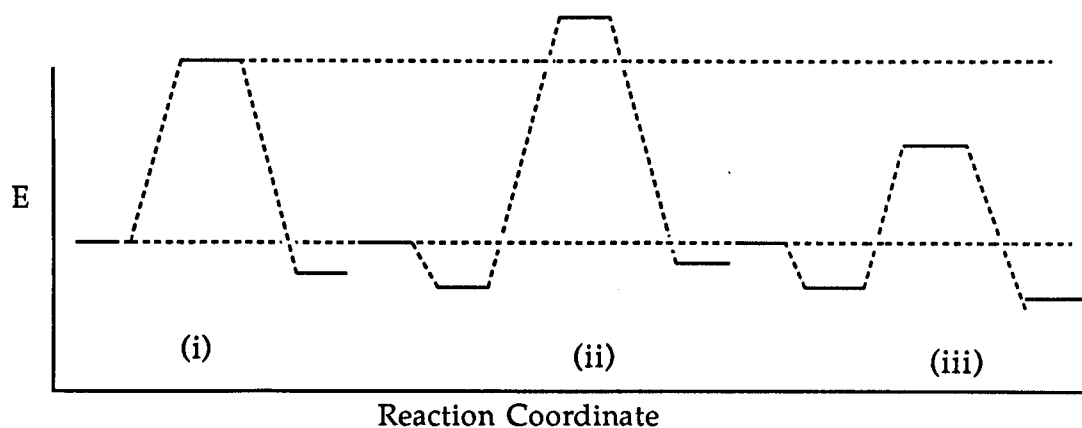


Figure 2.3 Energy profile for the intramolecular reaction shown in Figure 2.2 with different template used. (i) without template, (ii) with terephthaloyl template and (iii) with isophthaloyl template.

how the reaction goes via the complex 38, in which the ground state is stabilised, but the transition state is destabilised and (iii) shows that in the complex 39, both product and transition state are stabilised with the transition state a little more favoured. The conclusion is that a good enzyme or template must not only bind the substrates, but also bring them close together in an orientation that favours the formation of transition state or give good transition state binding.

2.2 The Basic Requirements for a Replicating System

The molecular replicating system described in the chapter 1 can be illustrated by Figure 2.4. The two reactants A and B, each of which bears a

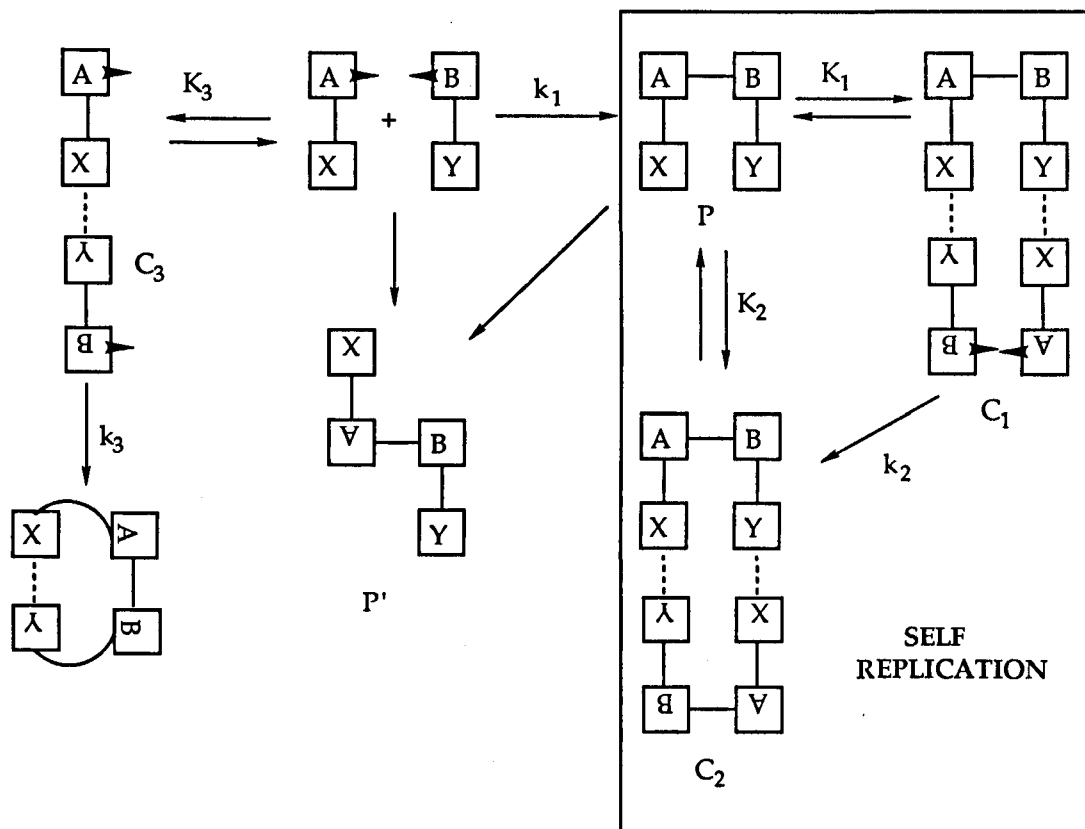


Figure 2.4 A basic replicating system. The arrows on the reactants A and B, which present the orientation of the reactants, pointing towards each other in complex C₁ and complex C₃ means that the conformation of the reactants is favourable for the reaction. Other unfavourable conformations may also exist.

complementary binding site X and Y, react together to give product P. The product P catalyses the reaction by forming the complex C₁. Then product dimer C₂ dissociates to give more template to catalyse the reaction in the next cycle. The dimer C₂ potentially inhibits the replication process unless

the magnitude of K_1 and K_2 are similar or $K_1 > K_2$. There may be many conformations of the reactants and product, which are not favourable for the reaction, depending on the rigidity of the molecules used. P' is another conformation of the product P, which gives no catalysis because of the bad orientation of binding sites which makes the substrates remote from each other. Any reaction that produces product P directly from C_3 is not a true replication process and there is no information transfer in this reaction, although there may be some rate enhancement. There may also be other non-productive conformations in C_1 caused by the rotation of the bonds between reactants and binding sites. So the minimum requirements for a successful replicating system are:

- (a) two mutually complementary binding sites X and Y incorporated into two reactants A and B,
- (b) a low energy conformation P of the reaction product that is a template for the catalysed process,
- (c) this conformation of the product P should be more suitable for transition state binding than for dimerisation.

Although the systems introduced in chapter 1 met these requirements to some extent, they are far from perfect.

Firstly, ideal kinetic characteristics have not been shown since the increase in the initial rate of reaction due to autocatalysis is only proportional to the square root of the concentration of the template, rather than directly proportional to the concentration of template. The proposed reason for this is that most of the product present in the solution is tied up by association in double helices, (C_2 in Figure 2.5) which inhibits catalysis by the template.

Secondly, the rate enhancements achieved by several groups are only at the lowest level for enzyme catalysed reactions. This could be for three possible reasons:

1) Polar solvents were used (in nucleotide cases) or less efficient binding sites were used (in other cases), so that a large binding energy between templates and substrates was not achieved. As discussed in section 2.1, this binding energy is essential to overwhelm the big entropy loss during the formation of the template-substrate complex.

2) Too flexible templates or spacers between reactants and binding sites allow too many non-productive conformations in the reaction complex C_2 .

3) The position of the substrates bound by the simple templates used do not fit the orientation of the transition states of the reactions very well.

Thirdly, a clear sigmoidal curve for product concentration against time, which is a characteristic of autocatalytic reactions, has not been achieved. A fast background reaction between reactants A and B or acceleration of the reaction by another route, such as a significant contribution by k_3 in Figure 2.4 which make the back ground rate look faster, can make the induction time too small to be observable.^{22b}

Fourthly, for all examples of molecular replicating systems, the information transfer is limited since the information in templates is only represented by the sequence of two binding sites X and Y. Although as many as six bases were used in nucleotide cases, there were only two patterns of sequences.

Finally, in all cases, stereochemical information has not been involved although it is important in biological replication processes. So building a more efficient molecular replication system carrying more information to transfer is not only a challenge for chemists, but also has implications for molecular recognition, molecular templating, artificial enzyme design, enzymatic catalysis, and replication processes in both biotic and abiotic systems.

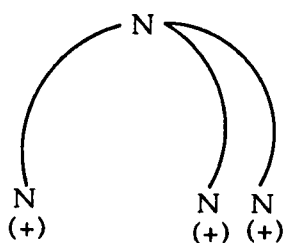
As discussed above, to design an efficient molecular replication system, the following requirements should be met: a large binding energy between the two complementary binding sites, potentially rich information storage and transfer, a comparatively rigid molecule to avoid non-productive conformations in complex C_2 , or pseudo rate enhancement via C_3 , and a suitable reaction with a transition state which could be stabilised by a simple product template with reduced dimerization.

2.3. Binding Sites

As we have seen a complementary binding pair of reactants with large binding energy is essential for a templated replication process. After the initial coupling reaction of the two reactants, the product has two binding sites, each of which will only bind its complementary reactant to catalyse the templated reaction. The large binding energy is normally obtained by using non-covalent interactions particularly when multiple interactions are used. The advantages of using these non-covalent interactions are that the association process is very fast and dissociation is easier after the catalytic reaction to regenerate monomeric templates which can catalyse the next cycle of replication.

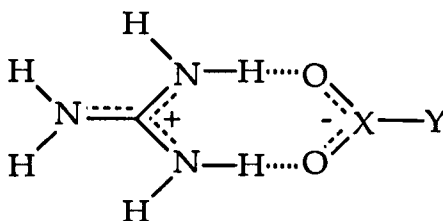
Positively and negatively charged molecules could be used as a complementary binding pair. It has long been known that anionic substrate binding plays an important role in biological systems. The exploration of artificial anion receptors of both cyclic and acyclic type started very soon after the discovery of cation recognition by crown ethers. Protonated amines were first used as anion binding sites.^{27,28,30} The quaternary ammonium salt was later introduced into the artificial anion receptor to eliminate the pH dependence of protonated amines.^{28,29,30}

However, it is difficult to include both protonated amine or ammonium group in the template of a replicating system since open chain compounds containing multiple protonated amine or ammonium groups, such as 40, show little molecular recognition although they may bind some anionic molecules strongly. It is not easy to find a suitable complementary anionic molecule for these compounds. Another problem is that flexible binding sites in the template will not bring the reactants into close proximity as required by a replicating system.

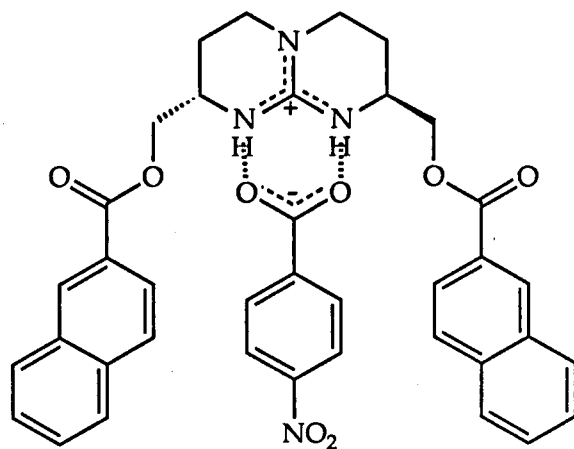


40

The guanidinium group is unique and presents some interesting features: i) It remains protonated over a much wider range of pH than does the ammonium group due to its much higher pKa (13.5 for guanidinium itself). ii) It may form characteristic pairs of zwitterionic hydrogen bonds $N-H^+ \cdots X^-$ which provide binding strength by their charge and structural organization in arrangements which are seen in the crystal structures of many guanidinium salts. The general type of binding pattern is as follows:



This type of binding pattern has already been found in biological systems. The guanidinium group of arginyl residues in proteins has an important function in protein tertiary structure through internal salt bridges with carboxylate anions, as well as in binding and recognition of anionic substrates by enzyme receptor sites and antibodies. When the guanidinium group is incorporated into synthetic receptors,^{30,31} both macrocyclic and acyclic compounds show ability to bind anionic molecules such as carboxylates and phosphates. For example, the values of stability constants ($\log K_S$) of some guanidinium based receptors for complexation with PO_4^{3-} are from 2.4 to 4.0 in water.^{31b} The more interesting characteristic is that when guanidinium and carboxylate associate together, they are held coplanar by the two hydrogen bonds formed between them; this will provide rigidity for the template if they are used as a complementary binding pair in a replicating system. This property has been developed to provide a chiral recognition receptor **41** with a rigid



41

guanidinium group and chiral carboxylate compounds. For instance, **41-SS** and **41-RR** have different binding ability towards sodium (S)-mandelate.^{31d} Subsequently, the guanidinium and carboxylate groups were incorporated into a replication system²³(Figure 1.17, chapter 1). The

disadvantage of this binding pair is its poor solubility in non-polar organic solvents and it only shows a modest association constant in polar solvents (around 100 M^{-1}). This problem could be solved by modifying the side chain of the compounds. It has been shown that with more lipophilic side chains, the association constant between a guanidinium cation and a carboxylate anion in **41** could reach 10^4 M^{-1} in chloroform.^{31d}

The coordination between a Lewis acid and electron rich molecules is another kind of non-covalent force which has been of interest to build into molecular receptors. Metalloporphyrin is another molecular unit which has been paid much attention in this field ³² because of its special role in nature. The coordination bond between the metal atom of the metalloporphyrin and a heteroatom such as nitrogen is very strong. For example, porphyrin **42** binds to 4,4'-dipyridyl with association constant 3.5

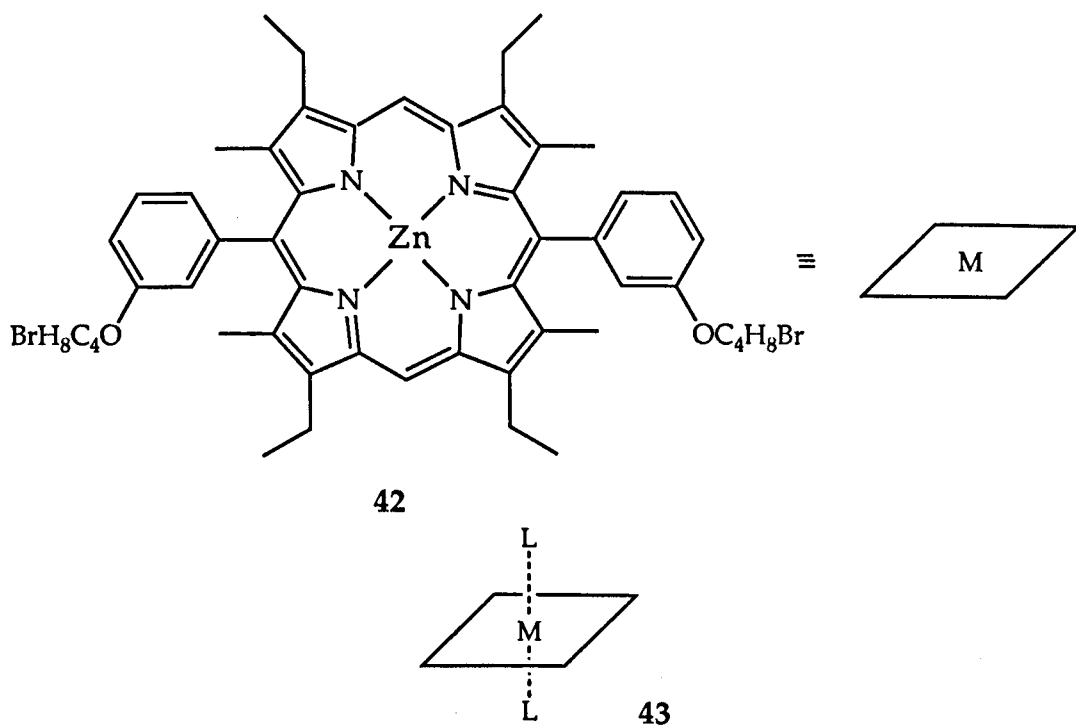
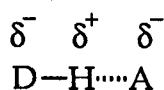


Figure 2.5 Coordination between a porphyrin derivative and ligands

$\times 10^3 \text{ M}^{-1}$. The association constants are even bigger when more basic ligands are used.^{32h} Porphyrins which can complex with nucleobases ^{32d} and amino acids ^{32g} have also been explored, but there are some problems with using a porphyrin as one of binding sites of an artificial template. One problem is that the two faces of the porphyrin have little selection towards the ligand as shown in 43, which can cause deficiency of the binding. Another problem is that the coordination bond is nearly vertical to the porphyrin face, and this special geometry makes some difficulty in the design of a template. Recently, by carefully choice of geometry, J. Sander's group in Cambridge made an artificial template based upon a cyclic porphyrin trimer, which can catalyse some intermolecular reactions.³³ This example will be discussed in more detail later on in this chapter.

Among non-covalent forces, hydrogen bonds are the most popular, they have been intensively studied and their properties are well defined. The hydrogen bond is the force between a hydrogen atom covalently attached to an electronegative atom and another electronegative atom. The hydrogen bond is usually represented by dotted lines as below,



where D and A are electronegative atoms and are called hydrogen donor and hydrogen acceptor respectively. F, O and N are the most common electronegative atoms in hydrogen bonds. D and A can be in different molecules or in the same molecules. Hydrogen bonds exist everywhere in living systems and they are essential factors in the 3-D structure of proteins and nucleic acids. They may also be the major force between enzymes and substrates and can exist in the aqueous cytoplasm in a cell.

Their important role in molecular recognition has been described in chapter 1. Figure 2.6 shows some typical examples of hydrogen bonding between molecules.

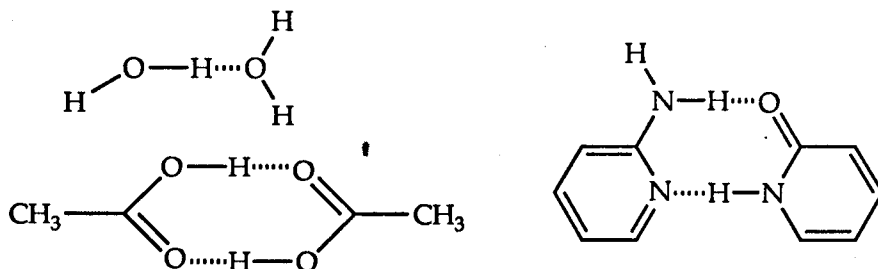


Figure 2.6 The example of hydrogen bonds.

The energy of a single hydrogen bond varies from 50 kcal/mol (FH...F) to 3 kcal/mol (NH...N), but most OH...O bonds and NH...N bonds have energies in the range 5-10 kcal/mol. To a first approximation, the strengths of hydrogen bonds increase with increasing acidity of D—H and basicity of A and lie between those of covalent bonds (50-100 kcal/mol) and weak non-bonding interactions such as van der Waals forces (<1 kcal/mole). In solution hydrogen bonds rapidly form and break. The mean lifetime of NH₃...H₂O hydrogen bonds is 2×10^{-12} second. These characteristics make the hydrogen bond very useful as a source of binding energy, especially in cases where more than one hydrogen bond exists between two molecules. The relatively small bond energies allow rapid hydrogen bond breaking when it is needed.

The geometry of hydrogen bonds is generally linear but because of the low bond energy it can show deviation from linearity up to a maximum of 30°. So the O—H...O and N—H...O bond angles in intermolecular hydrogen-bonded systems vary from 140° to 180° and from 130° to 180° respectively. This approximate linearity gives specific

arrangements in solution and in the solid state when molecules are associated by hydrogen bonding.

Because in the hydrogen bond, D—H is the hydrogen donor and A is the hydrogen acceptor, together with the linear geometry, hydrogen bonding gives molecules the capability of molecular recognition. If there are two or more hydrogen bonding pairs in two molecules, then more than one hydrogen bond can be made by the hydrogen-donors and hydrogen-acceptors. This not only provides more binding energy but also enhances the molecular recognition property of such molecules. Figure 2.7 shows two different ways of combining D and A in two intermolecular hydrogen bonds.

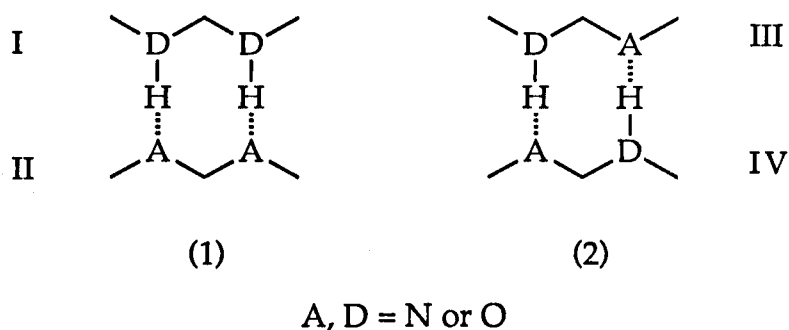


Figure 2.7 Two different combinations for double hydrogen bonds between molecules

If the hydrogen bonds are formed with the geometrical relationships shown, although the bond energies are similar in both type (1) and type (2), they have different recognition properties. In type (1), species I can only bind with complementary species II or vice versa, neither I nor II can bind with themselves or with species III or IV. If one of the species flips 180° about the vertical axis, they can still form two hydrogen bonds because both molecules have a C_2 symmetry. In other words, this pattern of intermolecular hydrogen bonding has poor ability for stereo recognition. In type (2) neither species III nor IV has C_2 symmetry, full hydrogen binding is not possible if one of species flips 180°

about the vertical axis and the stereo recognition is consequently improved. However, molecules of this type have poorer capability of molecular recognition because both species have the same pattern for hydrogen bonding and they can bind not only to each other, but also to themselves. What is going to happen if one of these binding types is built into a replicating system? Suppose choosing type (1) as the complementary pair and assigning I as X and II as Y. After the coupling reaction between reactants A and B, a template is formed (See Figure 2.4). When this template is used to bind the reactants, there will be three possible binding modes according to the recognition pattern of the binding sites (Figure 2.8). Among these three patterns, differentiated by the black wedges which represent productive orientation of the reaction sites, only the first one has proximity between the two reaction sites, the other two patterns have a remote relationship between reaction sites. If the bonds between A—X and B—Y are rigid, there will only be catalysis in the first case. The other two patterns will be non-productive binding which will inhibit some template molecules in a reaction. So type (1) is not a good complementary binding pair for a replicating template.

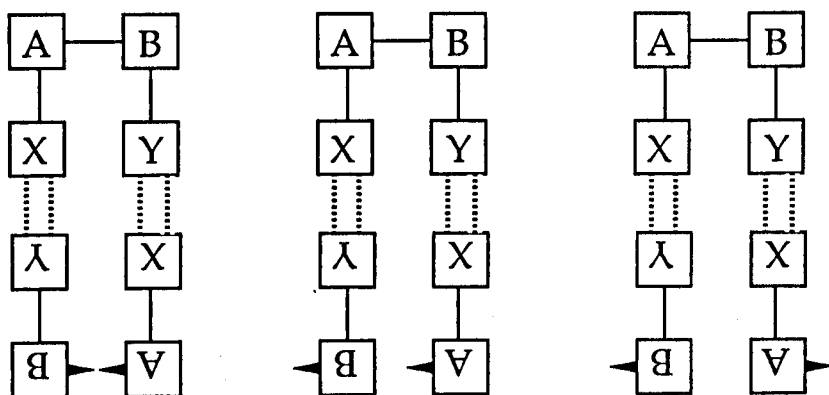


Figure 2.8 Three binding combination in a templating system using type (1) of double-hydrogen bonded (shown in Figure 2.7) as bonding pattern. Species I is assigned as X and species II as Y.

In type (2), there is no problem of the type found for type (1) because of the different molecular recognition property. The two molecules only form double hydrogen bonds in one direction, however, species III and IV have the same hydrogen bonding pattern and can also bind to themselves. This self-complementary character could also inhibit the efficiency of the template when used in a replicating system as shown in Figure 2.9 where species III is assigned as X and IV as Y. In the last two binding modes, the template is inhibited by binding two reactant molecules of the same species while the second pattern is as same as the third pattern in Figure 2.8, which is also a non-productive binding mode if the bonds between A-X and B-Y are rigid.

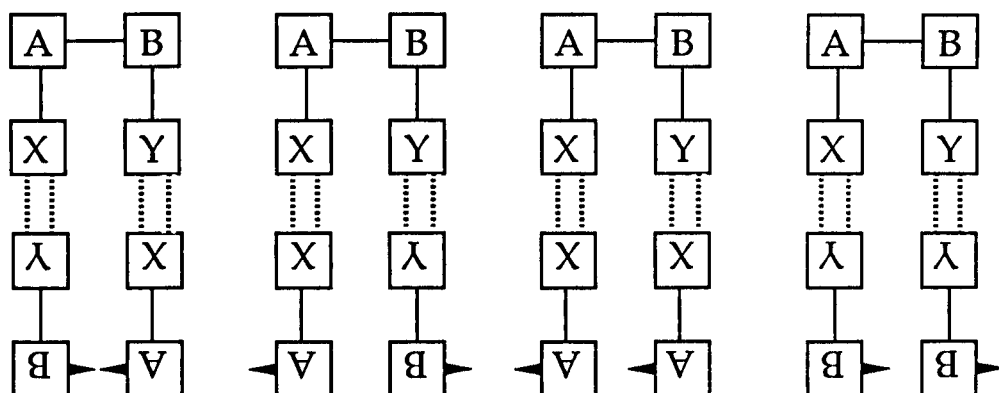


Figure 2.9 Four different hydrogen bonding combinations using type (2) (shown in Figure 2.7) as bonding pattern, where species III is assigned as X and IV as Y.

In view of the above considerations, obviously the two-hydrogen-bonded complementary pair is not a very good strategy for a self-replicating system. Furthermore the binding is not strong enough to give a large catalytic effect since strong binding is essential to obtain a good catalytic effect as discussed in Section 2.1.

The combination of more hydrogen bonds has also to be considered. There are three possibilities when three hydrogen bonds are used for

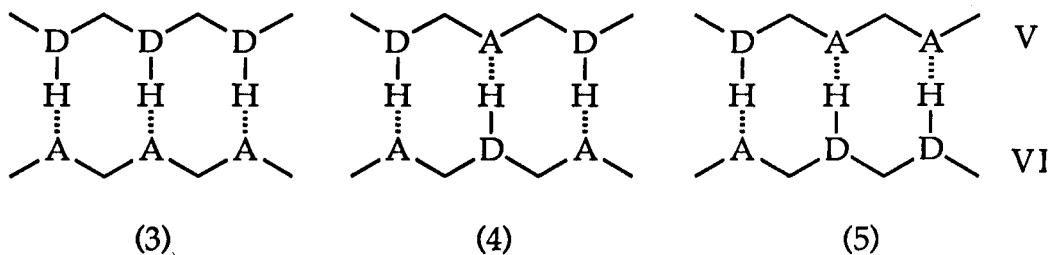


Figure 2.10 Bonding patterns using triple hydrogen bonds

complementary binding (Figure 2.10). The first two types (3) and (4) have the same recognition property as the doubly-hydrogen-bonded type (1) (Figure 2.7). These binding patterns have C_2 symmetry and they can associate with their complementary partner with face up or face down, which may cause some problems when they are built into a molecular replicating template. However, binding pattern (5) is unique since both species in this type form triple hydrogen bonds from one direction with their complementary partner and they can not bind with themselves. This specificity of molecular recognition will hold the reactants firmly together and optimise the proximity of the reaction sites. This type of binding pattern has been adopted in biological systems, such as cytosine-guanine pairing in DNA (see Figure 1.1 in chapter 1, page 1), and the specificity plays an important role in gene replication.

Apart from the specificity of molecular association, recent research shows that the binding energy of multiple hydrogen bonding is not a simple multiple of the binding energy of the corresponding isolated hydrogen bonds particularly when three hydrogen bonds are lined up in close proximity as those in the cytosine-guanine pair.³⁴ In view of the partial positive charges on H and partial negative charges on N and O, there are three different patterns of secondary interactions for the three bonding types of Figure 2.10. There are four attractive secondary interactions for type (3), four repulsive interactions for type (4), and two

attractive and two repulsive interactions for type (5) (see dotted lines in Figure 2.11).

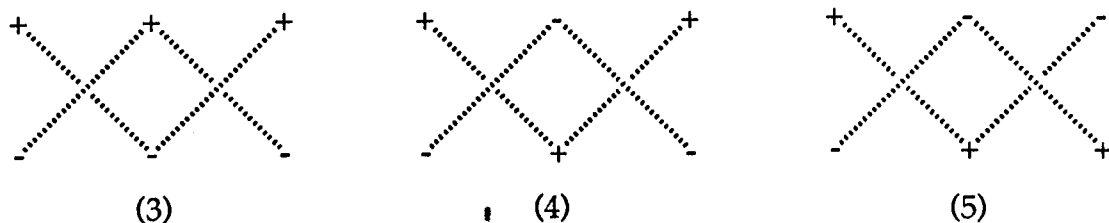
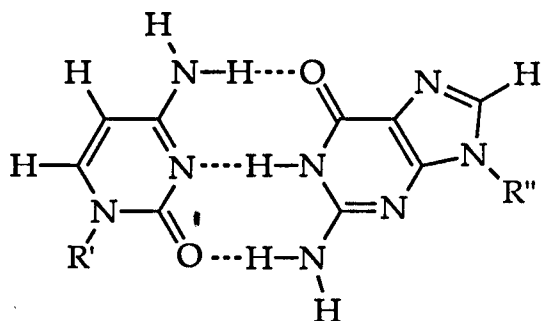


Figure 2.11 The secondary interactions in triply-hydrogen-bonded systems. + represents the partial positive charge δ^+ on hydrogens and - represents the partial negative charge δ^- on electronegative atoms hydrogen-bonded with hydrogens.

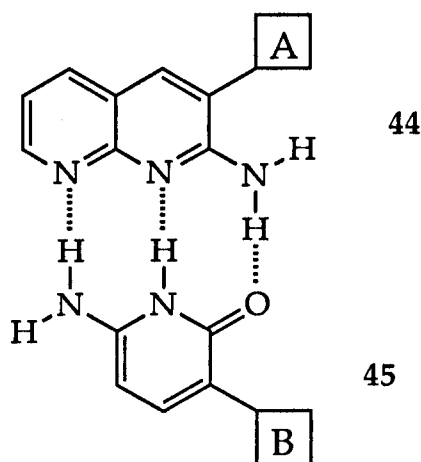
The four repulsive secondary interactions in (4) offset the strength of the hydrogen bonding to give this pattern a low binding energy as indicated by a low association constant (K_a about 10^2 M^{-1}), which is in the range for the doubly-hydrogen-bonded system. Although type (3) may have the biggest association constant, its poorer specificity is a disadvantage as discussed above. Experimental results show that type (5) gives an association constant of more than 10^4 M^{-1} in chloroform, which is far higher than for doubly-hydrogen-bonded pairs and the additional good specificity means that type (5) should be a good choice for a replicating system.

The derivatives of guanine and cytosine have been studied since the 1950's, but their unreactive purine ring and pyrimidine ring make it difficult to introduce non-polar groups to make them soluble in non-polar solvents. The reaction sites may be attached at position 3 in the cytosine ring and position 9 in the guanine ring, but spacers are needed to link the

reactants to the binding sites which may lead to loss of rigidity of the template.



The simpler analogue of this binding pattern provided by 2-amino-1,8-naphthyridine and 2-amino-pyrid-2-one ²¹ seems to be better. This binding pair has a similar binding constant ($1.7 \times 10^4 \text{ M}^{-1}$) to the guanine cytosine pair and it is easier to introduce non-polar groups into both the pyridone ring and the naphthyridine ring. In addition it may not be necessary to use a spacer to link the reactants A and B to the binding sites as shown in 44 and 45.



2.4 The Reactants

Many kinds of bimolecular reactions that have been shown to be catalysed by the proximity effect could be used as a basis for reactants A and B in a molecular replicating system as shown in Figure 2.4. The original coupling reaction in DNA replication is the esterification of an OH group on one nucleotide by the phosphate group on another nucleotide. In living systems the reaction is catalysed by the polymerase enzyme helped by a DNA template, but it has already been shown that this reaction can also be catalysed by an oligonucleotide template in an artificial replication system. In both the living systems and the artificial system, the phosphate needs to be activated. *In vivo*, phosphates are activated as their triphosphates and *in vitro*, some activating agents (coupling agents) are used *in situ* to help the formation of the phosphate ester (Figure 2.12). Carbodiimides⁸ such as dicyclohexylcarbodiimide (DCC) are commonly

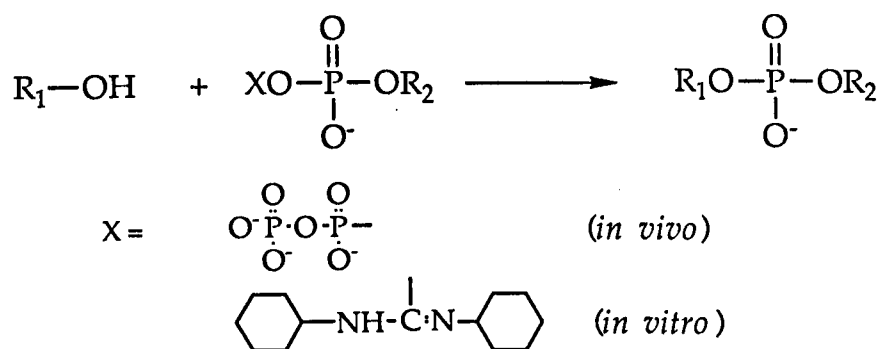


Figure 2.12 The esterification of phosphate in nucleotides was used in the first molecular replication system.

used as coupling agents in nucleic acid research but this kind of coupling agent can cause numerous side reactions. One major side reaction is that the activated phosphate group can be attacked by another phosphate group to form a pyrophosphate⁸ (Figure 2.13). This by-product makes it difficult

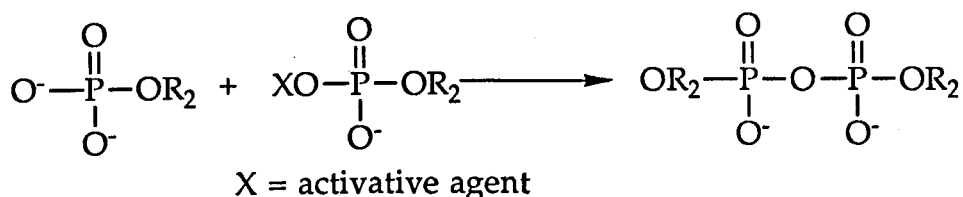


Figure 2.13 A side reaction of esterification of phosphate in nucleotide

to estimate the real reaction rate. To minimize by-product formation, other coupling agents may be used such as aromatic sulfonyl chlorides but HCl released during the reaction may cause other side reactions for acid sensitive functional groups. This problem may be solved by replacing the chlorine with imidazole or tetrazole leaving groups so that no acid is generated during the coupling reaction. Another method is to use an amino group instead of hydroxy group to form an amide with phosphate, since the amino group is more nucleophilic than the hydroxyl group. Amidation will dominate over pyrophosphate formation. There are two examples ^{9,10} that show that the amidation product is the only product formed during the replication reaction (Figure 2.14). Another disadvantage of using the nucleotide coupling reaction is the polar solvent that must be used for the reaction. The polar solvent will weaken the binding strength between the template and the substrates so that the catalytic effect will be reduced.

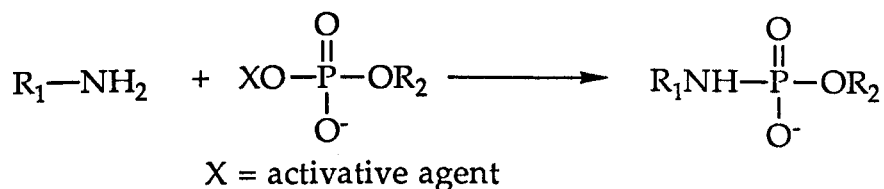


Figure 2.14 Amidation of phosphate in nucleotide catalyzed by simple template

The amidation of a carboxyl group by an amino group is another important reaction in living systems (Figure 2.15). In living cells, amino acids are lined up with the aid of their carrier, t-RNA, on the template mRNA and the amidation reactions are catalysed by the enzyme peptide synthase. A simple molecular replication system²² has already shown that amidation may be catalysed *in vitro* and many intramolecular reactions of this type (lactam formation)^{35a} have also shown big rate enhancements as compared with analogous intermolecular reactions.

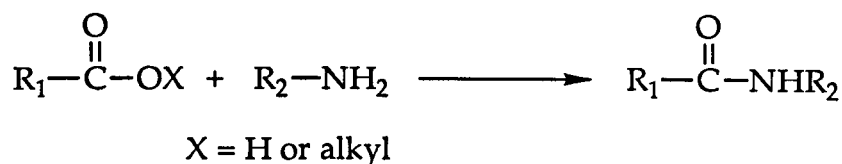


Figure 2.15 Amidation of carboxylic acid catalysed by both enzymes and simple template.

Another two reactions, analogous to amidation, which are catalysed by enzymes in living system are esterification and thioesterification of carboxylic acids (Figure 2.16). The main esterification reaction in living systems is the attachment of amino acids to t-RNAs by an ester linkage

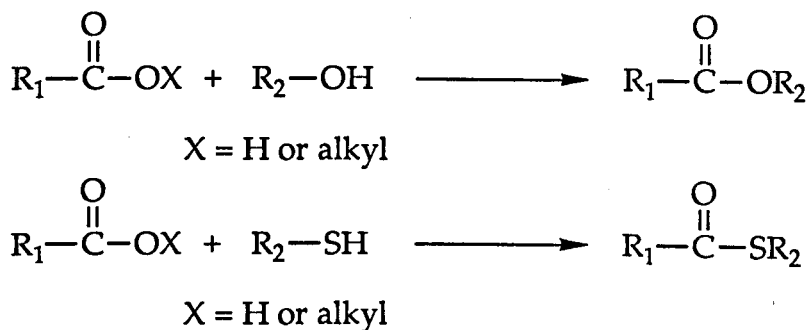


Figure 2.16 Esterification and thiol esterification catalysed by an enzyme and an artificial mimic.

so that they can be transported to the ribosome to produce proteins. The reaction of each amino acid with t-RNA is catalysed by the appropriate synthase. Thiol ester formation in living systems, which mainly involves carboxylic acids and the thiol group of coenzyme A, is also catalysed by synthases. Artificial catalysis of these two types of reaction has already been reported by using macrocyclic compounds as enzyme mimics to catalyse the acyl transfer reactions.^{20d,e,36} Some intramolecular reactions can be accelerated by a simple template and the lactonization in Figure 2.17 is an example of rate enhancement in an intramolecular reaction as compared with an intermolecular reaction.^{35c}

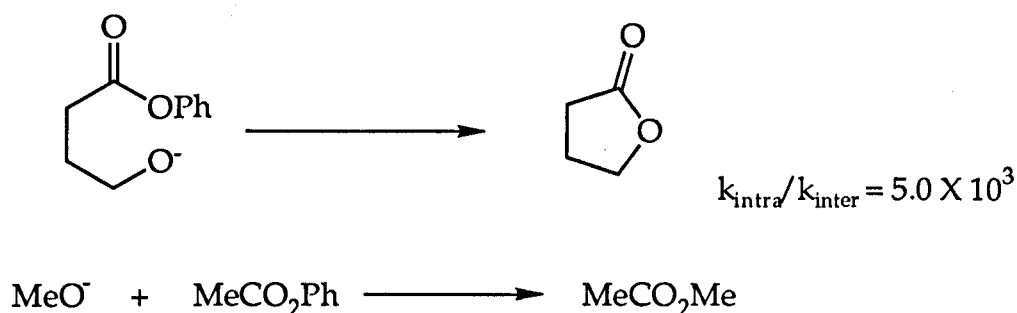


Figure 2.17 An example of rate enhancement in an intramolecular esterification

Anil formation between an aldehyde and an amine is the first abiotic reaction which has been used in a simple replicating system²³ and many other reactions which do not exist in living systems but show rate enhancement in intramolecular reactions could also be used in replication systems. These include nucleophilic substitution and anhydride formation, examples are listed in Figure 2.18.^{35c} However, in all these reactions no stereochemical relationships are involved and they are not going to enrich information storage and transfer if they are employed in an artificial replication system. There is another important but difficult point which should be considered in choosing a reaction for an efficient

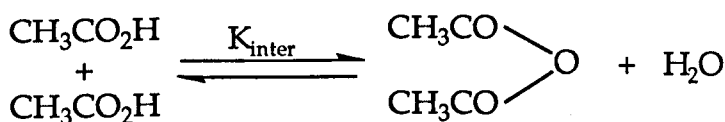
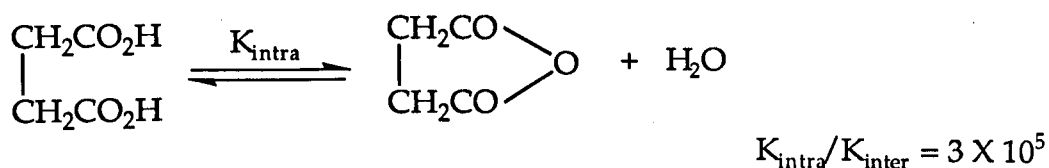
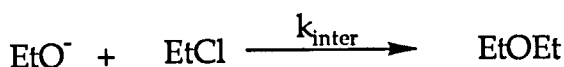
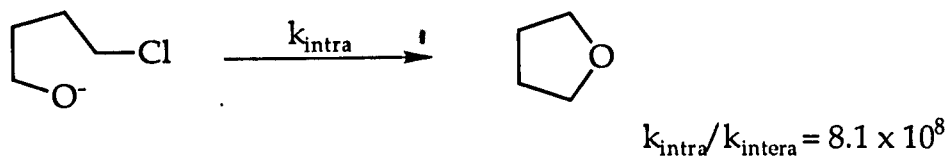
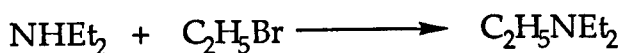
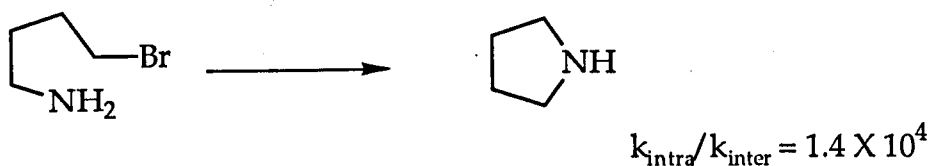


Figure 2.18 Some reactions which show rate enhancement in their intramolecular reactions could be used for a molecular replicating system.

replicating system, this is the transition state of the reaction. As has been discussed in section 2.1, the greatest rate enhancement for an enzymatic reaction would be achieved when the enzyme helps the formation of the transition state, or in other words, the enzyme lowers the energy of the transition state. A simple template only brings reactants close together in a head to head fashion but for all of the reactions mentioned above, transition state formation does not involve simple head-to-head approach of the reactants.

Carbon-carbon bond formation is an important reaction which is of great interest to chemists although there are relatively few reaction types

used for C-C bond formation in living systems. Some intramolecular carbon-carbon bond formation reactions have shown rate enhancement^{35c} (Figure 2.19) but the strongly basic reaction conditions which are required would destroy the binding site of the template if this kind of reaction were employed in a molecular replicating system.

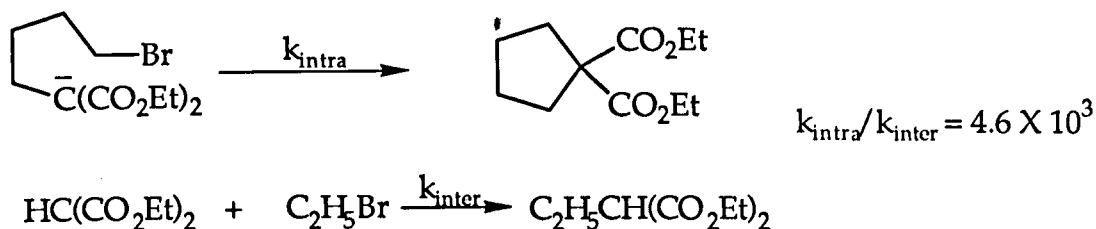


Figure 2.19 Intramolecular carbon-carbon bond formation in basic conditions is not a good candidate for use in a replicating system.

However, the Diels-Alder reaction, which is a widely used for carbon-carbon bond formation in synthesis, can be carried out under very mild conditions. The Diels-Alder reaction involves cyclo-addition of a 1,3-conjugated diene and an alkene (called the dienophile). The reaction has several features which make it a very good candidate for use in a molecular replicating system:

i) According to the principles of orbital symmetry, the Diels-Alder reaction is a $[4\pi_s + 2\pi_s]$ reaction which is symmetry allowed and goes through a thermal pathway because it involves 4 π electrons from the diene and 2 π electrons from the dienophile. Many Diels-Alder reactions go very fast without any activating agent or catalyst and the reaction has been widely used in organic synthesis including many intramolecular examples.³⁷

ii) The transition state of the Diels-Alder reaction has been intensively studied. All available data from theoretical and experimental

studies are consistent with describing the reaction as a concerted process and the reaction is a syn (suprafacial) addition with respect to both the alkene and the diene (Figure 2.20).

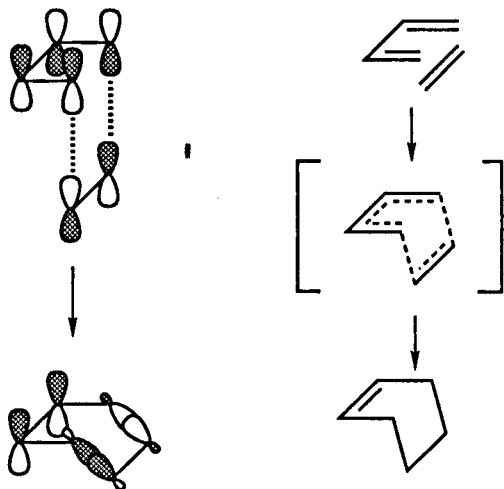


Figure 2.20 Syn-suprafacial addition of Diels-Alder reaction

The concerted nature of the reaction means that there will be no intermediates generated during the reaction and that the transition state is relatively well defined. Many intramolecular Diels-Alder reactions have demonstrated that the Diels-Alder reaction can be facilitated by proximity if the molecular structure helps to form the transition state for concerted syn addition, as shown in Figure 2.20. If the diene and alkene are brought into proximity by the template with the correct head to head relationship, it will help the formation of the transition state of the reaction although the precise position of diene and alkene in the transition state is face to face.

iii) Stereochemical information will be involved if an asymmetrically substituted diene or dienophile is used in the reaction. For example, a reaction with both asymmetric diene and dienophile gives eight possible stereoisomers (Figure 2.21).

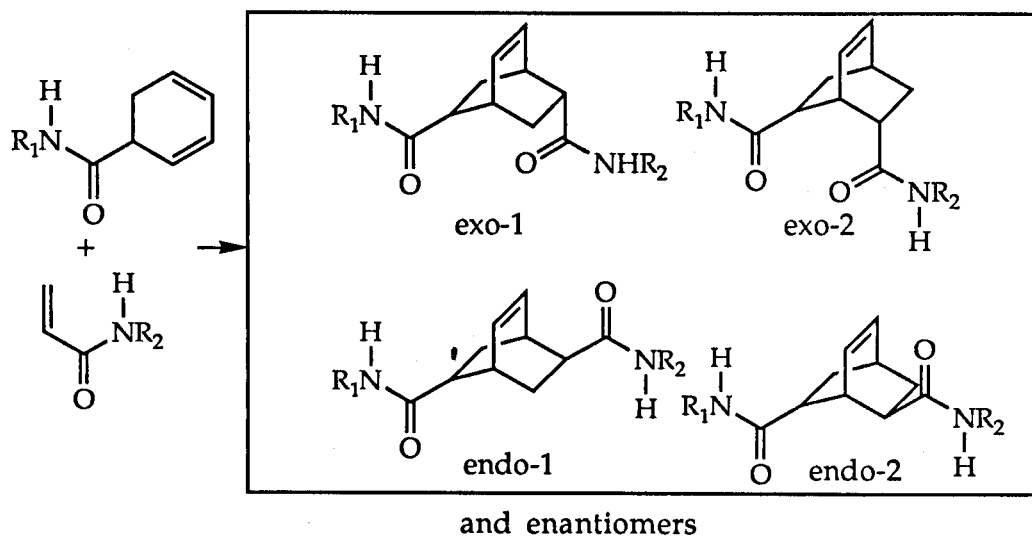


Figure 2.21 Possible stereoisomers formed in a Diels-Alder reactions with both asymmetric ene and diene.

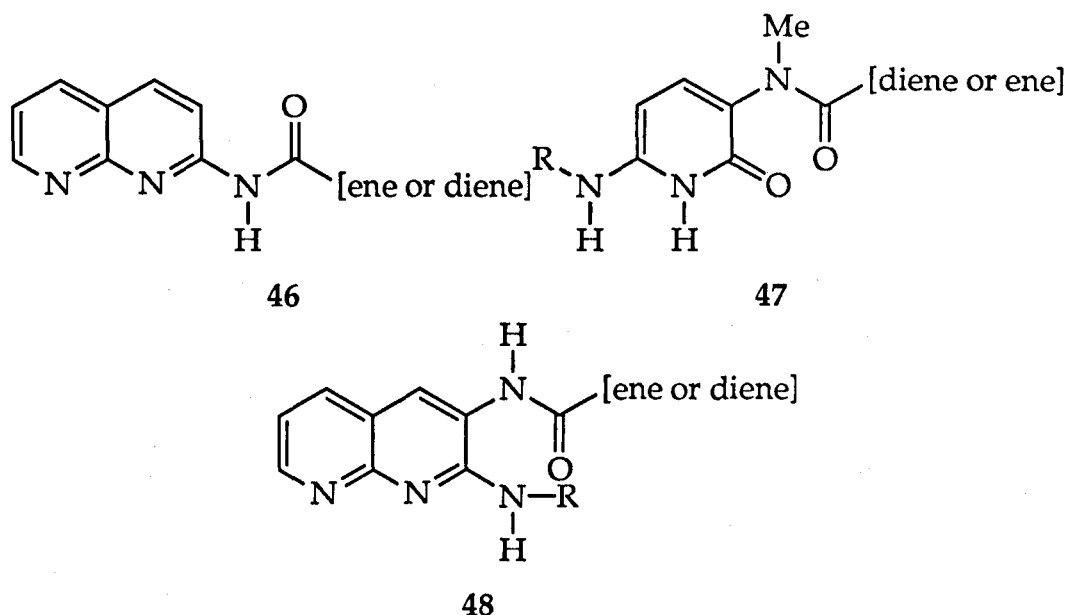
Studies of the Diels-Alder reaction have shown that the reaction is often highly stereo-selective, so if a Diels-Alder reaction provides the template of a replication system, each stereoisomeric product can potentially act as a template for its own formation but may also act as a template for the formation of its enantiomer and other isomers. This potentially greatly enriches the information storage for a simple molecular template. It is therefore of interest to study how the stereochemistry of the template influences the stereochemistry of the newly formed product from the substrates during the replication process.

iv) The reaction can proceed in non-polar solvents, such as chloroform, suitable for a hydrogen bonding interaction between template and reactant binding sites.

v) The reacting diene and ene groups can easily be attached to the components of the binding sites 44 and 45 chosen in section 2.3 through a simple linkage, such as an amide connection. All these features suggest

that attachment of a diene and an ene group to the complementary binding components would give a product template through a Diels-Alder reaction which could become an efficient, information rich, simple, cleanly reacting, and easily examined molecular replication system.

Compounds 46 and 47 are molecules designed initially for a replication reaction and compound 48 is an alternative for the compound 46. The R groups are aliphatic groups which make the compounds more soluble. However, in comparison with compound 48, compound 46 has some advantage. Firstly, synthetic routes to compound 46 are simpler; secondly, there is possible disturbance of the hydrogen bonding between the template and substrates by a carbonyl group on position 3 in 48 which is eliminated in compound 46. Moreover, as has been discussed, the



transition state of the Diels-Alder reaction involves suprafacial addition and placing the reacting groups as indicated in 46 and 47 appears to be particularly suitable for generating this suprafacial relationship between the ene and diene systems of bound reactants as shown in Figure 2.22.

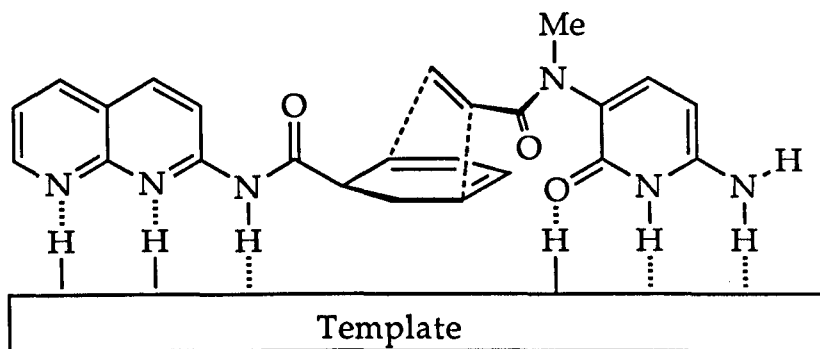


Figure 2.22 The transition state of templated Diels-Alder reaction.

In line with the above discussion, a full molecular replication system which potentially possesses autocatalytic and information transfer characteristics has been designed and the replication process based upon this system is shown in Figure 2.23. Template 51 is made from its precursors 49 and 50 by a Diels-Alder reaction between them. This template 51 then binds unreacted compounds 49 and 50 to form a complex 52, in which the Diels-Alder reaction between the substrates is catalysed by proximity and new template is formed within the complex 52 to give product dimer 53. This dimer 53 then dissociate into two free templates 51 to continue replicating the reaction in the next cycle.

Shortly after this project had started, J. Sander's group in Cambridge reported an example of using an artificial template to accelerate an intermolecular Diels-Alder reaction.^{33a} In their experiment, a trimeric porphyrin host was used as a template to hold ene and diene reactants which are attached to two pyridine molecules by pyridine/metal coordination. One molar equivalent of template enhanced the initial reaction rate 200-fold at 60 °C as compared with the reaction without template. The shift in the equilibrium position in the presence of template corresponds to an increase in the effective bimolecular equilibrium

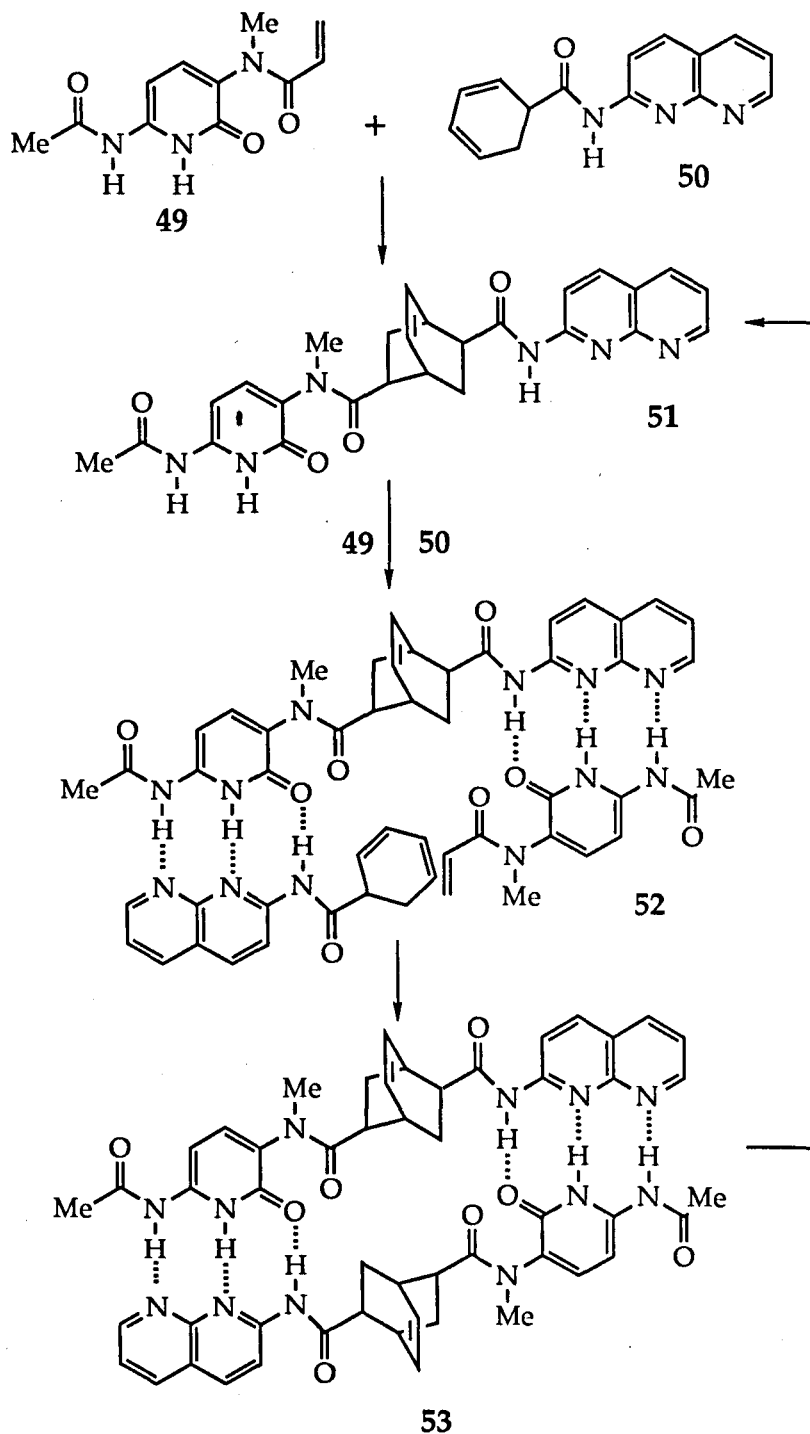


Figure 2.23 The replication process of a designed molecular replicating system based on a Diels-Alder reaction.

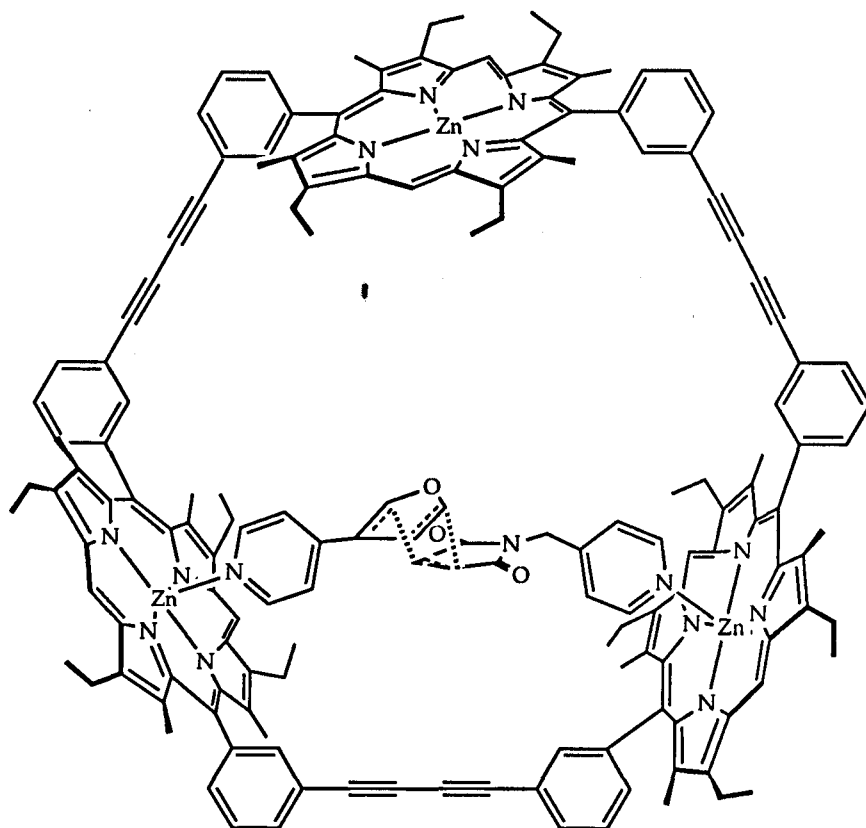


Figure 2.24 The Diels-Alder reaction catalysed by an artificial template based on a cyclic porphyrin trimer.

constant for the reaction between reactants from $\sim 300 \text{ M}^{-1}$ for the uncatalysed reaction to $\sim 6000 \text{ M}^{-1}$. The explanation for the exclusive *exo*-adduct, instead of usual *endo*-adduct is that the template binds the reactants in a way that only favours the *exo*-transition state, which is shown in Figure 2.24.

This example shows clearly that the Diels-Alder reaction can be catalysed by proximity. It also shows that templating the transition state of a reaction plays a key role in catalysis by proximity.

CHAPTER THREE

SYNTHESIS

3.1 Pyridone Compound

As discussed in chapter 2, in order to maximize the binding energy of the template, firstly the replication reaction should be carried out in non-polar organic solvent, secondly the reaction temperature should be kept lower than the boiling point of the solvent used such as dichloromethane or chloroform. These two criteria mean that all compounds must be soluble in non-polar solvents and reactants must be sufficiently reactive for the reaction to be followed at low temperature. The synthetic work started with the pyridone derivative which is one of the components of the template of the designed replicating system (compound 49 in Figure 2.24 Chapter 2). It is obvious that the precursor of this compound is 6-acylamido-3-amino-pyrid-2-one 54, which could be prepared by reduction of 6-acylamino-3-nitro-pyrid-2-one 56. The nitro compound may be made from 6-aminopyrid-2-one. It has long been known that 2-pyridone is the tautomer of 2-pyridol or 2-hydroxypyridine, so synthesis of 6-amino-pyrid-2-one is equivalent to the synthesis of 2-amino-6-hydroxypyridine 55. Figure 3.1 shows the synthetic route to this component.

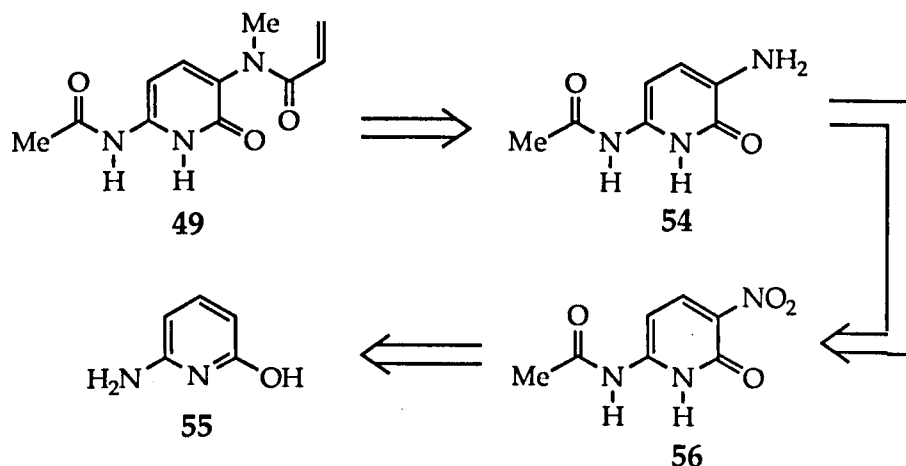


Figure 3.1

Although there are many methods for making aminopyridones, the methods to make 6-amino-2-pyridol and 6-amino-3-nitro-2-pyridol are limited. Generally there are four methods for making this kind of compound. (a) Nucleophilic substitution on the pyridine ring; (b) hydrolysis of aminopyridine derivatives; (c) rearrangement of pyridine N-oxides; (d) cyclisation of acyclic compounds. There are many examples of reducing nitropyridine to aminopyridine derivatives, but it is rare to use reducing methods for making 2- or 6- aminopyridines because it is difficult to make the 2- or 6-nitrocompounds. The first report of 6-amino-2-pyridol was in 1923, in which the strong base sodium amide was used to substitute the hydrogen at the 6-position of a 2-pyridol.³⁸ This is the so called Chichibabin reaction (Figure 3.2). Because of the biological activity of some aminopyridone derivatives, the synthesis was explored by many groups

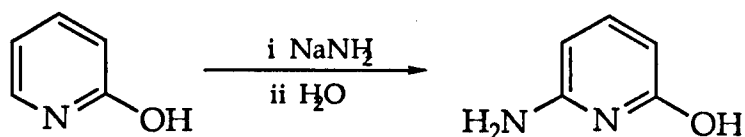


Figure 3.2 Chichbabin reaction to make aminopyridone

in Europe through the 1930's to 1950's. Den Hertog's group in Holland tried to use halopyridine derivatives as starting material to carry out the substitution reactions.³⁹ Obviously, halide anions are better leaving groups than the hydride anion, so the yields are higher than in the Chichbabin reaction. If there is another electron-withdrawing group, such as a nitro group, on the pyridine ring, the reaction can be carried out at lower temperature and higher yields obtained (Figure 3.3). The alkoxy products of these reactions can easily be converted into pyridones by treating them with acid.

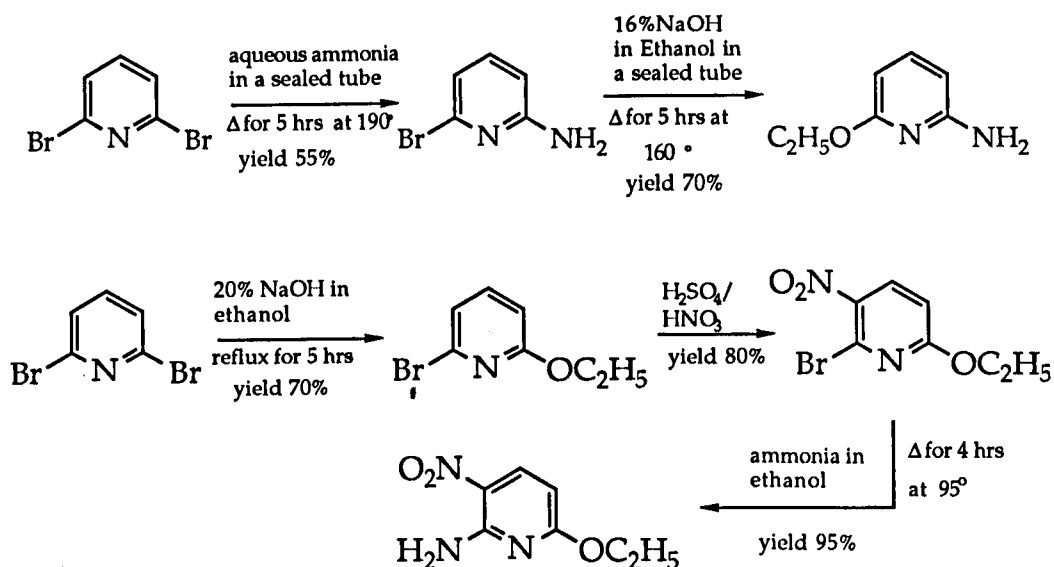


Figure 3.3 Examples of using nucleophilic reaction to make amino alkoxy compound which can be easily converted to hydroxy compound

At the same time, the technique of hydrolysis of 2,6-diaminopyridine to make 6-amino-2-pyridinol had been developed by two other groups.⁴⁰ The conditions for this type of reaction are much milder than for nucleophilic reactions with fewer reaction steps and simpler work up (Figure 3.4). This method can be used for large scale synthesis. The

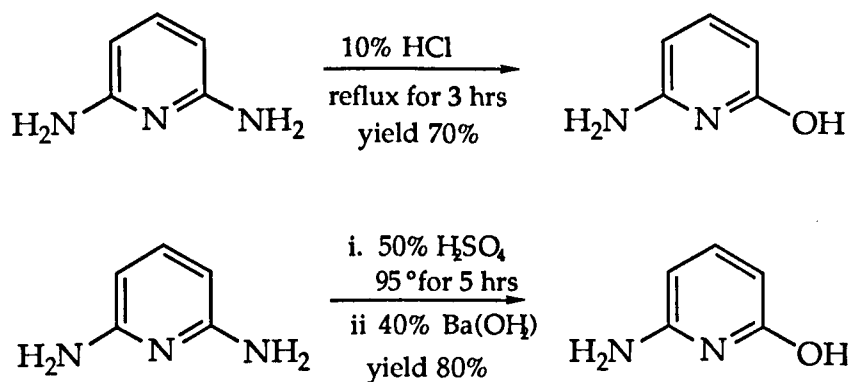


Figure 3.4 Hydrolysis reaction of diaminopyridine to make 2-amino-6-hydroxypyridine

mechanism is believed to involve acid catalysed nucleophilic displacement of the amino group by water as outlined in (Figure 3.5).^{40b}

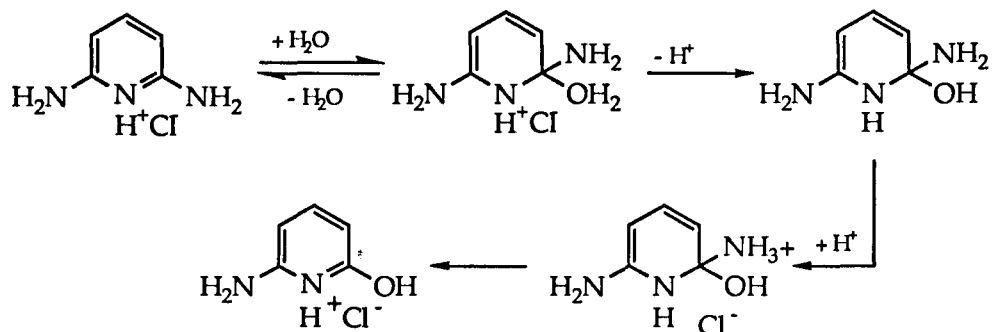


Figure 3.5 The mechanism of hydrolysis of diaminopyridine

The rearrangement of pyridine -N- oxide derivatives was not investigated until 1951, when a Japanese group reported that pyridine -N-oxide rearranged on heating with acetic anhydride to form 2-acetoxypyridine.^{41,21} This reaction was then used for other substituted pyridines and it was found that in most cases the acetoxy group rearranges

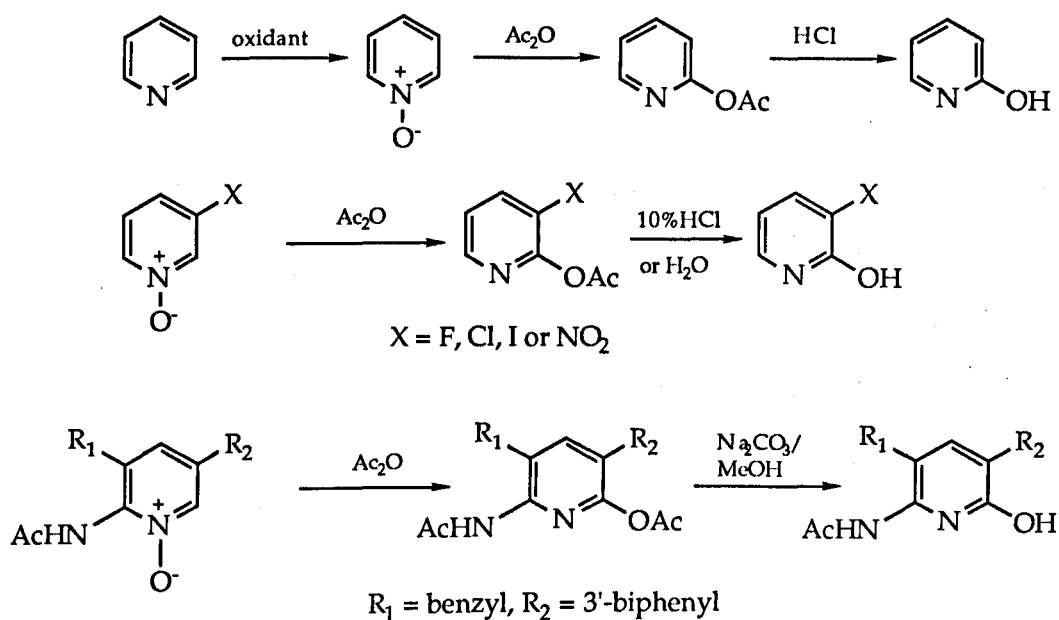


Figure 3.6 The rearrangement of pyridine-N-oxides to make hydroxy pyridines

to the 2-position when there is a deactivating group on the 3-position (Figure 3.6). One 6-acetoamido-pyrid-2-one derivative has been made by this method recently^{21b} (the third reaction in Figure 3.6). The advantage of this method is that the positions of all functional groups on the pyridine ring are defined but the overall yield is moderate, particularly for the reaction of rearrangement, the yield is only 20-40%. The mechanism for the rearrangement has also been explored but the exact pathway is still uncertain.⁴² It is believed that there is an intermediate or at least a transition state involving an ion pair (B in Figure 3.7) rather than the free cation (C in Figure 3.7). However the key argument is whether the reaction is through an intramolecular rearrangement or an intermolecular reaction.

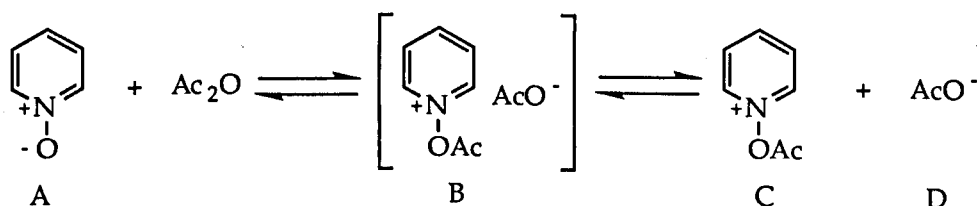


Figure 3.7 Possible mechanism of rearrangement of 1-N-Oxide pyridine

The ring closure of acyclic compounds has been used to make all kinds of pyridine derivatives, including amino pyridones.⁴³ Most methods for making 6-amino-2-pyridol or its ethers involve using reaction of malonic acid derivatives, such as cyanoacetoamide or malononitrile, with carbonyl compounds. Generally, strong base is needed for catalysis of the reaction. In most malononitrile cases, the reactions have a similar pathway, in which an intermediate 1,1,3,3-tetracyanopropene anion is involved. This intermediate can be either pre-prepared or generated *in situ*. A couple of examples are given in Figure 3.8. However, reactions of this type produce multiple substituted

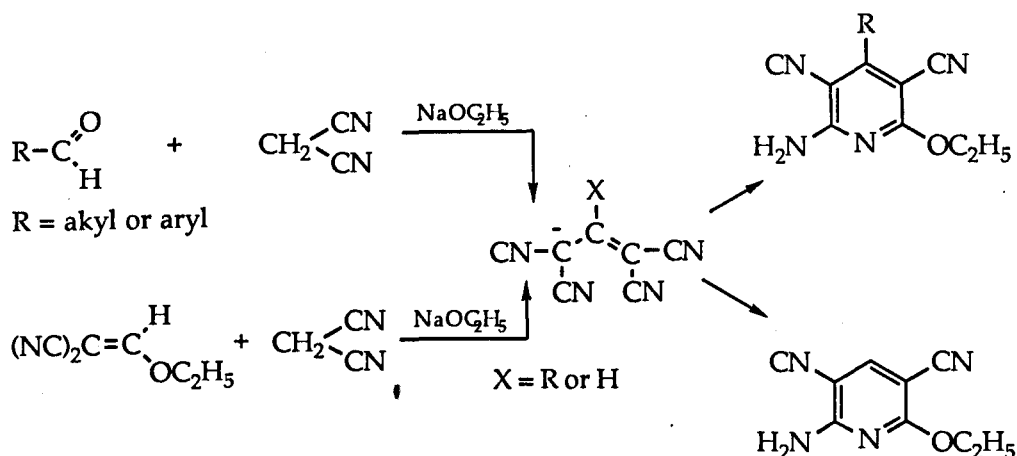


Figure 3.8 Ring-closure reaction to make aminopyridone derivatives

cyano-aminopyridones on which there is no room for introducing a 3-nitro group on the pyridone ring. These cyano groups may also cause complications during replication reactions and decyanation of this type of compound has also been reported (Figure 3.9).⁴⁴ The reaction started from cyanoacetoamide instead of malononitrile to give an aminopyridone with only one cyano group on the 3-position which could be removed with HBr to give 6-amino-5phenyl-2-pyridol which is a potential candidate for one component for the designed replicating system.

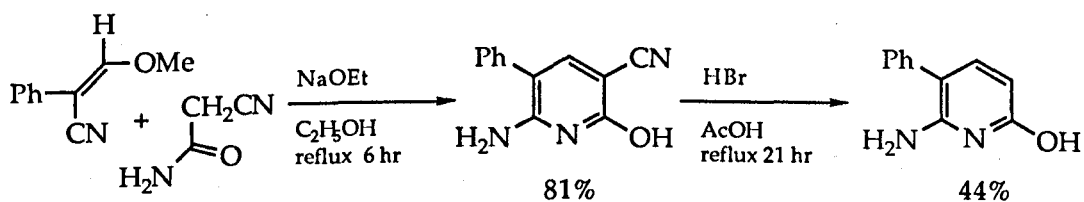


Figure 3.9 An useful ring-closure reaction to make aminopyridone derivatives

After reviewing all of the methods discussed above, the synthetic experiments began with nucleophilic substitution because the starting material, 2,6-dibromopyridine **57** was at hand (Figure.3.10). The first substitution step by sodium methoxide proceeded in high yield.³⁹ In order

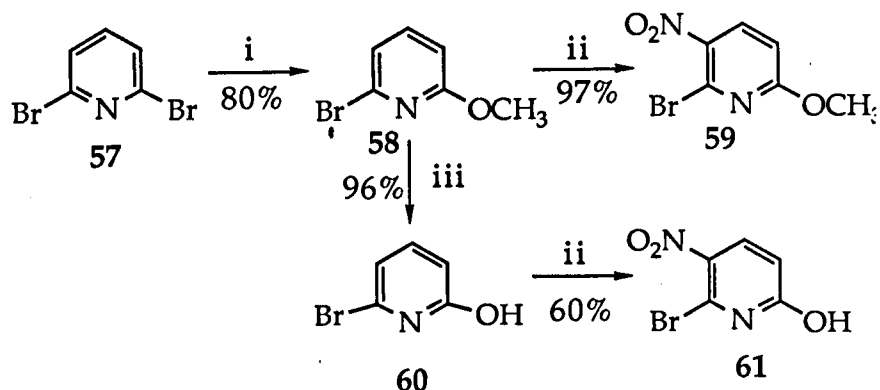


Figure 3.10 i. MeONa/MeOH , reflux; ii. conc. HNO_3 /conc. H_2SO_4 , 0° ;
iii. HBr/AcOH , reflux.

to make the second nucleophilic reaction easier, nitration was carried out as the second step.⁴⁵ Unfortunately, the nitro group was introduced at the 5-position, adjacent to the bromo group rather than to the methoxy group **59**. This result was not surprising since similar results have been reported (see Figure 3.3, second reaction). Knowing that unlike their ether derivatives, many free pyridones were nitrated at the 3-position, the demethylation was carried out by treating 6-bromo-2-methoxypyridine with HBr in acetic acid to give 6-bromo-2-pyridinol **60**.⁴⁶ Surprisingly, the nitration still occurred at the 5-position so blocking position 5 is obviously required. The nitration was done again after the 5-position had been brominated. The spectrum of the product demonstrated that it was the required 3-nitroderivative, but the yield was very low (10%) and the product was very insoluble. An attempt to do the amination first on the

2,6-dibromopyridine by the Chichibabin reaction failed and this approach seems to be unsuitable for the synthesis of 6-amino-3-nitro-2-pyridol 56.

The method involving hydrolysis of 2,6-diaminopyridine was tried with success ^{40b} soon after the substitution method was abandoned. 6-Amino-2-pyridol 55 was obtained by basification after hydrolysis of the starting material 62 with 50% H₂SO₄. The nitration product 64 and the acetamidonitropyridone 65 were also obtained by two successive reactions (See Figure 3.11). However, the same question arose again. Where is the

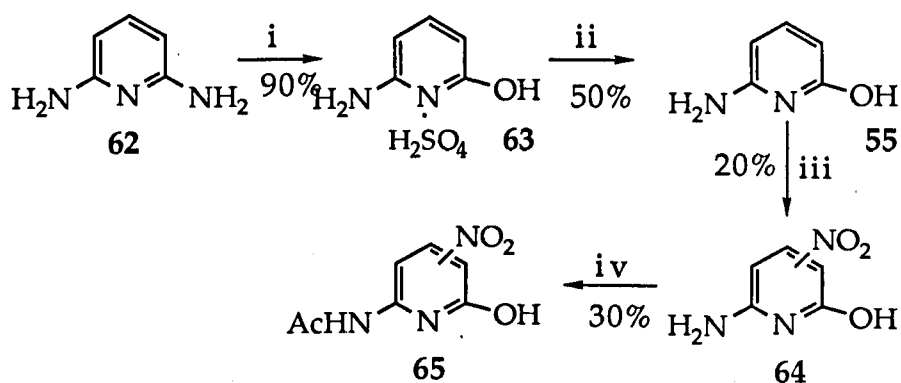


Figure 3.11 i. 50% H₂SO₄ aqueous solution, 95°C, 5 hrs; ii. 40% Ba(OH)₂, 70°C, 2 hrs;
 iii conc. HNO₃/conc. H₂SO₄, 0°C; iv. Ac₂O, 100°C, 2 hrs.

nitro group, adjacent to the amino group or the hydroxy group? To answer this question, the rearrangement of a suitable pyridine N-oxide compound was examined because this would lead to defined positions of all substituents on the pyridine ring. The experiment was started from 2-aminopyridine 66 ^{21b} (Figure 3.12). In the first step nitration occurs at the 5-position ⁴⁵ para to the amino group, this is a well known reaction. After acetylation, the product 68 was treated with peracetic acid to produce the N-oxide 69. The rearranged compound 70, 2-acetoxy-6-acetylamino-3-nitropyridine, was obtained by heating compound 69 with acetic anhydride.

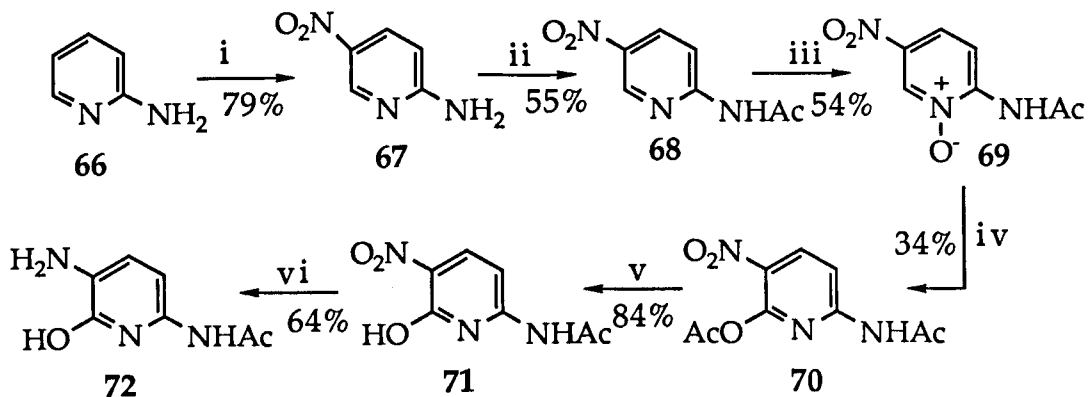


Figure 3.12 i. conc. HNO_3 /conc. H_2SO_4 , $0\text{ }^\circ\text{C}$; ii. $(\text{CH}_3\text{CO})_2\text{O}$, $100\text{ }^\circ\text{C}$;
 iii. $\text{CH}_3\text{COOOH}/\text{CH}_3\text{COOH}$, $80\text{ }^\circ\text{C}$; iv. $(\text{CH}_3\text{CO})_2\text{O}$, $140\text{ }^\circ\text{C}$; v. H_2O ,
 boiling; vi. $\text{H}_2/\text{PtO}_2/\text{MeOH}$, room temperature.

Hydrolysis of the 2 - acetoxy substituent gave the expected product, 6-acetylamino-3-nitro-2-pyridol **71**. This is the first 3-nitro derivative of 6-amino-2-pyridol. The NMR spectrum of compound **71** was compared with the NMR spectrum of compound **65**. The difference in chemical shift of protons on the pyridine ring is 0.33 ppm for the 4 position of both compound and 0.15 ppm for the 3 position and the 5 position respectively (position 5 in **71** and position 3 in **65**). These data show that compound **71** and **65** are different and the nitro group in compound **65** must be at position 3. This is also matches a result reported in the literature sixty years ago ⁴⁷ which was found after this stage of the work had been completed. Knowing the position of the nitro group in compound **71**, the reduction of the nitro group was examined. The first reaction using hydrazine as the reductive agent and palladium on carbon as the catalyst,⁴⁸ failed, since under these conditions the acyl group was removed by the strongly nucleophilic hydrazine. The second attempt using hydrogenation with a platinum oxide catalyst ⁴⁹ was successful and the 3-amino compound **72** was obtained. However the insolubility of both the nitro and amino compounds (**71** and **72**) was very discouraging since as has been

mentioned at the beginning of this chapter, the solubility of replication components in non-polar organic solvent is very important.

Back to 2-amino-5-nitropyridine (67 in Figure 3.12), hexanoylation was carried out using hexanoic anhydride in order to increase the solubility of the target 2-pyridone. After the oxidation reaction, the rearrangement reaction was tried using acetic anhydride but after heating the solution at 140 °C, the reaction gave only a product identical to compound 70 (Figure 3.13). Stirring a solution of hexanoylamidopyridine N-oxide in acetic anhydride at room temperature showed that the hexanoyl group was substituted by an acetyl group with no rearrangement. An attempt using hexanoic anhydride as the rearrangement reagent was not successful.

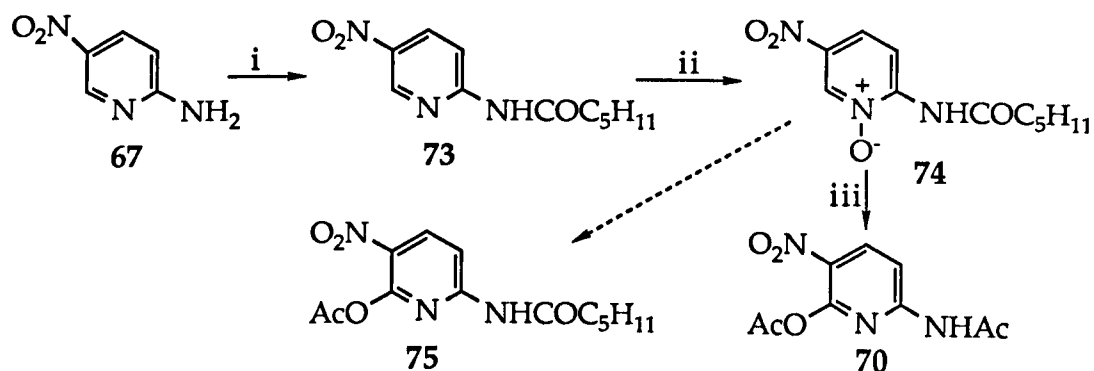


Figure 3.13 i. $(C_5H_{11}CO)_2O$, 100 °C; ii. CH_3COOOH/CH_3COOH , 80 °C;
iii. $(CH_3CO)_2O$, 140 °C.

Considering that although the amino group in 6-amino-2-pyridone (compound 55) activates the ortho position more than para position, the acylamino group may deactivate the ortho position more than the para position, the reactions shown in Figure 3.14 were undertaken.

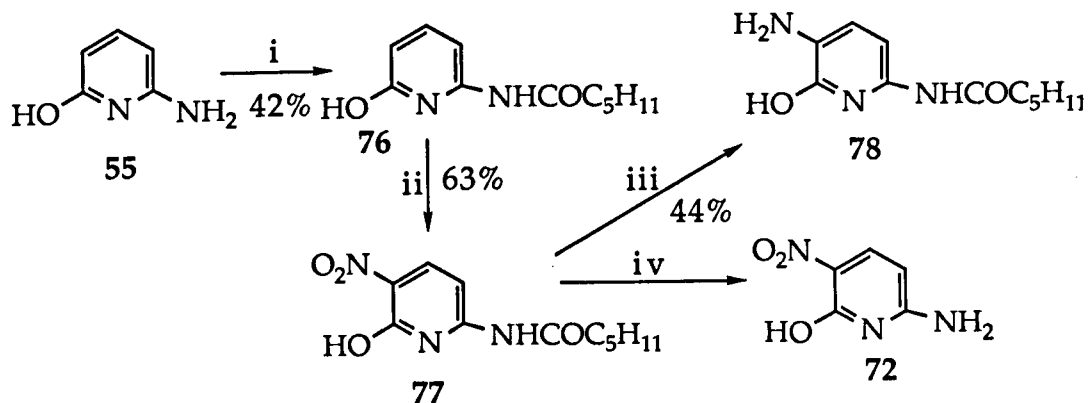


Figure 3.14 i. $(C_5H_{11}CO)_2O$, $120\text{ }^\circ C$; ii. conc. $HNO_3/AcOH$, cold water bath;
 iii. H_2 , $PtO_2/MeOH$, r.t.; iv. $NH_2NH_2 \cdot H_2O/MeOH$.

The conditions of the reactions are the same as those described before except for the nitration reaction in which acetic acid was used instead of concentrated sulphuric acid to avoid hydrolysis of the hexanamido group. Compound 77 was obtained in good yield. Comparing the proton NMR spectrum of 77 with that of compound 71, the absorptions in the aromatic region are nearly identical (for compound 77, the chemical shifts of the NMR absorption in the aromatic region are δ 8.55, doublet and δ 6.44, doublet; for compound 71, they are δ 8.55, doublet and δ 6.45, doublet). This implies that the position of the nitro group in these two compounds is the same and the nitro group is ortho to the hydroxyl group. To confirm this result, the hexanoyl group on compound 77 was removed under basic condition to give a nitro derivative of 6-amino-2-pyridol (compound 72). A sample of this compound was mixed with compound 64 (See Figure 3.11) and the 1H NMR of this mixture examined. The spectrum showed that they were different compounds since there are two pairs of doublet peaks in the aromatic region (Figure 3.15).

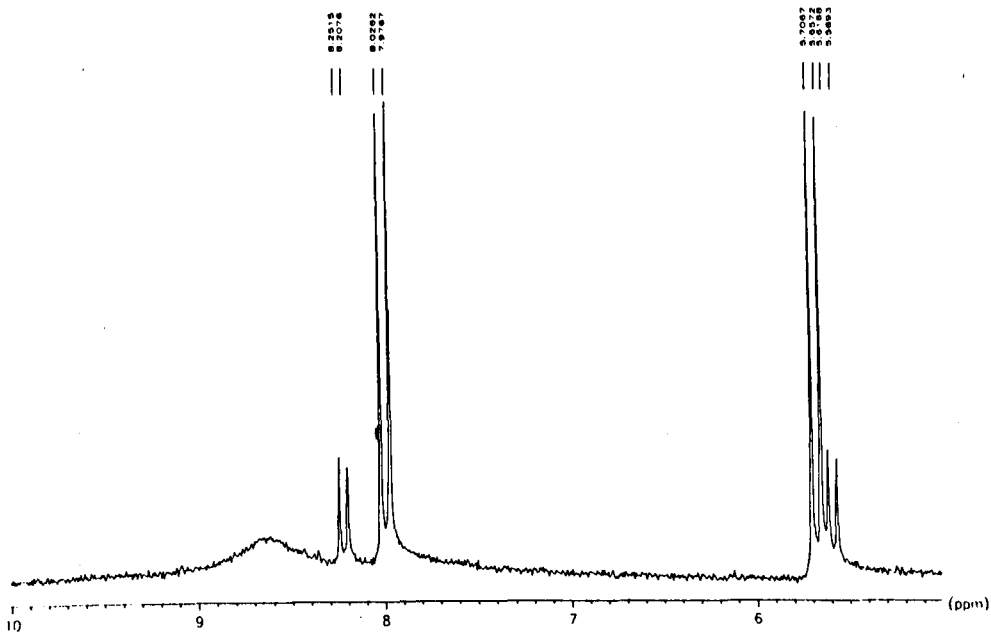


Figure 3.15 The ^1H NMR of mixture of compounds 72 and 64, two higher doublets belong to compound 72 and lower ones belong to 64.

The reduction of the nitro compound to give the 3-amino compound was conducted by hydrogenation with platinum oxide as the catalyst. The reaction was straightforward and the crude product can be used without further purification.

According to the initial synthetic scheme (Figure 3.1), the next reaction should be mono-methylation of the amino group and then synthesis of the acrylic amide. However, since methylation of pyridone derivatives may produce 1-methylated derivatives as by-products this proposed synthesis was likely to be difficult to achieve. Furthermore, an acrylic amide is not a very active dienophile and the slow Diels-Alder reaction of an acrylic amide with a diene may cause difficulty in measuring the rate of the replication process. These considerations led to a change in strategy and a more reactive maleimide derivative of the 3-amino-2-pyridone was adopted as the target ene.

The intermediate maleic amide was readily obtained by adding a THF solution of maleic anhydride to a THF solution of the aminopyridone 78 at room temperature⁵⁰ (Figure 3.16). The reaction was complete in half an hour. The ring closure of compound 79 was done by a conventional procedure using acetic anhydride, the product is the O-acetyl derivative of the required maleimide (compound 80). The last step, the hydrolysis of the acetoxy group of compound 80 was not as straightforward as expected. The imide ring was reopened during the hydrolysis of the acetoxy group under both basic and acidic conditions. Finally, diethylamine was used as the reagent since it would give diethyl acetamide as the cleavage product and no nucleophile would be generated to attack the imide ring. This time the imide ring survived. Compound 81 was obtained as yellow crystals from chloroform, which were soluble in dichloromethane.

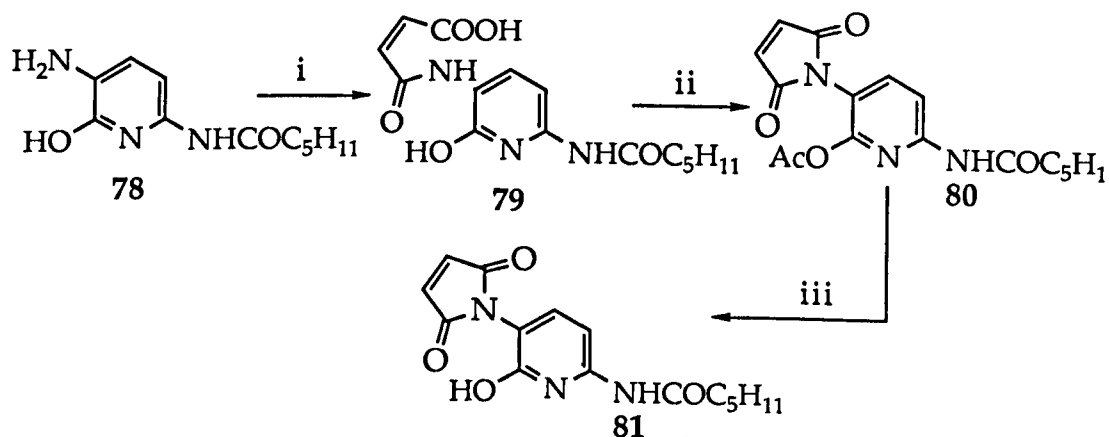


Figure 3.16 i. Maleic anhydride/THF, room temperature; ii. Ac₂O/NaOAc, 100 °C; iii. HN(C₂H₅)₂/dichloromethane, room temperature.

From the above reactions, it can be seen that the nitration was a key reaction. The properties of 6-amino-2-pyridone are somewhat similar to those of aniline or phenol. The hydroxy and amino groups activate the

pyridine ring and make nitration easy but these groups also make the pyridine ring more easily oxidized during the nitration by nitration reagents such as H_2SO_4 and HNO_3 . The amino group makes the situation more complicated. On the one hand, the amino group is an activating substituent which facilitate the electrophilic nitration but on the other hand, the basicity of the amino group make it easily protonated to form an ammonium group which is, a deactivating group. Actually, when 6-amino-2-pyridone was used in nitration directly with $\text{H}_2\text{SO}_4/\text{HNO}_3$, the yield was very low (20%) because of decomposition and dinitration. If mild conditions were used, such as acetic acid with nitric acid, a white precipitate of pyridone nitrate formed immediately.

From the theory of aromatic electrophilic reactions, it is not difficult to predict the orientation of nitration. The hydroxyl and amino groups are all ortho-para directing groups. The nitrogen in the pyridine ring is equivalent to a meta directing group. All three groups are located so that the directive influence of one reinforces that of the other, so that nitration should be either at the 3-position or 5-position. But which position would be preferred? Study of 2-aminopyridine shows that a two step reaction is involved in the nitration process⁵¹ (Figure 3.17). In the first step, a

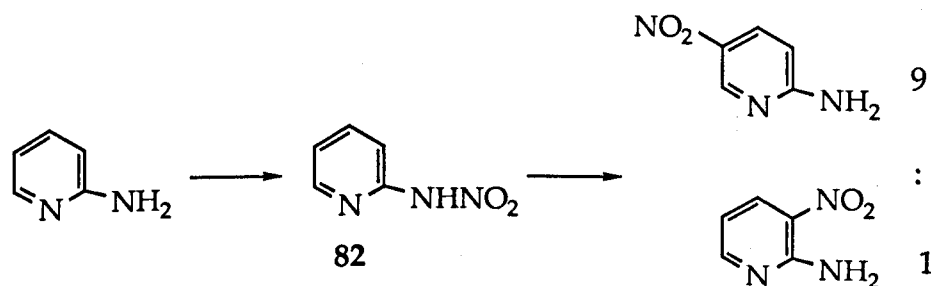


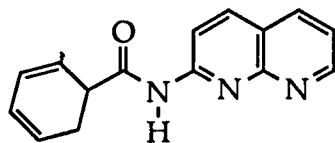
Figure 3.17 Mechanism of nitration of pyridine

nitroaminopyridine 82 is formed at low temperature, but when the reaction temperature is raised to about 30 °C, the nitroaminopyridine rearranges under acid conditions to form 2-amino-5- or 3-nitropyridine in a 9:1 ratio. The mechanism of the reaction is believed to be either intramolecular⁵² or intermolecular rearrangement.⁵³ Most experiments support the intermolecular rearrangement in which a free radical process is involved.⁵⁴ The situation for pyridone derivatives is different. For ether derivatives, that is the alkoxy pyridines, most nitration is at the para-position to the alkoxy group, while for pyridone or hydroxypyridine, most nitration is at the ortho-position.⁵⁵ Although the mechanism of this phenomenon is not clear, it is not likely that a transition state involving hydrogen-bond participation by OH, the so-called chelation effect as has been suggested for ortho-nitration of phenol,⁵⁶ is responsible for the formation of 3-nitro-pyrid-2-one since 2-pyridones are nitrated mainly as the free base and are probably in the pyridone form.⁵⁷ For 6-amino-2-pyridol, the amino group and hydroxyl (or carbonyl group) should reinforce the directive influence of each other and the nitration should be on the position which is para to the amino group and ortho to the hydroxy group. Unfortunately, the nitration product is not as expected when 6-amino-2-pyridone itself was used (Figure 3.11) and nitration took place at the ortho-position to the amino group in compound 64! Obviously, the real situation is more complicated than expected and the mechanism of the reaction needs further study. When the amino group is acylated, the troublesome basic amino group has disappeared and the reaction seems to be simpler and nitration follows the rules which have been discussed above and 6-acylamino-3-nitro-2-pyridol 77 was obtained (Figure 3.13).

3.2 The Naphthyridine Component

The second component of the designed replicating system is a diene linked to a 2-amino-1,8-naphthyridine 50 (see Figure 2.23, chapter 2) The

first



50

approach was based upon cyclohexadiene carboxylic acid or its ester. According to frontier orbital theory, a diene with an electron-withdrawing group will be very inactive so to obtain a reasonably active diene, the double bonds of the diene should not be conjugated with the carboxylic acid group as in 2,4-cyclohexadiene-1-carboxylic acid.

There were some reports of making 2,4-cyclohexadiene-1-carboxylic acid or its ester. An early synthetic experiment was reported in 1948 by a German group.⁵⁸ In their method, 2,4-cyclohexadiene-1-carboxylic acid butyl ester or ethyl ester were made by condensing 1 equivalent of butyl or ethyl acrylate with 2 equivalents of acetylene catalysed by triphenylphosphine nickel bromide $(\text{Ph}_3\text{P})_2\text{NiBr}_2$ (Figure 3.18). Although the starting materials are cheap, the high pressure of acetylene (15 atm) and the high temperature (150 °C) needed in the reaction limit the laboratory use of this method, furthermore the yield of the reaction was not reported.

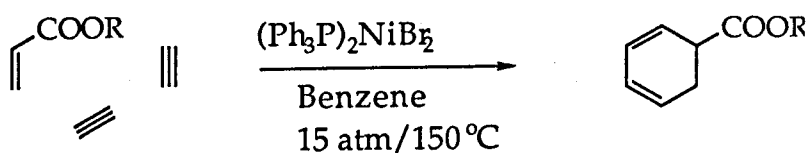


Figure 3.18 High pressure method of making 2,4-cyclohexadiene-1-carboxylic acid

The pyrolysis method was reported much later in 1962.⁵⁹ The acrylate ester was again used as one of the starting materials, it reacted with 1-acetoxy-1,3-butadiene to form 1-cyclohexene-3-acetoxy-4-carboxylate. This compound was pyrolysed at 435 °C to give a mixture of three cyclohexadiene carboxylic acid methyl esters with a 71% total yield which consisted of 2,4-cyclohexadienecarboxylate, 1,3-cyclohexadienecarboxylate and 1,5-cyclohexadienecarboxylate in a 1:6:2 ratio respectively. So the actual yield of 2,4-cyclohexadienecarboxylate is only 7.9% (Figure 3.19).

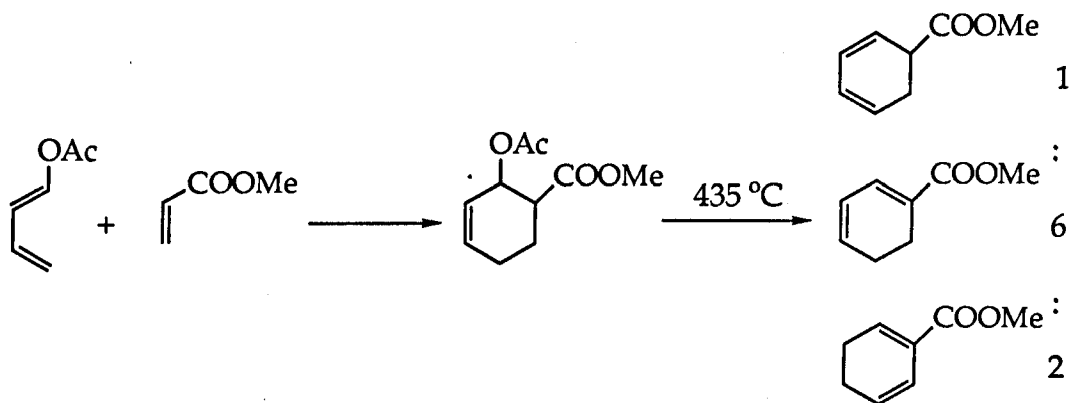


Figure 3.19 Pyrolysis method of making 2,4-cyclohexadiene-1-carboxylic acid

A newer method which was reported in 1979,⁶⁰ uses a palladium catalyst for the elimination of the acetoxy group instead of high temperature pyrolysis (Figure 3.20). The yield of elimination products is

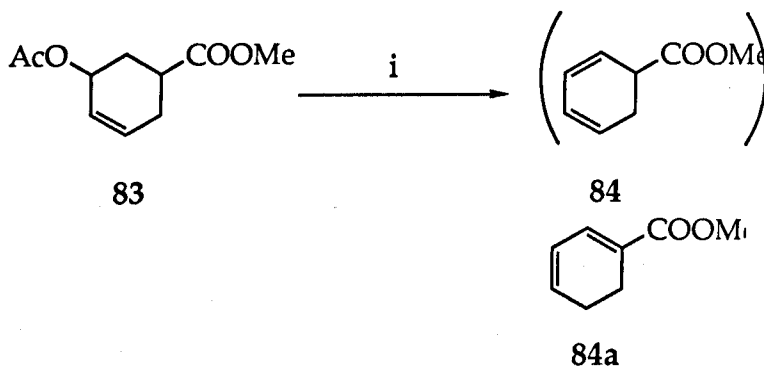


Figure 3.20 i. $(\text{Ph}_3\text{P})_4\text{Pd}/\text{NEt}_3/\text{THF}$, reflux for 8 hours

87% which is quite good. The starting material for elimination, methyl 3-acetoxycyclohex-1-ene-5-carboxylate **83**, can be made from 1-cyclohexene-3-carboxylic acid in four steps (Figure 3.21).⁶¹ The mild conditions and good yields of all these reactions offset the disadvantage of too many reaction steps so this method was chosen to make the diene for the replication system.

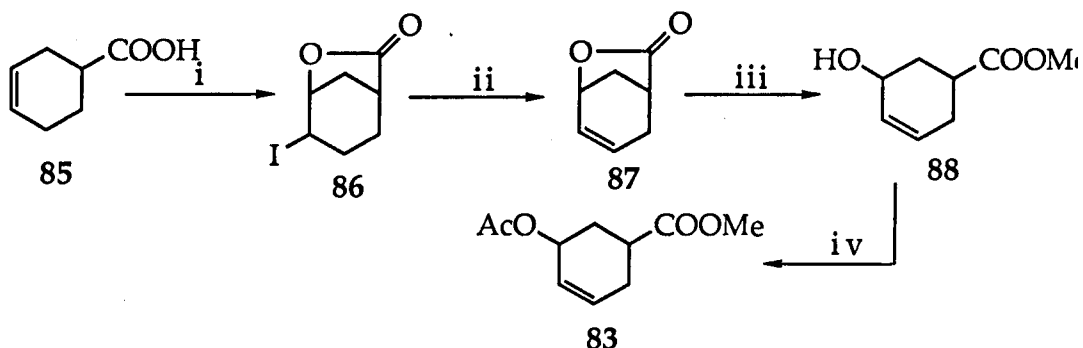


Figure 3.21 i. KI/Na₂CO₃/H₂O, dark, r.t.; ii. DBU/Toluene, 80 °C, 8 hours;
 iii. MeOH/NaOH, r.t.; iv. Ac₂O/N(C₂H₅)₃/4-dimethylaminopyridine.

The first four reactions went smoothly but the yield of the second step was lower than that reported. The result of the final elimination reaction was different from that reported in the literature. When the reported procedure was followed, in which 5% tetrakis-(triphenylphosphine)palladium(0), [(Ph₃P)₄Pd] and one equivalent of triethylamine were used, the product was not 2,4-cyclohexadiene-1-carboxylic acid methyl ester as reported. The ¹³C NMR spectrum of the product showed that it was 1,3-cyclohexadiene-1-carboxylic acid methyl ester **84a** and obviously, a rearrangement had occurred during the reaction (see Figure 3.22). Since triethylamine might induce the rearrangement of double bonds, the reaction was carried out again as before but without the

triethylamine. This time 2,4-cyclohexadiene-1-carboxylic acid methyl ester 84 was obtained with some aromatization which is also in contrast to the literature report.

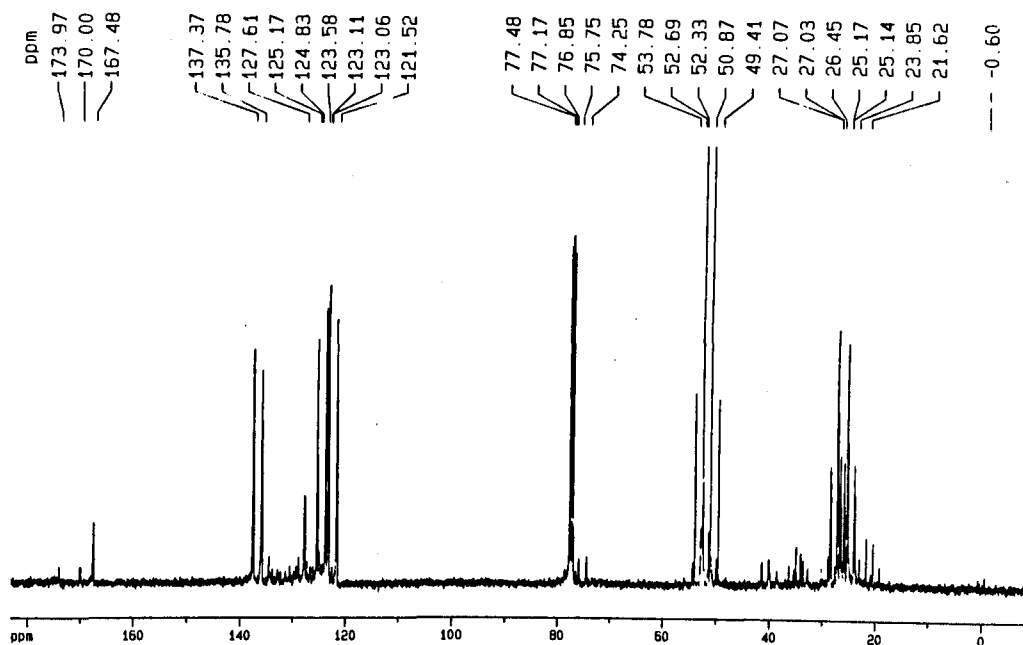


Figure 3.22 Off resonance ^{13}C NMR of compound 84a. It is clearly shown that only 3 doublet peaks with a singlet peak in the olefinic region ($\delta = 120 - 140$ ppm) and two triplet peaks in the saturated carbon region.

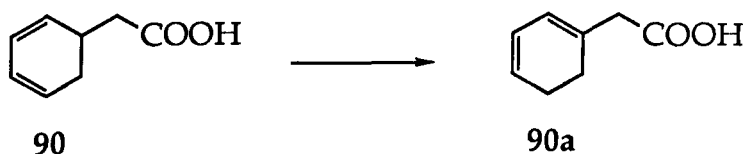
The hydrolysis of the methyl ester of 2,4-cyclohexadiene-1-carboxylic acid 84 under basic condition again showed rearrangement with exclusive

formation of the conjugated acid product, 1,3-cyclohexadiene-1-carboxylic acid 89. Because of the difficulty in obtaining 2,4-cyclohexadiene carboxylic



acid, direct amidation of its ester with 7-amino-2,4-dimethyl-1,8-naphthyridine was investigated, but the experiment failed under mild conditions since the amino group on the naphthyridine ring is very inactive as a nucleophile.

Upon realizing that it would be difficult to avoid the rearrangement of double bonds in 2,4-cyclohexadiene-1-carboxylic acid during either the hydrolysis reaction or subsequent amidation reaction, the homologue, 2,4-cyclohexadiene-1-acetic acid 90 was considered as a replacement. The basic consideration for using 2,4-cyclohexadiene-1-acetic acid is that if the rearrangement of double bonds in this compound is still inevitable, the product of the rearrangement, 1,3-cyclohexadiene-1-acetic acid 90a, will still be reactive enough for the Diels-Alder reaction.



The earliest report of making 2,4-cyclohexadiene-1-acetic acid (impure), was in 1946.⁶² The starting material for the reaction was 3,6-dibromocyclohexene which reacted with $\text{NaCH}(\text{COOEt})_2$, the crude product was hydrolyzed and decarboxylated to obtain 2,4-cyclohexadiene-1-acetic acid (Figure 3.23). Obviously, the first step of the reaction could give

a mixture of mono or di-substituted product and severe reaction conditions can cause rearrangement of double bonds.

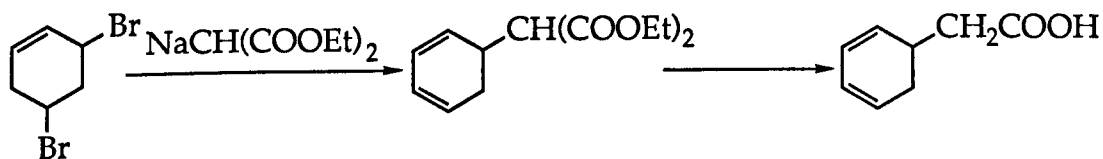


Figure 3.23

A more reliable method for making 2,4-cyclohexadiene-1-acetic acid was reported in 1985.⁶³ In this method a tricarbonyldienyliron cation complex was used as an intermediate (Figure 3.24). The reactions started with complex formation of dihydroanisole with pentacarbonyliron in benzene. The product is a mixture of tricarbonyl-1-methoxy-cyclohexa-1,3-dien-iron and tricarbonyl-2-methoxy-cyclohexa-1,3-dien-iron in a ratio of

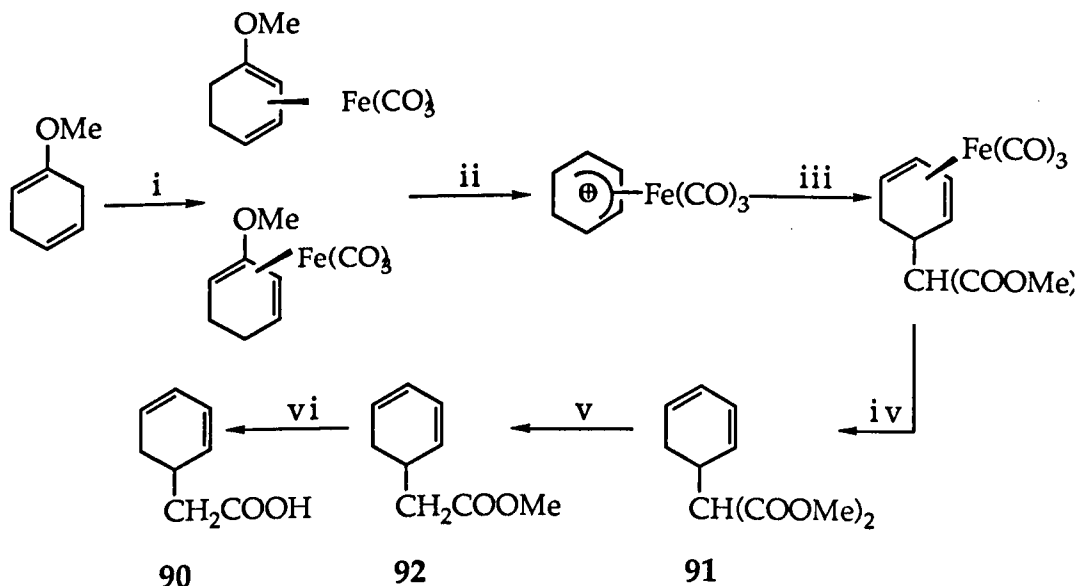


Figure 3.24

i. $\text{Fe}(\text{CO})_5$ /Benzene

iii. $\text{NaCH}(\text{COOMe})_2$ /THF, 0 °C.

v. DMSO/ H_2O / NaCN , 110 °C.

ii. conc. H_2SO_4 / $\text{NH}_4^+\text{PF}_6^-$.

iv. DMF/Trimethylamine oxide, r.t.

vi. MeOH/ KOH , r.t.

2:1. This mixture was used directly for removal of the methoxy group by adding concentrated H_2SO_4 followed by ammonium hexafluorophosphate to form a cation salt. The reaction of this dienyl complex with $\text{NaCH}(\text{CO}_2\text{Me})_2$ occurs virtually instantaneously in THF at $0\text{ }^\circ\text{C}$ to give the required diester derivatives in quantitative yield. This complex was smoothly demetallated by a modification of Shov and Hazum's method,^{63e} in which trimethylamine oxide in *N,N*-dimethylacetamide was used, giving the cyclohexadienyl malonic ester **91** in high yield. This diester was converted to the monoester **92** by sodium cyanide in DMSO. The ester was hydrolyzed to the carboxylic acid **90** by aqueous potassium hydroxide. As expected, the double bonds in the 2,4-cyclohexadiene-1-acetic acid methyl ester **92** were more stable than those in 2,4-cyclohexadiene-1-carboxylic acid methyl ester **84** and the rearrangement did not occur.

A newer method for making 2,4-cyclohexadiene-1-acetic acid **90** was reported by a Swedish group. During their research into stereoselective reaction by organopalladium catalysis, a new method for making 2,4-cyclohexadiene-1-acetic acid was discovered (Figure 3.25). The reaction

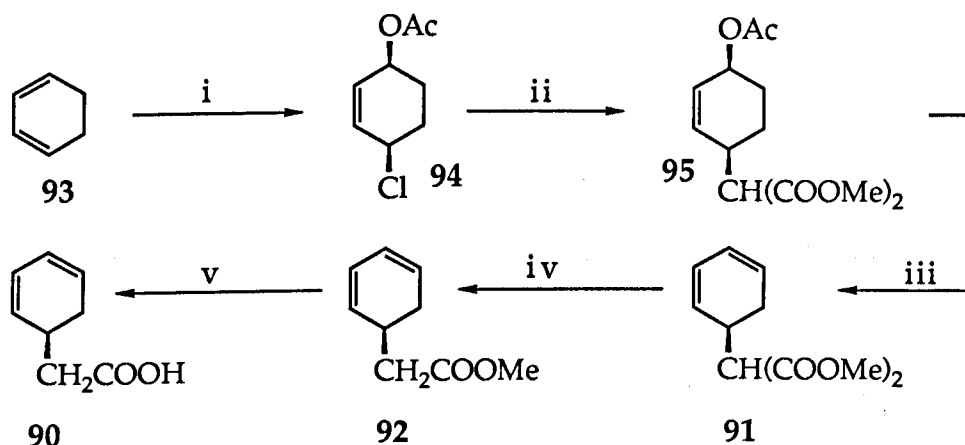


Figure 3.25 i. 2.5% $\text{Pd}(\text{OAc})_2/\text{LiCl-LiOAc}/p\text{-benzoquinone}/\text{HOAc-pentane}$, $25\text{ }^\circ\text{C}$.
 ii. 2% $\text{Pd}(\text{OAc})_2/8\% \text{PPh}_3$, $\text{NaCH}(\text{COOMe})_2/\text{THF}$, $25\text{ }^\circ\text{C}$.
 iii. $\text{Pd}(\text{dba})_2/\text{dppe}/\text{Triisobutylamine}/\text{Toluene}$, Reflux for 2 hr.
 iv. $\text{DMSO}/\text{H}_2\text{O}/\text{NaCN}$, $110\text{ }^\circ\text{C}$. v. MeOH/KOH , r.t.

starts from 1,4-functionalization of conjugated 1,3-cyclohexadiene to form 1-acetoxy-4-chloro-2-cyclohexene using a palladium catalyst, which is then converted into dimethyl (cis-4-acetoxycyclohex-2-en-1-yl)malonate. A palladium catalyst was used again to eliminate the acetoxy group to give dimethyl (2,4-cyclohexadiene-1-yl)malonate. The decarboxylation and hydrolysis of this malonic acid dimethyl ester derivative into the acetic acid derivative is carried out by the same method as those described for the tricarbonyliron-complex method (see Figure 3.24). This method was chosen to make the diene which is needed for the replicating system because it contains fewer reaction steps with a full experimental description for the first two reactions in "Organic Synthesis".^{64e} All reactions went smoothly confirming that the rearrangement did not occur during the last two reactions which were decarboxylation and hydrolysis.

In the synthesis of both 2,4-cyclohexadiene-1-carboxylic acid and 2,4-cyclohexadiene-1-acetic acid, there was a very similar reaction but with two different results, this was the elimination of acetic acid by a palladium catalyst. In the carboxylic acid case, the elimination reaction took place with rearrangement of double bonds under basic conditions, while under neutral conditions, there is no rearrangement. In the acetic acid case, there is no rearrangement even under basic condition. The mechanism for elimination of acetic acid with a palladium catalyst from an allyl acetoxy compound generally involves an intermediate π -allyl complex, but the exact path of the reaction is not clear. Two proposals have been made for the reaction mechanism.⁶⁵ In one proposal (Figure 3.26), the palladium(0) catalyst adds to the double bond to form a complex cation **96**, in an oxidative addition. The acetic anion associates with the cation complex like a salt, then the cation complex undergoes β -elimination to produce a palladium hydride complex **97** which can dissociate to release the diene **84**

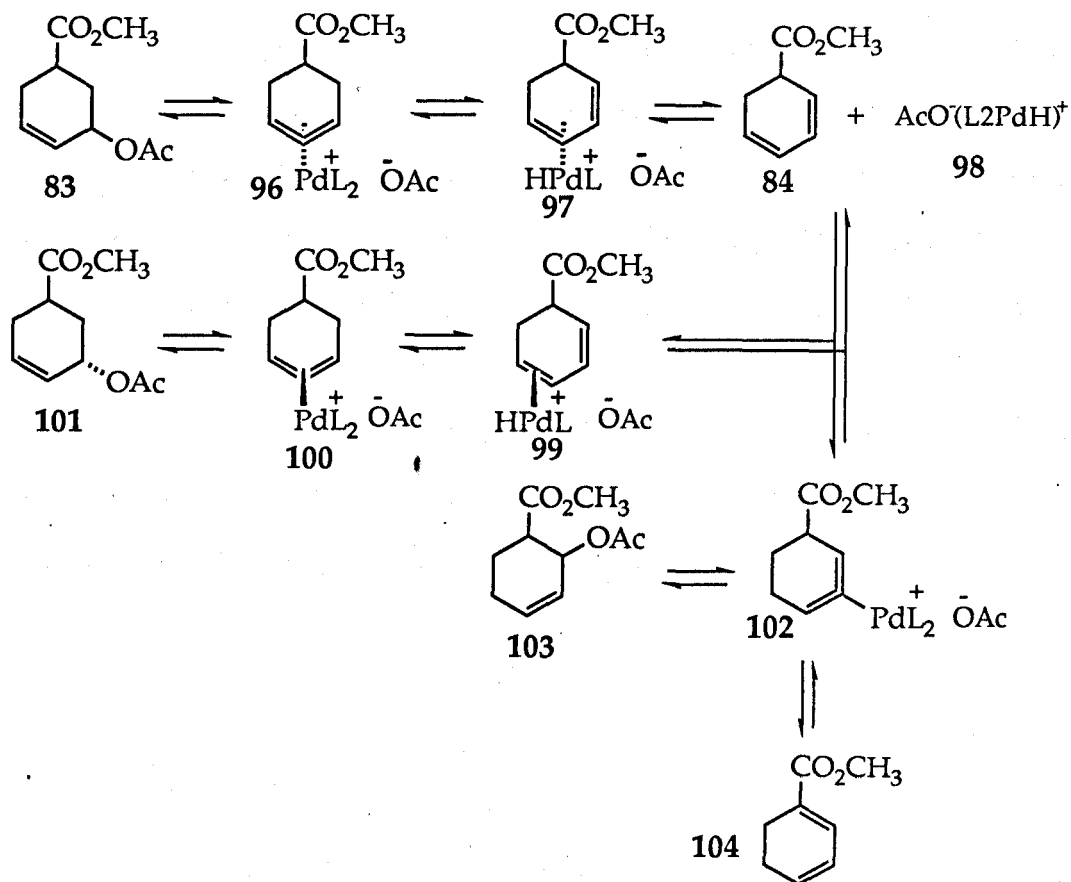


Figure 3.26 A proposed mechanism for the elimination of acetic acid from allyl acetate by a palladium catalyst.

and a palladium complex **98**. This palladium complex could recomplex with diene and since recomplexation could occur on either face of the cyclohexadiene, hydropalladation could thus establish the π -allyl complex as a mixture of stereoisomers **96** and **100**. Nucleophilic attack by acetate would then regenerate an isomeric mixture of allyl acetates **83** and **101**, and this mechanism could explain the isomerisation of allyl acetates. However, if this mechanism were operative, the hydropalladation of the diene would reasonably be expected to produce another regioisomeric complex **102** which could consequently produce the regioisomer of the allyl acetate **103**. Since no products derived from complex **102** were observed, the intermediacy of the diene and the palladium hydride

complex in the acetate isomerization appears unlikely. The elimination of acetic acid to give 2,4-cyclohexadiene-1-carboxylic acid (in neutral conditions) or cyclohexadienylacetic acid seem to support this literature result, because if the free diene and palladium hydride recomplexed, it would produce a mixture of regioisomeric dienes 84 and 104. This was not observed in the synthesis.

Another more likely mechanism for this process is that the acetate anion coordinates with the palladium during the formation of the π -allyl complex 105 or 106 (Figure 3.27). Then, acetic acid could be eliminated by

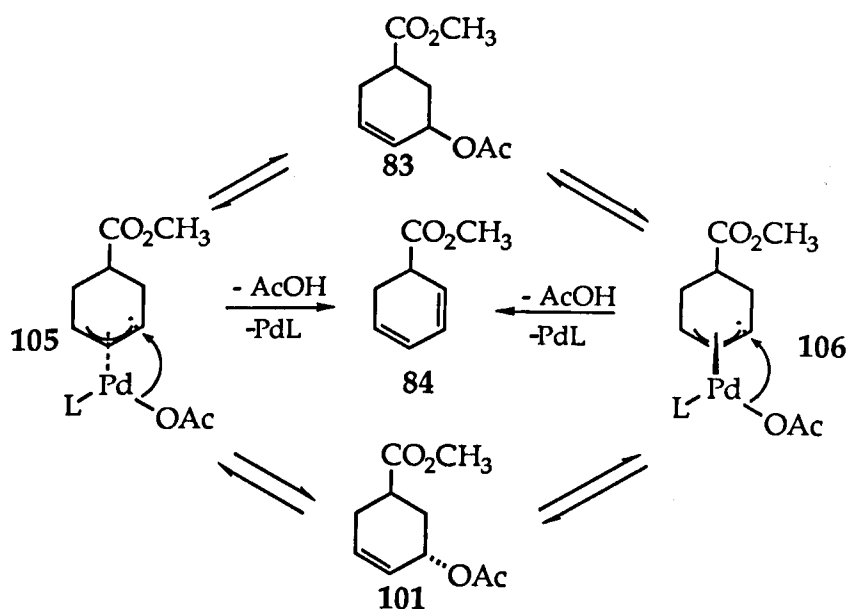


Figure 3.27 A more reasonable mechanism for elimination of acetic acid from acetoxy allyl compound by palladium catalyst.

either a thermal or base-promoted method to produce diene and regenerate the Pd(0) catalyst, which can not form a complex with product diene. The internal delivery of acetate from the same face as palladium could provide a pathway for acetate isomerisation. In this mechanism, the 2,4-diene is the final product and its formation is irreversible. This

matches the result for the elimination of the acetic acid. Other work has also provided some indirect evidence supporting this mechanism. One piece of the evidence is that when there is a competitive ligand, such as carbon monoxide, in the reaction system, the acetate anion would be removed from the inner coordination sphere of the metal and would produce allyl acetate in good yield. A further piece of evidence is that for some nucleophiles, the nucleophile attacks palladium first and is then transferred to the carbon.

The reason for observing the rearrangement of double bonds under basic condition during the elimination of acetic acid from 3-acetoxycyclohex-1-ene-5-carboxylic acid methyl ester **83** is probably due to the acidic proton at the 1-position of the cyclohexadiene. This proton is adjacent to the carboxylic group and at same time is on an allylic position to the double bond, therefore, it is very easily removed to generate a stable delocalised carbanion **107**, which leads to rearrangement (Figure 3.28).

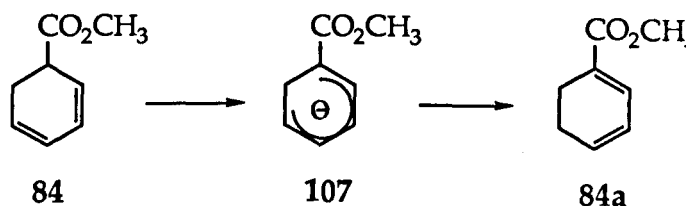


Figure 3.28 A possible mechanism for the rearrangement of **84** to **84a**

In 2,4-cyclohexadiene-1-acetic acid, the proton at the 1-position is not adjacent to the carboxyl group and it therefore less easily removed and the double bonds do not rearrange.

The next task is to make a suitable amino-1,8-naphthyridine to link with the 2,4-cyclohexadiene-1-acetic acid. There is one amino-1,8-

naphthyridine derivative commercially available, 2,4-dimethyl-7-amino-1,8-naphthyridine, but it only dissolves in protonic solvents such as methanol. However its more soluble acylated derivative could be a good candidate for use as one component of the replication system. Some attempts were made to obtain more soluble 2-amino-1,8-naphthyridine derivatives. The general method for making 1,8-naphthyridine derivatives is by fusing 2,6-diaminopyridine with a 1,3-dicarbonyl compound, such as ethyl acetoacetate or acetylacetone and their derivatives. The earliest report of using this method is by O. Seide in 1926.^{66a} 2-Hydroxy-4-methyl-7-amino-1,8-naphthyridine was prepared by heating 2,6-diaminopyridine with ethyl acetoacetate at 150 °C without any other solvent (Figure 3.29). This method was modified later by using an

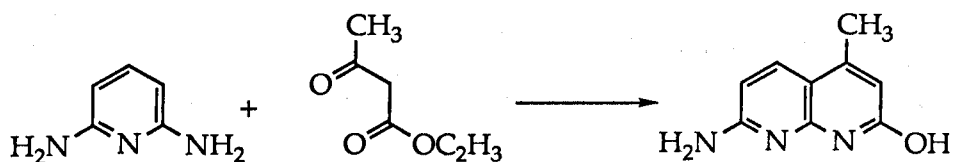


Figure 3.29 Reaction condition: 150 °C.

acidic medium such as phosphoric acid with a lower reaction temperature (around 100 °C).^{66d} The mechanism of the reaction is presumably that the amino group of 2,6-diaminopyridine attacks one of carbonyls of the 1,3-dicarbonyl compounds to form an anil 108. Then the pyridine ring functions as a electron donor and the other carbonyl group in the side chain serves as an electron acceptor, and they react together in the way that is analogous to other electrophilic substitutions into aromatic rings such as the Friedel-Crafts type of reaction. (Figure 3.30)^{66b,c} Actually the

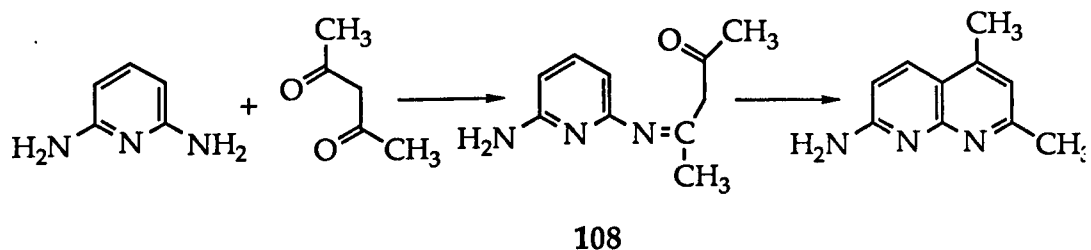


Figure 3.30

intermediate, anil, is isolable and the reaction can be divided into two steps. The reaction can also be carried out in a high boiling solvent such as diphenyl ether.^{66b,c}

Another method, not using 2,6-diaminopyridine as a starting material, has been reported by D. G. Wibberly's group.^{66e} In their method, 2-aminonicotinaldehyde was used as the starting material and was condensed with activated methylene derivatives using base (piperidine) catalysis in ethanol. The 2-aminonicotinaldehyde can be made from ethyl 2-aminonicotinate (Figure 3.31). Many examples of the synthesis of 2,3-

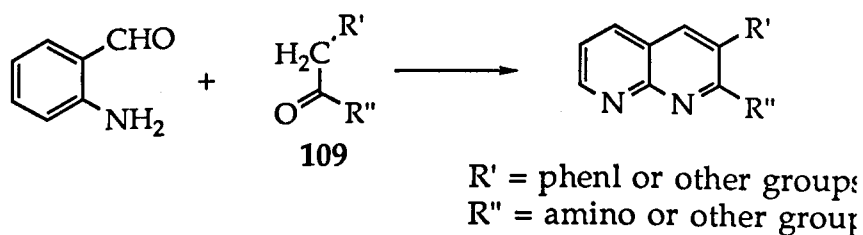


Figure 3.31

substituted 1,8-naphthyridine derivatives by this method have been reported in the literature. However, the method is not suitable for making alkyl or phenyl 2-amino-1,8-naphthyridine derivatives, because alkyl or phenyl groups deactivate the methylene group in compound 109. The only example of this type of compound given in the literature is 2-amino-3-phenyl-1,8-naphthyridine which needed a reaction time of 5 days. The many reaction steps needed for making 2-aminonicotinaldehyde also make this method disadvantageous.

Three different 2-amino-1,8-naphthyridines were made by the 2,6-diaminopyridine method (Figure 3.32). Compound 110 was not expected to be more soluble than 2,4-dimethyl-7-amino-1,8-naphthyridine and it was confirmed that this compound is only slightly soluble in chloroform or dichloromethane, although in the literature procedure chloroform was used to extract the product. Compound 111 does not show any improvement of the solubility in organic solvents although there is a benzyl group on the 3-position. Compound 112 is soluble in organic solvents, but the many reaction steps cause a low overall yield, additionally, the large phenyl group on the 2-position is likely to interfere with the hydrogen bonding between template and substrates during the replication process. These disadvantages probably rule out the use of compound 112.

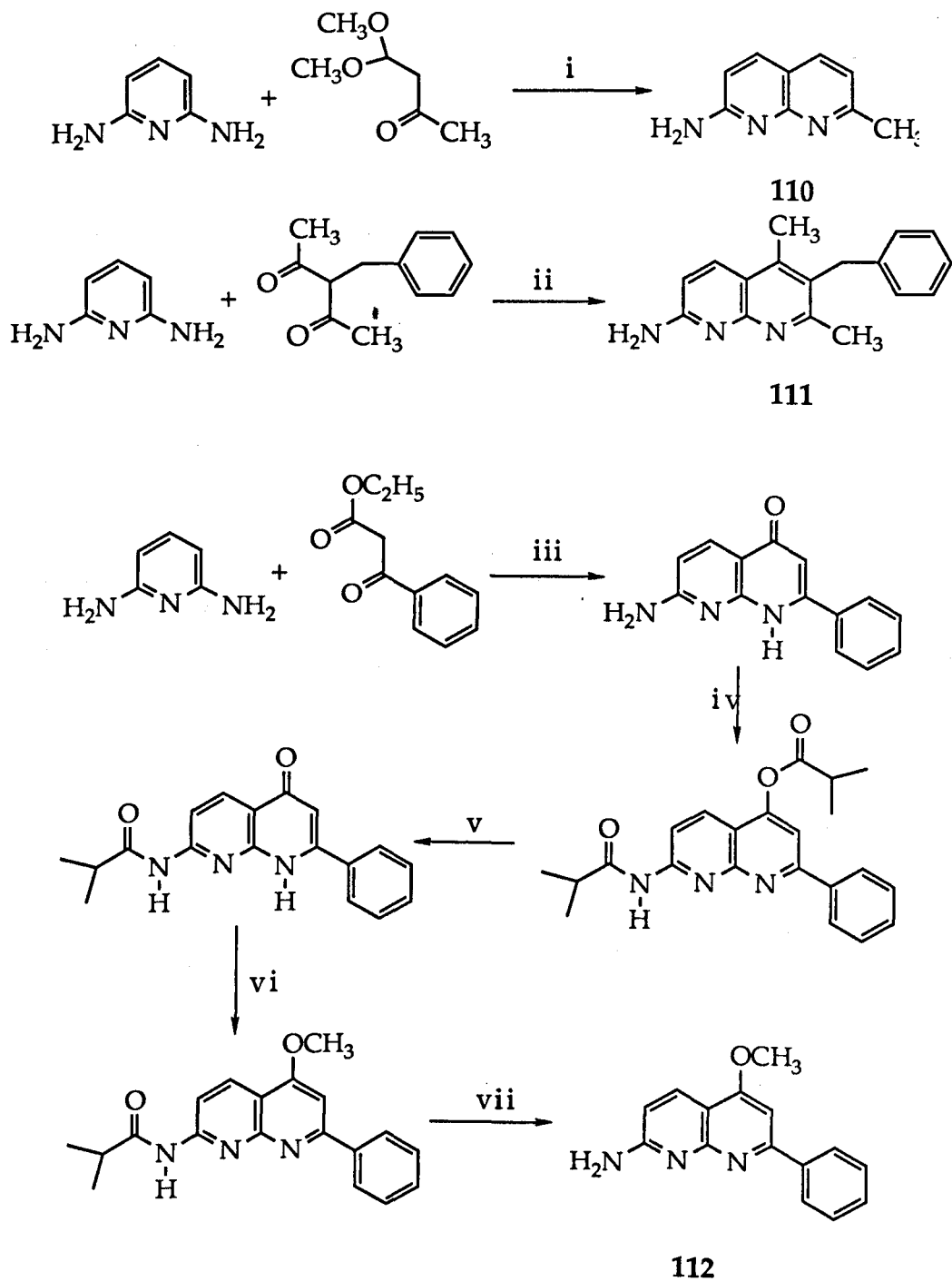


Figure 3.32 i, $\text{H}_3\text{PO}_4/90^\circ\text{C}$, 3 hr. ii, $\text{H}_3\text{PO}_4/90^\circ\text{C}$, 3 hr. iii, PhOPh , 130°C .
 iv, $[(\text{CH}_3)_2\text{CHCO}]_2\text{O}$, 60°C . v, $\text{MeOH}/\text{Na}(\text{CO}_3)_2$, r.t.
 vi, $\text{CH}_3\text{I}/\text{Ag}_2\text{O}/\text{CH}_3\text{COCH}_3$, reflux. vii, $\text{MeOH}/10\%\text{NaOH}$, r.t..21b

The last step of the synthesis, attaching 2,4-cyclohexadiene-1-acetic acid **90** to 2,4-dimethyl-7-amino-1,8-naphthyridiene **113**, was carried out in DMF solution using a mixed anhydride method.⁶⁷ Because of the low activity of the amino group, the reaction required a temperature of 100 °C, but the double bonds remained stable and no rearrangement was observed (Figure 3.33).

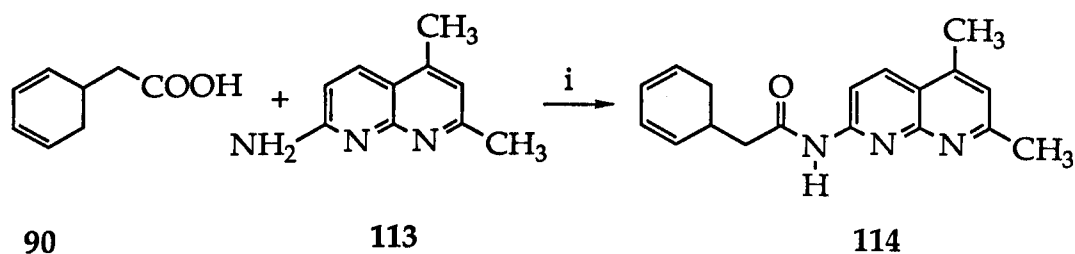


Figure 3.33 i. ClCOOEt/ $N(C_2H_5)_3$ /DMF, 100 °C, 1 hr.

CHAPTER FOUR

RESULTS AND DISCUSSION

4.1 The Kinetic Results from Experiments and Computer Simulations

With the two target compounds 81 and 114 at hand, the Diels-Alder reaction shown in Figure 4.1 was investigated.

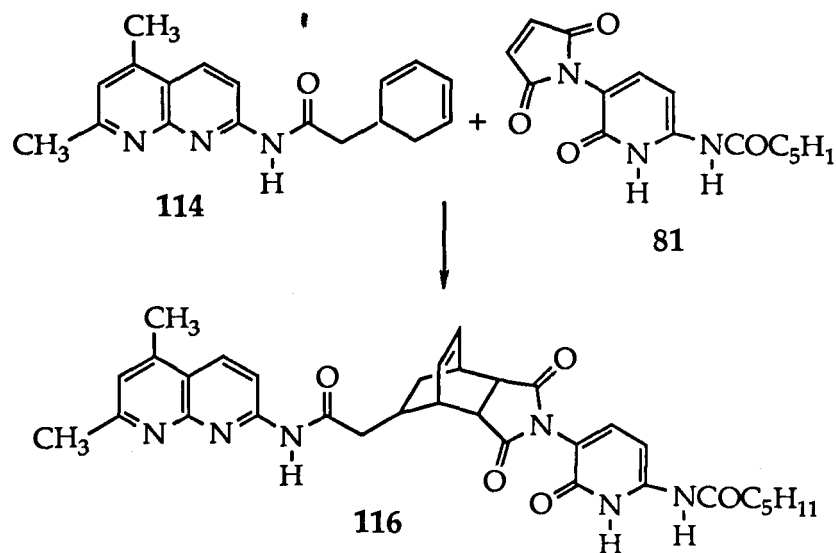


Figure 4.1 Diels-Alder reaction of replicating system

The reactions were carried out in a 5mm NMR tube with d_2 -dichloromethane as solvent. The reactions were followed by ^1H NMR and the change of concentrations of diene, ene and products were calculated according to the integration of ^1H NMR spectra. The aromatic proton signals of the compound were used as references because these integrations did not change throughout the reactions. (raw data of the experiments are listed in Appendix 2 and Appendix 3)

The first experiment was done at 40 °C with 0.015 M concentrations of each reactant and the initial result was very exciting. The spectra of the product showed that the Diels-Alder reaction did occur and the reaction

rate increased rapidly after about 30 minutes of induction time. A very clear sigmoidal (S shape) reaction curve of concentration vs time was obtained, which matches the character of autocatalytic reactions (curve a. in Figure 4.2). The catalytic effect of product templating was further confirmed by another two experiments in which 5% and 10% equivalent of product 116 were added to the initial solution of the starting compounds 114 and 81 and the results showed that the initial reaction rates increased dramatically with increasing initial product concentration. (curve b and c in Figure 4.2). Then three similar reactions were carried out at 23 °C with the concentration 0.015 M for each reactant and 0, 5% and 10% equivalent of product. The results also confirmed that the autocatalytic process did exist in the system (Figure 4.3). The induction time of

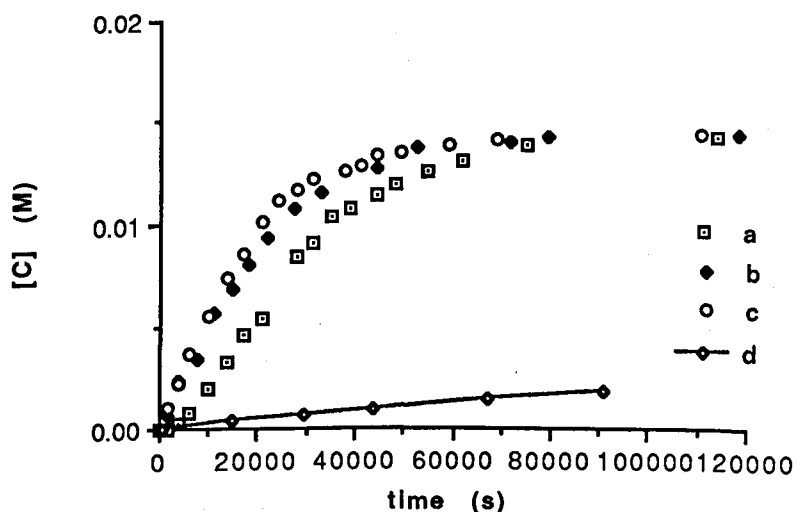


Figure 4.2 The Diels Alder reaction course of replication system 114 and 81 at 40 °C.

The concentration for each reactants is 0.015 M.

a. without addition of template 116. b. with 5 % of template 116.

c. with 10% of template 116.

d. calculated background reaction

course using a rate constant $3.5 \times 10^{-5} \text{ M}^{-1} \text{ s}^{-1}$.

the reaction without addition of product increased to about 200 minutes (curve a in Figure 4.3) and the initial rate increase was also very obvious in the reaction after addition of 5% and 10% equivalent of product.

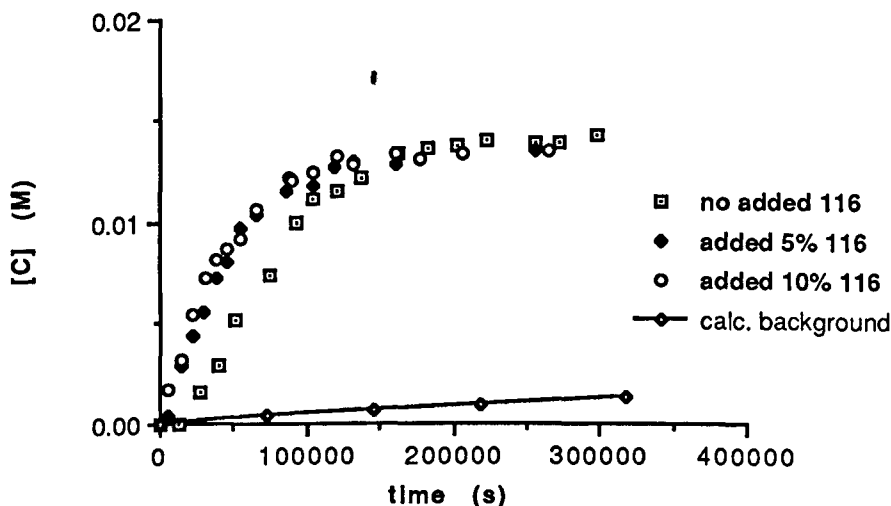


Figure 4.3 The Diels Alder reaction course of replication system 114 and 81 at 23 °C. The concentration for each reactants is 0.015 M.

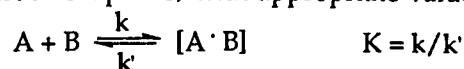
a. without addition of template 116. b. with 5 % of template 116.
 c. with 10% of template 116. d. calculated background reaction course using a rate constant $7 \times 10^{-6} \text{ M}^{-1} \text{ s}^{-1}$.

Because this reaction is supposed to be a product templated and catalysed reaction, the equation for the reaction rate is very complicated and rate constants are difficult to determine by simple calculation. Accordingly, a computer program was used to simulate the reaction, in which concentrations of all reactants, intermediates and products are

computed numerically for a given reaction set and equilibrium processes * and with various trial rate constants until the calculated reaction curves match the experimental reaction curves.⁶⁸

To start the simulation, the reaction scheme shown in Figure 4.4 was proposed (molecular structures for every species are shown in Figure 4.5). In this reaction scheme there are 4 main complexation equilibria and 4 reactions. At the beginning of the reaction, there are two processes accompanying each other. One is the reaction of two reactants 114 and 81 to produce product 116 with a rate constant k_1 and another is the aggregation of these two reactants to form reactant complex 115 with an association constant K_1 because the two reactants are complementary binding species. The product 116 acts as a template which binds the two reactants with association constant K_2 to form a reaction complex 117, in which the two reactants are held in proximity. Reaction complex 117 can also be formed through a reaction between two reactant complexes 115 with a rate constant k_2 and this actually is a major pathway to the reaction complex 117 since in a very short time after the replication process starts, most of the reactants will be in the form of reactant complex 115 because of the big association constant K_1 , hence k_2 is a major contribution to the background rate rather than k_1 . k_3 is the rate constant for the reaction of complex 117 to form product dimer 118. This is the catalytic reaction which is the key reaction of the whole replication process. K_3 is the dimerisation

* Equilibrium processes involving complex formation are treated as a pair of reactions (details see experiment part in chapter 6) with appropriate values for k and k' .



Values were chosen for the various k and k' so that complexation equilibria were rapid compared with reactions.

constant for free product template 116 and its value determines the turnover efficiency of the template. There is another possible route to product 116 involving an intramolecular reaction with a rate constant k_4 within the reactant complex 115 to give the intramolecular complex 119 which then gives product 116 with an equilibrium constant K_4 . These two process could dominate the whole reaction if the spacer or tether between the reaction site and binding site of the reactants is flexible and long enough as has been discussed in section 2.2 in chapter 2.^{22b}

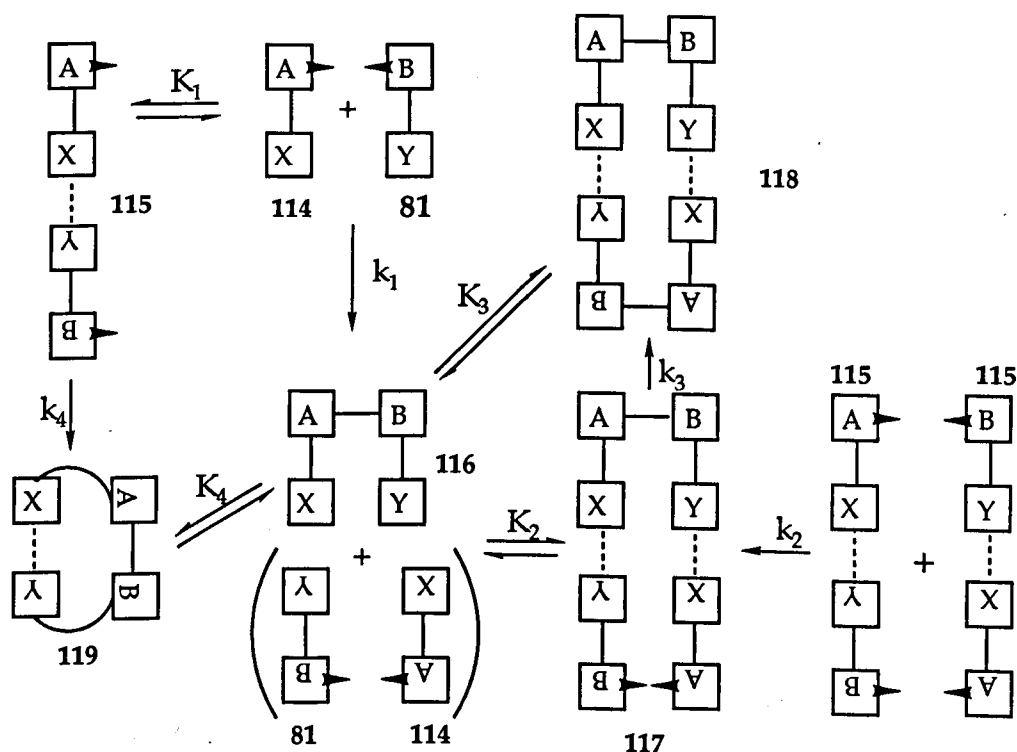
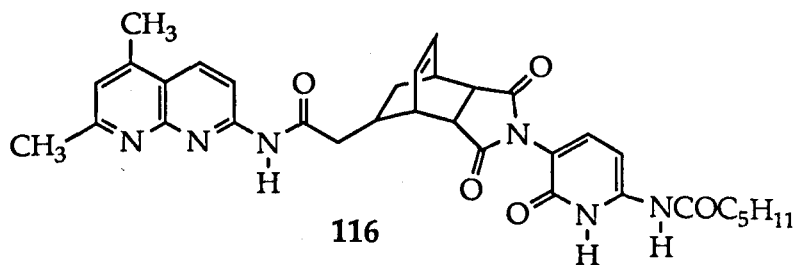
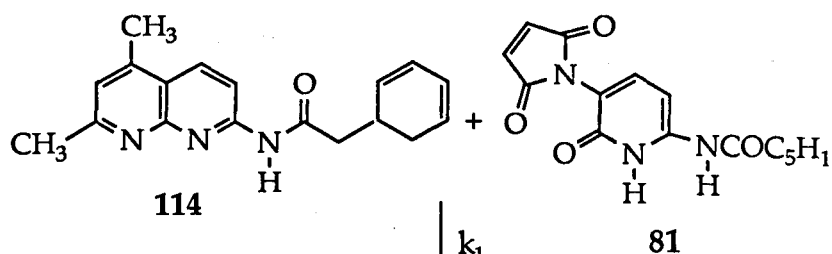
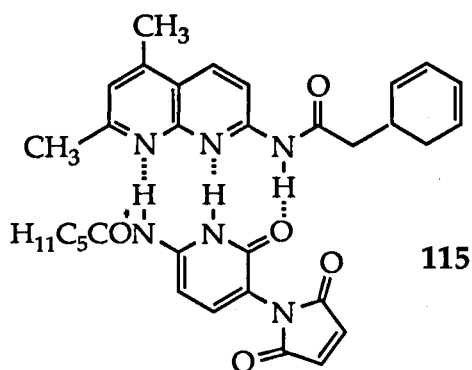
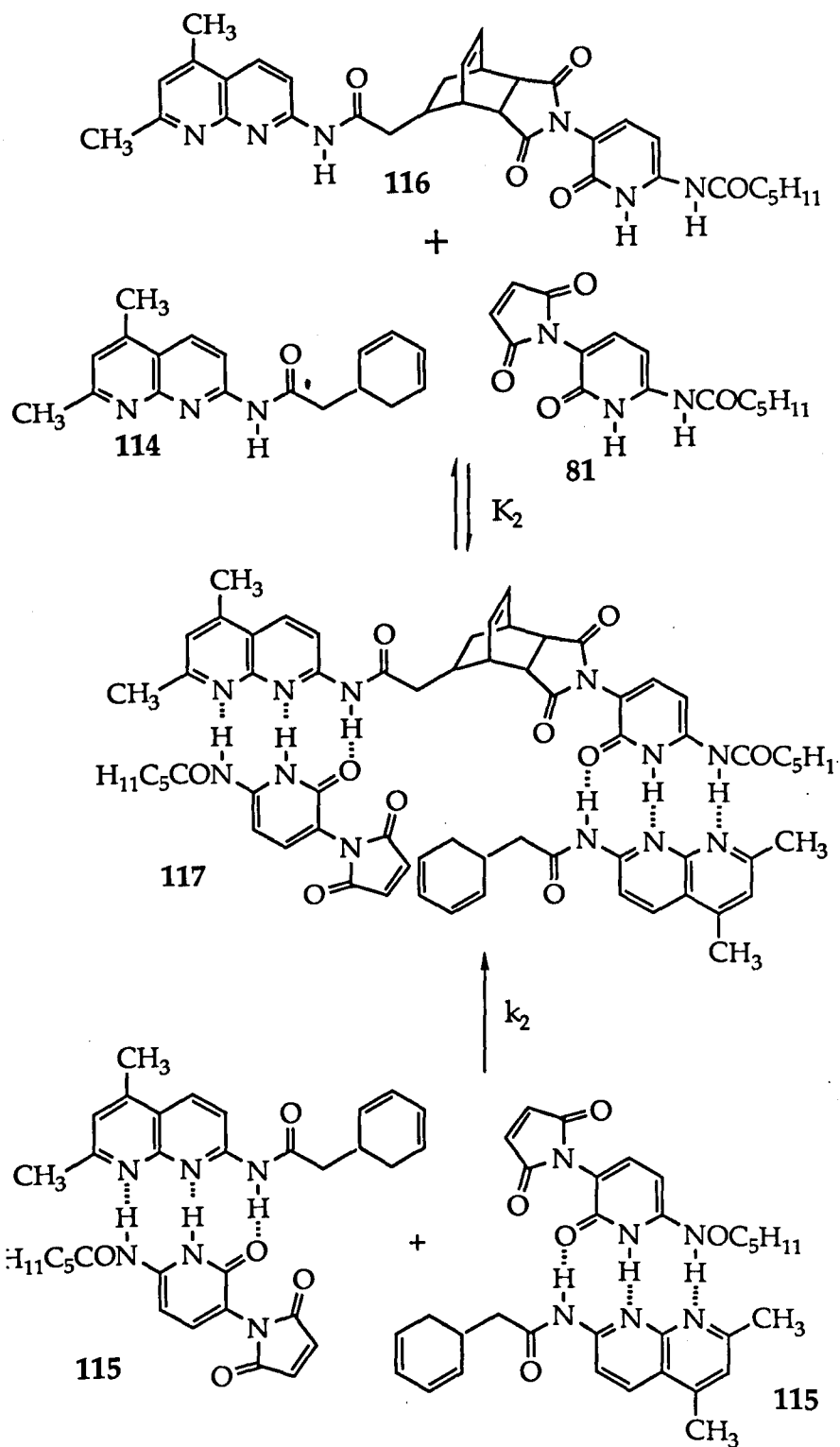
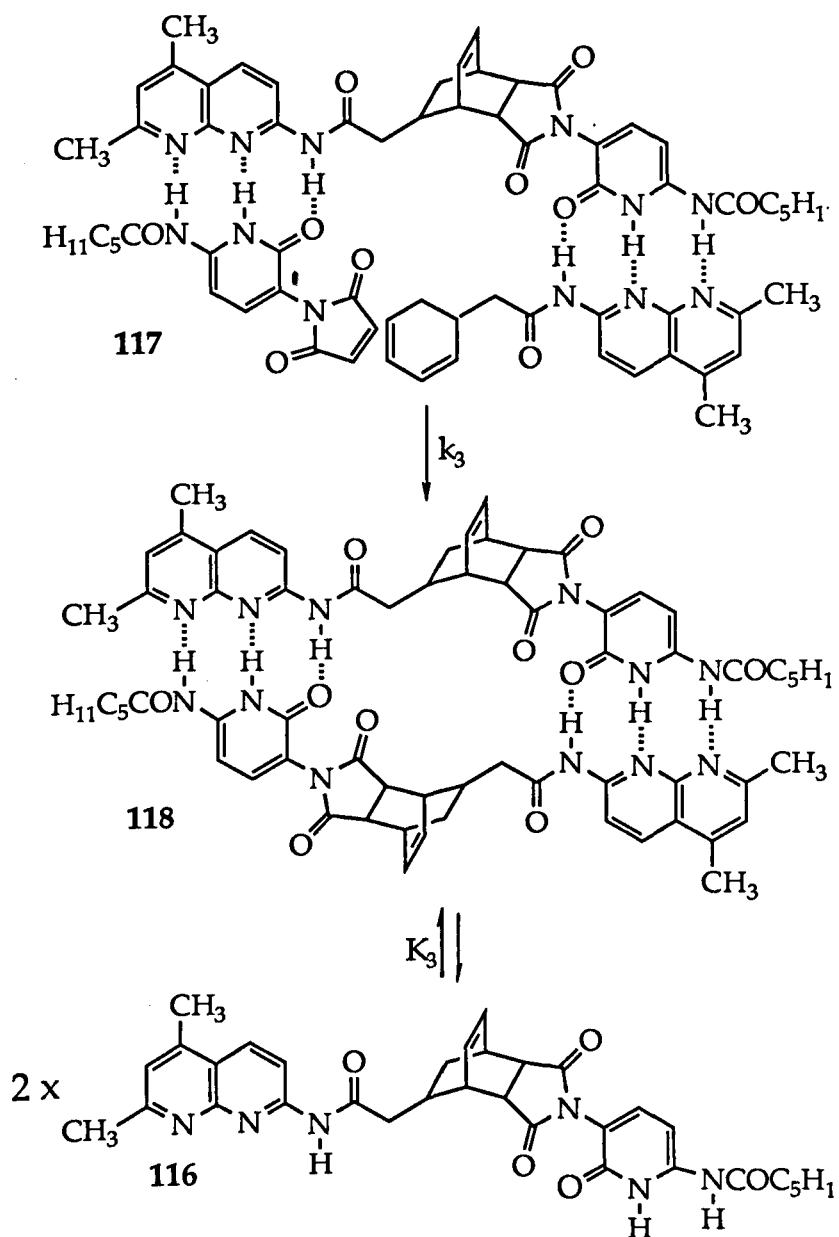


Figure 4.4 A reaction scheme proposed for the self replication system. A and B represent the reaction sites ene and diene, X and Y represent the binding sites pyridone and naphthyridine. The molecular structures for every species see Figure 4.5.







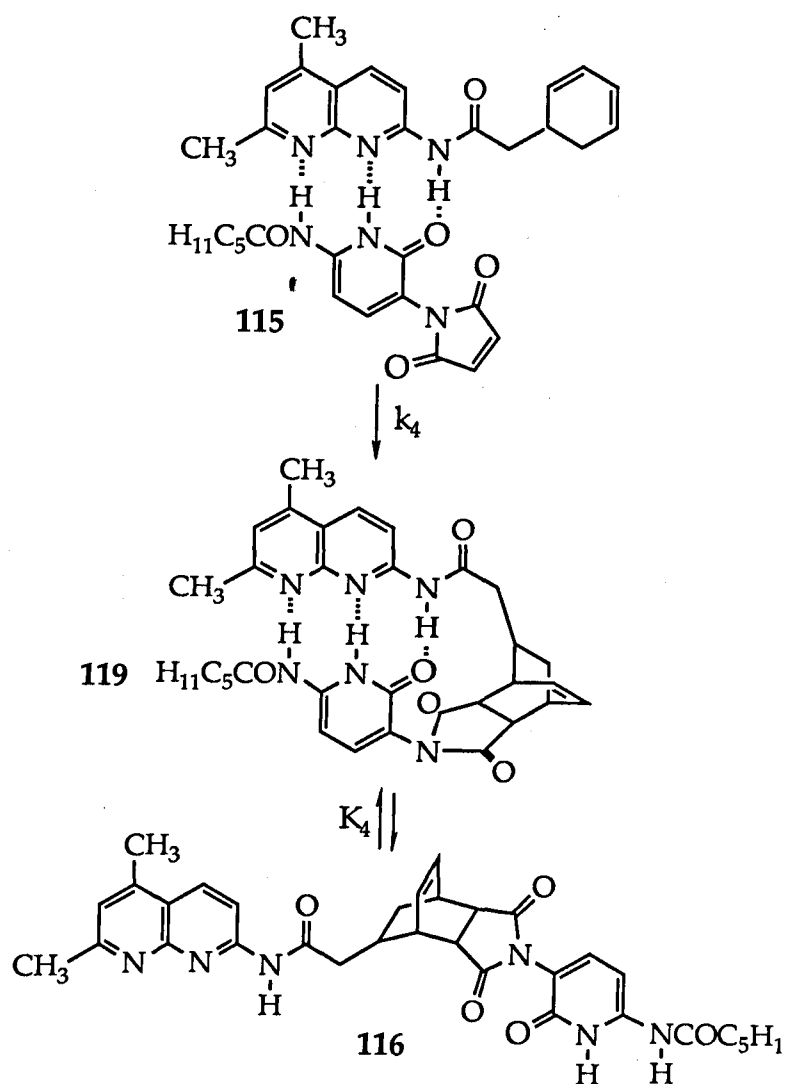


Figure 4.5 The molecular structures of species presented in Figure 4.4.

To make the computer simulation reliable, it is better to determine the values of these rate constants and equilibrium constants by direct experiments as far as possible. To make a better guess for the rate constant of the background reaction (k_1 or k_2), two model compounds **120** and **121** were used to carry out an uncatalysed Diels-Alder reaction under the same conditions (Figure 4.6). This reaction should be a simple second order bimolecular reaction and follow the second order rate law, so the reaction rate can be determined by using simple second order rate equations.

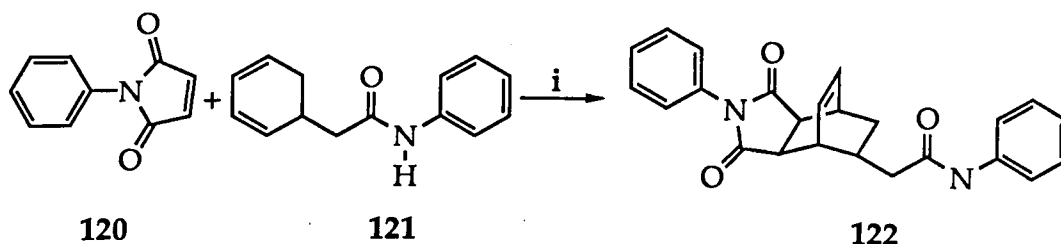
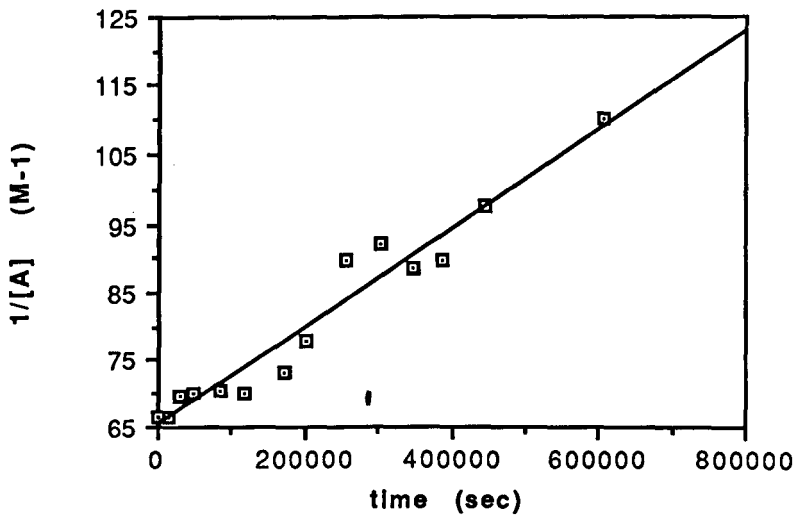


Figure 4.6 The model Diels-Alder reaction. Reaction conditions: i. 0.015 M for each reactant and reactions were carried out in DCM at 23 °C and 40 °C.

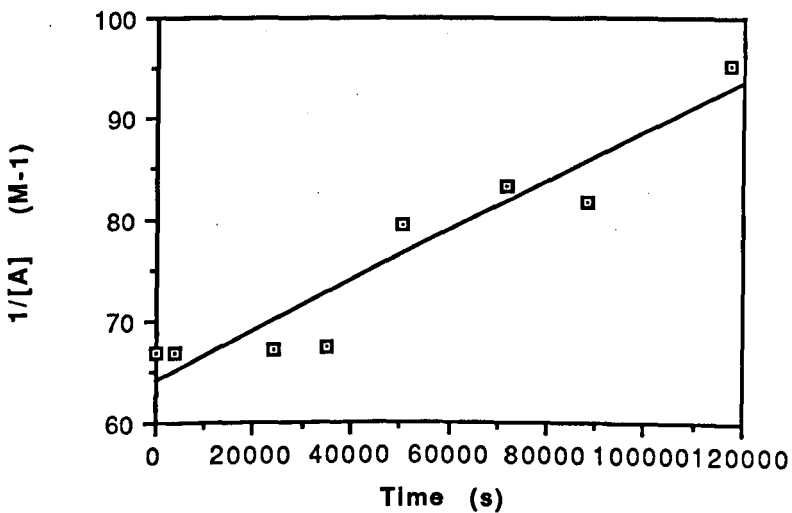
According to the second order rate law, the concentration of the reactants and reaction time should have a relation as follows,

$$\frac{1}{[A]} - \frac{1}{[A_0]} = kt \quad (4.1)$$

where $[A]$ is the concentration of the reactant, $[A_0]$ is the initial concentration of the reactant, k is the rate constant and t is the reaction time. So when $1/[A]$ is plotted against time, a straight line should be obtained and its slope is the reaction rate constant. Figure 4.7 shows the



(a)



(b)

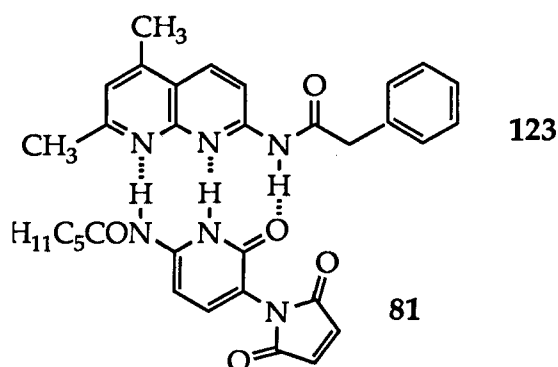
Figure 4.7 The plots based on the equation 4.1, using the data from reaction shown in Figure 4.6. [A] represents the concentrations of reactants.

(a) is for the reaction at 23 °C and (b) is for the reaction at 40 °C.

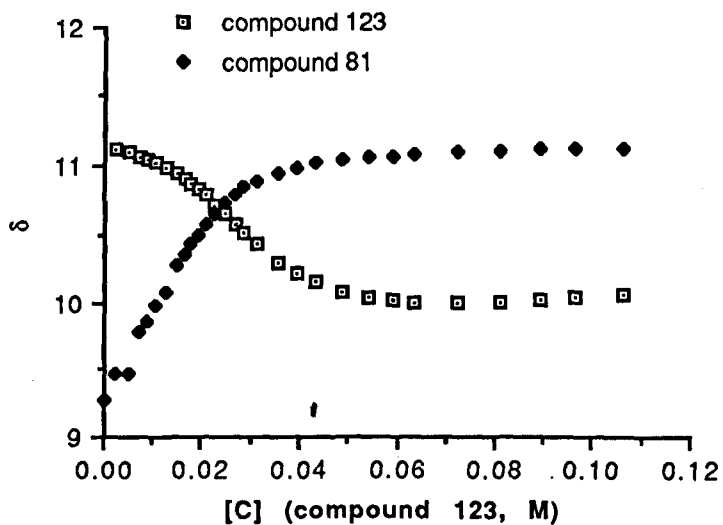
plots using the data from the experiment based on the model reaction. The rate constants of this model reaction determined from these plots are

$6.98 \times 10^{-5} \text{ M}^{-1}\text{s}^{-1}$ and $2.81 \times 10^{-4} \text{ M}^{-1}\text{s}^{-1}$ for the reaction at $23 \text{ }^\circ\text{C}$ and at $40 \text{ }^\circ\text{C}$ respectively. These values were used as approximations for k_1 in Figure 4.4.

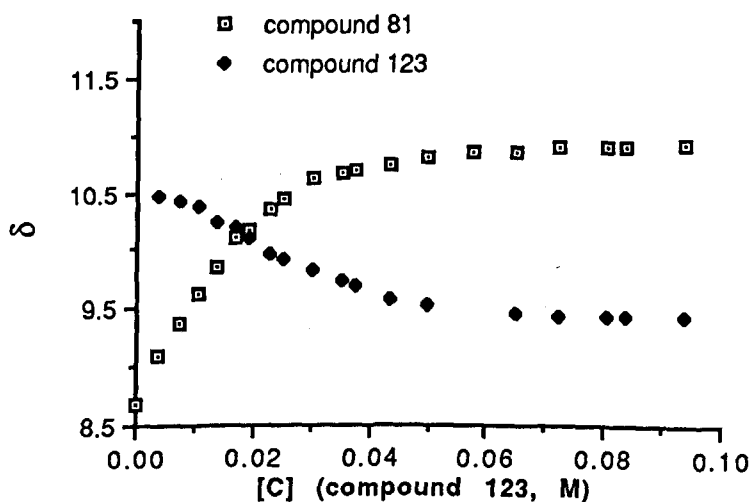
To obtain the equilibrium constant K_1 , an analogue of compound 114, 7-phenylacetamido-2,4-dimethyl-1,8-naphthyridine 123, was made, and the association constant between 123 and amidopyridone 81 was determined by a ^1H NMR titration experiment 21^b which was carried out at



two reaction temperatures ($23 \text{ }^\circ\text{C}$ and $40 \text{ }^\circ\text{C}$). The concentration of amidopyridone 81 was kept constant, while the concentration of compound 123 was increased from 0.1 equivalent of 81 to about 4 equivalent of 81. The chemical shift of the amide protons in both compounds were recorded and the results are shown in Figure 4.8. The association constants were calculated by trial and error using a computer programme which is based on the normal method for calculating association constants in host-guest chemistry.⁶⁹ The best fitting K 's are 228 M^{-1} for $23 \text{ }^\circ\text{C}$ and 163 M^{-1} for $40 \text{ }^\circ\text{C}$ and these values were used for K_1 in the simulation.



(a)



(b)

Figure 4.8 The plots of NMR titration for association of compound 81 and 123.

(a) at 23 °C. (b) at 40 °C.

The attempt to obtain the dimerisation constant K_3 failed because all the NH peaks were broad in the NMR spectra of product 116, so its value had to be determined by computer simulation along with the other rate constants and equilibrium constants.

The simulation started for the reaction at 23 °C. The value 228^2 (5.20×10^4) is a reasonable approximation for the association constant K_2 for the formation of reaction complex 117. If this equilibrium is a two step process, template T (116) binding reactant A (81) to form complex A:T then binding reactant B (114) to form A:T:B, then we have two equilibrium processes:



For these two equilibria, we can have two association constants K' and K'' :

$$K' = \frac{[A:T]}{[A][T]} \qquad (4.2)$$

$$K'' = \frac{[A:T:B]}{[B][A:T]} \qquad (4.3)$$

and both K' and K'' should have values very close to that of K_1 . Combining the two equations, we have:

$$\frac{[A:T:B]}{[A][B][T]} = K' \cdot K'' = K_1^2 \qquad (4.4)$$

The dimerisation constant K_3 should be around 10 to $10^2 \times K_2$ if we only consider the entropy effect, but the steric effects in the rigid product may offset the entropy effect. So during the simulation various values of K_3 were chosen.

As has been discussed above, k_2 possibly makes a major contribution to the background rate. It controls the rate of intermolecular reaction between two reactant molecules in the complex 115. It could be smaller than k_1 because complexation may somehow inhibit the reaction, but it could also be the same as k_1 . Initially it was set to the same value as k_1 ($6.98 \times 10^{-5} \text{ M}^{-1}\text{s}^{-1}$).

For simplicity, k_4 and K_4 were set to zero in the initial simulation. This is very likely to be correct because any significant contribution of k_4 will eliminate the induction time^{22b} while our system has shown clearly a significant induction time.

So in summary, the initial set of rate constants and equilibrium constants for the computer simulation are listed in Table 4.1.

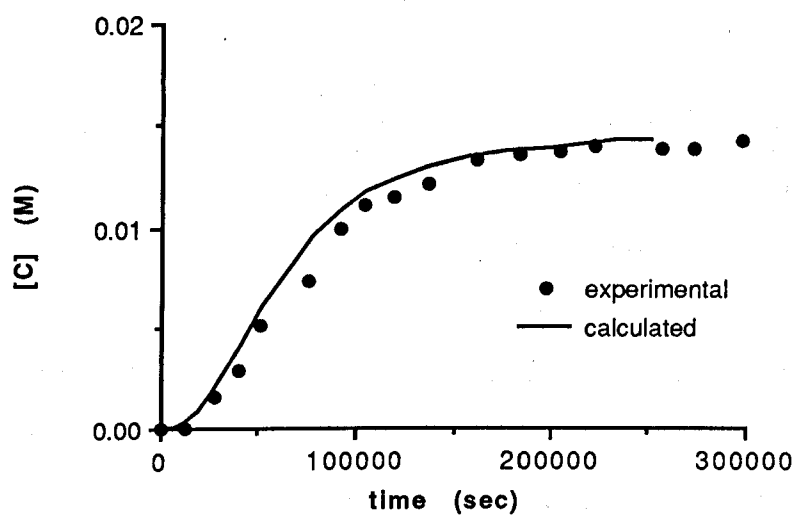
k_1	k_2	k_3	k_4	K_1	K_2	K_3	K_4
6.98 $\times 10^{-5}$	6.98 $\times 10^{-5}$	variable	0	228	5.20 $\times 10^4$	variable	0

Table 4.1 The rate constants and equilibrium constants for initial computer simulation of the replication reaction at 23 °C.

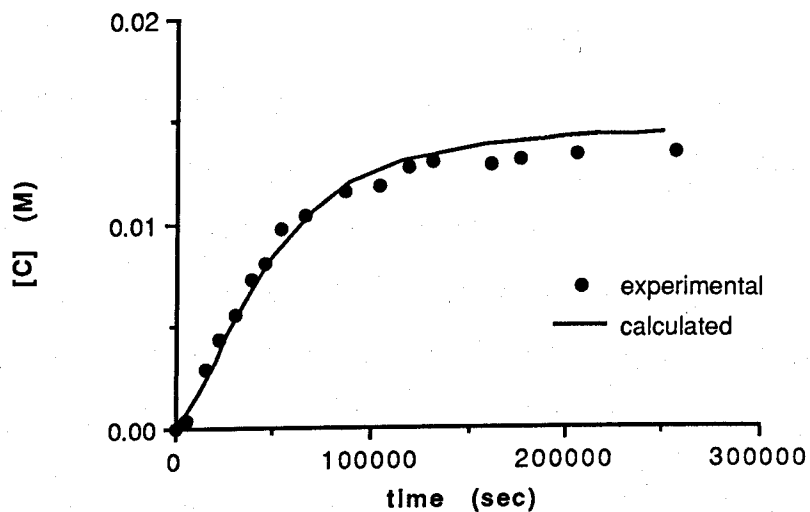
Putting these values and the initial concentrations of reactants and template into the computer program gives calculated curves representing the reaction at 23 °C. However, the simulation was not successful using this set of parameters and no matter what values are used for k_3 and K_3 , the calculated curves can only fit one of the experimental curves in Figure 4.3 but not fit all three curves simultaneously. In particular, the calculated curve for reaction without added template had a shorter induction time than that observed (curve a in Figure 4.3). It seemed that the values used for background rate constants k_1 and k_2 were too big. Reducing the background rate constants k_1 and k_2 by a factor of 10 gave a set of data which matched all three curves. The data are listed in Table 4.2 and calculated curves based on these data are shown in Figure 4.9.

k_1	k_2	k_3	k_4	K_1	K_2	K_3	K_4
6.98	6.98	8.3	0	228	5.2	7.3	0
$\times 10^{-6}$	$\times 10^{-6}$	$\times 10^{-4}$			$\times 10^4$	$\times 10^4$	

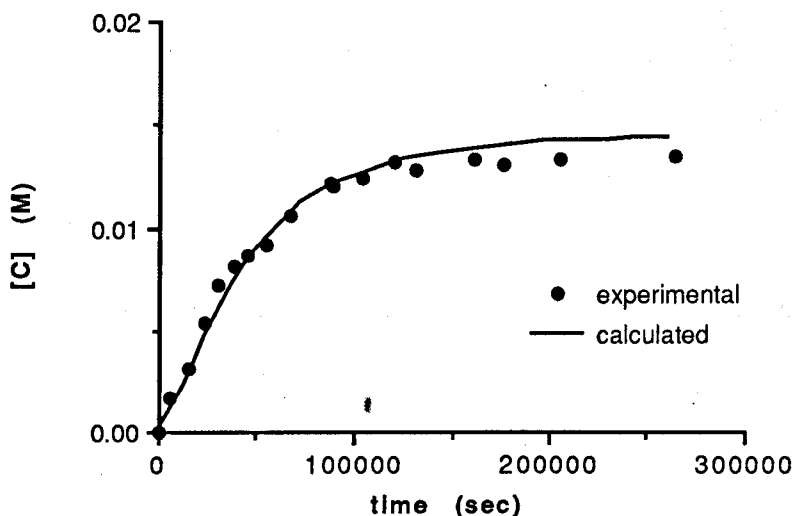
Table 4.2 A set of rate constants and equilibrium constants used in the simulation gave the results which match the experimental curves in Figure 4.3.



(a)



(b)



(c)

Figure 4.9 The calculated and observed reaction curves for the Diels-Alder replication reaction at 23 °C. (a) no added template, (b) 5% equivalent template, and (c) 10% equivalent template at start of reaction.

From Table 4.2, the effective molarity of the template catalysis at 23 °C can be calculated easily from k_3 / k_1 which is 119 M.

Using the data in Table 4.2, a simulation for the full reaction scheme (with variable values for k_4 and K_4) was carried out to check if the system does have the ability to form product 116 by the route $115 \rightarrow 119 \rightarrow 116$. The simulation results show that any significant value for k_4 eliminates the induction time of the reaction with no initial addition of template. So we are confident in stating that there is little product formed by the direct intracomplex reaction of 115.

Since several groups have used the simple reaction scheme shown in Figure 4.10 to analyse their results from replication systems,^{8,9,10,22} the calculation based on this scheme was also carried out for our system.

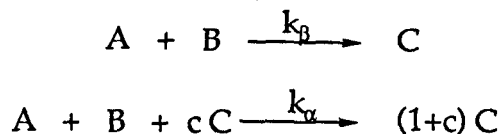


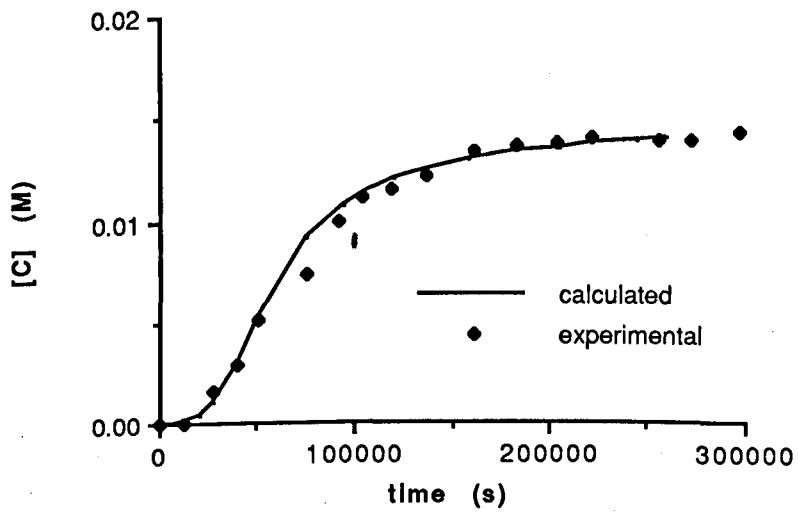
Figure 4.10 A simple scheme for replication reaction

From this reaction scheme, the following rate law can be evolved,

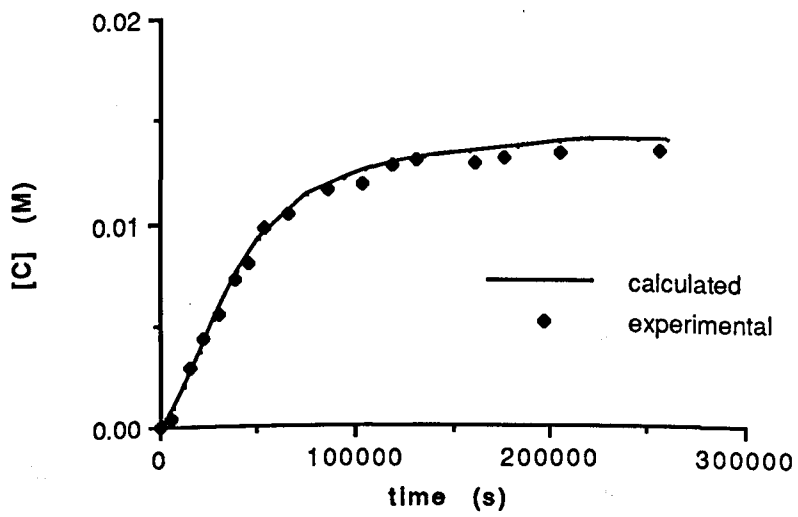
$$\frac{dC}{dt} = k_{\alpha}[A][B][C]^c + k_{\beta}[A][B] \quad (4.5)$$

where [A], [B] and [C] are the concentrations of the two reactants and the product, and k_{α} and k_{β} are the rate constants for catalytic and non-catalytic reactions respectively (see eqn. 1.3, Chapter 1). The quotient k_{α}/k_{β} , 'the autocatalytic excess factor ϵ ', has been used to express the efficiency of the autocatalytic templates. In our calculation, k_{β} was kept as same as k_1 (6.98×10^{-6}), [A], [B] and [C] were the initial concentrations of reactants and template used in the experiments. Three groups have claimed that a square root law was observed ($c = 1/2$), so the calculations started with $c = 1/2$ with variable k_{α} . However, no calculated curves fitted the experimental curves whatever values were chosen for k_{α} . By trying other values for c , it was found that $c = 0.8$ gave the best fit for observed and calculated curves with the value of $k_{\alpha} = 0.133 \text{ M}^{-1.8}$ ($19000 \times k_{\beta}$) (see Figure 4.11).

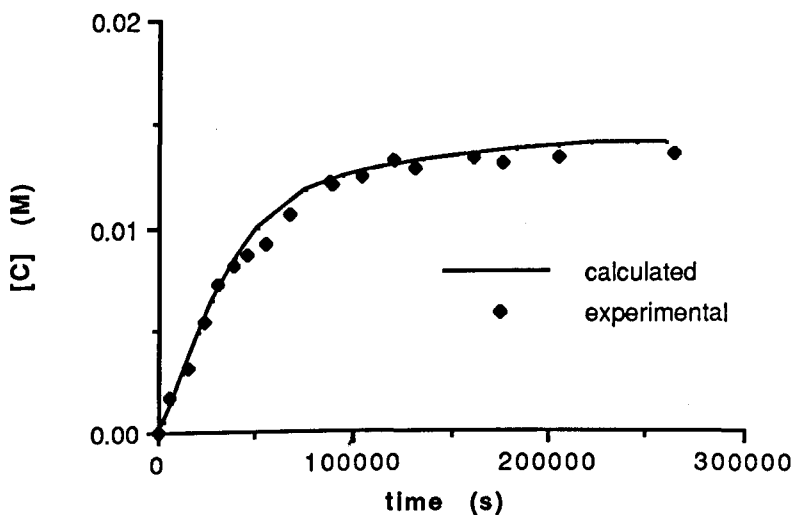
The same procedure was used for simulation of the Diels-Alder replication reaction at 40 °C. Again, when the value of $2.81 \times 10^{-4} \text{ M}^{-1} \text{ s}^{-1}$ which was obtained from the model reaction in Figure 4.6 was used as the values of k_1 and k_2 for a full reaction scheme, the calculation did not give any curve to fit observed curves until reducing the values of k_1 and k_2 to 3.5×10^{-5} . Table 4.3 lists a set of rate constants and equilibrium constants



(a)



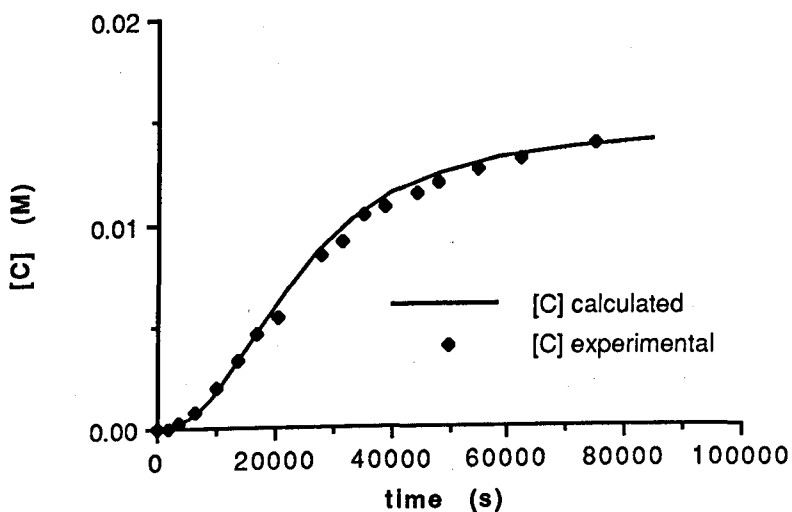
(b)



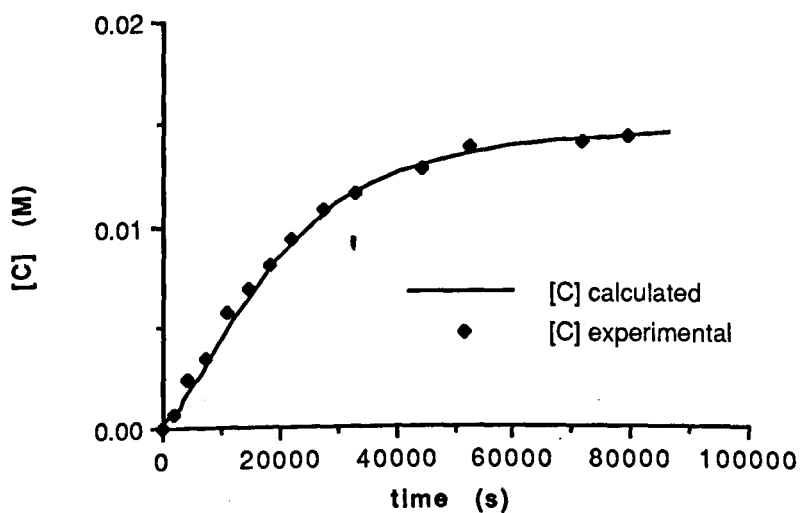
(c)

Figure 4.11 Calculated and observed reaction curves for the Diels-Alder reaction at 23 °C based upon equation 4.5 ($k_{\alpha}=0.133 \text{ M}^{-1.8}\text{s}^{-1}$, $k_{\beta}=6.98 \times 10^{-6} \text{ M}^{-1}\text{s}^{-1}$, and $c=0.8$). (a) No added template, (b) 5% equivalent template and (c) 10 % equivalent template.

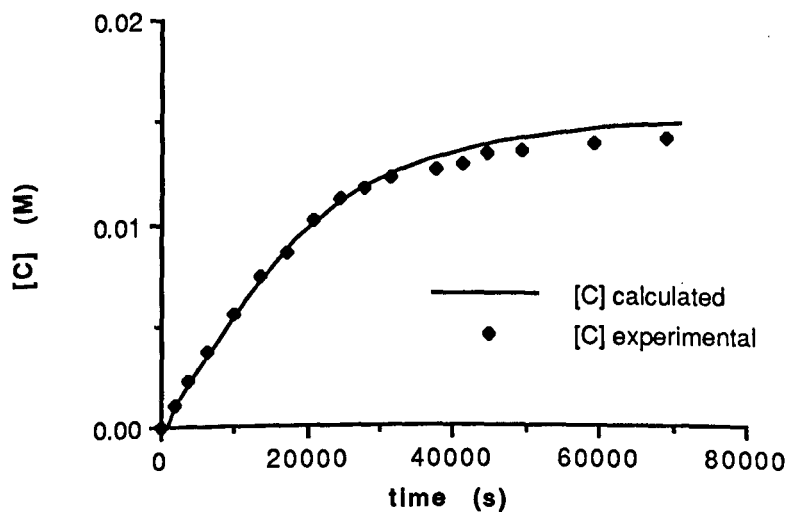
which gave the best fit for calculated curves (full reaction scheme) and observed curves, which are shown in Figure 4.12. The effective molarity is 66 M (k_3/k_1).



(a)



(b)



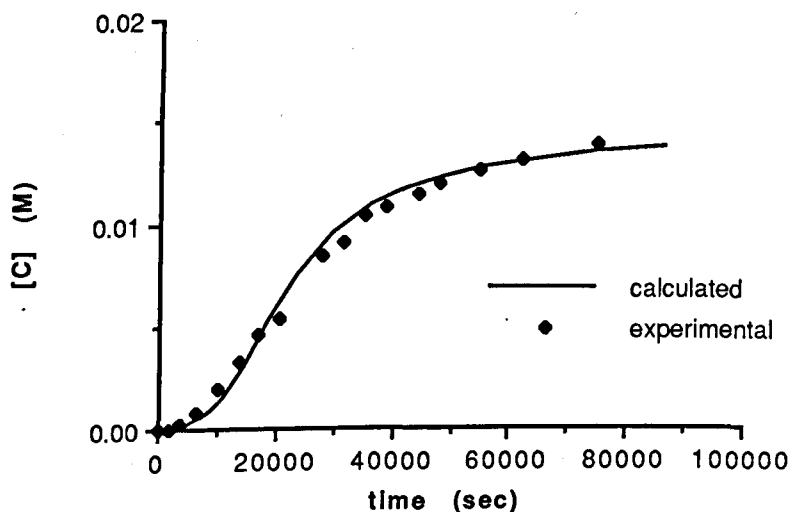
(c)

Figure 4.12 Calculated and observed reaction curves for the Diels-Alder replication reaction at 40 °C. The calculation is based on a full reaction scheme in Figure 4.4, using the parameters in table 4.4. (a) no added template, (b) 5% equivalent template, and (c) 10% equivalent template at start of reaction.

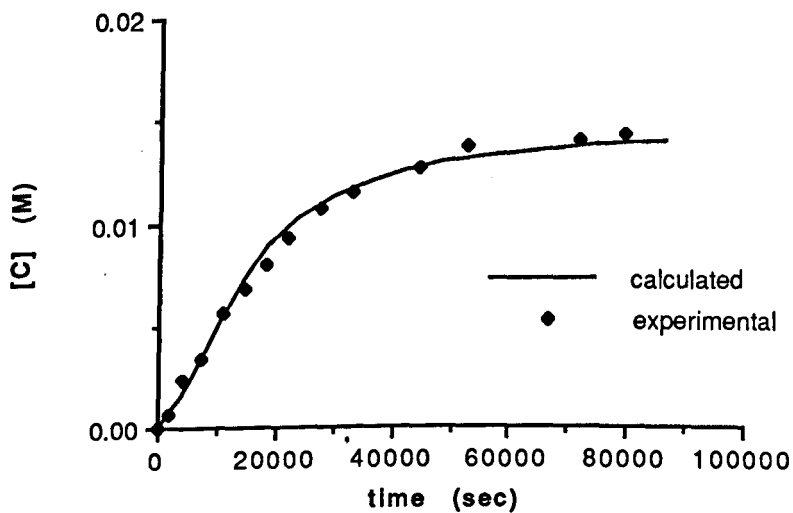
For the simple reaction scheme, it was found that the best fit for c and k_{α} were 0.8 and $0.35 \text{ M}^{-1.8}\text{s}^{-1}$ respectively when used the value of k_1 in Table 4.3 which was 3.5×10^{-5} as the value of k_3 in the simulation. The curves calculated compared with observed curves for the simple reaction scheme are shown in Figure 4.13.

k_1	k_2	k_3	k_4	K_1	K_2	K_3	K_4
3.5	3.5	2.3	0	163	2.66	3.66	0
$\times 10^{-5}$	$\times 10^{-5}$	$\times 10^{-3}$			$\times 10^4$	$\times 10^4$	

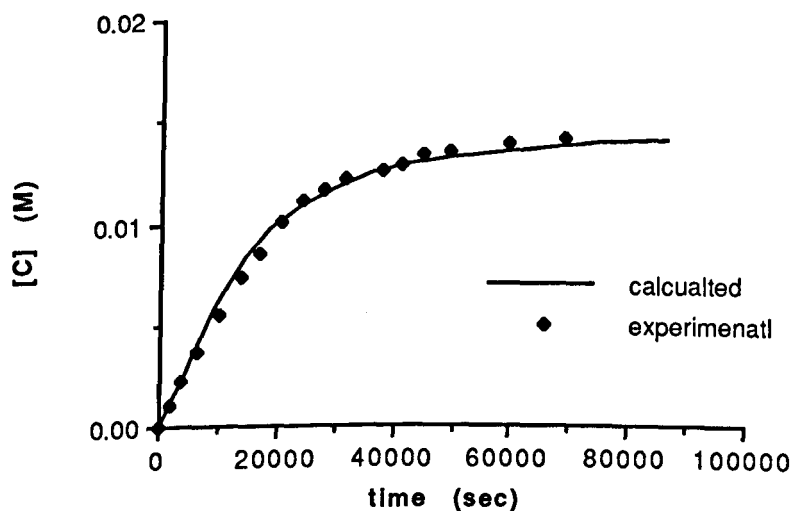
Table 4.3 The rate constants and equilibrium constants used for the simulation of the Diels-Alder replication reaction at 40°C .



(a)



(b)



(c)

Figure 4.13 Calculated and observed reaction curves for the Diels-Alder replication reaction at 40 °C. The calculation is based on the equation 4.5, using $k_{\alpha} = 3.5 \times 10^{-5} \text{ M}^{-1.8}\text{s}^{-1}$, $k_{\beta} = 0.35 \text{ M}^{-1}\text{s}^{-1}$ and $c = 0.8$.

- (a) no added template, (b) 5% equivalent template, and
(c) 10% equivalent template at start of reaction.

Table 4.4 gives values of rate constants obtained from the above simulations and compares them with those reported in literature.

Model	k_{α}^a	k_{β}^a	c^a	ϵ^a	k_{bi}^b	k_{uni}^b	E.M
Kiedrow. ^{8,10}	7.43	1.77×10^{-2}	0.5	420			
Orgel ⁹	5.71×10^{-2}	1.66×10^{-4}	0.5	340			
Rebek ^{22a,b}	9.87×10^{-2}	1.24×10^{-3}	0.5	80	2.3×10^{-2}	7×10^{-2}	3
Sanders ^{33a,b}					2.2×10^{-4}	1.0×10^{-3}	4
81,114,116 23 °C	6.98×10^{-6}	1.33×10^{-1}	0.8	19000	6.98×10^{-6}	9.5×10^{-4}	119
81,114,116 40 °C	3.50×10^{-5}	3.50×10^{-1}	0.8	10000	3.50×10^{-5}	2.3×10^{-3}	66

a. For scheme in Figure 4.11, ϵ is the ratio k_{α}/k_{β} .

b. For reaction scheme in Figure 4.4, k_{bi} is equivalent to k_1 and k_{uni} is equivalent to k_3 .

E.M.-- effective molarity.

Table 4.4

The 'autocatalytic excess factor ϵ ' (k_{α}/k_{β}) was used by von Kiedrowski's group to characterise the efficiency of the template. However, it only has some meaning when a reaction is compared with another reaction with the same order c . The effective molarity is a proper way to assess the efficiency of the template, this is the quotient of a unimolecular rate constant k_{uni} with a bimolecular rate constant k_{bi} .

Initial rate is another parameter which has been used to assess rate enhancements of artificial catalytic systems by many groups. It is also interesting to compare our system with others in this way. However, the initial rate depends on the initial concentrations of reactants and template and it also depends on the temperature. It is meaningless to compare the results with different initial concentrations and temperature with each

other. In our experiment, it was difficult to measure initial rates because NMR spectroscopy is not sensitive enough at low concentrations. The errors would be even bigger when the reaction has a small induction time. For comparison, equation (4.5) was used to calculate the initial rates for our system with different initial concentrations of reactants and template. It should be reasonably reliable because the calculated reaction curve fits the experimental curve so well. Table 4.5 gives results obtained by other groups at a similar temperature to that used in our experiments and the corresponding calculated rate enhancements based on equation (4.5) for our system.

Model	Conditions			Initial rate enhance. (fold)	Initial rate enhance. (calculated for system 81, 114 and 116 ^a)
	°C	Initial conc. (reactants) (mM)	Initial conc. (template) (equiv)		
Rebek (1) ^{22b}	22	8.2	0.2	1.43	113
	22	8.2	0.5	1.73	235
	22	16.5	0.2	1.32	198
	22	16.5	0.55	1.57	442
Rebek (2) ^{22c}	22	50	0.2	2	478
Kelly (1) ^{21a}	25	4	1	6	230
	25	20	1	16	832
Kelly (2) ^{21b}	25	4	1	12	230
Sanders ^{33b}	30	9	1	1000	440

a. The calculated results are based on the equation 4.5 using data for the reaction at 23 °C (the values of $k_{\alpha} = 1.33 \times 10^{-1}$, $k_{\beta} = 6.98 \times 10^{-6}$ and $c = 0.8$) and the conditions specified in the model.

Table 4.5

4.2 Discussion

Since an autocatalytic reaction is a complicated process, the simplest way to obtain kinetic data is by using computer modeling. However some problems may occur during the computer calculation. If several data need to be tried simultaneously, the calculation can cause significant error because many different sets of data can fit a particular experimental curve. However, there are not many sets of data that fit all the experimental curves. During the simulation we found that the curves calculated with different concentration of template respond to a change of rate constants and equilibrium constants differently. For example, if k_1 and k_2 were kept variable and other parameters in Table 4.2 are fixed, we found that the curve with zero initial concentration of template responded significantly to a change in the background rate constants k_1 and k_2 , while the curves calculated with 5% and 10% initial concentration of template hardly changed when background rate constants changed. Figure 4.14 shows two sets of curves calculated using two different background rate constants, 6.98×10^{-5} and 6.98×10^{-6} (the former one is the rate constant obtained from the model reaction in Figure 4.6). From the figure we can see that two sets of the curves with added template fit so well and the curves without added template do not fit at all. These two sets of curves have a common feature which is that curves with 5% and 10% template (b, c and e, f) are very close each other while the curves without added template are far apart from them. But the curve d (with lower background rate) is further apart from the curves e and f than the curve a (with higher background rate) from the curves b and c. In other words, the three curves with higher background rate are closer to each other. This was the reason why initially we could not find a set of curves to fit our experimental results when we used 6.98×10^{-5} as the value for background rate constants k_1 and k_2 because

the three curves were always too close to each other whatever other parameters were used, unless we reduced background rate constant by a factor of 10.

So all this means that if a set of data fits all experimental curves it should be reasonably accurate.

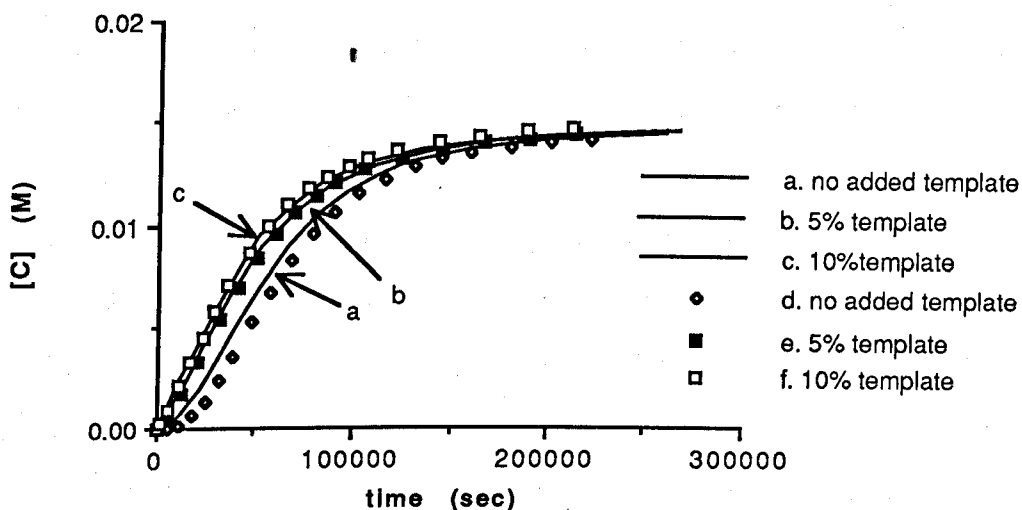


Figure 4.14 Two sets of calculated curves for the reaction at 23 °C based upon the full reaction scheme. All parameters used for calculation of these two sets of curves are the same as those listed in Table 4.2 except for k_1 and k_2 .

For solid lined curves, k_1 and k_2 are 6.98×10^{-5} , for scattered curves k_1 and k_2 are 6.98×10^{-6} .

In the reactions at both 23 °C and 40 °C, the calculated background rate constants k_1 and k_2 for the reactions are lower than the rate constants obtained for the reaction of model compounds 120 and 121. One possible reason for this difference is that some properties, such as solubility, of compounds 81 and 114 are very different from those of compounds 120 and 121. The solubility of 81 and 114 is much lower than that of 120 and

121 and the poorer solubility in dichloromethane may make the reaction of 81 and 114 slower than that of 120 and 121. Another possible reason is that a significant contribution to the background rate is from the reaction involving complex 115 because at the beginning of the replication process compounds 81 and 114 form the complex quickly and they are possibly not so accessible for the reaction as the uncomplexed molecules. So in the real situation, the values of k_1 and k_2 are probably quite different, with k_1 close to 6.98×10^{-5} and k_2 lower than 6.98×10^{-6} . The value of 6.98×10^{-6} used in the simulation for both k_1 and k_2 may well be an average of the actual values of k_1 and k_2 .

Apart from k_1 and k_2 , k_4 actually presents a third contribution to the background rate if it does have a significant value. We did some simulation with variable k_4 using the parameters listed in Table 4.2 and adding in another fixed value 0.5 for K_4 (considering that there may be some strain in the complex 115). All parameters are listed in Table 4.6 and results are shown in Figure 4.15. In Figure 4.15 a calculated curve obtained previously (Figure 4.9a) is used as a reference curve (scattered curve). From results we can see that any curve with a value of k_4 larger than 6.89×10^{-8} has a shorter induction time and does not fit the reference curve. We could obtain a curve which fits the reference curve by fixing k_4 at the value of 6.98×10^{-6} and reducing the values of k_1 and k_2 , but this is unreasonable because from the model reaction shown in Figure 4.6 we know that the k_1 and k_2 should not too much smaller than $6.98 \times 10^{-5} \text{ M}^{-1}$.

k_1	k_2	k_3	k_4	K_1	K_2	K_3	K_4
6.98 $\times 10^{-6}$	6.98 $\times 10^{-6}$	8.3 $\times 10^{-4}$	variable	228	5.2 $\times 10^4$	7.3 $\times 10^4$	0.5

Table 4.6

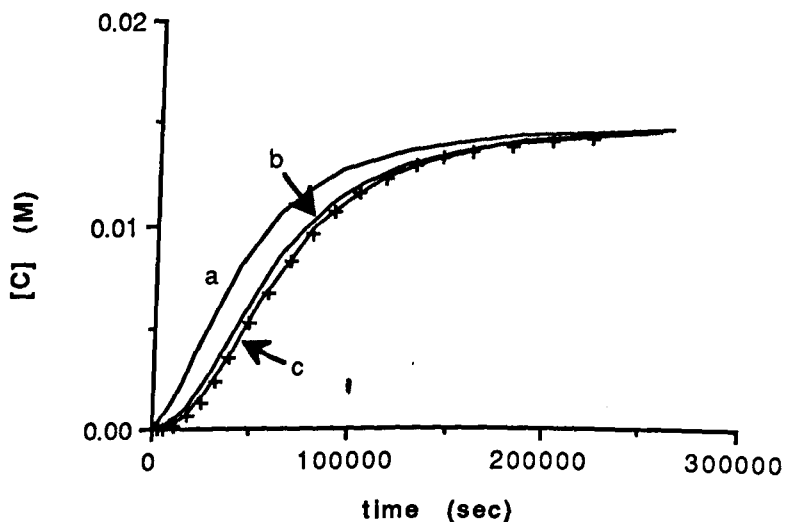


Figure 4.15 Calculated curves for the Diels-Alder replication reaction at 23 °C. The calculation is based on a full reaction scheme in Figure 4.4, using the parameters in table 4.6. All curves represent the reaction without added template with different k_4 . a. $k_4 = 6.98 \times 10^{-6} \text{ s}^{-1}$. b. $k_4 = 6.98 \times 10^{-7} \text{ s}^{-1}$. c. $k_4 = 6.98 \times 10^{-8} \text{ s}^{-1}$. + $k_4 = 0$ and $K_4 = 0$.

The influence of K_4 for the reaction is actually the same as the dimerization constant K_3 . The bigger the value of K_4 , the more inhibition for the reaction. In the simulation we can use a big K_3 with a small K_4 or vice versa or intermediate values for both to obtain the same curve. So precisely speaking, the values of K_3 we obtained from the previous simulations (see Table 4.2 and Table 4.3) are the average values of K_4 and K_3 . But from the structure of **116**, we can estimate that K_4 should not be significant because the spacer between the two binding sites is short and rigid. So, using a zero value for both k_4 and K_4 should not cause serious error for the results of simulation.

Apart from K_4 , there are three equilibrium constants in the system but the values used for K_2 and K_3 are determined by the measured values of K_1 . The bigger the value of K_1 , the bigger the values of K_2 and K_3 . The values of K_1 obtained from measuring the association constant between **81** and **123**, 228 M^{-1} ($23 \text{ }^\circ\text{C}$) and 163 M^{-1} ($40 \text{ }^\circ\text{C}$), are smaller than those of some similar binding systems reported by other groups,^{21,70} However, they are reasonable values because computer modelling shows that the methyl at the 2-position of the acylaminonaphthyridine **123** interacts with the hexanoylamido group in the pyridone **81**, so that the complexation between the two molecules is partially inhibited (Figure 4.16). A very similar situation found for an analogous binding system by Zimmerman's group⁷¹ supports this observation.

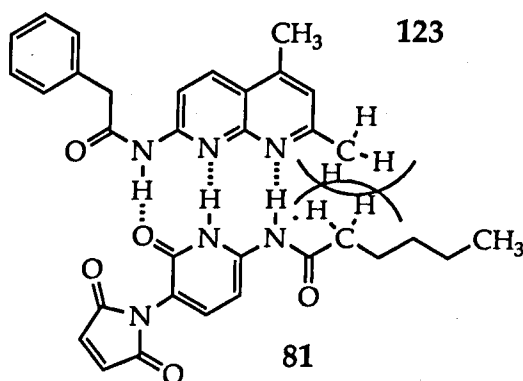


Figure 4.16 The interfere of methyl group in compound **123** with hexnoyl group in compound **81**.

The values of equilibrium constants K_2 and K_3 are crucial in the replication system. A large value of K_2 accelerates the reaction while a larger K_3 inhibits the reaction. The competition between these two equilibria determines the efficiency of the replication system. However, increasing K_1 will increase both K_2 and K_3 . This is the most difficult

problem to solve in designing an artificial template. Generally, K_3 would be 10 – 100 times larger than K_2 because of the entropy contribution. If the template is designed to bind the transition state perfectly, the product is likely to stay on the template after the reaction and inhibit it due to a small turnover number. This is one of main reasons why reported artificial templates are not very efficient. The values of K_2 and K_3 from the simulation of our system show that K_3 is only slightly bigger than K_2 . (1.40 fold for the reaction at 23 °C and 1.41 fold for the reaction at 40 °C, see Table 4.2 and 4.3) and the reliability of this relation between K_3 and K_2 is supported by the results obtained using equation (4.5) derived for the simple reaction scheme (see Figure 4.11 and Figure 4.13). The value of c in equation (4.5) is an indication of the efficiency of the template. The smaller the value of c , the stronger the inhibition, whereas if the template is not inhibited by the dimerisation the value of c should be 1, which would reflect a very low value of K_3 . The calculations for our system give $c = 0.8$ (for both reactions at 23 °C and 40 °C) that fits the reaction curves best. This means that our system approaches the objective of no inhibition. Hence K_3 must have relatively low values in our system. The rigidity of the product 116 and the interference between the methyl group at the 2-position of the naphthyridine and the hexanoylamido group on the pyridone ring are possible factors which offset the entropy contribution to the dimerisation. In reaction complex 117, the reactants 114 and 81 are free to adopt a minimum energy position, which minimises this unfavourable interaction to complex with template 116. However, in the product dimer both components 116 are rather rigid and minimisation of the unfavourable interaction is not achievable, the resulting increase in enthalpy offsets the advantage of the more favourable entropy for bimolecular association as compared with termolecular association. So it seems that the synthetic problem which forced us to use the 2-methyl

aminonaphthyridine turned out to be a lucky feature for our replication system and gave the system values of K_2 and K_3 which make it efficient.

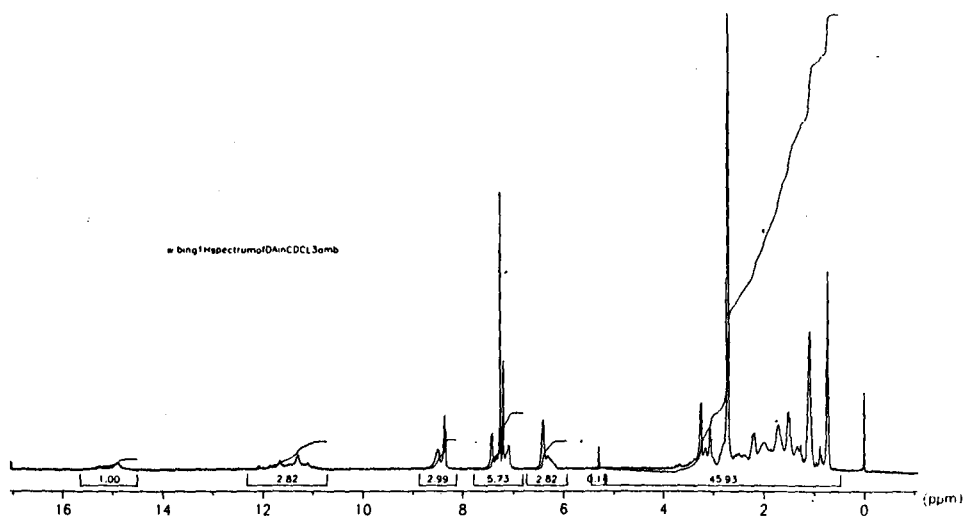
The data listed in table 4.4 and 4.5 show that the system we made is quite efficient. The calculated effective molarity is about 119 M at 23 °C and 66 M at 40 °C, which are quite in line with a system with a loosely bound transition state or product. As has been discussed in chapter 2, for a loosely bound system the entropy contribution can give a rate constant enhancement of about 10^2 M (effective molarity) (see table 2.2 chapter 2). Because of the limited number of binding sites, our system and other similar artificial systems should belong to the class of loosely bound systems. The calculated initial reaction rates show that our system is more efficient than other reported systems. One thing that should be mentioned is that the concentrations of the template used in the calculation for our system reported in table 4.5 are the total concentrations of the template, the actual concentrations of free template are smaller than this because of the dimerisation. Yet, they still give very big enhancement of initial reaction rates.

4.3 The Stereochemistry of the System.

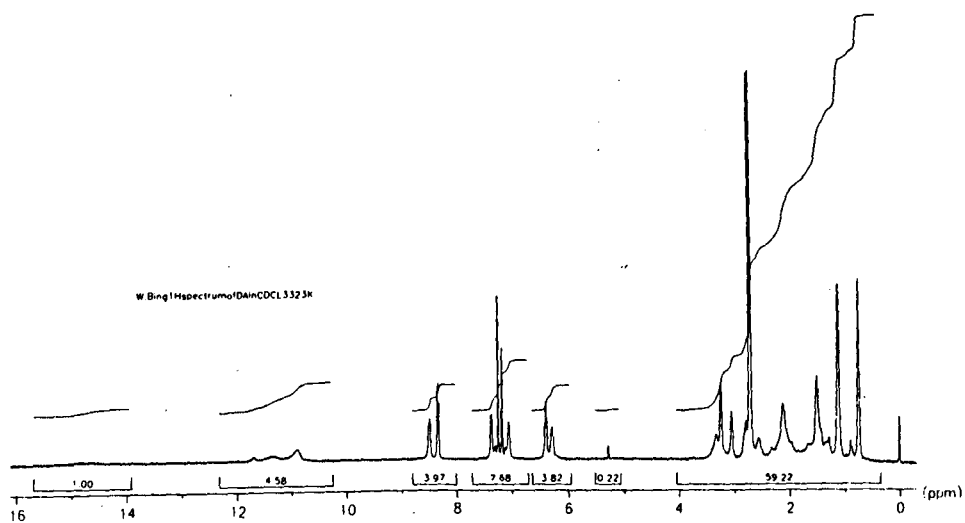
As has been discussed in chapter 2, the system has enriched information content because of stereochemistry. In reactant 114 there is a chiral centre and the Diels-Alder reaction can generate possible isomers. It is interesting to investigate the system to see if there is stereoselectivity or stereo-amplification during the replicating process. Using a high resolution NMR (400 MHz) spectrometer, the ^1H spectrum of product 116 was recorded at ambient temperature and at 50 °C (Figure 4.17). The spectra are consistent with significant diastereoselectivity. There are two pairs of doublet peaks (δ 7.0 – 7.5) which are assignable to the protons of the

pyridone ring showing clearly that there are only two diastereoisomers in the product in a ratio about 4 : 1. There could be a total of 8 stereo isomers generated from the reaction since racemic **114** was used (see Figure 2.23 in chapter 2), but in view of the *endo* preference of the Diels-Alder reaction, there should be just 2 pairs of enantiomers in product **116** which are assigned as RR, SS, SR and RS in Figure 4.18. It is assumed that the major product involves *endo* attack of the ene **81** at the less hindered face of the diene **114** to give the RR or SS product as a racemate. The minor product is probably the RS/SR racemate but *exo*-diastereoisomers are also a possibility.

The ^1H NMR spectrum at ambient temperature provides some other information about the stereochemistry of the product **116**. There are more than 3 peaks at low field between 10 – 16 ppm although there are only three NH's in the molecule. Presumably there is more than one binding pattern for 'dimers' of the product. Two peaks at around 15 ppm (NH of the pyridone ring) indicate that there are two binding patterns in the product in a ratio of 2 : 1. At 50 °C exchange is rapid on the NMR time scale and a single broad NH signal was observed in the same region. Supposing that only the RR and SS stereoisomers contribute to these two peaks (the NH peak of minor RS / RS product may too small to be observed) there should be three possible binding patterns, RR – RR, SS – SS and RR – SS. Since the RR – RR and SS – SS complex are a pair of enantiomers, their signals should be indistinguishable, while the RR – SS complex should be different from them. If this is the case, it would mean that there is some stereoselection in the dimerisation. If the RS and SR stereoisomers do contribute to these signals, the situation would be very complicated. A reaction using template **116** derived from homochiral **114** would indicate whether the transition state complex, that controls the catalysed process, shows similar diastereoselectivity. This would be of



(a)



(b)

Figure 4.17 ^1H NMR spectra of compound 116 in CDCl_3 .

a. recorded at ambient temperature (20 °C); b. recorded at 50 °C

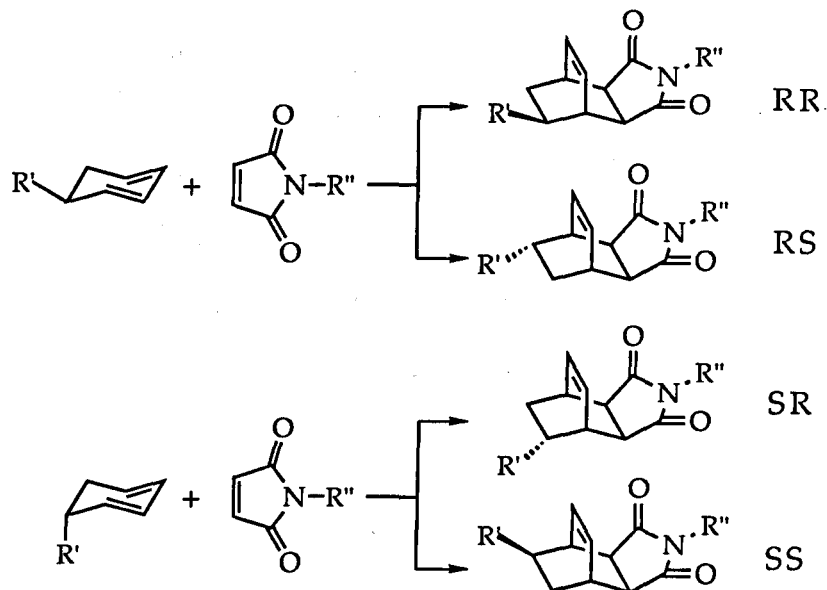


Figure 4.18 Four possible *endo*-isomers of the compound 116.

#

4.4 More Stable Transition State?

From the kinetic results discussed above, the new replication system is more effective than those described in other work. The first possible reason is that a template with a bigger binding energy is used. Although the association constant of the two reaction components is not as big as expected, 228 M^{-1} (23°C) is still bigger than some cases in which the association constants between the two components are less than 100 M^{-1} ^{22,23}. This effect has already been shown from our results obtained from experiments at different temperatures (see table 4.4). The system at lower temperature has a larger association constant K_2 and has a bigger effective molarity. Secondly, as has been discussed in section 4.2, the inhibition of the template by the dimerization is partially prevented by the more rigid template which is formed by the Diels - Alder reaction. Thirdly, the rigid template also minimizes the non-productive conformations of

the bound reactants. Flexible templates have more non-productive conformations in which the substrates are widely separated.^{21b} Fourthly, because of the careful design of the hydrogen bonding pattern of the binding sites, inhibitory binding is prevented. As has been shown in chapter 2 (section 2.3), the templates could bind two molecules of a single substrate, which deactivates the template, if an unsuitable bonding pattern were chosen. Finally, the most important reason for the more efficient catalysis achieved is probably because the Diels-Alder reaction is more suitable for catalysis by this simple template method than other reactions, or more clearly, the simple linear template is very suitable for stabilising the transition state of the Diels-Alder reaction.

For every reaction, the correct direction of approach of each reactant molecule to form the transition state is essential. Any condition which facilitates the formation of the transition state will accelerate the rate of the reaction, or vice versa. Most molecular replication systems and some artificial enzymes use linear templates. These simple templates can only bring substrates together from head to head or side by side. However, for many reactions, the formation of the transition states is by reactants approaching each other from a direction other than head-to-head. For example, phosphate esterification is known to go through a pentacoordinate intermediate. The geometry of this intermediate is a trigonal bipyramid, in which the dsp^3 hybridization scheme provides five non-equivalent bonding orbitals. The three shorter bonds, which are called equatorial, lie in a plane, while two longer bonds, which are called apical, are perpendicular to that plane from opposite directions. During the esterification reaction of an initially tetrahedral phosphate, the entering group would approach in a perpendicular direction to the plane containing three ligands so that it will be perpendicular to the plane of the equatorial atoms in the pentacoordinate intermediate and it will be

attached by the long bond of an apical ligand. Similarly, the leaving group can only depart from an apical position (Figure 4.19). The organophosphate reaction does not necessarily proceed by this simple

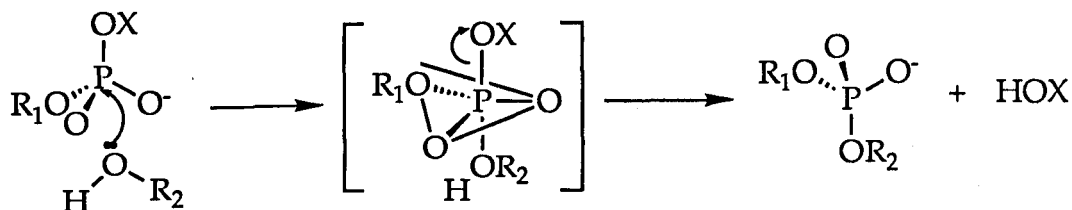


Figure 4.19

displacement mechanism since in many cases, a process called *pseudo-rotation* occurs in the pentacoordinate intermediate before the leaving group departs. This process exchanges equatorial and apical groups so that an appropriate leaving group can become apical if it is initially equatorial (Figure 4.20). After *pseudo-rotation* two equatorial bonds become apical bonds and two apical bonds become equatorial bonds. Because groups can only enter or leave from apical positions, the pseudo-rotation allows former equatorial groups to leave. The driving force for the process is the transformation of a good leaving group from an equatorial to an apical geometry. This pseudo-rotation allows a group to leave from any position so that the reaction becomes less orientation demanding.

The S_N2 reaction is another process with a well defined transition state. The nucleophile attacks the substrate molecule from the side opposite to the leaving group, with bond formation occurring simultaneously with bond breaking between the carbon atom and the

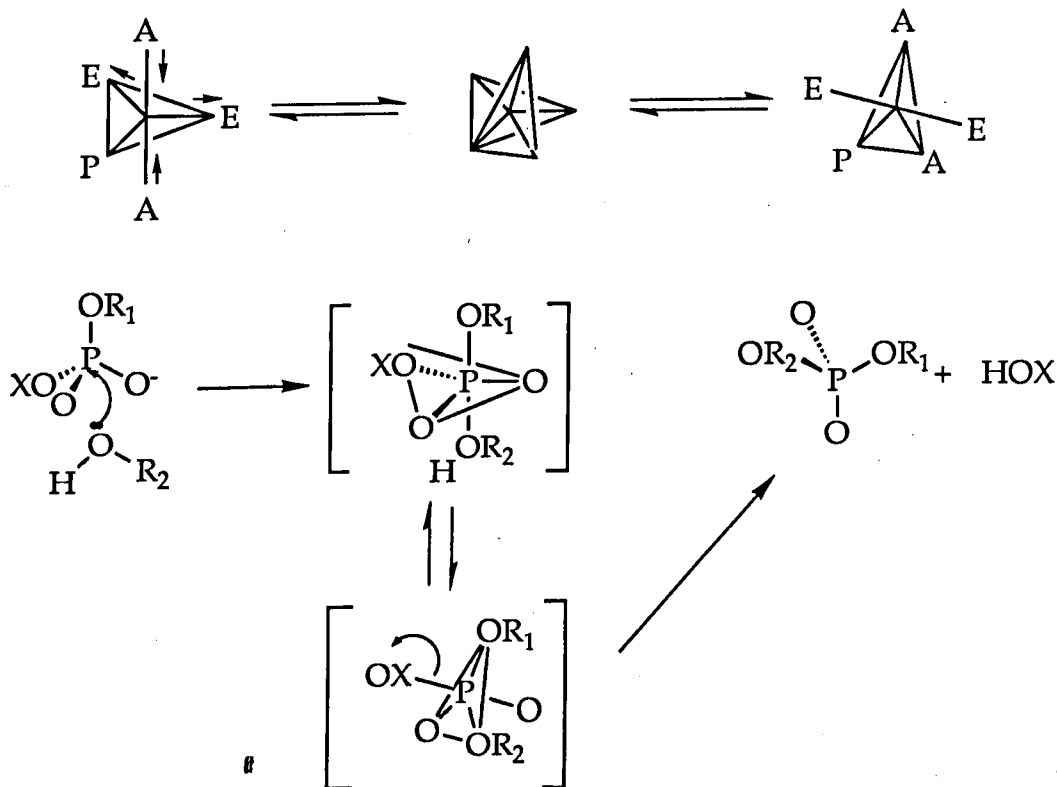


Figure 4.20 *Pseudo-rotation in phosphate esterification*

leaving group (Figure 4.21). The transition state also involves trigonal bipyramidal geometry at a pentacoordinate carbon. The nucleophile and leaving group are both coordinated to the central carbon in the transition state and the leaving group leaves from the opposite direction to the attacking group. The central carbon returns to tetrahedral structure with inversion of configuration, no *pseudo-rotation* can occur in the transition state, so the leaving group can only leave from the opposite direction to

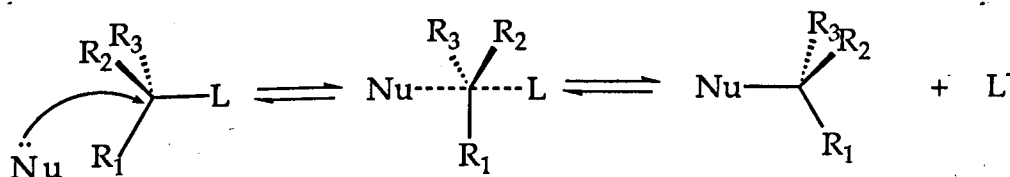


Figure 4.21 The transition state of S_N2 reaction

the attacking group. Consequentially, the S_N2 reaction is more orientation demanding than the esterification of phosphate. Obviously, if the template brings the substrates together from directions which do not match this backside attack, it will have less catalytic effect. This is possibly the key reason for the difficulty in designing an efficient template for the S_N2 reaction. In the S_N2 case,^{21b} even if the reaction complex 25 has the non-productive conformation similar to that of an intramolecular reaction, the rate enhancement is only 12 folds which is still far lower than the 5×10^3 times of the intramolecular reaction which is geometrically favoured (Figure 4.22).

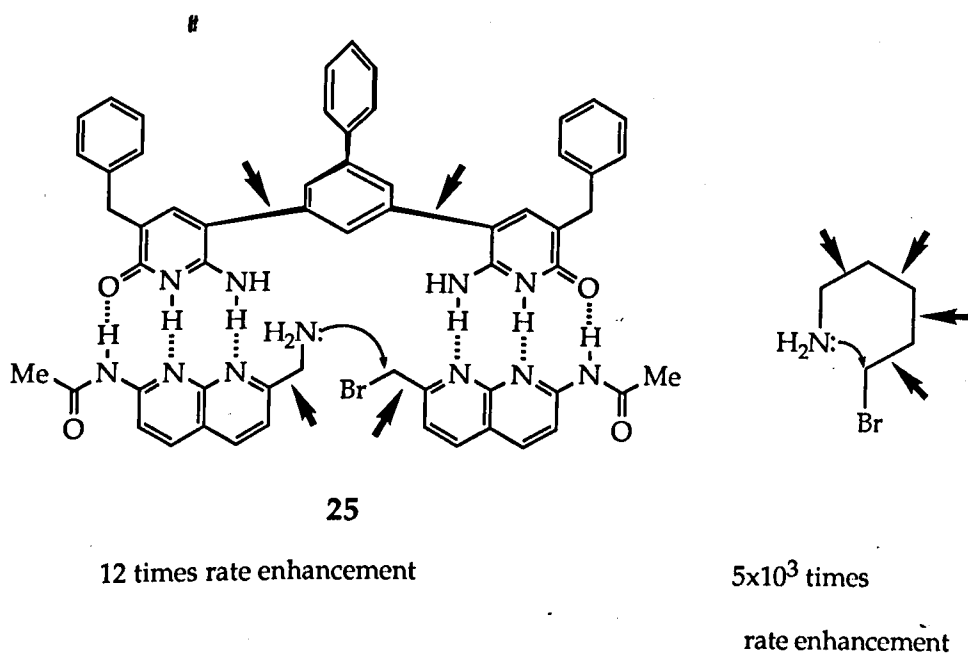
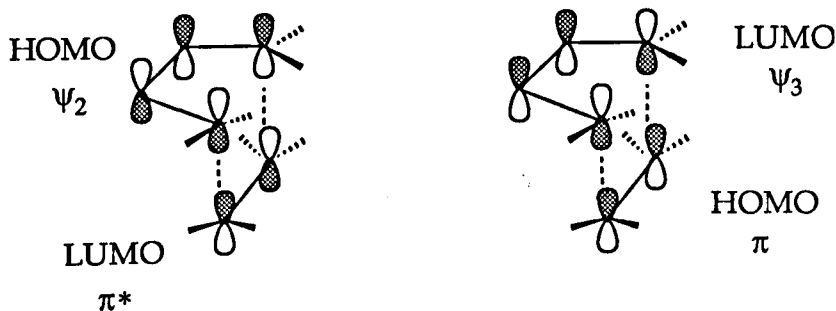


Figure 4.22

For the Diels-Alder reaction, the geometrical demands of the transition state are completely different from these two reactions. According to frontier orbital theory, the best orientations for the Diels-Alder reaction are those in which there is maximum overlap between the π orbitals of ene and diene, i. e.,



so that HOMO/LUMO interactions are maximised.⁷² Consequently, ene and diene need to approach each other suprafacially and as long as the two reactants are able to reach this suprafacial position, it does not matter how the reactants approach each other. Simple linear templates can bring two reactants from a head to head relationship to meet the suprafacial orientation required for the Diels-Alder reaction so that big rate enhancements can be observed. Sander's work seems to support this point of view. The porphyrin trimer template catalyses the Diels-Alder reaction very efficiently (see section 2.4 chapter 2)^{33a} and it can also catalyse the acyl transfer reaction with similar efficiency.^{33c} The acyl transfer reaction is another type of reaction which should be catalysed efficiently by a simple template because formation of the transition state is not too geometrically demanding. The attacking group could approach the carbonyl group from either of side of its sp^2 plane to form a tetrahedral intermediate (see Figure 4.23). Other group have also demonstrated efficient templated acyl transfer reactions.^{19,20}

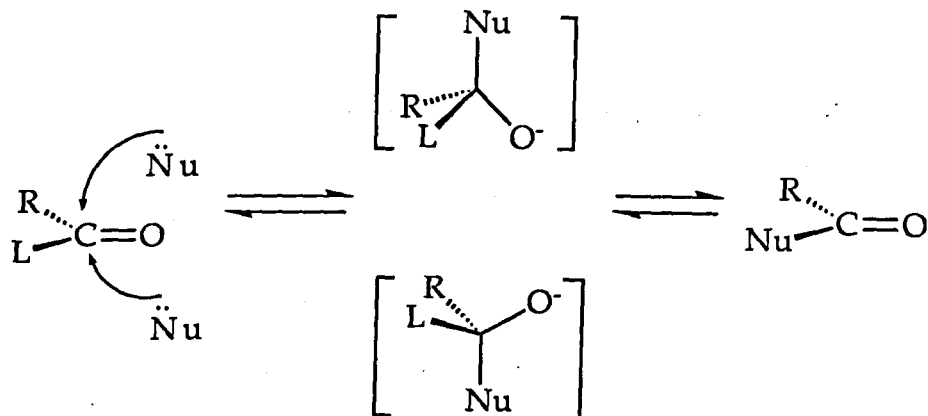


Figure 4.23

4.5 Future Work

The immediate future work involves exploration of the stereochemistry of the replication process. It has been shown that during the replication process, there were some stereoisomers involved. To determine whether the template is chirally selective, the replicating process would have to be conducted in a chiral environment. For example, the Diels-Alder reaction could be carried out by using the R- or S-naphthyridine-diene 114 to react with the pyridone-ene 81 in the presence of pure R-template. Reaction rates could be examined to see whether the R-template accelerates the reaction of the R-reactant more than that of the S-reactant. Pure chiral reactant and template could be made by using enantiomerically pure 2,4-cyclohexadiene-1-acetic acid 90 which could be obtained by resolving the racemic mixture. Generally, an acid can be resolved by reacting with a chiral amine to form two diastereoisomeric salts. These diastereoisomeric salts can be separated according to their different physical properties, such as solubility and the acid can then be regenerated.

Some other simple dienes would also be used to study the stereoselectivity of simple templates of this type. The large rate enhancement of the Diels-Alder reaction demonstrated in this project makes it possible to have a wide choice of ene or diene, including some of which were previously thought to be too inactive, such as 1,3-cyclohexdiene-1-carboxylic acid **84a** or 2,4-hexadienoic acid which is commercially available. The use of these achiral dienes would reduce the number of product isomers to 4 and they would be easier to examined.

Other reactions may also be used for the study of chiral selectivity of simple templates although the rate enhancement by the template may not as large as that for the Diels-Alder reaction. Two nucleophilic substitution reactions involving amines are good candidates for this study. One is a substitution reaction and the other is ring opening of an epoxide.(Figure 4.24). In both reactions, chiral centre are involved during the reaction. The

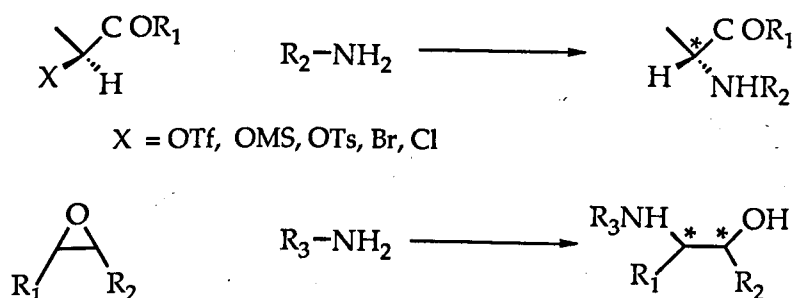


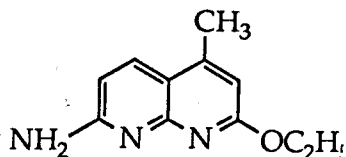
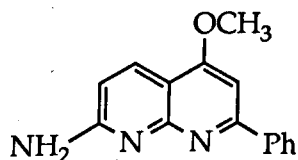
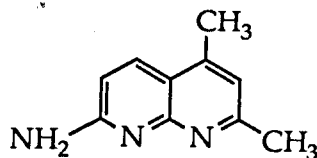
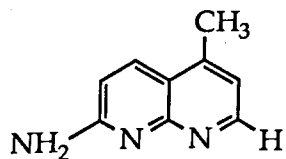
Figure 4.24

chiral selectivity of the template could be assessed by using chiral starting material to compare the ee of the products of self-replication reaction and self-replication reaction in the presence of a homochiral template. The conditions for all these reactions are mild and the reactants are synthetically accessible.

Another interesting question has already been raised. How does the association constant between two reactants influence the catalytic effect of

the template. The relation of three association constants K_1 , K_2 and K_3 in Figure 4.4 has already been discussed. Because the values of K_2 and K_3 are determined by the value of K_1 and they have opposite influences on template catalysis, the question is whether there is a crucial or best value for K_1 which gives the maximum rate enhancement for the replicating process. Although computer modeling can help to give an answer to this problem, the chemical experiment is still essential because correct values of K_2 and K_3 , which are needed for computer modeling, are difficult to determine theoretically. The results of this project have shown that substituents on the 2-position of naphthyridine will influence the association constant of two complementary binding components. Hence an interesting project would be to synthesize a series of aminonaphthyridines with different substitution at the 2-position, to incorporate these into a series of replication systems, and to measure the association constant of each pair of replication components and examine the Diels-Alder reaction of each system. The relationship between the association constant of the two replication components and reaction rate enhancement could then be found and this relationship may be useful for the other design templates.

Some aminonaphthyridine which are synthetically accessible are shown below,



CHAPTER FIVE

A NEW APPROACH TO OPTIMISE IONOPHORES

#

5.1 An Introduction to Combinatorial Chemistry

The traditional procedure for making a good ionophore is the same as for making other useful compounds, that is synthesis, isolation or purification, identification or characterisation and finally the examination of the properties. Although modern technology shortens these procedures, purification is still a laborious, time-consuming and sometimes a frustrating task. Besides, in many cases, the properties of target compounds when they are finally obtained are as not good as expected, although nowadays some molecules can be designed. It has been a long time since chemists tried to investigate mixtures without purification, but recently a new field called 'combinatorial chemistry' has emerged. At the heart of this method is a chemical library which is generated and then screened. This library contains a large array of different molecular entities into which chemical diversity is built by systematic, but random, covalent connections.

Work to generate molecular diversity began in the early 1980's and was done by biochemists. Mario Geysen's group introduced the pin peptide synthesis.⁷³ Using an ELISA-plate with 8 x 12 plastic pins arranged on it, the synthesis of individual peptides on each of these pins was possible. In this way, 96 different peptides per plate (one per pin) could be generated in a relatively economical and time-efficient manner. A year later, Richard Houghten's group in La Jolla introduced the 'tea-bag method' in which multiple peptides are synthesized in small polypropylene tea-bag-like packets.⁷⁴ The field of peptide libraries was accelerated by several independent reports at the start of the 1990s that described different practical approaches for generating peptide libraries. For example, George Smith introduced the 'bio-panning' method which allows for enrichment of a biologically active peptide sequence displayed

on the surface of a bacterio-phage. Later he combined this bio-panning procedure with a combinatorial phage display method (displaying multiple different peptides on the surface of phages) to create a peptide library selection system.⁷⁵ However, the inherent limitation of phage-display methods to only the 20 naturally encoded amino acids as building blocks limited the direct impact of these methods in drug design and development. Therefore, the appearance of two alternative synthetic chemical methodologies in the same issue of Nature in 1991 ⁷⁷ excited immense interest among medical and synthetic organic chemists.

Solid phase synthesis, which was first introduced by R B Merrifield in 1963,⁷⁶ was a revolution for peptide synthesis. In this method, the peptides are made on small polystyrene beads instead of by traditional solution synthesis. To find a good peptide that binds with high affinity to a biological acceptor (enzymes, antibodies), Lam et al used the solid phase method and systematically made a peptide library which contained millions of peptides with the entire collection representing the universe of possible random peptides in roughly equimolar proportion.^{77a} It is not enough to just use a random mixture of activated amino acids in a peptide synthesis protocol, because the widely different coupling rates of different amino acids will lead to unequal representation and because each bead will contain a mixture of different peptides. What they did is that in step 1, they put equal amounts of beads into several reaction vessels (the number of vessels used depending on how many amino acids used), then they added different amino acids into each of the different vessels so that only one particular amino acid is added to each vessel. In step 2, after the coupling reactions were finished the beads from all the reaction vessels were combined and then divided equally again into the reaction vessels followed by adding only one kind of amino acid to each vessel followed by the second peptide coupling; Repeating the above steps gave a random

library of oligopeptides. Figure 5.1 shows a process for making a tripeptide library. By this procedure a library containing up to 2,476,099 (19^5) individual pentapeptides of differing sequence, with only one peptide attached to each bead, was made after 5 steps by using 19 amino acids. This method is now called the 'split synthesis method'. Then they developed a

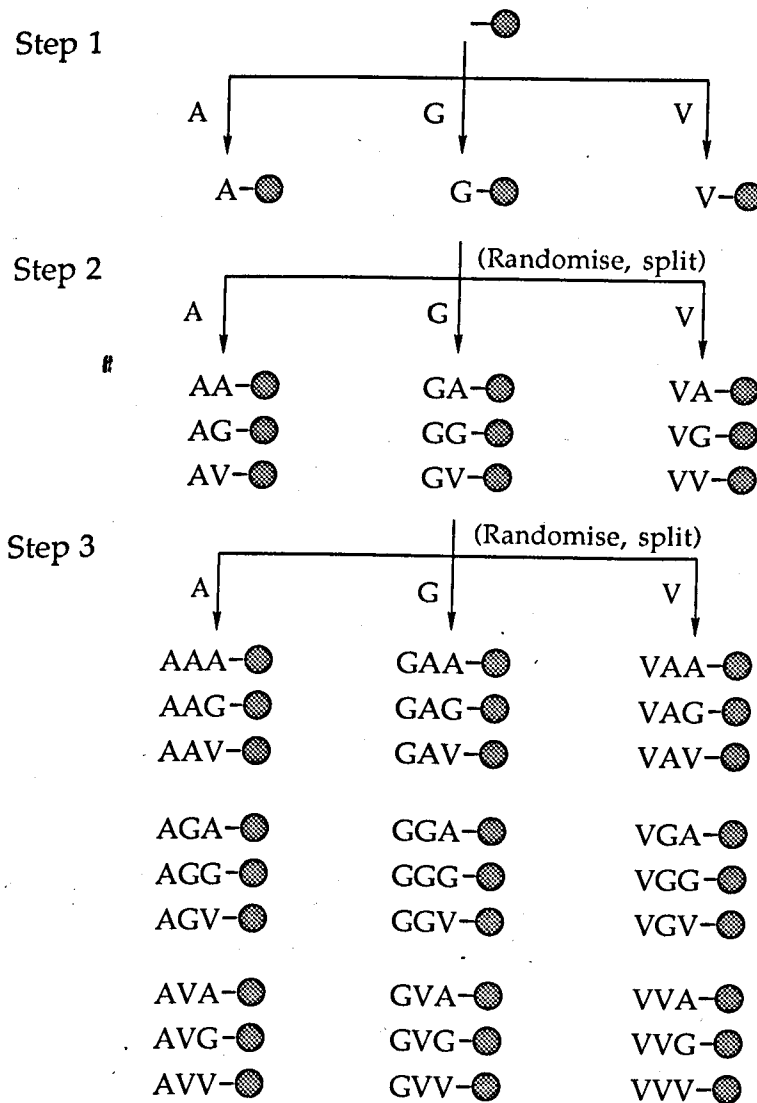


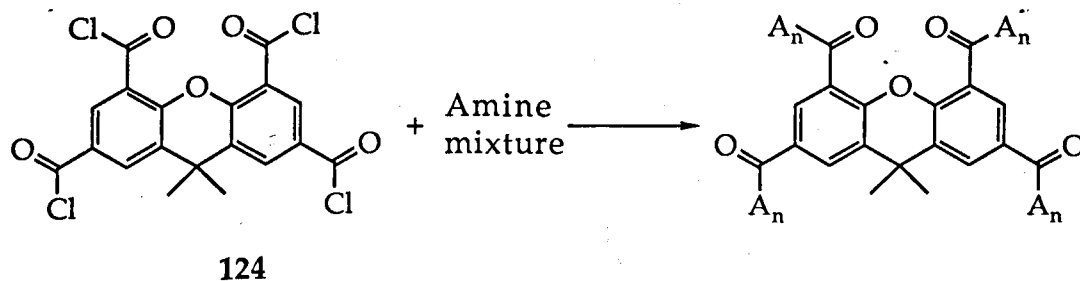
Figure 5.1 An example library containing 27 different tripeptides with three different amino acid generated by a solid phase 'split synthesis method'

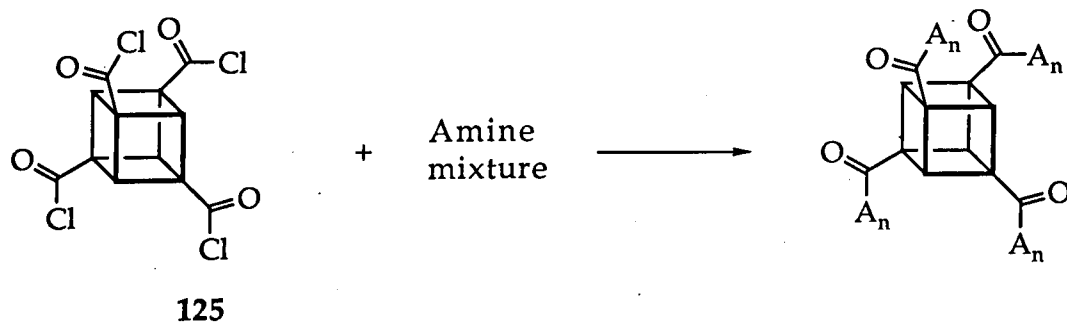
rapid method for screening the library to find solid beads containing peptides able to bind to any particular acceptor molecule. The acceptor molecules were coupled to an enzyme (alkaline phosphatase) or to fluorescein and added in soluble form to the peptide library. Typically, the beads linked with peptides which can bind the acceptor were intensely stained and were visible to the naked eye and easily seen with a low-power dissecting microscope against a background of colourless, nonreactive beads. With the aid of tiny forceps coupled to a micromanipulator, the intensely stained beads could be removed for analysis by removing the acceptor complex and then determining the peptide sequence contained on the beads. A library containing several million beads each of which contains a peptide⁶ could be screened in an afternoon. This work obviously demonstrates a powerful new tool for the study of molecular recognition in biochemistry.

However, if the biological target is insoluble it is necessary to present the library of compounds in solution. This led Houghten to develop an iterative deconvolution approach.^{77b} He used a similar split synthesis process, based upon tea-bag chemistry, and developed a synthetic scheme for generating soluble peptide libraries. Omitting two amino acids from the naturally encoded 20 amino acids, Houghten synthesized 324 (18^2) different hexapeptide mixtures with the first two amino acids defined, $\text{Ac-O}_1\text{O}_2\text{XXXX-NH}_2$, in which Ac is an acetylated N terminal and NH_2 is an amidated C terminal, O_1 and O_2 represent two defined amino acids and X's represent randomised amino acids from the 18 selected amino acid building blocks. Thus, each of the 324 libraries consisted of more than a hundred thousand peptides (18^4). Because all of the compounds in a library are dissolved in the solution, only the total activity of a library towards a biological target can be detected after first step of the screening. Therefore, only the most active library can be selected.

That means that only 2 positions of the most active peptide have been defined (O_1 and O_2). To find out the optimum sequences of the other four positions, XXXX, sub-libraries need to be made. So the second step, following the iterative pattern, was to prepare 18 new libraries $O_1O_2O_3XXX$, where now O_1O_2 are based upon the best results obtained from the previous experiment and O_3 was varied systematically with X again being randomised among the 18 selected amino acids. This iterative scheme was followed until the sixth and final residue of the best active peptide was identified. Although this method requires considerably more effort and manpower, and larger amounts of peptides than Lam's method, it produces soluble peptide libraries which can be used directly in a series of already existing assays.

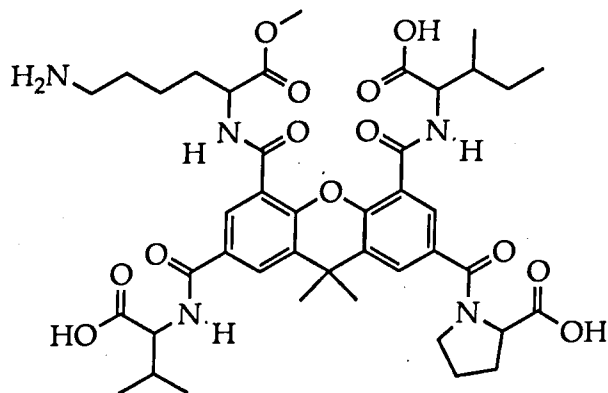
After these two reports, there have been many other reports about how to generate and screen peptide libraries.⁷⁸ Some libraries for oligonucleotides made by array synthesis have also been reported.⁷⁹ But most of them used similar chemical diversity in their libraries based upon the sequence of amino acids in peptides or nucleotides in oligonucleotides, called linear diversity. However, Rebek's group developed chemical diversity of amino acids into three dimensions⁸⁰ because the activity of some peptides is not only decided by the sequence, but also by their conformation. They used a xanthene derivative **124** and a cubane **125**



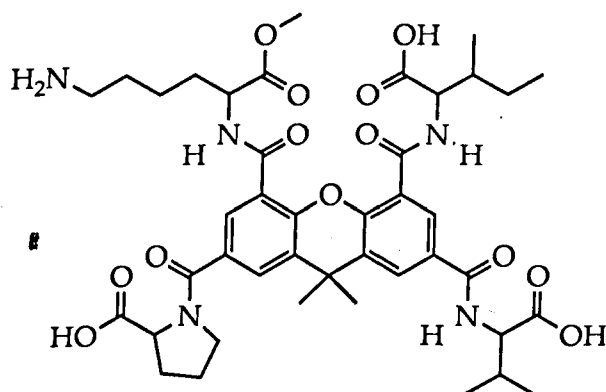


which possess multiple reactive functional groups (acid chloride groups) as core molecules and let them react with a mixture of small reactive organic building blocks (amines) to give libraries which contain compounds with a random selection of amines arranged randomly on the core molecules. The randomness of the libraries is based on the assumption that all amines react with acid chlorides at a similar rate. Thus with up to twenty-one different amines, predominantly L-amino acid derivatives and small heterocycles, two soluble libraries were made of 97,461 different compounds using the xanthene core molecule 124 and over 16,611 compounds using the cubane core molecule 125. (The diversity of the library decreases with increasing symmetry of the core molecule).^{80a}

The screening procedure Rebek used was based on a trypsin assay as performed by Houghten's group. Each library was examined for activity as a protease inhibitor by enzymatic study. According to screening results, inactive core molecules and amino acids were eliminated and possible good amino acids were divided into groups to make sub-libraries. After four steps, two compounds 126 and 127 were discovered as micromolar inhibitors of trypsin from a mixture of tens of thousands of possibilities.^{80b} Interestingly, compound 126 is more active than compound 127 although they are very similar. This matches the original assumption.



126



127

This successful experiment shows that the methodology of combinatorial chemistry can be used not only for compounds like peptides, but also for other small molecules.

5.2 An Introduction to Calixarenes

Calixarenes are a family of macrocyclic host compounds for ions and small molecules made up of phenol units linked by methylene bridges.⁸¹ (Figure 5.2) The synthetic methods for making different calixarenes of different cavity size have been established. The simplest way to obtain calixarenes is condensation of phenols with formaldehyde catalysed by base.⁸²

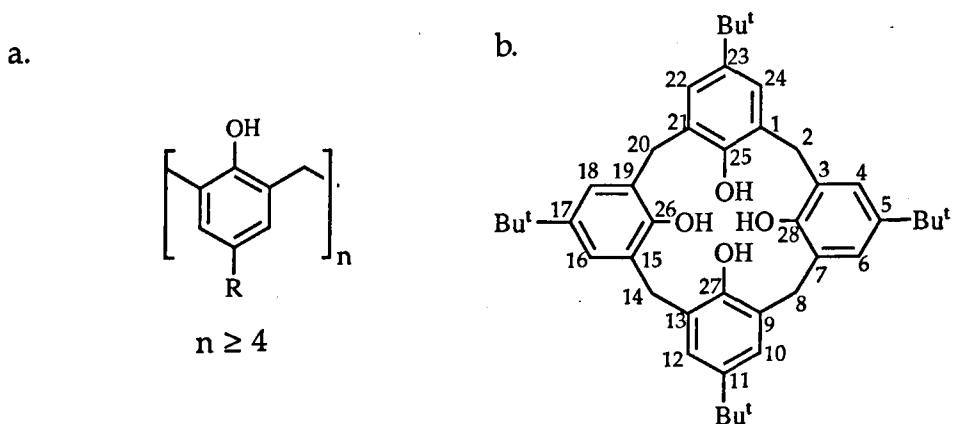


Figure 5.2 a. Simplified structure of calixarenes. b. 5,11,17,23-tetra-*tert*-butyl-25,26,27,28-tetrahydroxycalix[4]arene. The terms "upper rim" and "lower rim" used in the text refer to the R positions and HO positions respectively.

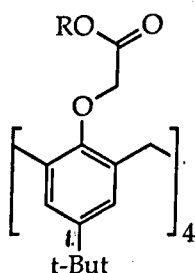
Host-guest chemistry related to calixarenes has recently been developed. Besides their attractive architecture, the unique structure of calixarenes provide both an upper rim and a lower rim for modification for various purpose. Several groups have succeeded in demonstrating that calixarenes serve as an excellent "platform" for the design of a receptor site for the specific binding of guest atoms and molecules. The first demonstration of the complexing abilities of the unmodified calixarenes was reported by Izatt in 1983 who discovered that although they are ineffective cation carriers in neutral solution, in strongly basic solution they transport alkali metals.⁸³ Gutsche and Shinkai, have found that water-soluble calixarenes can form a variety of inclusion complexes with organic guests in aqueous solution,⁸⁴ and Ungaro, McKerverey and Chang have studied calixaryl esters which show high alkali metal ion affinity.⁸⁵

Examples of the industrial applications of calixarenes ⁸⁶ are the recovery of caesium and uranium,^{86b,c} separation of neutral organic molecules,^{86d} and applications in catalysis.^{86e,f,g,h} These discoveries

suggest that an intensive study of calixarenes has potential for new applications.

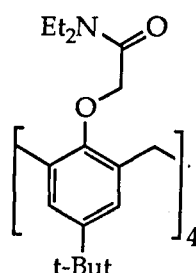
Published reports show that many factors affect the complexation ability and selectivity of calixarenes.

Like other macrocyclic acceptors, the size of calixarene cavity plays an important role for their coordinating property. It has been shown that the calix[4]aryl esters **128** and **129** exhibit remarkably high selectivity



128 R = Et

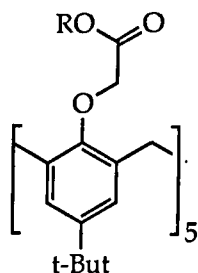
129 R = Me



130

towards sodium ^{85b,87} comparable to cryptand **222**. This is attributed to the size of the ionophoric cavity composed of the four OCH₂CO groups, which is similar to the ionic radius of Na⁺. Similarly, X-Ray crystal structures of the calixarene tetraamide **130** and its 1:1 KSCN complex show the cation completely encapsulated in an eight-oxygen antiprism.⁸⁸ The hexameric, calix[6]arene esters favour the larger cations with preference for Cs⁺, reflecting the larger receptor cavity.⁸⁹

Although there are many examples of calix[4], [6] and [8]aryl ionophores, there are few examples of ionophores based upon calix[5]arene^{90a} in the literature and it has recently become a matter of interest to determine how the calix[5]arene derivatives behave. Accordingly, the synthesis and complexation properties of two calix[5]aryl esters **131** and **132** has been reported^{90b} and it has been shown that both



131. R = Et

132. R = *t*-But

pentamer esters are much more effective in extraction of cations than either their tetramer or hexamer counterparts, favouring the larger cations with little discrimination between K^+ , Rb^+ and Cs^+ .

Along with the ring size, conformation is another important aspect of the complexation properties of calixarene derivatives because of their unique structure.⁶ In the case of calix[4]arene there are four possible conformational isomers (Figure 5.3), cone, 1,2-alternate, partial cone and 1,3-alternate, which are interconverted by rotation of the phenol groups

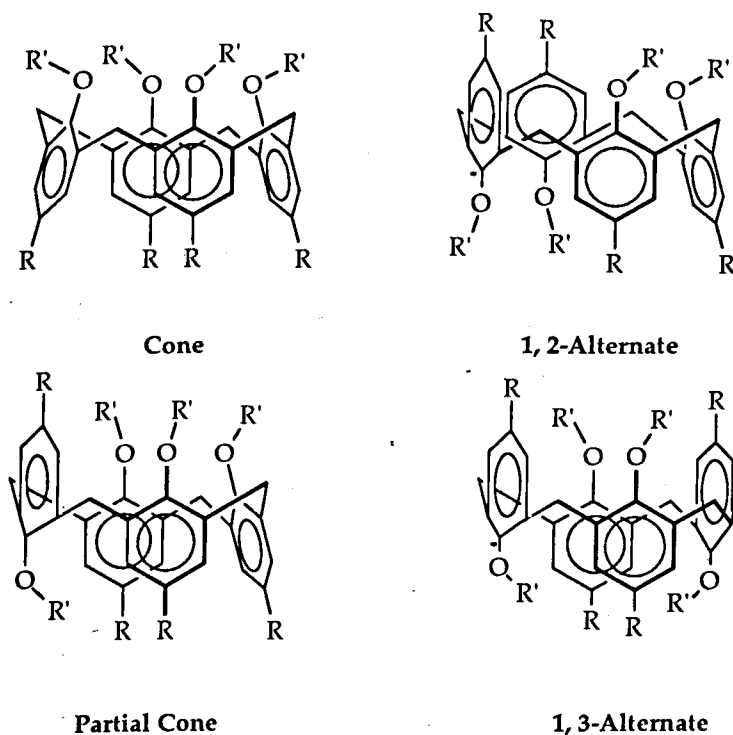
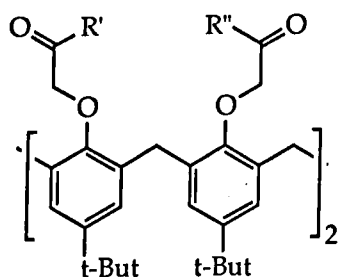


Figure 5.3 4 types of conformation of calix[4]arene

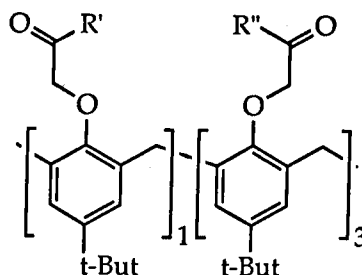
bonded to the bridging methylene units. Usually, the cone conformation gives the best complexing ability. Early experiments showed that unmodified calixarenes are not effective cation carriers although they are free to adopt all conformations by free rotation of the phenol rings. The introduction of four ester, amide or keto ligating functional groups on the phenolic hydroxy groups of *p*-*tert*-butylcalix[4]arene fixes the macrocycle in the cone conformation and these ligands show complexing properties comparable with those of cryptands and have selectivity towards cations with high charge density such as Na⁺, Ca²⁺ and lanthanides. The calix[6]aryl esters exhibit a broader ion selectivity probably because of the flexibility of the calix[6]arene framework. The conformational freezing of *p*-*tert*-butylcalix[6]arene has been achieved from the introduction of amide and ester binding groups to the symmetrical 1, 3, 5-trimethoxy-*p*-*tert*-butylcalix[6]arene fixing it in the cone conformation.^{89c} The relationship between ring size and ion radius mentioned previously requires the cone conformation for complexation of cations. Recently, the synthesis and ion selectivity of all four conformational isomers of calix[4]arene ester **128** has been reported.⁹¹ Investigation by two-phase solvent extraction has established that the cone conformer shows Na⁺ selectivity, whereas the remaining three conformers show K⁺ and Cs⁺ selectivity. The 1,3-alternate conformation **128** is less sterically crowded than cone-**128**, as the ionophoric cavity consists of only two ester groups, and it displays high K⁺ and Cs⁺ binding.^{91c} Interestingly, it can be shown that 1,3-alternate-**128** can form both a 1:1 and a 2:1 metal/calixarene complex and the two metal binding sites display negative allostericity. The partial cone-**128** skeleton shows poor ionophoricity, probably because the inverted phenol unit sterically interferes with the binding of a cation. The 1,2-alternate-**128** is also a poor ionophore because of two defects in the ionophoric cavity in that the flattened ester groups do not act as efficient ligands and two

proximal ligands are not as effective as two distal ligands as in 1,3-alternate-128. Thus, the metal selectivity of ionophoric calixarenes can be varied not only by a change in ring size, but also by a conformational change and one can realise various metal selectivities by a careful combination of the two.

As well as conformational variation,⁹² substitution variation is another way of realising the potential of calixarene ionophores. Chemically modified ionophoric calix[4]arenes, such as 133-136, which include derivatives with more than one type of functionality around the calix, have been studied by McKervey et al.⁹³ Derivatives with mixed ligating functional groups at positions 1 and 3 of the four equivalent phenolic groups^{87b} have been used to construct new ion receptors with 133 showing a high affinity for Ag⁺.



133. R' = NEt₂, R'' = OEt



134. R' = OH, R'' = OEt

135. R' = NEt₂, R'' = OEt

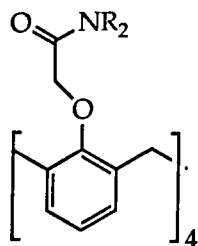
136. R' = OEt, R'' = OCH₂C≡CH

The calix[4]arene tetraethyl ester 128 is hydrolysed under mild conditions with the loss of only one ester group⁹⁴ to form the monoacid triester 134. Such substituent variation in the ester podands of these

calixarenes can have a significant effect on cation binding selectivity, for example, the one amide group in **135** is sufficient to reduce Na⁺ selectivity by increasing the binding of K⁺. Although all the derivatives that have been studied have the cone conformation in solution, it is likely that the substituents influence the disposition of the ligating atoms around the hydrophobic cavity and therefore their binding ability as with **134** and **135** which exhibit low ability for cation extraction, suggesting poor pre-organisation of the binding sites.

So, to make a good calixarene ionophore, all those three factors require to be considered and usually, in the selection procedure, two of them are fixed and only one factor is variable. Comparing these three factors which influence the capability of coordinating and selectivity, substituent effects can obviously be more easily converted into chemical diversity and more easily built into libraries if it is chosen for the selection of good ionophores by combinatorial methodology. Rebek's work, especially some similarity between the activity of peptides affected by the arrangement of the amino acids in the space and the cation binding ability of calixarene molecules affected by their side chains, gives us inspiration to introduce the methodology of combinatorial chemistry to the selection of good ionophores based upon a calixarene core.

A calix[4]arene system **137** with a cone conformation was chosen to build up libraries which contain a mixture of the derivatives of amide calixarenes with different side chain. One more reason for choosing **137** is that the calixarenes without t-butyl groups on the upper rim have not been paid as much attention as their t-butyl counterparts, and analogues of **130**, which have shown to be good ionophores for Na⁺. It is therefore of interest to investigate a library based upon **137** for its ability to bind Na⁺.



137. R = aliphatic or aromatic, cyclic or acyclic substituents.

5.3 A Unique Screening Method

Extraction of cations by ionophore libraries looks like a counterpart of biological assay for soluble peptide libraries. Using a whole library to do the extraction study will give a total result for the mixture and it has already been shown that this kind of method requires several steps of elimination so that many sublibraries need to be made. However, for ionophore study, mass spectrometry is possibly an alternative simple and accurate method for the assay of selectivity and complexation.

Since its inception, fast atom bombardment mass spectroscopy (FAB MS) has gained universal usage as a soft ionization technique⁹⁵ and it was quickly applied to the study of the binding of alkali metals to crown ethers. Unlike previous techniques, the FAB method involves bombardment of substances on a surface with fast atoms (usually xenon or argon) and it results in ionized species being desorbed without being volatilised. R. A. W. Johnstone's group in 1983 did pioneering work using FAB MS for assay of the binding capability of crown ethers. They made an assumption⁹⁶, by considering FAB ionisation mechanisms of an equilibrium or non-equilibrium nature, that the observed mass spectral peak heights for desorbed ionic species should be proportional to the concentrations of these species in solution, which could be expressed by the following equation:

$$C_{\text{complex}} = t \cdot p \quad (5.1)$$

where C_{complex} is the concentration of crown ether-cation complex in solution, p is the peak height observed in the mass spectrum at the m/z value for the crown ether-cation complex and t is a proportionality constant, termed the "transfer coefficient". To examine this assumption they explored the relation between the concentration of crown ether complexes with alkali metal cations and the peak height observed in the mass spectrum at the m/z value for the crown ether-cation complexes $[M+\text{Na}]^+$ or $[M+\text{K}]^+$. Generally, for a metal ion (M_1^+) in equilibrium with a crown ether in solution (eqn. 5.2), the corresponding stability constant (K_1) is given by eqn. (5.3) in which r is the concentration of the crown ether-cation complex and c, a are the respective initial concentrations of crown



$$K_1 = \frac{r}{(c-r)(a-r)} \quad (5.3)$$

ether and metal ion. By inserting values for K_1, c and a into equation (5.3), the concentration of crown ether- M_1^+ complex (r) can be calculated. By comparing a curve, which was obtained by calculating the concentrations (r) for successive addition of potassium chloride with $K_1 = 20,000$ (an approximate value estimated from equilibrium constants for K^+ complexed with 18-crown-6 in methanol and water at 25° and $c = 0.008\text{M}$, each addition increasing the concentration of KCl by 0.001M), with a second curve, which was obtained from observed peak heights in the FAB mass spectrum for 18-crown-6- H^+ at m/z 265 and for 18-crown-6- K^+ at m/z

303 produced under the same conditions as those for the first curve (Figure 5.4), they found that two features of the curves are immediately obvious. Firstly, the variation in peak heights at m/z 303 for the 18-crown-6- K^+ complex is very similar to the calculated variation in concentration for a crown ether- K^+ complex in solution. Secondly, as the peak height for the 18-crown-6- K^+ complex at m/z 303 increases with increasing molar

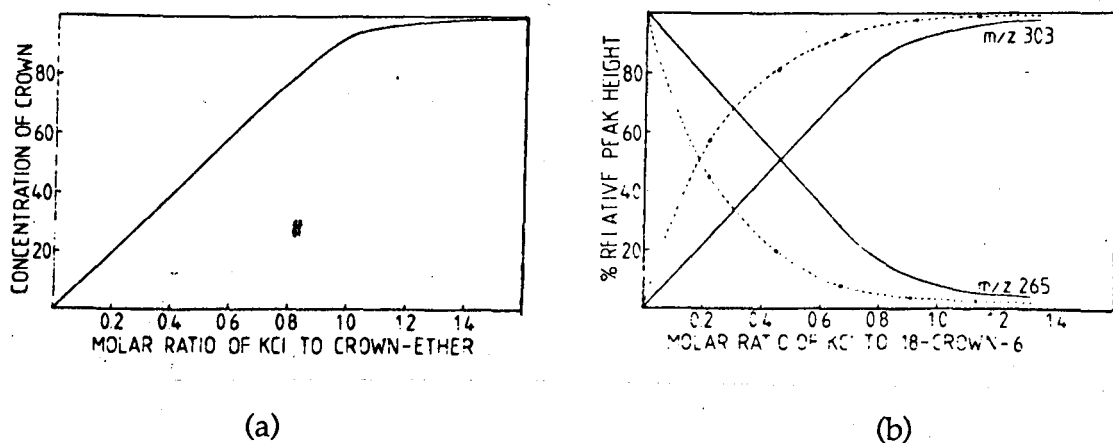


Figure 5.4 (a) Calculated variation in concentration of crown ether $\cdot K^+$ complex using a starting concentration for 18-crown-6 of 0.008 molar and as stability constant $\log K = 4.3$.
 (b) The variations in observed percentage relative peak heights of FAB MS for 18-crown-6. The dotted lines represent the observed experimental data. The solid lines represent corrected data.

ratio of KCl to crown ether, the peak height at m/z 265 corresponding to 18-crown-6- H^+ , decreases and reaches a limiting value when almost all the crown ether is complexed to K^+ . They claimed that these results strongly imply that the FAB technique is capable of giving quantitative information on phenomena occurring in solution. From the cross-over point for m/z 303 and m/z 265 which lies at 50% relative peak height and a molar ratio of 0.5, they further suggested that FAB spectroscopy can be

used to obtain data on stability constants of crown ether-cation complexes if the stability constant or the concentration of crown ether is sufficiently large. To test these calculations, a second experiment was done by treating a solution of dicyclohexyl-18-crown-6 in glycerol with aliquots of an aqueous glycerol solution containing KCl, NaCl and CsCl. After the addition of each aliquot, FAB mass spectral peak heights at m/z 395, 411 and 505 (corresponding to dicyclohexyl-18-crown-6 plus Na^+ , K^+ and Cs^+ respectively) were measured. Comparing the curve of relative peak height against the number of aliquots added with the curve of calculated concentration against aliquots, they found that the variations in mass spectral peak heights for the dicyclohexyl-18-crown-6 complexes of Na^+ , K^+ and Cs^+ correspond very closely to the calculated changes in concentrations of these complexes in solution. In another report published by same group,^{96b} FAB MS was used to examine the complexation selectivity of many kinds of macrocyclic ligands towards different cations. In the experiment, solutions of each macrocyclic ligand dissolved in glycerol-water and a mixed salt solution containing equal amounts of the iodides of lithium, sodium, potassium, rubidium, and caesium was prepared. Before measuring MS data, the ligand solution was mixed with the salt solution so that all the components were present in equimolar ratios. This results in the metal cations competing for a limited number of ligands. The FAB MS results showed that the variation in abundances of ions corresponding to metal cation complexes with each ligand was closely parallel to that expected from published stability constant data. For example, with 12C4 which is a poor ligand for alkali cations, no ions were observed corresponding to complex formation between 12C4 and alkali metal cations; while with the cryptand, C222, complexation was greatest for K^+ and ion abundances of cation-ligand complexes decreased in the order $\text{K}^+ > \text{Rb}^+ > \text{Na}^+$, which is as same as that for the relative

concentrations of these complexes in aqueous solution. All these results suggested that metal cation-ligand complex formation in solution for a wide range of metal cations and many different types of macrocyclic ligands can be assessed rapidly and semi-quantitatively by the FAB technique. Since this pioneering work of Johnstone's group, many groups have used FAB MS as a tool to estimate the selectivity and complexing ability for many kind of ionophores.⁹⁷ Distinct from the work of Johnstone's group where the binding abilities of crown ethers towards different cation were assessed, Medina and co-workers reported the first experiments where the binding ability of different acceptors, which were some ferrocene-crown derivatives and several reference compounds, towards a same cation was measured by examining the relative peak intensities of complexes, $[M+Metal]^+$, to free acceptors, $[M+H]^+$.^{97e} Meanwhile, other groups reported that significant ion intensities for 1:2 complexes ($[M+2Metal]^{2+}$) or 2:1 complexes ($[2M+Metal]$) were observed in the FAB mass spectra ^{97e,f,g} and semi-quantitative assessment has also been made by FAB MS.

From all the above examples, it appears that FAB MS could also be a good method for screening ionophore libraries. Theoretically, if there is no mass overlap in the mixture, MS can detect all compounds and complexes in the libraries and peak heights will give the relative abundance of the compounds in the mixture.

5.4 Library Generating.

Alkylation of hydroxy group on calixarene 138 is a widely used method for making ionophore amide derivatives of calixarene.^{88a} NaH is used so that Na^+ can be a template for making the cone conformation of the alkylated calixarenes and the method also gives a good yield (Figure

5.5). However, this approach has some apparent disadvantages. Firstly, it can not guarantee 100% cone conformation for all of the alkylated species in the libraries and, as has been shown early in this chapter, conformation plays a key role in complexation ability and cation selection. Variation of conformation will cause complications for screening the libraries and make results indecisive. Secondly, the variation of the rate of alkylation of

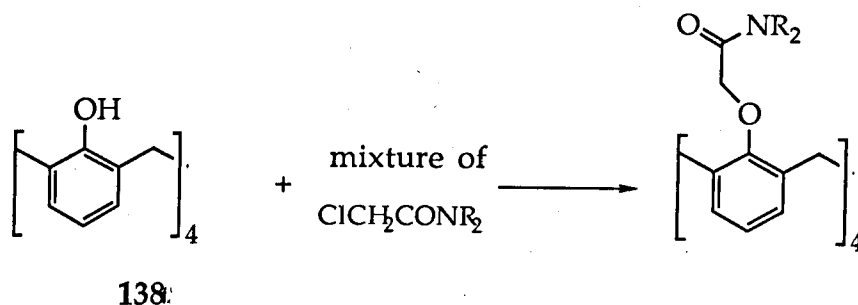


Figure 5.5 Reagents: NaH, NaI/THF

the tetrahydroxycalix[4]arene may be so large that randomness in the libraries can not be ensured. Eventually this method was abandoned although most of the species expected in some libraries made by this method were seen in FAB mass spectra. The method shown by Figure 5.6 is a better method if the precursor of the chloride **139**, calixarene tetracarboxylic acid, can be made. One member of the group had already explored the synthesis of the carboxylic acid by using basic hydrolysis of the

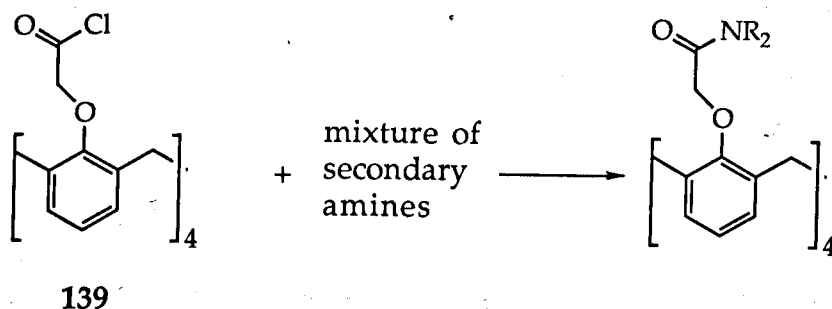


Figure 5.6 A good method for generating the library.

Reaction condition: DCM / $N(C_2H_5)_3$ / r.t.

ethyl esters in water, which is a reported method for making *t*-butyl calixarene carboxylic acids, but ended up with an impure product. So the easily hydrolysed *t*-butyl ester was tried. It was prepared in high yield under the same conditions as those used for making the ethyl ester (Figure 5.7),^{88a} but the NMR spectrum shows that the major product,

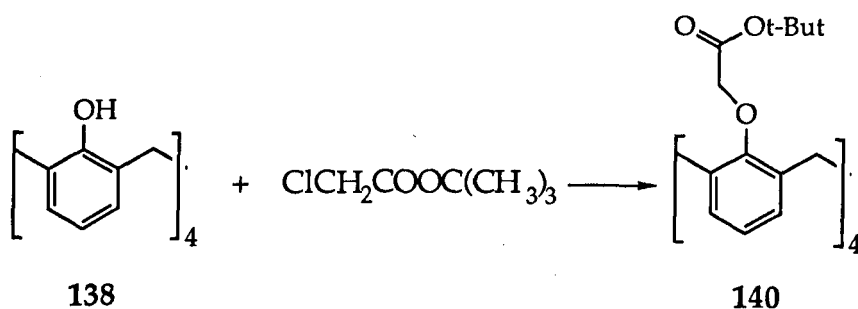


Figure 5.7 Reagent: NaH/THF

which is obtained as beautiful colourless crystals, has the partial-cone-conformation although some product with the cone-conformation was obtained by recrystallization. The *t*-butyl esters are easily hydrolysed by trifluoroacetic acid, so the reaction shown in Figure 5.8 was tried and initially the *t*-butyl ester was used with success. Then the ethyl ester 128, more easily obtained in the cone conformation, was used and hydrolysis

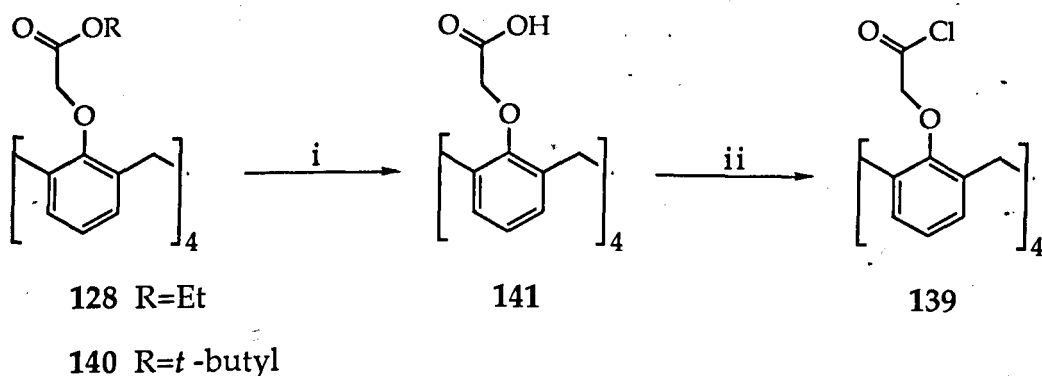
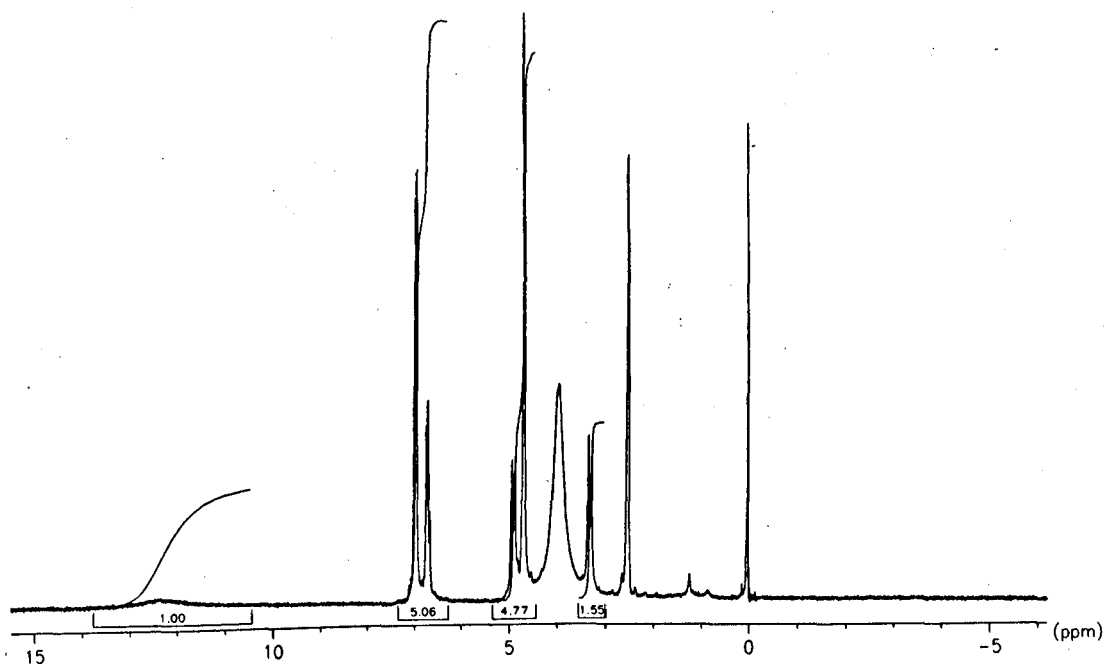
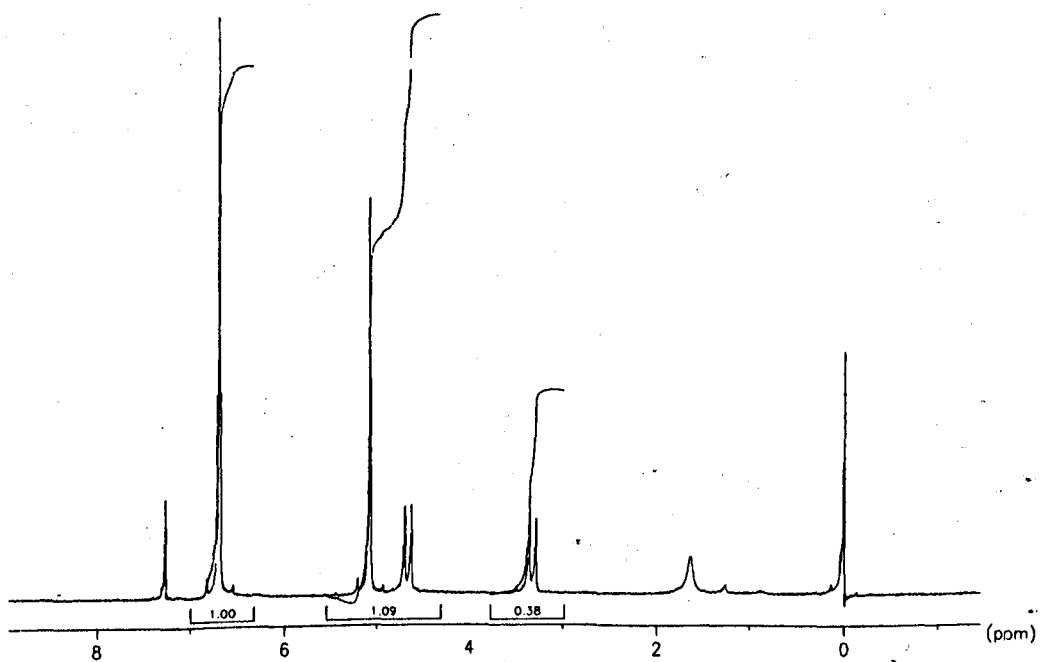


Figure 5.8 i. 70 % trifluoroacetic acid, 80 °C. ii. oxalyl chloride/DCM, r.t.



(a)



(b)

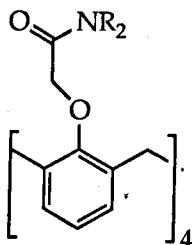
Figure 5.9 (a) ^1H NMR of compound 141. (b) ^1H NMR of compound 139.

with TFA also works well. After recrystallization in the same solvent, the tetracarboxylic acid **141** was obtained as the pure cone-conformation. Figure 5.9a shows the ^1H NMR spectrum of this compound. The corresponding tetra-acid chloride **139** was obtained by reacting the carboxylic acid **141** with excess oxalyl chloride (Figure 5.8) and its ^1H NMR spectrum is shown in Figure 5.9b.

All the libraries used in this project were made under the same conditions as shown in Figure 5.6. By using a mixture of different secondary amines, the libraries were expected to contain a random mixture of different ionophoric calix[4]arenes.

5.5 The Study of Calixarene Libraries by FAB Mass Spectroscopy

The study started with a library **142** having four different simple dialkylamide residues on the side chains of calix[4]arene, the amines used were dimethylamine, diethylamine, dipropylamine and dibutylamine.



142. NR₂ = N(CH₃)₂, N(C₂H₅)₂, N(C₃H₇)₂ or N(C₄H₉)₂.

Theoretically, there should be 55 different compounds in the library **142**, including distal and proximal disubstituted species. Table 5.1 shows all expected species in the library **142** with their masses and their statistical

relative molar ratio. The abbreviations M, E, P and B correspond to the amide substituents R, methyl, ethyl, propyl and butyl respectively and their sequence represents the sequence in which they appear on the periphery of the calix[4]arene system. Because of the overlapping in masses, only 13 different masses were expected in the mass spectrum.

The FAB Mass Spectrum of the library 142 was recorded using a 3-nitrobenzyl alcohol (3-NOBA) matrix with (a) no sodium (b) 10% equivalent of sodium and (c) 30% equivalent of sodium. The purpose of this experiment was to let the ionophore species in the library compete for insufficient sodium so that the relative intensities of peaks corresponding to the masses of both free calixarenes and their sodium complexes could be measured. By comparing the relative intensity of each free compound and its complex ($\text{Intensity [M+H]}^+ / \text{Intensity [M+Na]}^+$) the best ionophores should be detectable. Figure 5.10 shows the FAB mass spectra recorded under the first two conditions while the spectrum made under the third condition is omitted because the spectrum showed total sodium complexation and was not useful for the analysis.

The spectrum a shows free calixarene species as their $[M + H]^+$ peaks. From the spectrum, it is clear that all of the expected mass peaks occur (13 in total, see Table 5.1). This shows the capability of mass spectrometry to detect every species of different mass in a library of limited size. It is also clear, however, that the pattern of peaks deviates significantly from the expected statistical pattern. For example, statistically, the strongest peak should be at mass 933 but it is found at 990 in the spectrum. Theoretically the relative height of the peak at mass 1074 as compared with the peak at mass 933 should be 1:11 but in the spectrum this ratio is only 1:1.8 and the ratio as compared with the highest peak at mass 990 is only 1:2.5. The spectrum also shows some strong fragment peaks.

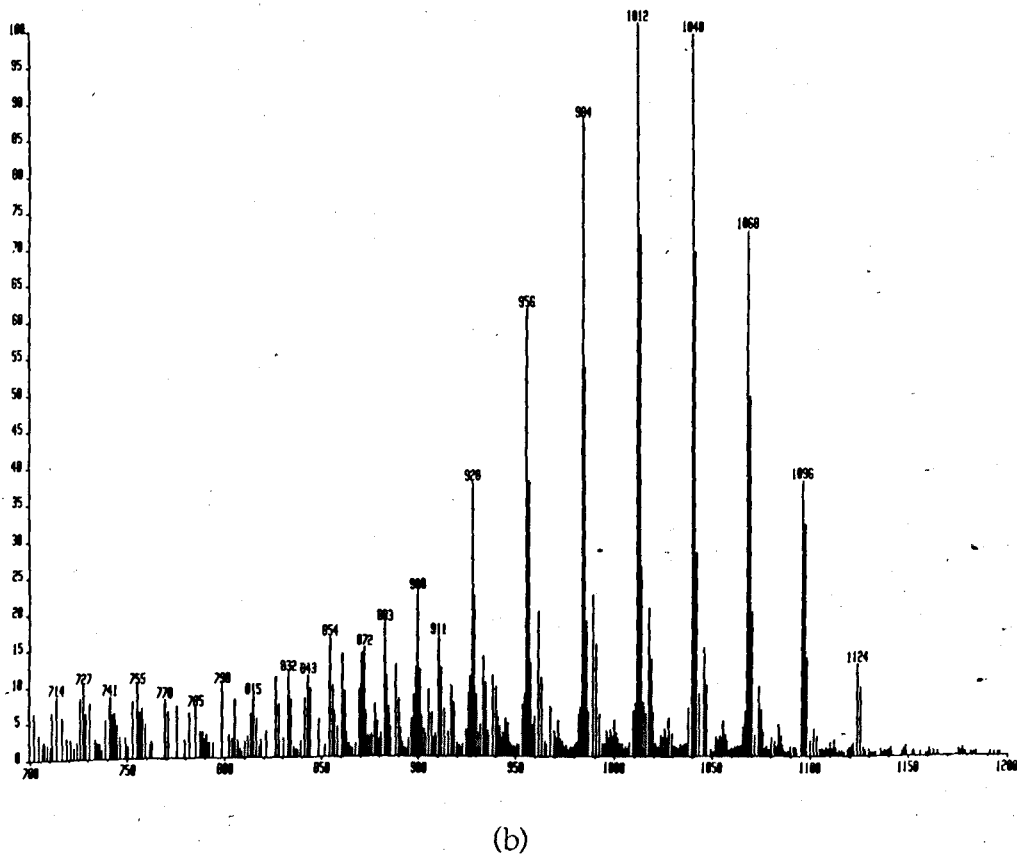
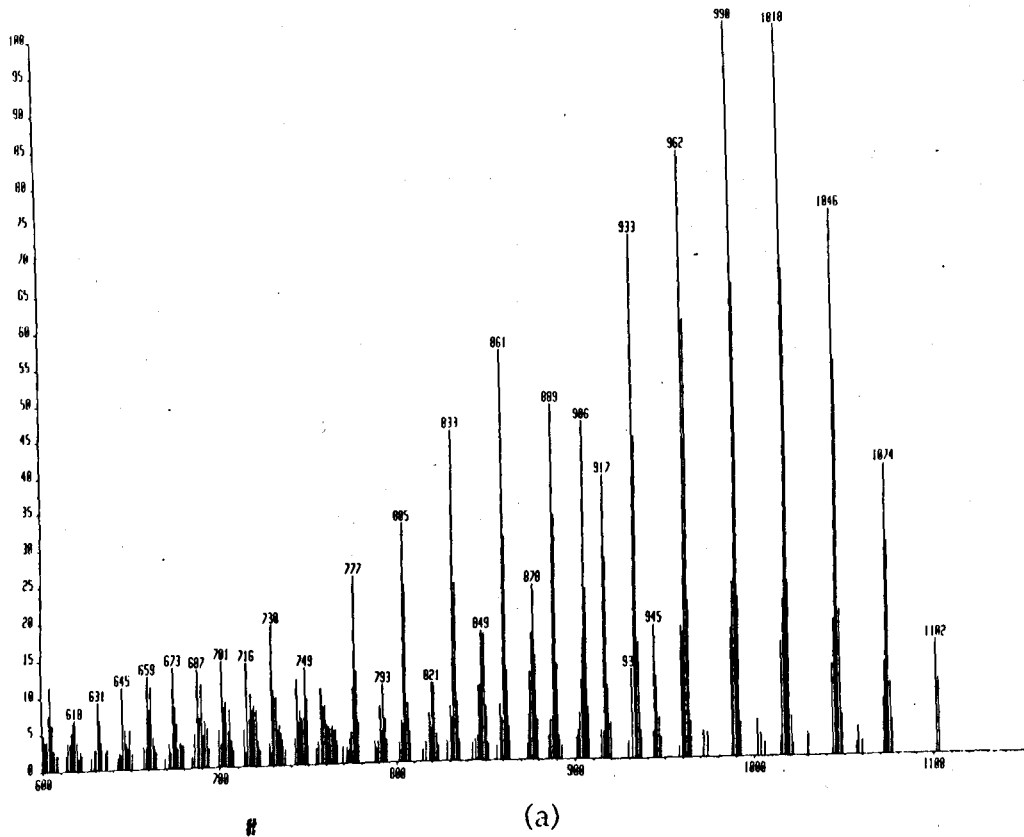


Figure 5.10 The FAB MS of library 142.

(a) without added NaNO₃. (b) with 10% NaNO₃.

Comp. (SMR)	Mass	Comp. (SMR)	Mass	Comp. (SMR)	Mass
MMMM (1)	764	EMEB (4)	904	MPPB (8)	960
MMME (4)	792	EMPP (8)	904	MPBP (4)	960
MMEE (4)	820	EPMP (4)	904	PPPE (4)	960
MMMP (4)	820	MMPB (8)	904	EEBB (4)	988
MEME (2)	820	MPMB (4)	904	EBEB (2)	988
MEEE (4)	848	EEEB (4)	932	EPPB (8)	988
MMEP (8)	848	MPPP (4)	932	EPBP (4)	988
MEMP (4)	848	EEPP (4)	932	MPBB (8)	988
MMMB (4)	848	EPEP (2)	932	MBPB (4)	988
EEEE (1)	876	EMBP (8)	932	PPPP (1)	988
MEEP (8)	876	MEBP (8)	932	EPBB (8)	1016
MEPE (4)	876	MBEP (8)	932	EBPB (4)	1016
MMEB (8)	876	MMBB (4)	932	MBBB (4)	1016
MEMB (4)	876	MBMB (2)	932	PPPB (4)	1016
MMPP (4)	876	EEPB (8)	960	EBBB (4)	1044
MPMP (2)	876	EPEB (4)	960	PPBB (4)	1044
EEEP (4)	904	EMBB (8)	960	PBPB (2)	1044
EEMB (8)	904	EBMB (4)	960	PBBB (4)	1072
				BBBB (1)	1100

Table 5.1 All expected compounds in library 142 with their masses. The figures in brackets are their expected statistical molar ratio (SMR). M, E, P, B represent methyl, ethyl, propyl and butyl, the R substituents in calixarene amides in the library.

In spectrum b, peaks for both $[M + H]^+$ and $[M + Na]^+$ ions were clearly seen with a similar pattern to that in spectrum a. According to the method discussed above, the bigger the ratio of the intensity of $[M + Na]^+$ to that of $[M + H]^+$, the stronger the ionophore. The Intensities of the $[M + H]^+$ and $[M + Na]^+$ peaks and the calculated ratios ($\text{Int } [M + Na]^+ / \text{Int } [M + H]^+$) are listed in table 5.2, which clearly shows that the relative intensities are highest for the medium-mass calixarenes. In other words, the medium-mass species have a stronger capability for binding sodium cations. Because there are too many compounds with the same masses, it

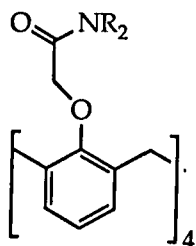
M + H (E. R. I)	Intensity # %	M + Na	Intensity %	Int(M+Na)/ Int(M+H)
765 (1)	0.79	787	1.22	1.54
793 (4)	1.13	815	2.62	2.36
821 (10)	1.12	843	3.47	3.09
849 (20)	1.58	871	4.69	2.96
877 (31)	2.23	899	7.15	3.20
905 (40)	2.86	927	11.76	4.11
933 (44)	4.32	955	19.29	4.46
961 (40)	6.22	983	27.52	4.42
989 (31)	6.98	1012	31.67	4.53
1017 (20)	6.37	1039	31.17	4.89
1046 (10)	4.65	1068	22.70	4.88
1074 (4)	2.98	1096	11.87	3.98
1102 (1)	1.15	1124	3.92	3.40

Table 5.2 FAB MS relative intensities of compounds in library 142.

E. R. I — expected relative intensity

is difficult to say which one is the best ionophore but it does mean that the calixarenes with medium size side chains (ethyl and propyl groups) have optimum binding capability. Is this deduction correct?

To confirm this result, four sublibraries 143, 144, 145, and 146 were made and screened in the same way. Each libraries contains 21 different compounds with three different residues by omitting one of amines used for the original library 142. The mass spectra were recorded under the same conditions as used for library 142. The spectra for the sublibraries with 5% added sodium are shown in Figures 5.11, 5.12, 5.13 and 5.14. Generally, all sublibraries show the expected peaks but with some deviation in intensities from the expected statistical pattern. The relative intensities of peaks^f in all the sublibraries are listed in Tables 5.3, 5.4, 5.5, and 5.6. The initials for side chain are the same as those used in Table 5.1.



143. $\text{NR}_2 = \text{N}(\text{CH}_3)_2, \text{N}(\text{C}_2\text{H}_5)_2$ or $\text{N}(\text{C}_3\text{H}_7)_2$

144. $\text{NR}_2 = \text{N}(\text{CH}_3)_2, \text{N}(\text{C}_2\text{H}_5)_2$ or $\text{N}(\text{C}_4\text{H}_9)_2$

145. $\text{NR}_2 = \text{N}(\text{CH}_3)_2, \text{N}(\text{C}_3\text{H}_7)_2$ or $\text{N}(\text{C}_4\text{H}_9)_2$

146. $\text{NR}_2 = \text{N}(\text{C}_2\text{H}_5)_2, \text{N}(\text{C}_3\text{H}_7)_2$ or $\text{N}(\text{C}_4\text{H}_9)_2$

The data in these four tables match the results obtained from Table 5.2. In Table 5.3, the intensity ratio $[\text{M} + \text{H}]^+ / [\text{M} + \text{Na}]^+$ gradually increases from low mass to high mass because the number of methyl groups gradually decrease in the calixarenes of higher mass. On the other hand, Table 5.6 shows the opposite tendency because this time the poor side chain is the largest one, butyl. In Tables 5.4 and 5.5, there is a similar

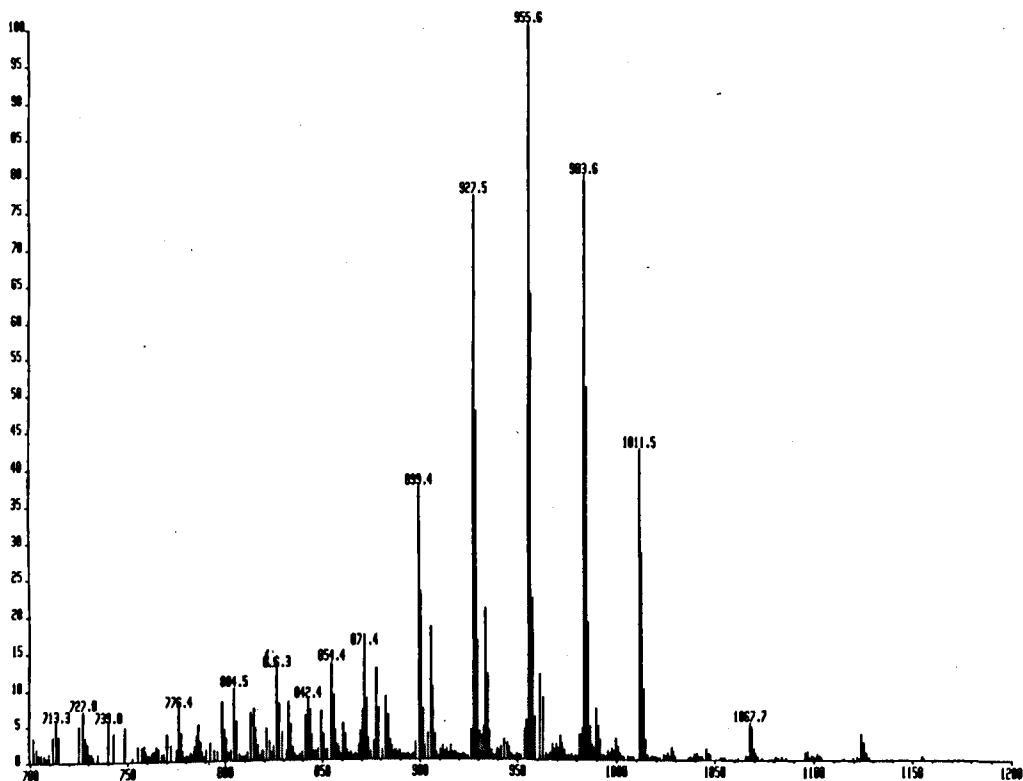


Figure 5.11 FAB MS of Library 143 with 10% NaNO₃.

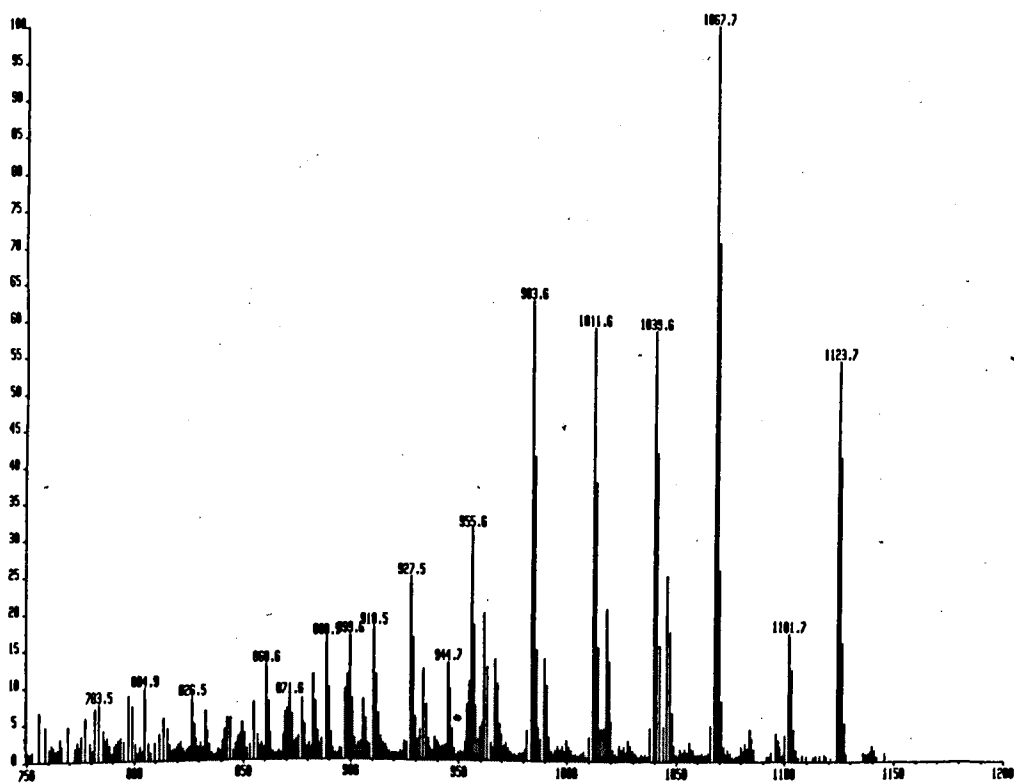


Figure 5.12 FAB MS of Library 144 with 10% NaNO₃.

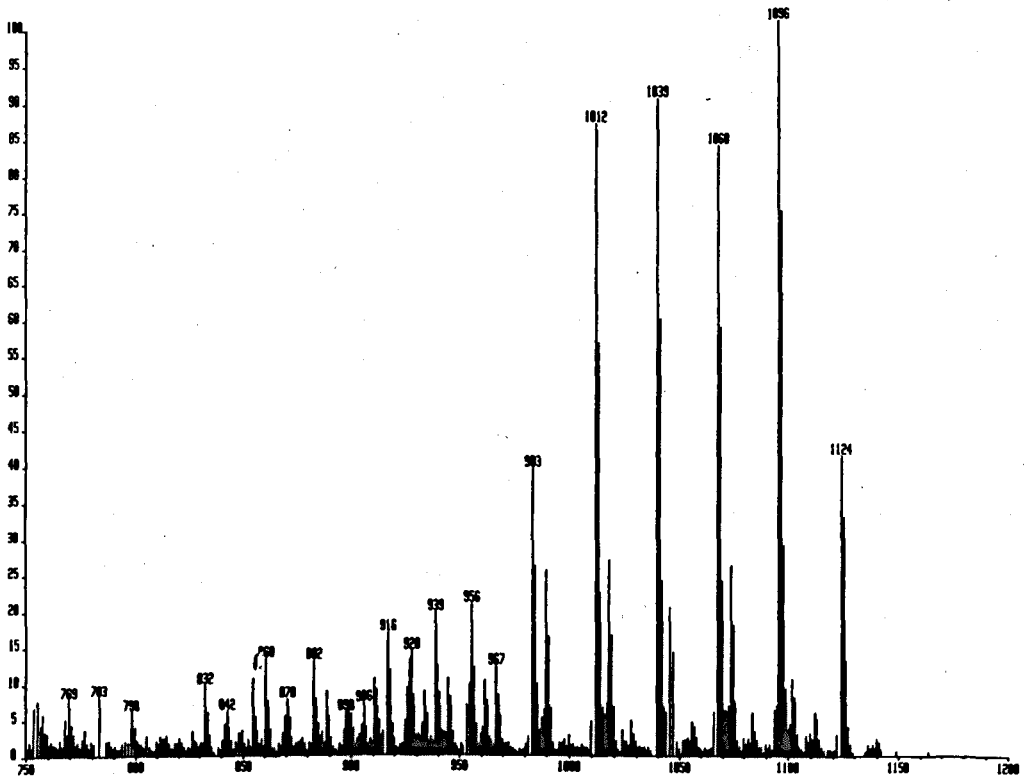


Figure 5.13 FAB MS of Library 145 with 10% NaNO₃.

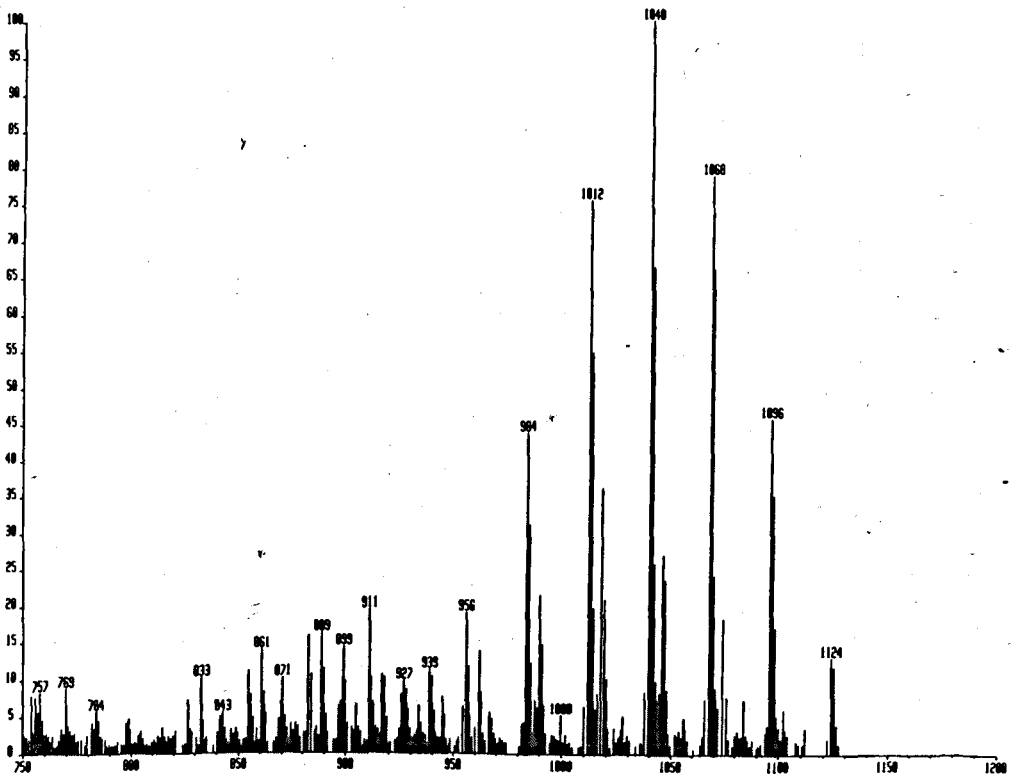


Figure 5.14 FAB MS of Library 146 with 10% NaNO₃.

Comp. (S. M. R)	M + H (E. R. I)	Intensity %	M + Na	Intensity %	Int(M+Na)/ Int(M+H)
MMMM(1)	765 (1)	0.88	787	2.21	2.50
MMME(4)	793 (4)	1.33	815	3.14	2.36
MMEE(4)					
MEME(4)	821 (10)	1.90	843	3.64	1.92
MMMP(2)					
MEEE(4)					
MMEP(8)	849 (16)	2.96	871	6.82	2.30
MEMP(4)	#				
EEEE(1)					
MEEP(8)					
MEPE(4)	877 (19)	5.54	899	16.45	2.97
MMPP(4)					
MPMP(2)					
EEEP(4)					
EMPP(8)	905 (16)	8.03	927	34.03	4.24
EPMP(4)					
MPPP(4)					
EEPP(4)	933 (10)	9.08	955	44.27	4.88
EPEP(2)					
PPPE(4)	961 (4)	5.21	983	35.11	6.74
PPPP(1)	989 (1)	3.16	1011	18.63	5.90

Table 5.3

FAB MS data of sub-library 143.

S. M. R — statistical molar ratio.

E. R. I. — expected relative intensity (see Figure 5.11).

Comp. (S. M. R)	M + H (E. R. I)	Intensity %	M + Na	Intensity %	Int(M+Na)/ Int(M+H)
MMMM(1)	765 (1)	0.62	787	0.74	1.19
MMME(4)	793 (4)	0.74	815	1.03	1.39
MMEE(4)	821 (6)	0.62	843	1.39	2.24
MEME(2)					
MEEE(4)	849 (8)	1.23	871	2.14	1.74
MMMB(4)					
EEEE(1)					
MMEB(8)	877 ^R (13)	2.06	899	4.19	2.03
MEMB(4)					
EEMB(8)	905 (12)	2.01	927	6.12	3.04
EMEB(4)					
EEEB(4)					
MMBB(4)	933 (10)	3.04	955	7.75	2.55
MBMB(2)					
EMBB(8)	961 (12)	4.89	983	15.46	3.16
EBMB(4)					
EEBB(4)	989 (6)	3.37	1011	14.57	4.32
EBEB(2)					
MBBB(4)	1017 (4)	5.06	1039	14.48	2.86
EBBB(4)	1045 (4)	6.18	1067	24.82	4.02
BBBB(1)	1101 (1)	4.29	1123	13.54	3.16

Table 5.4

FAB MS data of sub-library 144.

S. M. R — statistical molar ratio.

E. R. I. — expected relative intensity (see Figure 5.12).

Comp (S. M. R)	M + H (E. R. I)	Intensity %	M + Na	Intensity %	Int(M+Na)/ Int(M+H)
MMMM(1)	765 (1)	1.15	787	1.05	0.91
MMMP(4)	821 (4)	1.22	843	2.00	1.64
MMMB(4)	849 (4)	1.75	871	4.09	2.34
MMPP(4)	877 (6)	1.19	899	3.02	2.54
MPMP(2)					
MMPB(8)	905 (12)	3.78	927	7.68	2.03
MPMB(4)					
MPPP(4)					
MMBB(4)	933 (10)	4.67	955	11.07	2.37
MBMB(2)					
MPPB(8)	961 (12)	5.51	983	21.11	3.83
MPBP(4)					
MPBB(8)					
MBPB(4)	989 (13)	13.56	1011	46.66	3.44
PPPP(1)					
MBBB(4)	1017 (8)	14.33	1039	48.39	3.38
PPPB(4)					
PPBB(4)	1045 (6)	10.93	1067	44.99	4.12
PBPB(2)					
PBBB(4)	1073 (4)	13.97	1095	53.99	3.86
BBBB(1)	1101 (1)	5.65	1123	22.04	3.90

Table 5.5 FAB MS data of sub-library 145. S. M. R — statistical molar ratio.
E. R. I. — expected relative intensity (see Figure 5.13).

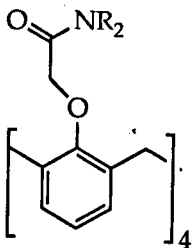
Comp. (S. M. R)	M + H (E. R. I)	Intensity %	M + Na	Intensity %	Int(M+Na)/ Int(M+H)
EEEE(1)	877 (1)	1.16	899	4.18	3.60
EEEP(4)	905 (4)	1.04	927	2.82	2.71
EEEB(4)					
EPPP(4)	933 (10)	1.85	955	5.56	3.00
EPEP(2)					
EEP(8)					
EPEB(4)	961 (16)	4.02	983	12.71	3.16
PPPE(4)	#				
EEBB(4)					
EBEB(2)					
EPPB(8)	989 (19)	6.26	1011	21.99	3.51
EPBP(4)					
PPPP(1)					
EPBB(8)					
EBPB(4)	1017 (16)	10.55	1039	29.18	2.77
PPPB(4)					
EBBB(4)					
PPBB(4)	1045 (10)	7.88	1067	23.08	2.93
PBPB(2)					
PBBB(4)	1073 (4)	5.33	1095	13.40	2.51
BBBB(1)	1101 (1)	1.73	1123	3.81	2.20

Table 5.6 FAB MS data of sub-library 146. S. M. R — statistical molar ratio.
E. R. I. — expected relative intensity (see Figure 5.14).

pattern of relative intensities. The relative intensities initially increase with higher mass, reach a maximum and then decrease as mass increases because these two sublibraries contain two poor residues, methyl which is smallest in mass and butyl which is biggest in mass.

From this data, another result could be deduced. In Table 5.3, the difference between the biggest relative intensity and the smallest relative intensity is 4.24, while in Table 5.6, this difference is only 1.4. So does this result mean that the difference of binding strength for methyl-containing calixarene amides and ethyl- or propyl-containing calixarene amides is bigger than that for butyl-containing calixarene amides and ethyl- or propyl-containing calixarene amides? In other words, does this result imply that methyl-containing compounds have a poorer binding strength than butyl-containing compounds? Similar conclusions can also be drawn from Tables 5.4 and 5.5, in which the differences of relative intensity in the first half of the table are always bigger than those in the second half.

How about ethyl and propyl groups? Which one is better? To answer these questions, a minilibrary 147 was made containing only ethyl and propyl residues. The FAB mass spectrum and relative intensities of peaks are shown in Figure 5.15 and Table 5.7. In this minilibrary there are



147. $\text{NR}_2 = \text{N}(\text{C}_2\text{H}_5)_2$ or $\text{N}(\text{C}_3\text{H}_7)_2$

148. $\text{NR}_2 = \text{N}(\text{CH}_3)_2$; 149. $\text{NR}_2 = \text{N}(\text{C}_2\text{H}_5)_2$;

150. $\text{NR}_2 = \text{N}(\text{C}_3\text{H}_7)_2$; 151. $\text{NR}_2 = \text{N}(\text{C}_4\text{H}_9)_2$.

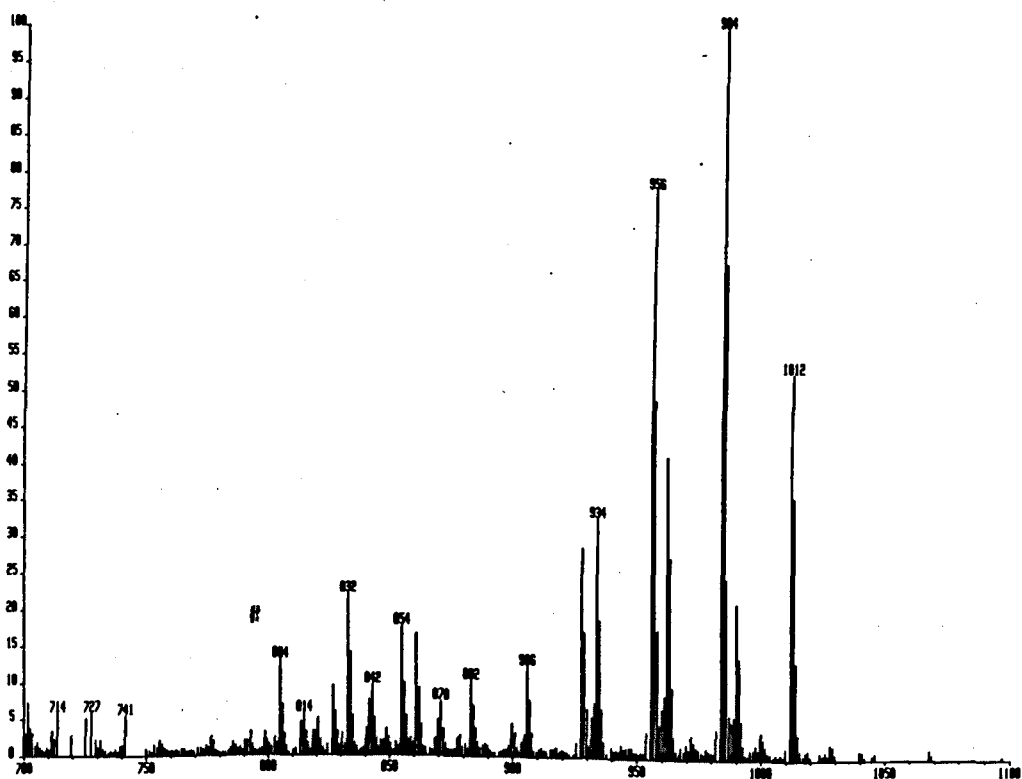


Figure 5.15 The FAB MS of minilibrary 147.

Comp. (S. M. R)	M + H (E. R. I)	Intensity %	M + Na	Intensity %	Int(M+Na)/ Int(M+H)
EEEE(1)	877 (1)	0.43	899	0.77	1.79
EEEP(4)	905 (4)	2.14	927	4.98	2.33
EEPP(4) EPEP(2)	933 (6)	5.67	955	13.6	2.39
PPPE(4)	961 (4)	7.21	983	17.46	2.42
PPPP(1)	989 (1)	3.70	1011	9.21	2.48

Table 5.7 FAB MS data of minilibrary 147. S. M. R — statistical molar ratio.
E. R. I. — expected relative intensity (see Figure 5.15).

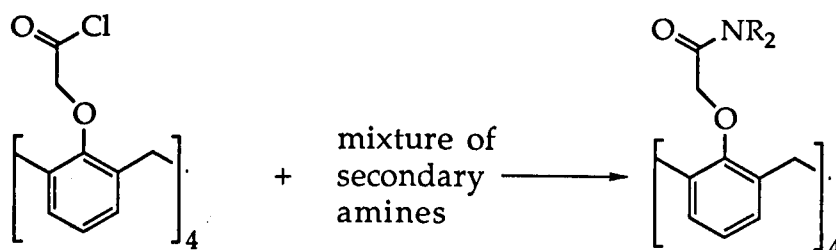
only 6 compounds with 5 different masses. The spectrum also shows a deviation from the statistical ratio and the relative intensities of peaks have a tendency to increase from low mass to high mass with a maximum difference of only 0.79. This means that calixarene amides containing these two kinds of residues have little difference in binding capability.

To confirm all the above deductions, extraction experiments were conducted. Because of difficulty in making unsymmetrical calixarenes, only four compounds, each with only a single type of side chain. were made (compound 148, 149, 150 and 151). Two phase extraction experiments were carried using these four compounds and sodium picrate. The percentage of sodium picrate extracted from an aqueous solution into an organic solution of the calixarene amides (in dichloromethane) was measured by the UV absorption of the aqueous phase. The results are listed in Table 5.8. The data clearly shows that the extraction capability of these 4 compounds is in the order of 149 ≈ 150 > 151 > 148, which means that the effect of side chain of the calixarene amide upon its binding strength is Ethyl ≈ propyl > butyl > methyl. This order exactly matches the results deduced from the FAB MS.

Host (10 ⁻⁴ M)	% Extraction of Na ⁺
148	54.2
149	75.4
150	78.6
151	65.2

Table 5.8 Extraction of Na Picrate (10⁻⁴M) by pure calix[4]arene amides 148, 149, 150 and 151.

After this first experiment, more libraries were made of calixarenes having different side chains and they were screened in the same way. In some libraries propyl or ethyl groups were built in as reference groups to see if any other better ionophores could be found. These libraries are summarized in Figure 5.16. Unfortunately, no compound was found with



Amines: $\text{HN}(\text{CH}_2\text{-CH=CH}_2)_2$ (A), HN (Py), HN (Mo),
 $\text{HN}(\text{CH}_2\text{-C}\equiv\text{CH})_2$ (Pg), $\text{HN}(\text{C}_2\text{H}_5)_2$ (E), $\text{HN}(\text{C}_6\text{H}_7)_2$ (P)
 $\text{HN}(\text{CH}_2\text{CH}_2\text{OCH}_3)_2$ (Bi)

152. $\text{NR}_2 = \text{Mo, Py or P.}$ 153. $\text{NR}_2 = \text{Mo or E.}$

Figure 5.16 Libraries made from up to 4 amines in the mixture. The letters in the brackets are their abbreviations used in the text.

better binding ability than compound 150. Figure 5.17 shows the FAB mass spectrum of one of these libraries, which was recorded in the absence of sodium salt. The library contains calixarenes with morpholinyl, pyrrolidyl and propyl side chains (library 152 in Figure 5.16). In addition to all the expected $[\text{M} + \text{H}]^+$ peaks there are also three $[\text{M} + \text{Na}]^+$ peaks. They are at m/e 981 ($958 + 23$), 997 ($974 + 23$) and 1011 ($988 + 23$) and represent the Na^+ complex of the calix[4]arene amides with the side chain PyPPP, MoPPP and PPPP respectively. This spectrum clearly indicates that among these three residues, propyl is the best one for the sodium ionophores based upon calix[4]arene amides. The sodium was accidentally introduced and the

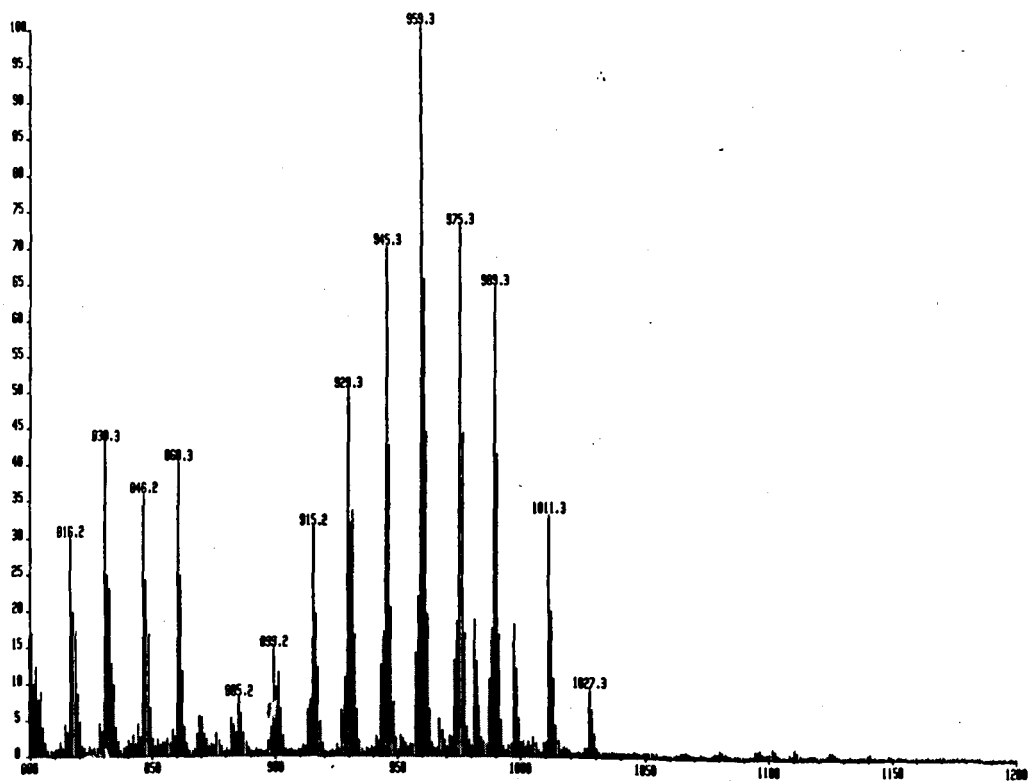
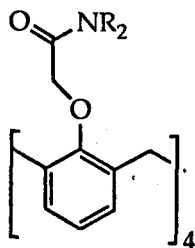


Figure 5.17 FAB MS of Library 152 (Mo, Py and P)

result suggests that a very low level sodium salt in the system will make this FAB MS screen more sensitive.

Five new symmetrical calixarene amides 154, 155, 156 157 and 158,



154. $\text{NR}_2 = \text{N}(\text{CH}_2\text{-CH}=\text{CH}_2)_2$

155. $\text{NR}_2 = \text{N}(\text{CH}_2\text{-C}\equiv\text{CH})_2$

156. N (pyrrolidine ring)

157. N (piperidine ring)

158. $\text{N}(\text{CH}_2\text{CH}_2\text{OCH}_3)_2$

each having one type of side chain (of a type used for making the libraries in Figure 5.16) were prepared and their extraction properties are listed in Table 5.9, which shows clearly that compounds with pyrrolidyl and morpholinyl as side chains are poor ionophores.

Host (10^{-4}M)	% Extraction of Na^+
154	62.8
155	26.2
156	56.6
157	19.2
158	67.7

Table 5.9 Sodium extraction results of calixarene amides 154, 155, 156, 157, and 158.

As has previously been mentioned several times, the patterns of the peak intensities in nearly all of the FAB mass spectra of the libraries have some deviation from the statistical molar ratio of the component compounds. There are several situations which could cause this deviation: (1) Different amines have different reaction rates towards the acid chloride during the formation of amides and the FAB mass spectra reflect the real molar ratio of the compounds in the mixture. However, this seems to be unlikely because dimethylamine or diethylamine should not be less active than dibutylamine, whereas in the spectra the deviation towards higher than expected intensity is in the high mass peaks; that is compounds with butyl residues have stronger peaks than they should have according to the statistical ratio. (2) Different compounds have different extents of fragmentation during the ionisation process in the mass spectrometer. In all of the spectra, fragmentation is a constant

phenomenon. For example Figure 5.18 is a full FAB mass spectrum for library 142 (in Figure 5.10a); there are some very strong peaks in the low mass region, such as m/e 43, 57, 72, 86, 100 and 128, with a 100% intensity for m/e 43. These peaks appear to be the fragment ions from the amine residues $[NR_2]^+$. But it is difficult to see which compounds fragment most

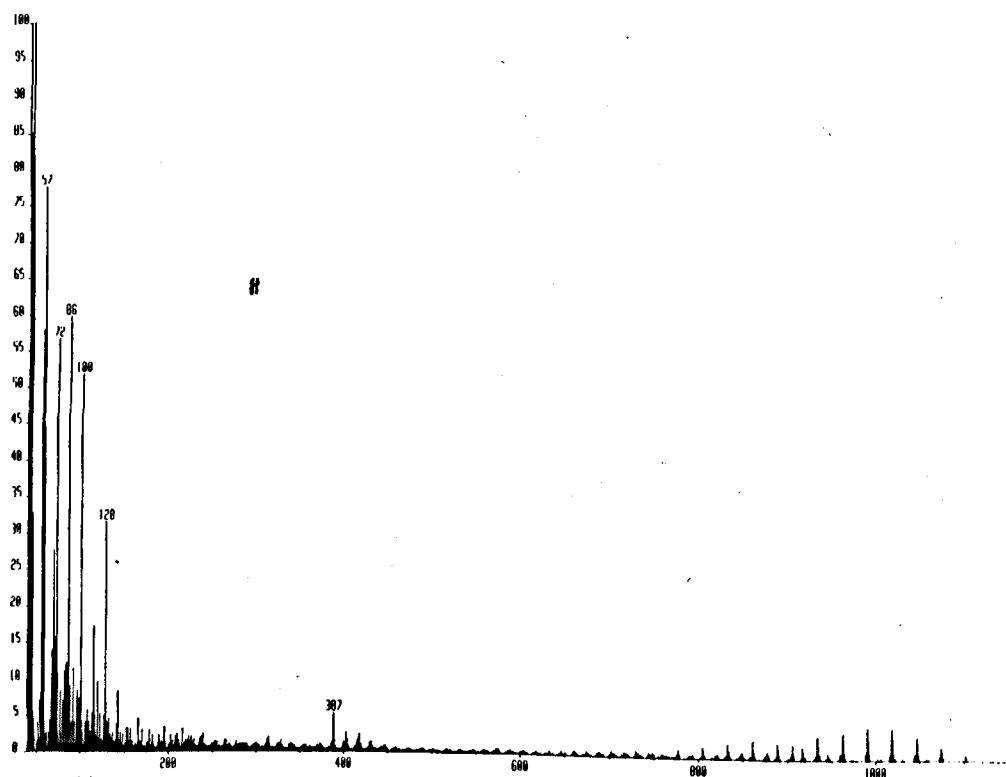


Figure 5.18 Full FAB MS of Library 142

because small fragment ions could be formed from bigger fragments. For example m/e 43 could be $[CH_3CH_2CH_2]^+$ which could come from propyl but also could come from butyl groups. The upwards deviation in intensity towards high mass does not seem to be the result of fragmentation since generally, high mass compounds fragment more easily than low mass compounds in the ionization source. (3) In FAB MS analysis of mixtures, the peaks for some compounds can sometimes be

depressed as compared with other compounds in the mixture. This phenomenon has already been reported⁹⁸ and the reason is that FAB ionization is a surface process since the xenon or argon atoms only bombard the surface of the sample matrix and obviously the spectra only show compounds which are on the surface of the matrix. This phenomenon is most apparent when there is a surfactant in the mixture. Is this the reason for the deviation in intensities in the spectra of the libraries? To answer this question, a mass spectrum was recorded using a mixture in which 4 compounds, 148, 149, 150, and 151 were mixed together in an equimolar ratio. Surprisingly, only one peak dominates the high mass region of the spectrum (Figure 5.19), the peaks at m/e 1102 and 1124 represents the tetrakis(dibutylcarbamoylmethoxy)calix[4]arene 151 and its Na^+ complex. The peaks for tetrakis(dipropylcarbamoylmethoxy)-calix[4]arene 150 and its sodium complex are very weak (990 and 1012), and those for tetrakis-(diethylcarbamoylmethoxy)-calix[4]arene 149 and

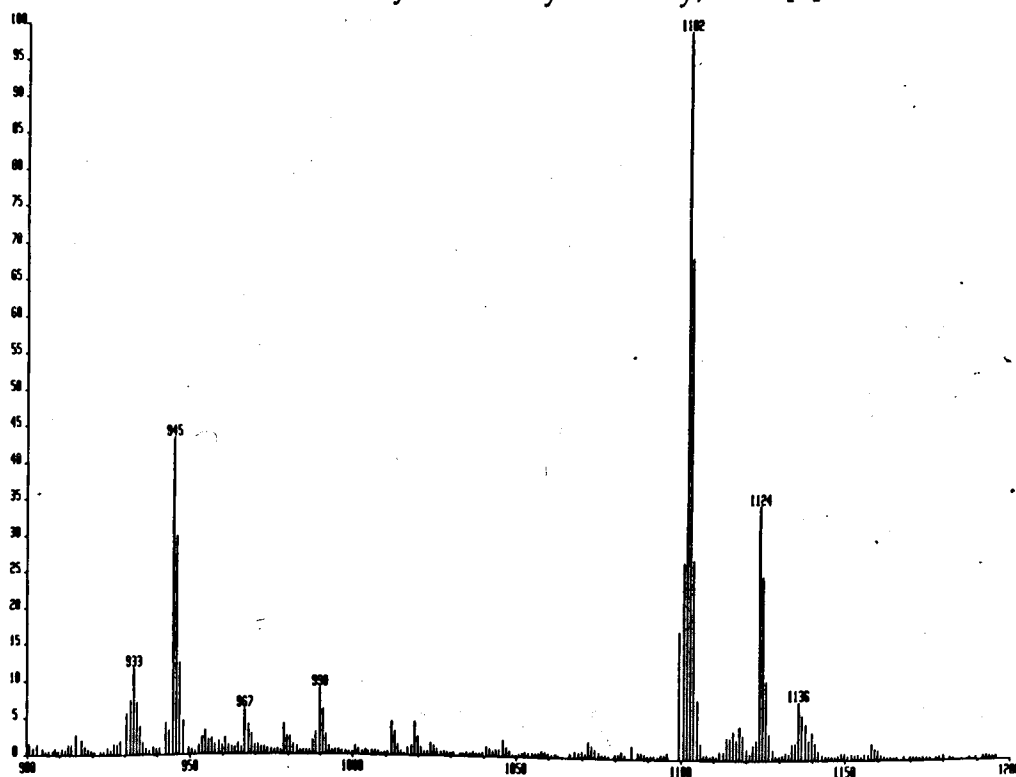


Figure 5.19 The FAB MS of a mixture sample of 148, 149, 150 and 151 with same equivalent.

tetrakis(dimethylcarbamoylmethoxy)calix[4]arene 148 are totally absent from the spectrum. This experiment clearly indicates that the butyl-containing calixarene 151 is a surfactant and in the surface of a 3-NOBA matrix, its concentration is far higher than those of the other three compounds. This is possibly because the compound 151 is more lipophilic than the other three compound and hence in 3-NOBA, which is a very polar solvent, the 151 is concentrated at the surface of the solution because it can not dissolve into the bulk of the solution like the other three compounds which are less lipophilic. So in the libraries, the more butyl groups that the calixarenes contain, the more surface effect they have, and the more they give rise to strong peaks in the mass spectra. This why most spectra have a positive deviation in intensity towards high mass. Fortunately, the statistical molar ratio of the compound 151 was very low in the libraries (1:8 towards most species in library 142), so it could not depress all of the peaks for the other compounds in the libraries. Obviously, this surface effect could introduce a big error into quantitative analysis using mass spectroscopy, especially when some peaks are totally depressed, However this was not the case for our libraries.

5.6 The Study of Calixarene Libraries By MALDI and ESI Mass Spectroscopy

There is a question still not completely answered. What is the randomness of the libraries generated by the method shown in Figure 5.6? It is obvious that FAB mass spectroscopy is unable to solve this problem. Apart from the surface effect, fragmentation, is another constant problem in FAB mass spectra. To avoid fragmentation, a soft ionization method is required. Recently, two new soft ionization methods for mass

spectrometry have been developed rapidly in the area of biochemistry. These methods are 'Matrix Assisted Laser Desorption/Ionization' (MALDI) and 'Electrospray Ionization' (ESI). Both methods have been demonstrated to be very successful for the analysis of large and fragile peptides, proteins and other biopolymers.

The laser desorption technique was conceived initially as early as the beginning of 1970's but was limited to small organic molecules. The breakthrough was achieved in 1987, when a Japanese group and a German group independently discovered that mass limitation of laser desorption could be overcome by placing samples in a solid or liquid matrix containing a highly UV-absorbing substance.⁹⁹ The major function of the matrix used in MALDI is absorption of energy from the laser to prevent decomposition of the species of interest. When molecules are ionized with a short-pulse laser, the ions are generated at a virtual point source, both in terms of space and time. This makes MALDI highly compatible with a time-of-flight (TOF) mass spectrometer in which the ions are released at one point and accelerated by an electric field. The masses of the ions are then determined by measuring the time required for them to traverse a fixed distance in a field-free drift tube. So one advantage of MALDI-TOF MS is that the mass range of a TOF analyzer is virtually unlimited, permitting determination of the mass of very large biomolecules. The Figure 5.20 illustrates the principle of the MALDI-TOF MS.

Along with the development of the MALDI technique, another very different technique – electrospray ionization – has also been developed. The first report of using ESI for a protein sample was made by an American group in 1988.¹⁰⁰ In ESI, highly charged droplets of the sample solution are dispersed from a capillary in a strong electric field at

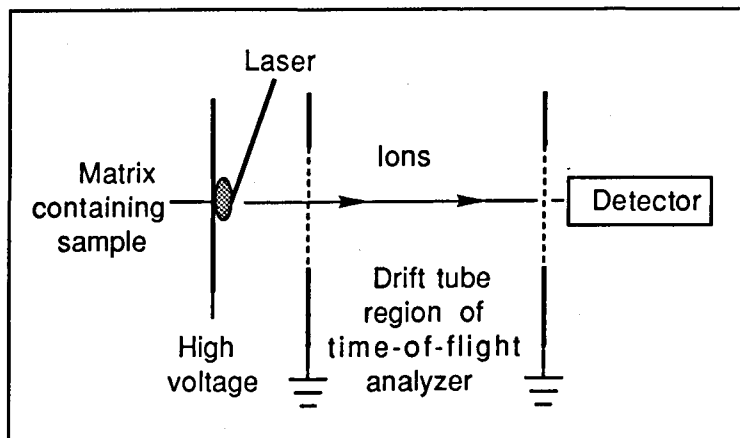


Figure 5.20 Illustration of MALDI-TOF MS

atmospheric pressure. Heat and/or dry gas are applied to the droplets to help evaporate the solvent. Multiply charged ions expelled from the droplets during the evaporation process are then drawn toward an inlet that admits them into the vacuum region of the spectrometer. The illustration of ESI is shown in Figure 5.21. Because molecules are multiply charged in the ESI process, the mass-to-charge ratio, m/z , is reduced,

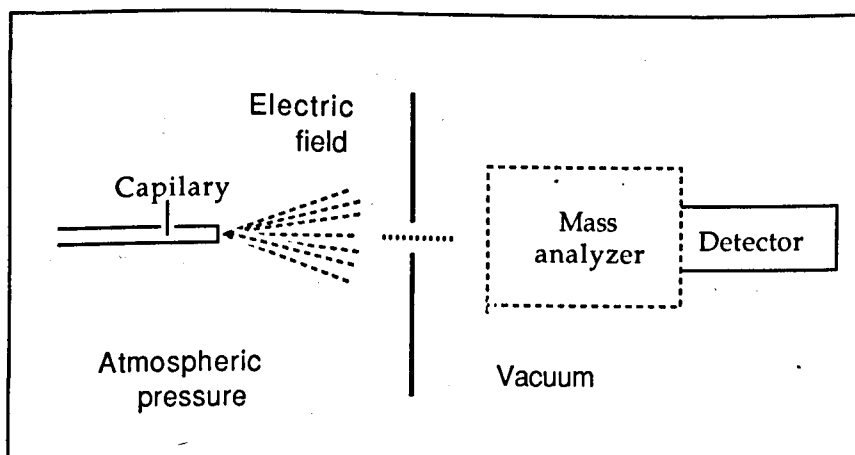


Figure 5.21 Illustration of ESI MS

which means that very large mass ions can be handled by any mass analyzer. The unique sampling technique of sending the sample solution directly into the instrument was extremely interesting to us because it means that the ions going to the analyzer are directly from the solution, which makes the mass spectrum reflect more precisely the composition of samples in the solution phase. There should be no surface effect at all as in the FAB sampling technique. Both ESI and MALDI MS have not been well studied for evaluating ionophores, so it was of considerable interest to compare these two techniques with FAB MS to see what their advantages are and what their limitations are.

The calixarene libraries used for ESI MS were used as solutions (2.0×10^{-4} M) in DCM. $20\mu\text{l}$ of each sample was injected into the mass spectrometer inlet and pumped into the capillary by a methanol stream before ionisation. Figure 5.22 and 5.23 show ESI spectra for the libraries 142 and 147. Three facts can be seen from these two spectra. (1) The libraries were saturated with sodium. This happened in all of the ESI experiments and only a couple of spectra showed $[\text{M} + \text{H}]^+$ peaks of reasonable intensity. The sodium probably comes from the relatively large volume of methanol which is used for pumping the sample into the mass spectrometer. (2) The patterns of peaks in the spectra match the statistical molar ratio in the mixtures very well (see Table 5.2 and Table 5.7). For example, in library 147, there should be 5 different masses for the compounds with a statistic ratio of 1:4 : 6: 4: 1. In Figure 5.22, the spectrum clearly shows that these 5 peaks ($[\text{M} + \text{Na}]^+$) have exactly the ratio expected. Comparing with the spectrum in Figure 5.15, this is a big improvement. This result demonstrates that the method used for generating the libraries can give a statistical molar ratio of the various component compounds. It also shows that the patterns of peaks in the FAB MS of libraries do not

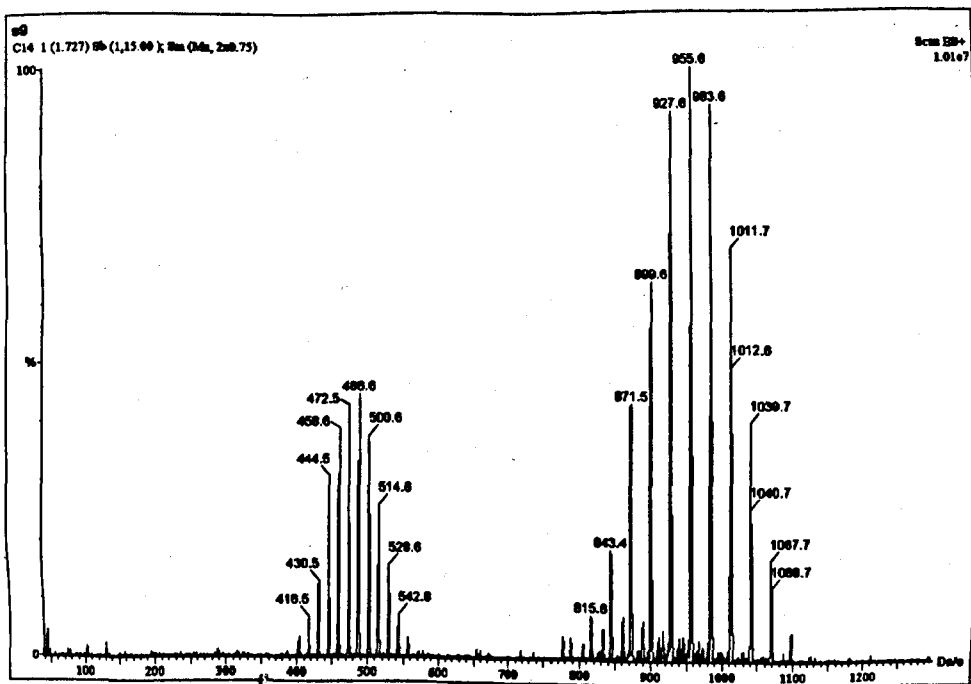


Figure 5.22 ESI MS of Library 142 (MEPB)

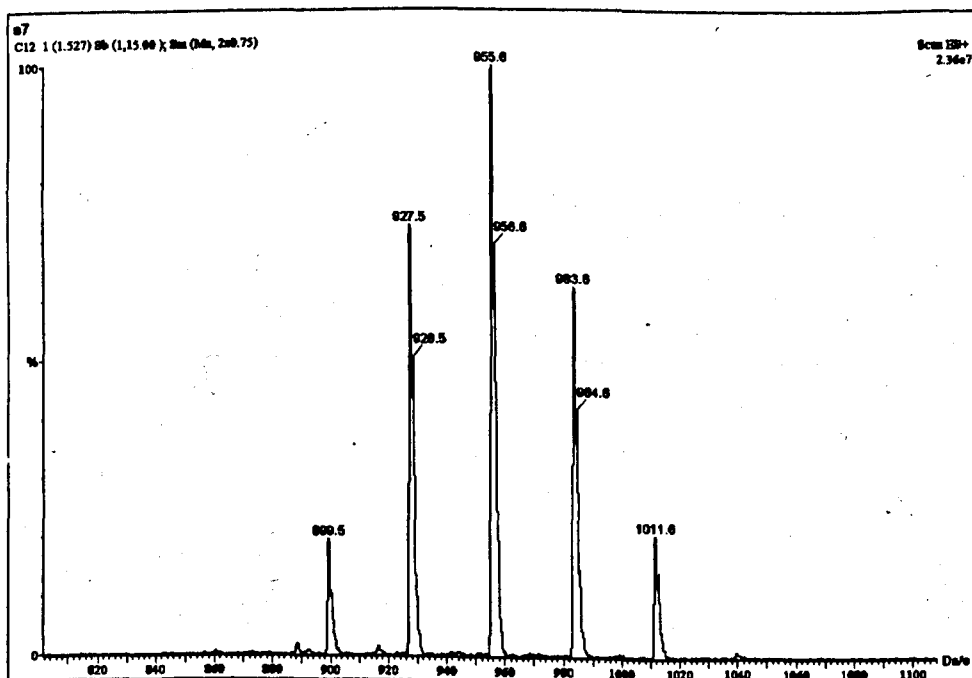


Figure 5.23 ESI MS of Library 147 (EP)

reflect the real molar ratio of the components of the mixtures because of the surface effect. (3) Doubly charged species do appear in the ESI MS of libraries, but the peaks are very weak as compared with peaks of singly charged species. In addition the peaks of doubly charged species have the same pattern as the peaks of singly charged ions. This means that the chance of doubly charging for every compound in a library is the same so that it should not disturb the statistical ratio of singly charged species in the libraries (Figure 5.22). According to calculation, these peaks of doubly charged species represent the ion $[M + Na + H_2O]^{++}$. Why water molecules are involved in these doubly charged ions is not fully understood.

When the sample is not saturated with sodium, ESI MS can be used for screening the ionophore libraries more precisely than FAB MS. For instance, Figure 5.24 is the spectrum for a minilibrary 153 in which only two side chain residues were used, diethylamino and morpholinyl. In the spectrum the peaks for $[M + H]^+$ are recognizable. The intensities of the peaks are listed in Table 5.10 and from this data, the tetrakis-

M + H (E. R.I)	Intensity %	M + Na	Intensity %	Int(M+Na)/ Int(M+H)
877 (1)	4.5	899	39.6	8.8
891 (4)	20.6	913	100	4.9
905 (6)	24	927	64.6	2.7
919 (4)	13.5	941	18.1	1.34
933 (1)	4.1	955	2.3	0.56

Table 5.10 Data of ESI MS for library 153. E.R.I — expected relative intensity (see Figure 5.24).

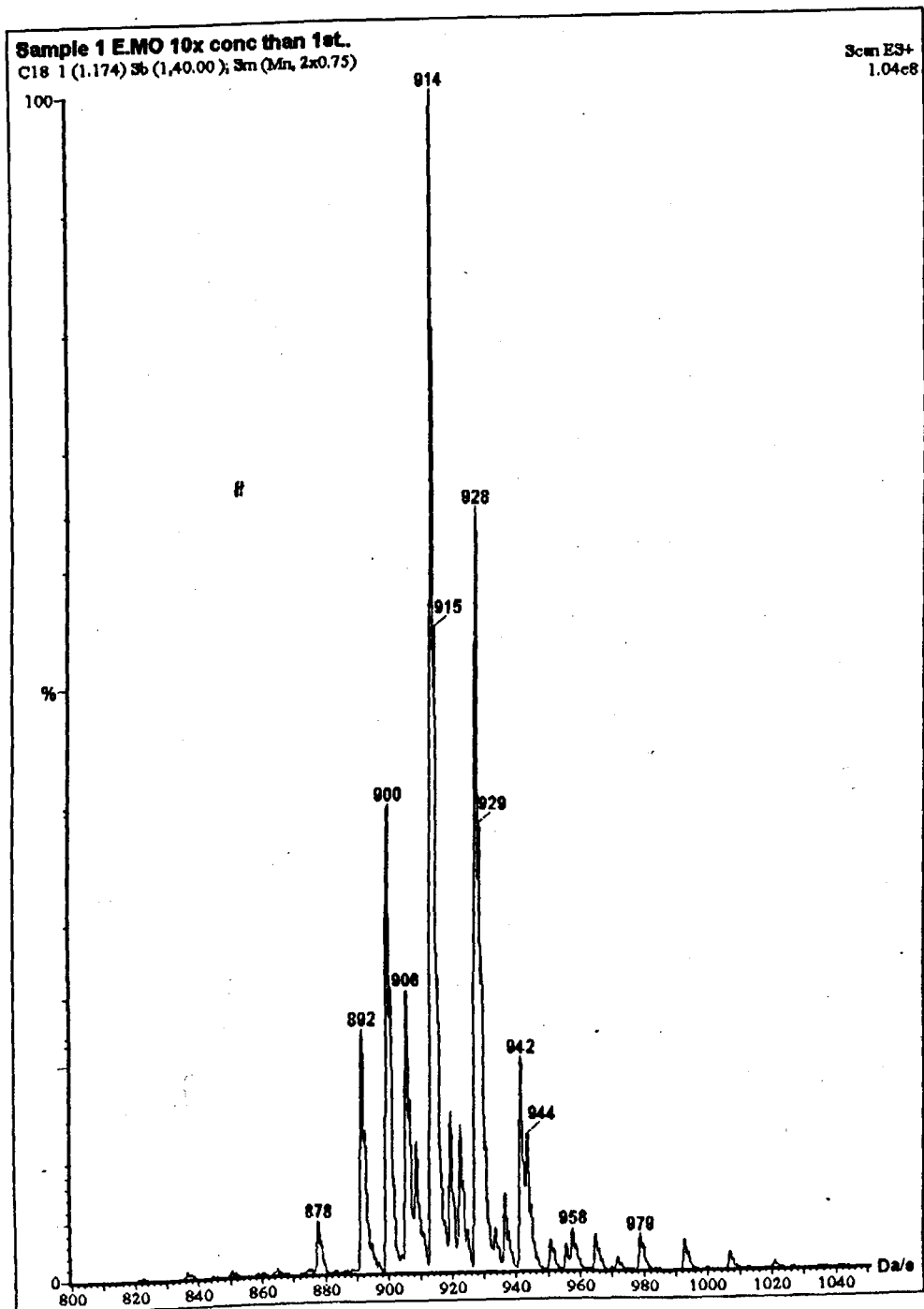


Figure 5.24 ESI MS of Library 153

(diethylcarbamoylmethoxy)calix[4]arene EEEE is the best ionophore in this library as proved by the extraction experiments.(see Table 5.8 and 5.9).

The MALDI-TOF MS were recorded under the usual conditions. The samples of the libraries and mixtures were made in a concentration of 1.0 pmol/ μ l as dichloromethane solution which were mixed with a UV absorbing matrix solution in dichloromethane (dithranol was used as matrix throughout the experiments). The spectra show that fragmentation is a common phenomenon and in all cases no spectrum without $[M + Na]^+$ peaks, which represents the library of free compounds, was obtained. Figure 5.25 shows spectra for library 146. Spectrum (a) is for a sample without the matrix and spectrum (b) is run for a sample in a dithranol matrix. For spectrum (a), a bigger laser energy (50%-63% of 180 microjoules) was used and this produces a lot of fragment peaks in the low mass region (not shown), but only $[M + Na]^+$ peaks are seen in the high mass region. Obviously, most of the sample was fragmented and the trace of sodium ions in the instrument help some of the molecules to ionise. In spectrum (b), both $[M + H]^+$ and $[M + Na]^+$ peaks can be seen clearly since a

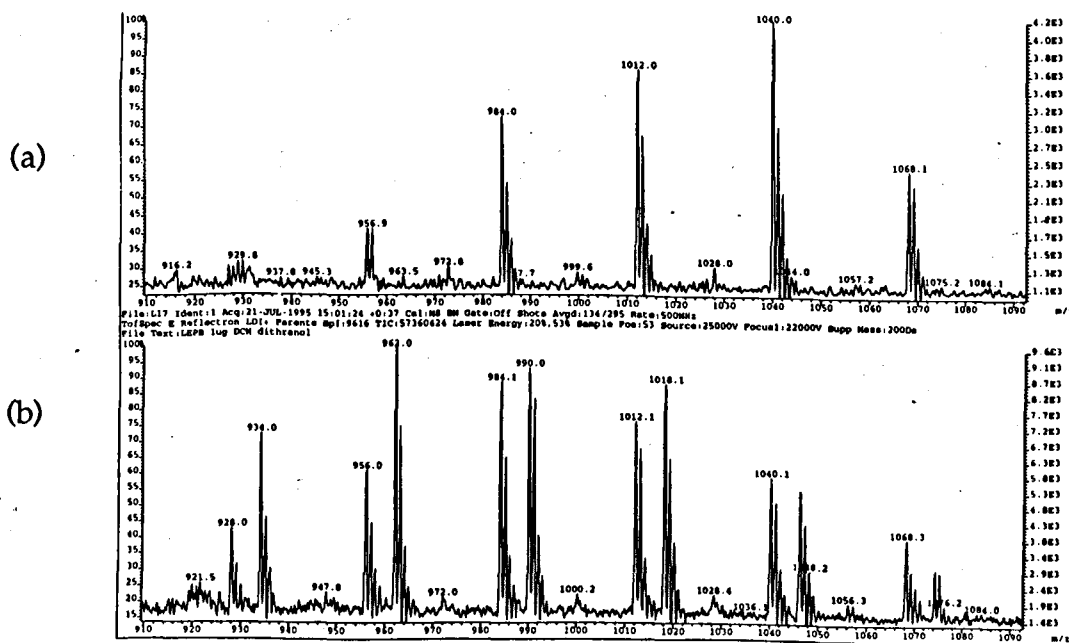


Figure 5.25 MALDI-TOF MS of Library 146 (EPB) (see Figure 5.14)

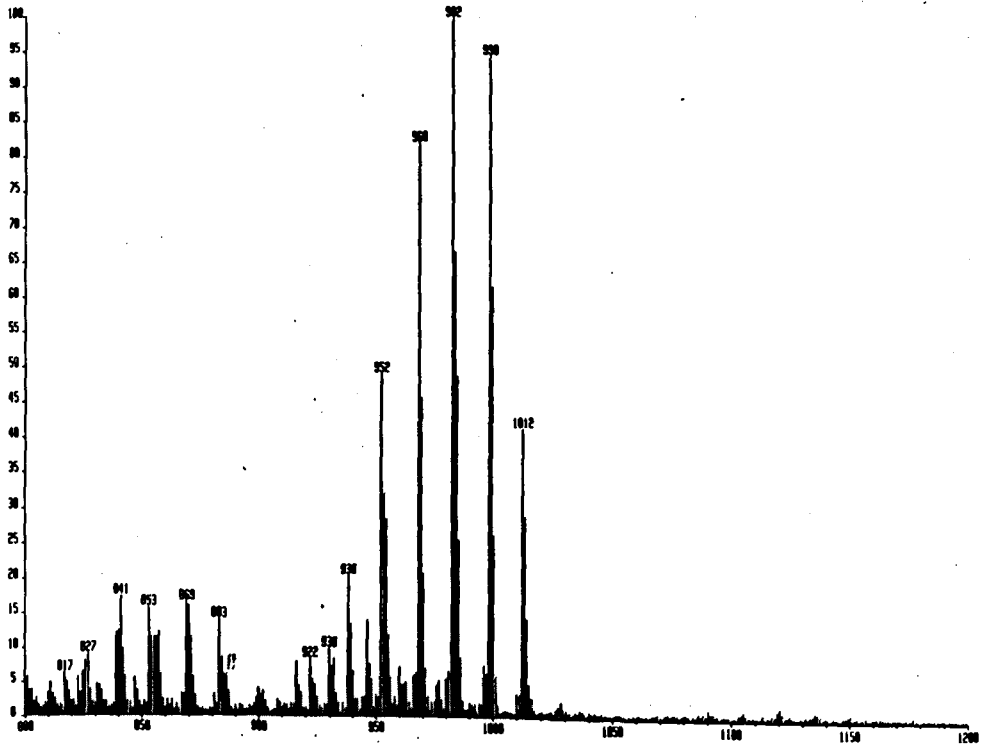
matrix was used. This spectrum and the FAB spectrum (Figure 5.14 in section 5.5) are very similar. The values of Intensity $[M + Na]^+$ /Intensity $[M + H]^+$ are also similar to the result shown in Table 5.6. Because no spectrum was obtained for a sodium free sample, it is difficult to estimate how much deviation of the heights of the $[M + H]^+$ peaks occurs with this technique. However, by saturating the sample with a sodium salt, it is possible to compare the $[M + Na]^+$ peaks with those seen in the ESI mass spectra. Figure 5.26 shows mass spectra for the library 152 with three side chain residues which are pyrrolidinyl, morpholinyl, and dipropylamino. Spectrum (a) is the FAB MS spectrum, (b) is the MALDI-TOF MS spectrum and (c) is the ESI MS spectrum. For (a) and (b) one equivalent of sodium nitrate was added to the sample and for all spectra only $[M + Na]^+$ peaks can be seen. The statistical molar ratio for all species in the library are shown in Table 5.11. From Table 5.11, the three strongest $[M + Na]^+$ peaks should be 937, 953 and 967 (the statistical molar ratios are all 12). In spectra (b) and (c) these three peaks are clearly seen (the masses have slightly different values from spectrum to spectrum because of the different calibration of each instrument). In spectrum (b), some low mass peaks seem to be slightly too weak, such as 891 and 907, while in spectrum (a), the strongest three peaks are at 967, 981 and 998 although for peaks 981 and 998 the statistical molar ratio is only 4. The peak at 937 is very weak, even weaker than the peak at 1101 for which the statistical ratio is only 1. So among these three spectra, ESI MS matches the statistical ratio the best, FAB MS the worst and MALDI-TOF MS is in between. The spectra obtained from MALDI-TOF MS are much better than expected. Initially, the spectra were expected to be similar to those from FAB MS since the two ionization techniques are very similar. The reason why the MALDI spectra are better is possibly because during the ionization process, the laser beam can be moved from place to place on the sample and also can be

focused on one point to 'dig a hole' on the sample which should cancel some surface effect.

Comp. (S. M. R)	M+H	M+Na
PyPyPyPy(1)	869	891
PyPyPyMo(4)	885	907
PyPyPyP (4)	898	921
PyPyMoMo(6)	901	923
PyPyMoP (12)	915	937
PMoMoMo(4)	917	939
PyPyPP (6)	929	951
MoMoPyP (12)	931	953
MoMoMoMo (1)	933	955
PPPyMo(12)	945	967
MoMoMoP (4)	947	969
PyPPP (4)	959	981
MoMoPP (6)	961	983
MoPPP (4)	974	997
PPPP (1)	989	1011

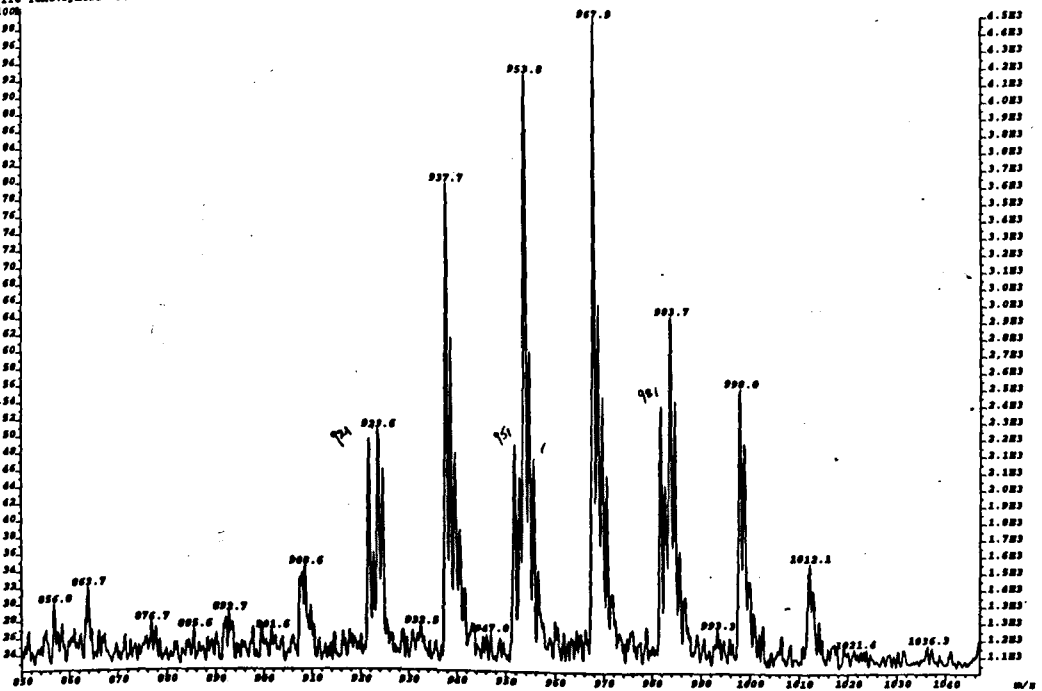
Table 5.11 Masses for species in Library 152.

S. M. R.- statistical molar ratio (see Figures 5.26a, b and c).

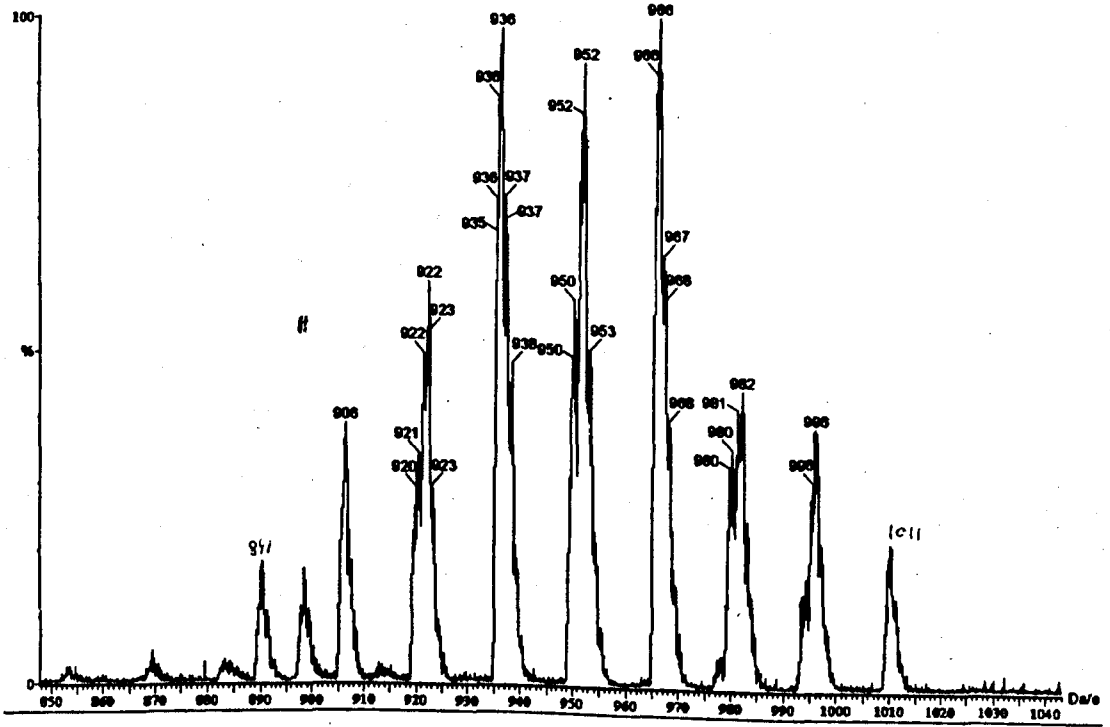


(a)

File:011 Ident:3 SMO(1.3) PWD(5.1, 9.0, 0.0%, 0.0, 0.0, 0.0, P, V) Acq:14-SEP-1995 12:23:42 +1:38 Cal:01 Mf Date:022 Photo Arpd:100/172 Rate:500MHz
 TopSpec 2 Reflectron LDI+ Parents RpI:1036 VIC:33772113 Laser Energy:304,32% Sample Pos:63 Source:33000V Focals:32000V Supp Mass:200Da
 File Name:PyroPr Sm 1 dithranol



(b)



(c)

Figure 5.26 Mass spectra of Library 152. (a) FAB MS

(b) MALDI-TOF MS

(c) ESI MS

5.7 Conclusions and Discussion

Combinatorial libraries of calix[4]arene-amides containing up to 55 different compounds in one library were made and their complexing ability for the sodium cation screened by three different mass spectroscopy techniques-FAB, MALDI-TOF and ESI. The mass spectra showed that the method used to generate amide libraries from acid chloride is good and gives the expected statistical molar ratio for every species in the libraries.

The experiments showed that using mass spectroscopy techniques to screen ionophore libraries of this type is feasible by comparing the intensities of $[M + \text{Na}]^+$ peaks with those of $[M + \text{H}]^+$ peaks. All three techniques have shown that they give correct results if samples containing amounts of sodium that give spectra including both $[M + \text{Na}]^+$ and $[M + \text{H}]^+$ peaks are used. Deviation of the patterns of peak intensities from their statistical ratio was observed for FAB MS spectra, because of the surface effect during the ionization process. This conclusion was proved by the spectrum of a mixture which contains one equivalent of each of four different calixarene amides. This deviation could cause serious errors during the screening process but this was not the case in our experiments, possibly because the deviations for $[M + \text{H}]^+$ peaks are similar to those for $[M + \text{Na}]^+$ peaks. MALDI-TOF and ESI MS gave much better spectra, particularly ESI MS which gave spectra in which the intensity of $[M + \text{Na}]^+$ peaks matched the statistical molar ratio of the compounds in libraries very well. The unique ESI ionization technique, in which the sample solution is injected into the machine directly and solvent is evaporated during the ionization process, makes the spectra reflect the composition of the sample solution precisely. This makes ESI MS the best candidate for screening libraries of sodium ionophores if the sodium level can be

completely controlled during the experiment and, in principle, every single peak in an ESI MS would indicate whether one or more of the compounds of that mass is a good sodium ionophore or not.

A mathematical problem has been noticed in which the maximum statistical molar ratio between compounds of one mass and compounds of another mass in a library becomes bigger as the library becomes bigger. For example, for three-residue libraries, the molar ratio between the most abundant species and the least abundant ones is 12 to 1 (see Table 5.3 or 5.4), while in four-residue library this ratio reaches a maximum of 24 to 1, because regio isomers and enantiomers have same masses. This difference become larger when masses of some compounds overlap with those of other compounds, thus in library 142 the biggest molar ratio between compounds of different mass is 44 to 1 (see Table 5.1). Obviously, it will be difficult to obtain a precise ratio of $[M + Na]^+ / [M + H]^+$ for different compounds under these conditions. However this problem could be overcome by reducing the number of reaction sites on the calix[4]arene. For example, by using a calix[4]arene-tricarboxylic acid chloride with one position protected or pre-made as an amide, the maximum molar ratio would be reduced to 6:1, no matter how many amines are used to generate libraries.

The screening results showed that calixarene-amides containing ethyl (diethylamino) and propyl (dipropylamino) side chains are the best ionophores. This result was partially confirmed by the extraction experiments using nine pure compounds (see Table 5.8 and 5.9). The results show that the complexing ability of calixarene-amides depends upon the side chain. Increasing the length of the alkyl side chain in the amide substituent leads to an increase in intramolecular interactions between these groups which may enhance the stability of the non binding C_{2v} conformation of the calixarene skeleton and bigger alkyl groups could

also decrease ion pairing in the organic phase, and therefore lead to inhibited binding. The steric properties of calixarenes containing cyclic side chains, such as morpholinyl and pyrrolidinyl may increase the relative rigidity of the ligands and this may make it difficult for the ionophore structure to adjust to a proper cavity size for binding the sodium cation and therefore the binding ability is decreased. Although allyl and propargyl have a similar size to the propyl group, their electron withdrawing character (their Taft electronic parameters σ^* are 0.56 and 2.18 for the allyl and propargyl groups, respectively) would possibly reduce the basicity of the carbonyl groups accounting for their poorer binding ability as compared with propyl amides.

From the results obtained in this project, an improvement on this study for future work would be to use an asymmetric calixarene to generate larger libraries and to use ESI MS to screen them. For example, libraries could be made from calix[4]arene-tricarboxylic chloride monoamide (Figure 5. 27) as has been discussed previously, by using this compound the maximum molar ratio between compounds in the library would be 6:1 (provided that there is no mass overlapping). The mass spectroscopy of such libraries would give better data so that screening results would be more reliable. The required calix[4]arene-tricarboxylic acid chloride is accessible by using the calix[4]arene tetraethylester (compound 5) as a starting material. A monocarboxylic acid triethylester can be made by partial hydrolysis under mild conditions,⁹⁴ which could be converted into a monoamide triethylester. This compound could then be converted into the monoamide tricarboxylic acid chloride. The successful screening of a library depends upon whether the sodium level can be controlled or not, this requires the cooperation of the spectrometer operator and the use of sodium free solvent and containers.

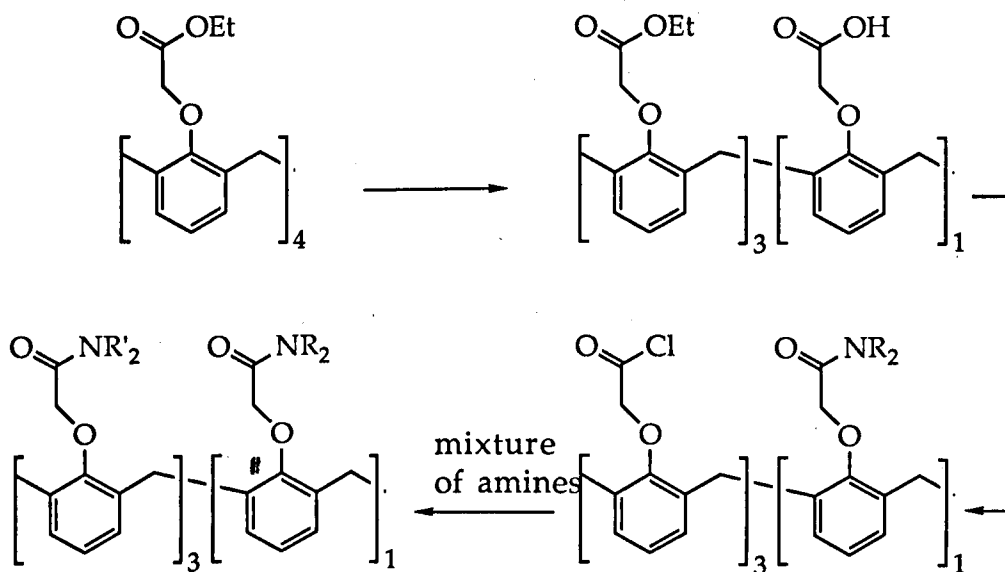


Figure 5.27

The combinatorial method, such as that used in this project, potentially gives a greater diversity of compounds using less time and materials than conventional synthesis. It should lead to a wider range of more powerful and selective ionophores in the future.

CHAPTER SIX

EXPERIMENTS

6.1 General

6.1.1 Procedures and Instruments

^1H and ^{13}C Nuclear Magnetic Resonance (NMR) spectra were recorded on a Bruker AC 200 spectrometer (200 MHz, 50 MHz) or a Bruker AMX 400 spectrometer (400 MHz) or a Bruker WM 250 (250 MHz). Deuteriochloroform (CDCl_3) was used as the solvent, unless otherwise stated. In all cases, chemical shifts are reported in parts per million (ppm) downfield from internal tetramethylsilane (TMS). The multiplicity of signals is expressed by the following symbols: s, singlet; d, doublet; dd, double doublet; t, triplet; q, quartet; m, multiplet and b, broad.

Routine mass spectra were obtained by direct insertion or GC/MS using a Fisons TRIO-1000 quadrupole spectrometer with electron impact ionisation (EI) source and connected with a GC-8000 gas chromatography system.

Fast Atom Bombardment (FAB) mass spectra, Chemical Ionisation (CI) mass spectra and high resolution mass spectra (HRMS) or accurate mass spectra were measured on a VG Analytical 7070E double-focusing magnetic sector mass spectrometer.

MALDI-TOF mass spectra were recorded by a VG ToFSpec-SE spectrometer with a 337 nm UV laser system.

The ESI mass spectra were run on a VG Quattro Triple Quadrupole mass spectrometer with an ESI interface attached to a Waters 600-MS HPLC system.

The symbol M^+ is used to indicate the molecular ion in Mass Spectrometry. $[\text{M} + \text{Na}]^+$ represents the complex ions of host molecule with sodium cation.

Infrared spectra (IR) were recorded on a Perkin-Elmer 883 or Perkin-Elmer 1320 infrared spectrometer using a KBr disk or liquid paraffin (Nujol) mulls of samples. Spectra were recorded in the range 4000 cm^{-1} to 600 cm^{-1} .

Ultraviolet (UV) and visible spectra were recorded on a Hewlett Packard 8452A diode array spectrometer.

Melting points were determined in Pyrex capillaries in a Gallenkamp melting point apparatus and are uncorrected.

Microanalyses were determined by the Departmental Microanalysis Laboratory.

Gas chromatography (GC) analyses were done on a DANI 3800 Gas Chromatography with either SE30 or FFAP capillary columns.

Whatman silicagel PE SIL G/UV plates (254nm) were used for analytical thin layer chromatography (TLC).

Flash column chromatography was performed using Merck silica gel 60 (average particle size $40\text{ }\mu\text{m}$) as absorbent under medium pressure.

Reactions sensitive to air or moisture were conducted in oven- or flame-dried glassware under an atmosphere of dry nitrogen.

With all ionophoric compounds, any complexed metal was removed by washing a solution of the ionophore in dichloromethane several times with freshly distilled water.

Hydrogenation reactions were performed using a low pressure hydrogenation apparatus.

In the text, the phrase "solvent was evaporated" or equivalent phrases mean that solvents were removed on a rotary evaporator at aspirator vacuum.

In all preparations, the organic phase was dried using a suspension of anhydrous magnesium sulphate unless otherwise stated.

6.1.2 Solvents and Reagents

Tetrahydrofuran (THF) and diethyl ether

AR THF or ether (1000 ml) together with sodium (3 g) and benzophenone (30 g) was heated until a deep blue colour was obtained. The mixture was refluxed for at least 1.5 hours under a nitrogen atmosphere and then was freshly distilled immediately before it was needed.

Dichloromethane and Toluene

Dichloromethane (DCM) or toluene were dried by refluxing AR grade solvent with calcium hydride for at least 2 hours under a nitrogen atmosphere and distillation immediately before using.

Methanol and Ethanol

Methanol (or ethanol) (100 ml) together with magnesium turnings (5 g) and iodine (0.5 g) was heated until the iodine colour disappeared. Methanol (or ethanol) (2000 ml) was then added and the mixture boiled under reflux for 1 hour. The resulting solution was distilled, the fraction boiling at 65 °C / 760 mm for methanol (or 78 °C / 760 mm for ethanol) was collected.

Dimethylformamide (DMF)

DMF (anhydrous) was purchased from Aldrich and used without further purification.

Petroleum ether refers to the fraction boiling from 35 to 50 °C.

6.2 Synthetic Work for the Replicating System

6.2.1 2-Amino-6-hydroxypyridine (55)

2,6-Diaminopyridine (10 g, 0.0917 mol) was placed in a 100 ml round-bottom flask with magnetic stirrer. 50% Sulphuric acid (50 ml) was added to the flask slowly with stirring, then the solution was heated at 95-100 °C for 5 hours. The solution was diluted with water (50 ml) and cooled to 45 °C and kept at that temperature for about 1 hour, the crystalline product was removed by filtration to give 2-amino-6-hydroxypyridine sulphate 63 (12 g). This product was ground well in a mortar and transferred to a 250 ml round bottom flask with 50 ml water. The solution was heated to about 70 °C with stirring and hot 30% barium hydroxide solution was added until the pH of the solution reached about 9. The solution was stirred for another 3 hours, BaSO₄ was removed by filtration and the filtrate was evaporated to about 10ml. The concentrated solution was kept in a refrigerator overnight to give the crude crystalline product (5.1g, 50 %), which was recrystallized from ethanol to give colourless crystals, m.p. 203-205 °C (literature 204-205 °C); IR ν_{\max} (Nujol) 3439 (OH), 3158 (NH), 1632, 1461, 1414 (Ar) cm⁻¹; ¹H NMR δ (DMSO-d₆) 10.52 (1H, b, OH), 7.08 (1H, dd, J= 7.68, 8.8 Hz, ArH), 6.02 (2H, b, NH₂), 5.35 (1H, d, J= 8.8 Hz, ArH), 5.26 (1H, d, J= 7.68Hz, ArH); MS (EI) m/z 110 (M⁺), 93, 82, 65, 55 (Found: C, 54.44; H, 5.48; N, 25.58 %. C₅H₆N₂O requires C, 54.54; H, 5.49; N, 25.44 %).

6.2.2 2-Hexanoylamido-6-hydroxypyridine (76)

2-Amino-6-hydroxypyridine 55 (4 g, 0.036 mol) and hexanoyl anhydride (10 ml) were placed in a round bottom flask heated to 100 °C for 5 hours. The solution was cooled to room temperature, 10% aqueous NaHCO₃ (100 ml) was added and stirred solution was warmed to about 60

°C for 1 hour. The precipitate was removed to give the product as white flakes (3.2 g, 50%), which was recrystallized from water, m.p. 144 - 145 °C; IR ν_{\max} (Nujol) 3210 (OH), 3150 (NH), 3097, 1667 (CO), 1589, 1460 (Ar) cm^{-1} ; $^1\text{H NMR } \delta$ (DMSO- d_6) 10.8 (1H, b, OH), 10.3 (1H, b, NH), 7.48 (1H, t, $J=8.24$ Hz, ArH), 6.97 (1H, d, $J=8.24$ Hz, ArH), 6.22 (1H, d, $J=8.24$ Hz, ArH), 2.34 (2H, t, $J=7.14$ Hz, COCH_2), 1.56 (2H, m, CH_2), 1.27 (4H, m, CH_2CH_2), 0.86 (3H, t, $J=6.6$ Hz, CH_3); MS (EI) m/z 208 (M^+), 152, 110 (100%), 82, 43 (Found: C, 63.63; H, 7.78; N, 13.50 %. $\text{C}_{11}\text{H}_{16}\text{N}_2\text{O}_2$ requires C, 63.44; H, 7.74; N, 13.45 %).

6.2.3 2-Hexanoylamido-5-nitro-6-hydroxypyridine (77)

A 50 ml round-bottomed flask was charged with 2-hexanoylamido-6-hydroxypyridine (3.0 g, 0.014 mol) and acetic acid (20 ml) and cooled by a cold water bath. To this solution 1 equivalent of nitric acid (conc. 67%) was added dropwise with vigorous stirring. After a third of the nitric acid had been added the solution turned sticky, the addition was halted and the solution was stirred until the solution became liquid before the addition of the remaining nitric acid. The solution was stirred for another half an hour at room temperature, diluted with ice water and neutralized with sodium hydroxide solution. The precipitate was removed by filtration to give the product as a dark green solid (2.3 g, 63%), which was recrystallized from methanol, m.p. 255 °C (decompose); IR ν_{\max} (Nujol) 3367 (OH), 3213 (NH), 1693 (CO), 1657 (CO), 1601, 1513, 1460, 1416 (Ar), 1377, 1330, 1272 cm^{-1} ; $^1\text{H NMR } \delta$ (DMSO- d_6) 11.31 (1H, b, NH), 8.55 (1H, d, $J=8.78$ Hz, ArH), 6.44 (1H, b, $J=8.78$, ArH), 2.54 (2H, t, $J=7.68$ Hz, COCH_2), 1.59 (2H, m, CH_2), 1.30 (4H, m, CH_2CH_2), 0.87 (3H, m, CH_3); MS (EI) m/z 253 (M^+), 197, 155 (100%), 108, 99, 71, 43 (Found: C, 51.85; H, 6.05; N, 16.89 %. $\text{C}_{11}\text{H}_{15}\text{N}_3\text{O}_4$ requires C, 52.17; H, 5.97; N, 16.59 %).

6.2.4 5-Amino-2-hexanoylamido-6-hydroxypyridine (78)

A 500 ml two-necked flask was equipped with a T shape valve one end of which was connected to a vacuum and the other end to a nitrogen cylinder. The other neck of flask was attached to a hydrogen source which had a mercury sealed outlet. A solution of 2-hexanoylamido-5-nitro-6-hydroxypyridine 77 (3.0 g, 0.012 mol) in methanol (100 ml) was added to the flask which was evacuated and filled with nitrogen three times. Platinum oxide hydrate (Adams catalyst) (0.2 g) was added and the flask was evacuated and filled with hydrogen three times. The solution was stirred for 2 hours under a constant pressure of hydrogen, insoluble material was removed by filtration and the solvent was evaporated to give the product as a crude purple solid (2.2 g, 61%). This compound was used for the next reaction without further purification, m.p. 116 – 119 °C; IR ν_{\max} (Nujol) 3320 (NH), 1649 (CO), 1593, 1461 (Ar) cm^{-1} ; $^1\text{H NMR}$ δ (DMSO- d_6) 11.3 (1H, b, OH), 10.80 (1H, b, NH), 6.50 (1H, d, $J=7.7$ Hz, ArH), 6.11 (1H, d, $J=7.7$ Hz, ArH), 4.73 (2H, b, NH_2), 2.26 (2H, m, COCH_2), 1.54 (2H, m, CH_2), 1.25 (4H, m, CH_2CH_2), 0.85 (3H, t, $J=6.6$ Hz, CH_3); MS (EI) m/z 223 (M^+), 125 (100%), 43; HRMS (EI), Found: M^+ , 223.13228, $\text{C}_{11}\text{H}_{17}\text{N}_3\text{O}_2$ requires M, 223.13208.

6.2.5 5-Maleoylamido-2-hexanoylamido-6-hydroxypyridine (79)

To a solution of 5-amino-2-hexanoylamido-6-hydroxypyridine 78 (2g, 0.009 mol) in THF (30 ml), 1.2 equivalent of maleic anhydride in THF was added slowly with vigorous stirring. The solution was stirred for another 1 hour after the addition of maleic anhydride. The precipitate was filtered off and washed with THF. A green solid product (2.45g, 85%) was obtained, which was then recrystallised from ethanol, m.p. 198 – 201 °C; IR ν_{\max} (Nujol) 3128 (OH), 1885 (CO), 1701 (CO), 1664 (CO), 1620 (C=C), 1546, 1461 (Ar), 1314, 1282, 1236 cm^{-1} ; $^1\text{H NMR}$ δ (DMSO- d_6) 12.1 (1H, b, COOH),

10.56 (1H, b, NH), 9.88 (1H, b, NH), 8.27 (1H, d, J= 8.26 Hz, ArH), 6.69 (1H, d, J= 12.1 Hz, =CH), 6.35 (1H, d, J= 12.1 Hz, =CH), 6.20 (1H, b, ArH), 2.34 (2H, m, COCH₂), 1.58 (2H, m, CH₂), 1.28 (4H, m, CH₂CH₂), 0.88 (3H, m, CH₃); MS (EI) m/z 321 (M⁺), 223, 205, 125 (100%), 43 (Found: C, 55.73; H, 6.05; N, 12.94 %. C₁₅H₁₉N₃O₅ requires C, 56.07; H, 5.96; N, 13.08 %).

6.2.6 5-Maleimido-2-hexanoylamido-6-acetoxypyridine (80)

A solution of 5-maleoylamido-2-hexanoylamido-6-hydroxypyridine 79 (0.5 g, 0.0016 mol) with sodium acetate (0.02 g) in acetic anhydride (5 ml) was heated to 90 °C for half an hour. The solution was cooled to room temperature and 10% aqueous NaHCO₃ solution (10 ml) was added and the solution was stirred for 5 hours at room temperature. The greyish solid was removed by filtration to give 0.4g (yield 72%) of product. This compound was used for the next reaction without further purification. m.p. 131 – 133 °C; IR ν_{\max} (Nujol) 3353 (NH), 1779 (CO), 1708 (CO), 1649 (CO), 1583, 1514, 1461 (Ar), 1309, 1111 cm⁻¹; ¹H NMR δ (DMSO-d₆) 10.84 (1H, b, NH), 8.15 (1H, d, J= 8.8 Hz, ArH), 7.90 (1H, d, J= 8.8 Hz, ArH), 7.25 (2H, s, CH=CH), 2.40 (2H, m, COCH₂), 2.17 (3H, s, COCH₃), 1.58 (2H, m, CH₂), 1.28 (4H, m, CH₂CH₂), 0.88 (3H, m, CH₃); MS (EI) m/z, 345 (M⁺), 303, 205 (100%), 58, 43; HRMS (EI), Found: M⁺, 345.13269, C₁₇H₁₉N₃O₅ requires M, 345.13247.

6.2.7 5-Maleimido-2-hexanoylamido-6-hydroxypyridine (81)

To a solution of 5-maleimido-2-hexanoylamino-6-acetoxypyridine (0.2 g, 0.00058 mol) in dry THF (5 ml), 1 equivalent of dimethylamine was added dropwise with stirring at room temperature. After completing the addition of the base, the solution was stirred for another half an hour and then the solvent was removed. 2 ml of chloroform was added to the flask and the precipitate was removed by filtration to give yellow solid product

(0.12g), which could be recrystallized in chloroform, m.p. 179 – 182 °C; IR ν_{max} (Nujol) 3350 (OH), 3230 (NH), 1890 (CO), 1732 (CO), 1589, 1504 (Ar), 1299, 1207, 1160 cm^{-1} ; $^1\text{H NMR } \delta$ (DCM- d_2), 12.25 (1H, b, OH), 9.28 (1H, b, NH), 7.34 (1H, d, $J = 7.7$ Hz, ArH), 6.81 (2H, s, CH=CH), 6.04 (1H, d, $J = 7.7$ Hz, ArH), 2.37 (2H, m, COCH₂), 1.66 (2H, m, CH₂), 1.30 (4H, m, CH₂CH₂), 0.90 (3H, m, CH₃); MS (EI) m/z , 303 (M⁺), 205 (100%), 82, 43 (Found: C, 59.11; H, 5.65; N, 13.85 %. C₁₅H₁₇N₃O₄ requires C, 59.40; H, 5.65; N, 13.85 %).

6.2.8 cis-1-Acetoxy-4-chloro-2-cyclohexene (94)

Lithium chloride (2.5 g, 0.06 mol), lithium acetate dihydrate (6.1 g, 0.06 mol), palladium acetate (0.34 g, 1.5 mmol), and p-benzoquinone (6.5 g, 0.06 mol) were added with stirring to acetic acid (100 ml) and after all chemicals were dissolved 300 ml of pentane was added. To the pentane phase was added 1,3-cyclohexadiene (2.41 g, 0.06 mol). The reaction mixture was stirred gently at room temperature for 4 hours, manganese dioxide (1.44 g, 0.033 mol) was added and the contents of flask were stirred for another 4 hours at room temperature. The organic phase was separated and saved. Another portion of manganese dioxide (1.44 g, 0.033 mol) and 10 ml of acetic acid were added to the acetic acid phase and the solution was stirred vigorously for 30 minutes. Lithium chloride (1.3 g, 0.03 mol), pentane (150 ml), and 1,3-cyclohexadiene (2.41 g, 0.030 mol) were added and the two phase solution was stirred gently overnight, saturated sodium chloride solution (35 ml) was added and the organic phase was separated and saved. The aqueous phase was filtered and extracted with pentane (2 x 150 ml) The combined pentane phases were washed with water, saturated aqueous Na₂CO₃, NaOH (2 M), water again and saturated NaCl solution, and then dried over MgSO₄. The solvent was removed to give the crude product as a yellow oil (7.5 g, 72%). After Kugelrohr distillation, the crude product afforded pure cis-1-acetoxy-4-chloro-2-cyclohexene (6.5 g). The

analytical data matched that reported in the literature. IR ν_{\max} (Nujol) 1740 (CO), 1600 (C=C), 1377, 1245, 1038 cm^{-1} ; ^1H NMR δ 6.02 – 5.77 (2H, m, CH=CH), 5.29 (1H, m, AcOCH), 4.57 (1H, m, ClCH), 2.08 (3H, s, CH_3), 2.20 – 2.92 (4H, m, CH_2CH_2); MS (CI) m/z 192, 194 ($[\text{M} + \text{NH}_4]^+$), 158, 139, 98.

6.2.9 cis-1-Acetoxy-4-(dicarbomethoxymethyl)-2-cyclohexene (95)

A solution of sodium dimethyl malonate in THF (255 ml of a 0.2 M solution, 0.055 mol, pre-made from equimolar amounts of sodium hydride and dimethyl malonate) was added to a mixture of cis-1-acetoxy-4-chloro-2-cyclohexene (8.7 g, 0.05 mol), palladium acetate (0.25 g, 1.1 mmol) and triphenylphosphine (1.2 g, 4.5 mmol) under an atmosphere of nitrogen at room temperature. The mixture was stirred for 2 hours, and saturated aqueous sodium bicarbonate (100 ml), water (50 ml) and ether (100 ml) were added. The organic phase was separated and the remaining aqueous phase was extracted with ether (3 x 150 ml). The combined organic phases were washed with brine (100 ml), dried over anhydrous magnesium sulphate, concentrated to approximately 200 ml, and then filtered through a short silica gel column to remove remaining palladium species and phosphine oxide. Evaporation of the solvent gave a light brown oil as crude product (14.5 g). Kugelrohr distillation of the crude product afforded 12 g (yield 90 %) of cis -1-acetoxy-4-(dicarbomethoxymethyl)-2-cyclohexene as a light brown oil. Analytical data matched that reported in the literature. IR ν_{\max} (Nujol) 1740 (CO), 1440 (C=C), 1375, 1250, 1150, 1030 cm^{-1} ; ^1H NMR δ 5.91 (2H, s, CH=CH), 5.19 (1H, m, AcOCH), 3.76 (6H, s, $(\text{COOCH}_3)_2$), 3.34 (1H, d, $J = 9.9$ Hz, $\text{CH}(\text{COOMe})_2$), 2.88 (1H, m, CH), 2.03 (3H, s, COCH_3), 1.85 (4H, m, CH_2CH_2); MS (CI) m/z 288 ($[\text{M} + \text{NH}_4]^+$), 228, 211, 150, 139.

6.2.10 5-(Dicarbomethoxymethyl)-1,3-cyclohexadiene (91)

To a solution of *cis*-1-Acetoxy-4-(dicarbomethoxymethyl)-2-cyclohexene **95** (3.0 g, 0.011 mol) in dry toluene (45 ml), tris(dibenzylideneacetone)dipalladium(0) (0.1 g, 0.17 mmol), 1,2-bis(diphenylphosphino)-ethane (0.179 g, 0.44 mmol) and triethylamine (1.68 g, 0.017 mol) were added with stirring under a nitrogen atmosphere. The resulting solution was heated at a bath temperature of about 100 °C for 5 hours under nitrogen. After being cooled down to room temperature, 25 ml of ether was added to the solution, which was washed with HCl (2M, 2 x 10 ml), water (10 ml), brine (10 ml), and dried over magnesium sulphate. The solvent was removed to give crude product as a yellow oil which was then purified by column chromatography to yield 2.10g (91 %) of diene. This product was used for the next reaction without further purification. IR ν_{\max} (Nujol) 1750 (CO), 1730 (CO), 1480, 1440 (C=C), 1330, 1260, 1150 cm^{-1} ; ^1H NMR δ 6.02 – 5.70 (4H, m, =CH), 3.75 (3H, s, COOCH₃), 3.73 (3H, s, COOCH₃), 3.54 (1H, d, $J = 9.34$ Hz, CH(COOMe)₂), 3.04 (1H, m, CH), 2.31 (2H, m, CH₂); MS (EI) m/z 210 (M⁺), 178, 146, 118, 91.

6.2.11 5-Carbomethoxymethyl-1,3-cyclohexadiene (92)

5-(Dicarbomethoxymethyl)-1,3-cyclohexadiene (4.17 g, 0.019 mol) was dissolved in dimethylsulfoxide (58 ml) together with sodium cyanide (4.86 g, 0.099 mol) and water (1.80 g, 0.10 mol) was added. The reaction mixture was heated to 70 °C for 30 hours. After cooling to room temperature, water (40 ml) was added, and the resulting solution was extracted with pentane/ether (9:1, 4 x 25 ml). The combined organic phases were washed with water (2 x 15 ml), brine (15 ml), and dried over MgSO₄. The solvent was distilled off at atmospheric pressure to give 2.5 g of crude product as an oil. Vacuum distillation (14 mm) of the crude product afforded 2.1 g (yield 72 %) of colourless product. IR ν_{\max} (Nujol) 1735, 1600,

1450, 1380, 1340, 1280, 1115 cm^{-1} ; $^1\text{H NMR}$ δ 5.94 – 5.67 (4H, m, =CH), 3.68 (3H, s, CH_3), 2.76 (1H, m, CH), 2.41 (2H, m, $\text{CH}_2(\text{COOMe})$), 2.37 (1H, m, CH_1), 2.11-1.93 (1H, m, CH); MS (EI) m/z 152 (M^+), 121.91, 79, 74, 43.

6.2.12 2,4-Cyclohexadiene-1-acetic acid (5-carboxymethyl-1,3-cyclohexadiene) (90)

To a solution of 5-carbomethoxymethyl-1,3-cyclohexadiene 92 (0.8 g, 5.3 mmol) in methanol (35 ml), an aqueous solution of KOH (2.5g in 15 ml H_2O) was added. The mixture was stirred under nitrogen at room temperature for 4 hours, and then the solution was slightly acidified with ice-cold 10% HCl and extracted with ether (2 x 30 ml). The ether solution was washed with water (2 x 10 ml) and dried over magnesium sulphate. The solvent was removed to give the product as light brown oil (0.66 g, yield 91 %), IR ν_{max} (Nujol) 3400 (COOH), 1700 (CO), 1400 (C=C), 1280 cm^{-1} ; $^1\text{H NMR}$ δ 10.34 (1H, b, COOH), 5.96 – 5.70 (4H, m, =CH), 2.77 (1H, m, CH), 2.46 (2H, m, CH_2COOH), 2.42 (1H, m, CH), 2.15-1.95 (1H, m, CH); MS (EI) m/z 138 (M^+), 136 ($[\text{M} - 2]^+$), 79.

6.2.13 2-(2,4-Cyclohexadienylacetamido)-5,7-dimethyl-1,8-naphthyridine (114)

A solution containing 5-carboxymethyl-1,3-cyclohexadiene 90 (0.66 g, 0.0048 mol), triethylamine (0.73 g) in dry DMF (15 ml) was cooled in an ice bath and ethyl chloroformate (0.52 g) was added dropwise. The mixture was stirred for half an hour at room temperature to allow complete reaction. To this mixture, a solution of 2-amino-5,7-dimethyl-1,8-naphthyridine (0.92 g 0.0053 mol) in dry DMF (10 ml) was added and the solution was heated at 100 $^\circ\text{C}$ for three hours. The solvent was evaporated and the residue was purified by flash column chromatography with DCM/Methanol as eluant to give the product (0.65 g, yield 46 %) as white

solid. Further purification could be done by recrystallization from toluene. m.p. 91 – 93 °C; IR ν_{\max} (Nujol) 3210 (NH), 1693 (CO), 1600 (C=C), 1512, 1460, 1410 (Ar), 1313, 1294 cm^{-1} ; ^1H NMR δ 8.63 (1H, b, NH), 8.46, 8.31 (2H, AB system, $J = 8.8$ Hz, ArH), 7.12 (1H, s, ArH), 5.98 – 5.75 (4H, m, =CH), 2.89 (1H, m, CH), 2.70 (3H, s, CH_3), 2.66 (3H, s, CH_3), 2.55 (2H, m, CH_2COOH), 2.50 (1H, m, CH), 2.15 (1H, m, CH); MS (EI) m/z 293 (M^+), 292 ($[\text{M} - \text{H}]^+$), 215, 173 (100%); HRMS (FAB), Found: $[\text{M} + \text{H}]^+$, 294.16035, $\text{C}_{18}\text{H}_{20}\text{N}_3\text{O}$ requires 294.16064.

6.2.14 N-Phenylmaleimide (120)

To a solution of maleic anhydride (2 g, 0.02 mol) in dry diethyl ether (25 ml), a solution of aniline (freshly distilled, 1.9 g, 0.02 mol) in dry ether (20 ml) was added dropwise. The resulting thick suspension was stirred at room temperature for 1 hour. The maleanilic acid was obtained by suction filtration as a fine, cream-coloured powder (3.7 g, yield 97%), m.p. 201 – 202 °C. The compound was used directly in the next reaction without further purification.

A suspension of maleanilic acid (3.2 g, 0.17 mol) together with anhydrous sodium acetate (0.65 g) in acetic anhydride (8 ml) was dissolved by stirring and heating on a steam bath for 30 minutes. The reaction mixture was cooled and then poured into 20 ml ice water. The precipitate was removed by filtration, washed with ice - cold water (3 x 5 ml) and petroleum ether, and dried to give crude product (2.1 g, yield 75 %) which was recrystallised from hexane to afford a product as yellow needles. m.p. 88 – 89 °C; IR ν_{\max} (Nujol) 3180 (Ar), 1724 (CO), 1593 (C=C), 1504, 1459 (Ar), 1310, 1207, 1160 cm^{-1} ; ^1H NMR δ 7.47 - 7.32 (5H, m, ArH), 6.81 (2H, s, CH=CH); MS (EI) m/z 173 (M^+), 77, 65 (Found: C, 69.01; H, 4.10; N, 7.84 %. $\text{C}_{10}\text{H}_7\text{NO}_2$ requires C, 69.36; H, 4.07; N, 8.09 %).

6.2.15 2,4-Cyclohexadienyl-acetyl-N-phenyl-amide (121)

A solution containing 5-carboxymethyl-1,3-cyclohexadiene 90 (0.3 g, 0.0022 mol), triethylamine (0.22 g) in dried DMF (5 ml) was cooled in an ice bath and ethyl chloroformate (0.24 g) was added dropwise. The mixture was stirred half an hour at room temperature to allow complete reaction. To this mixture, a solution of aniline (0.25 g, 0.0026 mol) in dry DMF (2 ml) was added and the solution was heated at 100 °C for three hours. The solvent was evaporated and the residue was purified by flash column chromatography with DCM as eluant to give the product (0.4 g, yield 85 %) as white solid. Further purification could be done by recrystallization from hexane. m.p. 65 – 67 °C; IR ν_{\max} (Nujol) 3286 (NH), 1649 (CO), 1598 (C=C), 1529, 1497, 1461 (Ar), 1309, 1204 cm^{-1} ; $^1\text{H NMR}$ δ 7.54 - 7.11 (5H, m, Ar), 7.22 (1H, b, NH), 5.94 - 5.81 (4H, m, =CH), 2.93 (1H, m, CH), 2.52 - 2.38 (3H, m, CH, CH_2CO), 2.05-2.2 (1H, m, CH); MS (EI) m/z 213 (M^+), 93, 77, 65, 55 (Found: C, 78.53; H, 7.18; N, 6.30 %. $\text{C}_{14}\text{H}_{15}\text{NO}$ requires C, 78.84; H, 7.09; N, 6.57 %).

6.2.16 2,4-Dimethyl-7-phenylacetamido-1,8-naphthyridine (123)

A solution containing phenyl acetic acid (2.0 g, 0.015 mol), triethylamine (1.51 g) in dry DMF (25 ml) was cooled in an ice bath and ethyl chloroformate (1.60 g) was added dropwise. The mixture was stirred for half an hour at room temperature to allow complete reaction. To this mixture, a solution of 2,4-dimethyl-7-amino-1,8-naphthyridine (2.60 g, 0.015 mol) in dry DMF (25 ml) was added and the solution was heated at 100 °C for three hours. The solvent was evaporated and the residue was purified by flash column chromatography with DCM/MeOH as eluant to give the product (3.6 g, yield 82 %) as white solid. Further purification could be done by recrystallization from toluene. m.p. >250 °C; IR ν_{\max} (Nujol) 3200 (NH), 1694 (CO), 1600, 1511, 1461, 1409 (Ar), 1342, 1314

cm⁻¹; ¹H NMR δ 8.50, 8.27 (2H, AB system, J = 9.34Hz, ArH), 8.20 (1H, b, NH), 7.42 - 7.32 (5H, m, ArH), 7.10 (1H, s, ArH), 3.83 (2H, s, CH₂), 2.67 (3H, s, CH₃), 2.63 (3H, s, CH₃); MS (EI) m/z 291 (M⁺), 91, 77, 65, 55 (Found: C, 73.95; H, 5.93; N, 14.23 %. C₁₈H₁₇N₃O requires C, 74.20; H, 5.88; N, 14.42 %).

6.2.17 2-Amino-5-nitropyridine (67)

To a solution of 2-aminopyridine (4.7g, 0.05 mol) in 40 ml conc. H₂SO₄ (98%, d = 1.84), a mixture containing conc. H₂SO₄ (10 ml) and conc. HNO₃ (3.2 ml, 70%, d = 1.42) was added dropwise with stirring in an ice bath. The solution was poured into 500 ml ice after 0.5 hour in the ice bath and 0.5 hour at room temperature. The solution was neutralized with aqueous NaOH solution and the precipitate was removed by filtration to give a crude product as a green solid which was purified by sublimation to afford the product as green needles (5.4 g, 79%), m.p. 185-187 °C; ¹H NMR δ (d₆-DMSO) 8.84 (1H, d, J = 3.3 Hz, ArH), 8.12 (1H, dd, J = 3.3, 9.34 Hz, ArH), 7.54 (2H, b, NH₂), 6.50 (1H, d, J = 9.34Hz, Ar); MS (EI) m/z 139 (M⁺), 93, 66.

6.2.18 2-Acetamido-5-nitropyridine (68)

2-Amino-5-nitropyridine (67) 1.6 g, 0.011mol) was heated in acetic anhydride (25 ml) at 45 - 50 °C under N₂ for 3 h then stirred at room temperature overnight. The acetic anhydride was evaporated and give a brown solid which was purified by flash column chromatography on silicagel, eluting with CH₂Cl₂/MeOH to afford a white solid (1.1 g, 55%), m.p. 193 - 195 °C; ¹H NMR δ (DMSO-d₆) 11.20 (1H, b, NH), 9.15 (1H, d, J = 2.76 Hz, ArH), 8.58 (1H, dd, J = 2.76, 10.0 Hz, ArH), 8.28 (1H, d, J = 10.0 Hz, ArH), 2.18 (3H, s, CH₃); MS (EI) m/z 181 (M⁺), 139, 43 (100%).

6.2.19 2-Acetamido-5-nitropyridine-N-oxide (69)

A solution of peracetic acid (7.7 ml, 8.5 g, 0.036 mol) (32 wt. % in acetic acid) was added to a solution of 2-acetamido-5-nitropyridine (68) (3.3g, 0.018 mol) in acetic acid (12 ml) dropwise at 80 °C and the resulting solution was heated at 80 °C for 5 h. The solvent was evaporated and the crude product was purified by flash column chromatography using ethyl acetate as eluant to give the product as yellow crystals (1.9 g, 54%), m.p. 220 - 222 °C; IR ν_{\max} (Nujol) 3210 (NH), 1695 (CO), 1540 (Ar), 1350 cm^{-1} ; ^1H NMR δ (DMSO- d_6) 10.91 (1H, b, NH), 9.20 (1H, d, $J = 2.2$ Hz, ArH), 8.47 (1H, d, $J = 9.28$ Hz, ArH), 8.22 (1H, dd, $J = 2.2$ Hz, $J = 9.28$ Hz, ArH), 2.33 (3H, s, CH_3); MS (EI) m/z 197 (M^+), 181, 155, 139, 43 (100%) (Found: C, 42.30; H, 3.50; N, 21.45 %. $\text{C}_7\text{H}_7\text{N}_3\text{O}_4$ requires C, 42.65; H, 3.58; N, 21.31 %).

6.2.20 2-Acetamido-5-nitro-6-acetoxypyridine (70)

A solution of 2-acetamido-5-nitropyridine-N-oxide (69) (1.8 g, 0.009 mol) in acetic anhydride (40 ml) was heated to 140 °C for 5 h with stirring. The solvent was evaporated and the residue was purified by column chromatography using $\text{CH}_2\text{Cl}_2/\text{CH}_3\text{COOC}_2\text{H}_5$ (4 : 1) as eluant to give the product as a yellow solid (0.75 g, 34 %), m.p. 185 - 190 °C; ^1H NMR δ (DMSO- d_6) 11.35 (1H, b, NH), 8.68 (1H, d, $J = 14.8$ Hz, ArH), 8.21 (1H, d, $J = 14.8$ Hz, ArH), 2.22 (3H, s, NCOCH_3), 1.90 (3H, s, OCOCH_3); MS (EI) m/z 239 (M^+), 197, 155, 43 (100%); HRMS (FAB), Found: $[\text{M}+\text{H}]^+$, 240.06234, $\text{C}_9\text{H}_{10}\text{N}_3\text{O}_5$ requires 240.06205.

6.2.21 2-Acetamido-5-nitro-6-hydroxypyridine (71)

A suspension of 2-acetamido-5-nitro-6-acetoxypyridine (70) (0.75 g,) in water (10 ml) was heated to reflux for 2 h. The solvent was evaporated to give the product as a yellow solid (0.5 g, yield 84%), m.p. 211-214 °C; ^1H NMR δ (DMSO- d_6) 11.8 (b, 1H), 8.55 (d, $J = 8.80$ Hz, 2H), 6.45 (d, $J = 8.80$ Hz),

2.21 (s, 3H); MS (EI) m/z 197 (M^+), 155 (100%), 43; HRMS (FAB), Found: $[M+H]^+$, 198.05122, $C_7H_8N_3O_4$ requires 198.05148.

6.2.22 2-Hexanoylamido-5-nitropyridine (73)

2-Amino-5-nitropyridine (67) 2.0 g, 0.014mol) was heated in hexanoyl anhydride (25 ml) at 100 °C under N_2 for 5 h then stirred at room temperature overnight. The hexanoyl anhydride was evaporated under vacuum to give a brown solid which was purified by flash column chromatography on silicagel, eluting with $CH_2Cl_2/MeOH$ to give a white solid (1.92 g, 58%), m.p. 85 - 88 °C; 1H NMR δ (DMSO- d_6) 11.19 (1H, b, NH), 9.16 (1H, d, $J = 2.74$ Hz, ArH), 8.58 (1H, dd, $J = 2.74, 9.34$ Hz, ArH), 8.26 (1H, d, $J = 9.34$ Hz, ArH), 2.46 (2H, t, $J = 7.14$ Hz, $COCH_2$), 1.56 (2H, m, CH_2), 1.28 (4H, m, CH_2CH_2), 0.86 (3H, m, CH_3); MS (EI) m/z 237 (M^+), 139 (100%) 43 (Found: C, 55.32; H, 6.27; N, 17.40 %. $C_{11}H_{15}N_3O_3$ requires C, 55.69; H, 6.37; N, 17.71 %).

6.2.23 2-Hexanoylamido-5-nitropyridine-N-oxide (74)

A solution of peracetic acid (2.8 ml, 3.2 g, 0.013 mol) (32 wt. % in acetic acid) was added to a solution of 2-hexanoylamido-5-nitropyridine (68) (1.6 g, 0.0067 mol) in acetic acid (10 ml) dropwise at 80 °C and the resulting solution was heated at 80 °C for 5 h. The solvent was evaporated and crude product was purified by flash column chromatography using ethyl acetate as eluant to give the product as yellow crystals (1.0 g, 59%), m.p. 153 - 155 °C; 1H NMR δ (DMSO- d_6) 10.9 (1H, b, NH), 9.19 (1H, d, $J = 2.2$ Hz, ArH), 8.49 (1H, d, $J = 9.34$ Hz, ArH) 8.22 (ArH, dd, $J = 2.2$ Hz, $J = 9.34$ Hz,), 2.67 (2H, t, $J = 7.14$ Hz, $COCH_2$), 1.52 (2H, m, CH_2), 1.28 (4H, m, CH_2CH_2), 0.86 (3H, m, CH_3); MS (EI) m/z 253 (M^+), 155 (100%), 139, 43 (Found: C, 51.98; H, 5.85; N, 16.54 %. $C_{11}H_{15}N_3O_4$ requires C, 52.17; H, 5.97; N, 16.59 %).

6.3 Kinetic Studies of Diels-Alder Reaction of Replicating System by ^1H NMR

The Diels-Alder reactions between **81** and **114** were followed by ^1H NMR in CD_2Cl_2 with the concentration of all reactants initially at 0.015 M. The reactions were carried out at two different temperature, 23 °C and 40 °C. In all reactions, the olefinic proton signals of diene **114** ($\delta = 5.80 - 5.90$ ppm) and the product **116** ($\delta = 6.20 - 6.40$ ppm) were monitored and their integration was used for calculating the change of concentrations of each species in the reaction. The olefinic proton signal of ene **81** ($\delta = 6.83$ ppm) was also monitored but the peak was overlapped by the signals of aromatic protons and therefore the integration is less accurate. The signal of protons at the 5- and 6- positions ($\delta = 8.42$ ppm) of the naphthyridine were used as a standard for integrations since all spectra showed that there were no changes for the integration and chemical shifts of these two protons throughout the reactions and the peak was not overlapped by other peaks. Although the shape of the naphthyridine signals changed during the reactions from an initial AB system to a multiplet because the naphthyridine unit was transferred from reactant to the product during the reaction, the total concentration of the unit was not changed. For the same reason, the aromatic proton signals were used as a standard for monitoring the reactions of model ene **120** and diene **121**. A Bruker - 200E 200 MHz spectrometer was used for recording the spectra. The spectrum of the reaction without added template at 23 °C was recorded at three-hour intervals for the first twelve hours, then at five-hour intervals thereafter. The spectra of the reactions with added template at 23 °C were recorded at two-hour intervals during the first fourteen hours, and then at four-to-eight-hour intervals thereafter. The spectra of all reactions at 40 °C were recorded at half-an-hour intervals during the first hour and then at one-

hour intervals for the next ten hours and at two-hour intervals thereafter. For every spectrum the same scanning number (64) was used to obtain stable signal/noise ratios which is a key factor for reliable integration. The concentrations of products and reactants were calculated by the following equation,

$$\frac{0.015 - X}{X} = \frac{\text{Int (diene)}}{2 \times \text{Int (product)}} = Y \quad (6.1)$$

where X is the concentrations of products, Int(diene) is the integration of the diene olefinic H and Int(product) is the integration of the product olefinic H. Because products only have 2 olefin protons while the dienes have 4, the integration of product signals needs to be multiplied by 2. By manipulating equation (6.1) we have concentrations of products X,

$$X = \frac{0.015}{Y + 1} \quad (6.2)$$

All data for the plots of concentration vs time for the reactions in Figure 4.2 in chapter 4 are based on this calculation. The data were processed by Macintosh Cricket Graph.

6.3.1 Diels-Alder Reaction Conditions

The pyridone-ene component 81 (2.27 mg, 0.75 mmol) and the naphthyridine-diene component 114 (2.19 mg, 0.75 mmol) were weighed accurately into a 5 mm NMR tube so that addition of 0.50 ml of CD₂Cl₂ gave a concentration of 0.015 M for all partners. The solvent was added just prior to the placement of the tube in the NMR probe and acquisition of spectra was started immediately.

6.3.2 Characterization of the Product 116 of the Replication Reaction

After the kinetic experiments were finished, the solutions were heated to 40 °C over night and then the solutions were checked by NMR spectroscopy before the solvent was evaporated to give the product 116 as a yellow solid which was dried by vacuum, m.p. 205 - 208°C; ¹H NMR δ(400 MHz, CDCl₃, 50 °C) 14.80 (b, 1H), 11.30 (b, 1H), 10.91 (b, 1H), 8.50, 8.34 (AB system J = 9.07 Hz, 2H), 7.38 (d, J = 7.3 Hz, 1H), 7.18 (s, 1H), 7.07 (d, J = 7.3Hz, 1H), 6.4 (t, J = 7Hz, 1H), 6.30 (br. 1H), 3.32 (m, 2H), 3.23 (m, 1H), 3.04 (br. d, J = 6.5Hz, 1H), 2.78, (m, 2H), 2.71 (s, 3H), 2.69 (s, 3H), 2.55 (m, 1H), 2.11 (m, 4H), 1.49 (m, 2H), 1.10 (br, m, 4H), 0.74 (m, 3H); MS (FAB) m/z 597 ([M + H]⁺), 294, 174 (100%), 55, 43; HRMS (FAB), Found: [M+H]⁺, 597.28460, C₃₃H₃₇N₆O₅ (M+H) requires 597.28254.

6.3.3 Characterization of the Product 122 from the Model Diels-Alder Reaction

The same procedure as used for compound 116 was used to obtain compound 122 as white crystals, m.p. 84-87 °C; IR ν_{max}(Nujol) 3340, 1772,1708, 1597, 1534, 1459, 1300, 1185 cm⁻¹; ¹H NMR δ(CD₂Cl₂) 7.49-7.16 (m, 10H), 6.39 - 6.23 (m, 2H), 3.26 (m, 2H), 3.08 (m, 2H), 2.50 (b, 1H), 2.33 (m, 1H), 2.25 - 2.06 (m, 2H), 1.27 - 1.11 (m, 2H); MS (FAB) m/z, 387 ([M + H]⁺), 214, 174, 77, 65, 55; HRMS (FAB), Found: [M+H]⁺, 387.17054, C₂₄H₂₃N₂O₃ (M+H) requires 387.17087.

6.4 Measurement of Binding Constant

An ¹H NMR titration method was employed for obtaining the data needed for calculation of binding constants between compound 81 and 123,

at 23 °C and 40 °C. The values used as an approximate data for K_1 for the computer modeling (see chapter 2). All measurements of chemical shifts were obtained in deuteriodichloromethane (CD_2Cl_2) at the NMR probe temperature required (23 °C and 40 °C) and are measured downfield from internal tetramethylsilane. In all cases exchange was observed to be rapid on the NMR time scale, and only averaged spectra were observed, rather than superposition of separate spectra of bound, unbound and self bound species.

A sample of **81** (equivalent to 0.02 M in 0.50 ml of CD_2Cl_2 for measurement at 23 °C and 0.015 M for measurement at 40 °C) was weighed into a 5 mm NMR tube and CD_2Cl_2 was added (0.03% TMS). The tube was placed in the NMR probe and spectrum was recorded to obtain the unbound chemical shifts of selected protons. To the NMR tube were added successive portions of compound **123** which were accurately weighed (each increment from 0.1 equivalent of **81** at the beginning of the measurement to 1 equivalent at the end) and spectra were recorded after each portion of **123** was added so that the chemical shifts of selected protons on each compound were recorded until the chemical shifts of these protons no longer changed upon further addition of compound **123**. The selected protons on each compound (**81** and **123**) are amide -NH- protons since their chemical shifts were most sensitive to the degree of binding. The plots of chemical shifts of -CONH- proton of both compounds vs concentration of **123** at both 23 °C and 40 °C are shown in Figure 4.8 in chapter 4. These data were put into a computer programme and association constants were calculated by a trial and error procedure to give a best fit for experimental and calculated data. Table 6.1 and 6.2 list the observed data and calculated data for association constant of $228 M^{-1}$ (for 23 °C) and $163 M^{-1}$ (for 40 °C).

Conc. for 123 (M)	Conc. for 81 (M)	Calculated δ for AcNH in 81 (ppm)	Observed δ for AcNH in 81 (ppm)	Observed δ for AcNH in 123 (ppm)
0.0023	0.0203	9.464724	9.4608	11.1200
0.0069	0.0203	9.806363	9.7795	11.0518
0.0105	0.0203	10.0461	9.9802	11.0161
0.0148	0.0203	10.29307	10.2659	10.9804
0.0164	0.0203	10.37296	10.3456	10.9364
0.0178	0.0203	10.43741	10.4226	10.9034
0.0192	0.0203	10.49685	10.4995	10.8677
0.0206	0.0203	10.55141	10.5655	10.8238
0.0225	0.0203	10.61805	10.6479	10.7798
0.0244	0.0203	10.6768	10.7221	10.7138
0.0268	0.0203	10.74092	10.7935	10.6506
0.0285	0.0203	10.78034	10.8375	10.5078
0.0312	0.0203	10.83426	10.8879	10.4226
0.0358	0.0203	10.90649	10.9502	10.2962
0.0393	0.0203	10.94895	10.9831	10.2165
0.0432	0.0203	10.98699	11.0106	10.1533
0.049	0.0203	11.03054	11.0381	10.0846
0.0545	0.0203	11.06177	11.0601	10.0434
0.059	0.0203	11.0822	11.0683	10.0159
0.0638	0.0203	11.10024	11.0821	10.0076

Table 6.1 The observed and calculated ^1H NMR chemical shifts for the amide proton in compound 81. The observed values were obtained from the titration experiment at 23 °C and the calculated data were obtained by computer calculation when 228 M⁻¹ was chosen

for the association constant. The initial δ for pure 81 is 9.2828. The r.m.s. are 0.06177 and 0.03396 for calculated and observed curves respectively.

Conc. for 123 (M)	Conc. for 81 (M)	Calculated δ for AcNH in 81 (ppm)	Observed δ for AcNH in 81 (ppm)	Observed δ for AcNH in 123 (ppm)
0.003814	0.015657	9.094292	9.1012	10.4587
0.007354	0.015657	9.425373	9.3712	10.4143
0.010454	0.015657	9.675358	9.630899	10.3848
0.013567	0.015657	9.888186	9.8427	10.2479
0.016694	0.015657	10.0656	10.0914	10.1973
0.0191	0.015657	10.1799	10.1659	10.1072
0.022962	0.015657	10.32937	10.3454	9.9636
0.025313	0.015657	10.40339	10.4344	9.9187
0.030289	0.015657	10.52771	10.6209	9.8335
0.035196	0.015657	10.6186	10.6773	9.7311
0.037595	0.015657	10.65466	10.7072	9.6793
0.043347	0.015657	10.72479	10.7532	9.5745
0.049835	0.015657	10.78392	10.7999	9.5244
0.057485	0.015657	10.83568	10.8506	9.4712
0.064639	0.015657	10.87235	10.8575	9.4530
0.072	0.015657	10.90199	10.8978	9.4369
0.080351	0.015657	10.9286	10.9013	9.4357
0.083656	0.015657	10.93757	10.9105	9.4323

Table 6.2 The observed and calculated ^1H NMR chemical shifts for the amide proton in compound 81. The observed values were obtained from the titration experiment at 40 °C and the calculated data were obtained by computer calculation when 163 M^{-1} was chosen

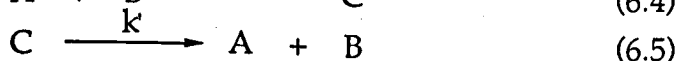
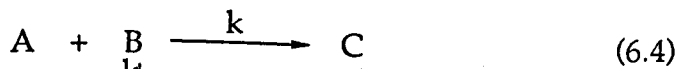
for the association constant. The initial δ for pure 81 is 8.6885. The r.m.s are 0.07055 and 0.03870 for calculated and observed curves respectively.

6.5 Computer Modelling of the Kinetics of a Self-Replication Process

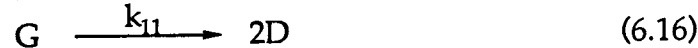
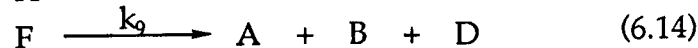
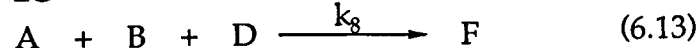
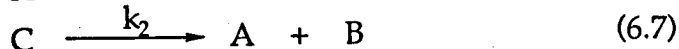
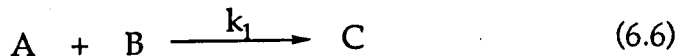
A computer package called 'Kinetics' (Version 1.0), which was made by S. Walker in the Department of Chemistry at the University of Liverpool, was used for kinetic modelling. To start modelling a reaction scheme has to be written in. An equilibrium process must be represented as two reactions in the reaction scheme. For example, an equilibrium like equation 6.3



must be written into the program as equations 6.4 and 6.5.



where $k/k' = K$ in equation 6.3. In all the cases of our modelling k' was set as value of 1 and k was variable. So the full reaction scheme presented in Figure 4.4 was written into the computer as follows:



in which the 4 pairs of equations (6.6 and 6.7, 6.10 and 6.11, 6.13 and 6.14, 6.16 and 6.17) represent the 4 equilibrium processes. According to this scheme, a rate law was computed for each species (see Appendix 1) and concentrations were calculated numerically¹⁰¹ based upon the given rate constants, the initial concentration of each reactant and product, step size (time interval), and error limit. For all the modelling, 1×10^{-6} (second) was used for the step size and 1×10^{-6} was used for error limits. The initial concentrations of the reactants and the product were the same as those used in the experiment. The calculated concentrations of each species at certain times, were printed and used in Macintosh Cricket Graph to compare with experimental results.

The calculation for the simple reaction scheme (Figure 4.10 in chapter 4) was carried out using a simple computer programme based upon equation 4.5. By putting in a time step size, k_α , k_β , c , and initial concentrations of the reactants and the product, the computer solved this equation numerically. The calculated results were printed and used in Cricket Graph to compare with the experimental results.

6.6 Synthetic Work for Calixarenes

6.6.1 5, 11, 17, 23-Tetra-*tert*-butyl-25, 26, 27, 28-tetrahydroxycalix[4]arene ⁸²

Para-*tert*-butylphenol (100 g, 0.67 mol), 37% aqueous formaldehyde solution (62.3 ml, 0.83 mol) and sodium hydroxide (1.2 g, 0.03 mol) were heated at 120 °C for 2 hours until a viscous yellow precursor was formed. The precursor was then suspended in diphenyl ether (800 ml), the contents of the flask heated to 250 °C with nitrogen blown rapidly over the reaction mixture to facilitate the removal of water, and subsequently heated to reflux for 3 hours. The reaction mixture was then cooled, treated with ethyl acetate (1000 ml) and stirred for 30 minutes. The precipitated material was filtered, washed twice with ethyl acetate (100 ml), once with acetic acid (200 ml) and once with water (100 ml) to yield the crude product. Recrystallisation from toluene (1000 ml) gave the product as a white crystalline solid (65 g, 53%), m.p. 342 °C (lit., 344 °C); ¹H NMR δ(CDCl₃) 1.22 (36H, s, C(CH₃)₃), 3.55 (4H, br d, ArCH₂Ar), 4.32 (4H, br d, ArCH₂Ar), 7.0 (8H, s, ArH), 10.22 (4H, s, ArOH); IR ν_{max}(nujol) 3189 (OH), 1461, 1377 (ArH) cm⁻¹; MS (EI) m/z 648 (M⁺), 57(100%) (Found: C, 82.59; H, 8.78 %. C₄₄H₅₆O₄ requires C, 82.65; H, 8.70 %).

6.6.2 25, 26, 27, 28-Tetrahydroxycalix[4]arene (138)

Para-*tert*-butylcalix[4]arene (13.3 g, 20 mmol), aluminium chloride (14.0 g, 105 mmol) and phenol (9.02 g, 96 mmol) were stirred in toluene (125 ml) at room temperature for 1 hour in a nitrogen atmosphere. The solution was then poured into hydrochloric acid (0.2M, 250 ml), the organic phase separated, dried and evaporated to leave a pale yellow oil. Upon the addition of methanol, a white precipitate formed which was recovered by filtration. Recrystallisation from chloroform/methanol gave the product as a white crystalline solid (6.93 g, 79%), m.p. 313-315 °C (lit.,

315-319 °C); IR ν_{\max} (nujol) 3160 (OH) cm^{-1} ; ^1H NMR $\delta(\text{CDCl}_3)$ 3.59 (4H, br d, ArCH_2Ar), 4.23 (4H, br d, ArCH_2Ar), 6.71 (4H, t $J = 7.7$ Hz, ArH), 7.03 (8H, d $J = 7.77$ Hz, ArH). 10.20 (4H, s, ArOH); MS (EI) m/z 424 (M)⁺, 211, 197, 119, 107, 91, 77, 65 (Found: C, 79.10; H, 5.65%. $\text{C}_{28}\text{H}_{24}\text{O}_4$ requires C, 79.23; H, 5.70%).

6.6.3 25, 26, 27, 28-Tetrakis[(ethoxycarbonyl)methoxy]calix[4]arene (128)

Sodium hydride (2.0 g of 60% NaH dispersed in oil) was washed with petroleum ether (50 ml) and added slowly to a solution of 25, 26, 27, 28-tetrahydroxycalix[4]arene (138) (2.0 g, 4.7 mmol) in dried THF (50 ml). After the reaction had subsided, the solution was treated with ethyl bromoacetate (8.0 g, 48 mmol) and refluxed for 24 hours under a nitrogen atmosphere. The reaction mixture was then cooled, quenched with a few drops of ethanol, and the solvent was removed by evaporation on a Rotovapor. The residue was partitioned between water and dichloromethane. The organic phase was separated and washed with distilled water three times. The solvent was evaporated and the yellow oily residue was dried in vacuum. The oil was heated with methanol, cooled down and solvent was evaporated to give a yellowish crude solid which was recrystallised by dissolving in ethanol and leaving at 0 °C for 12 hours to yield the product as colourless needles (2.52 g, 70%), m.p., 105-106 °C (lit., 108-109 °C); IR ν_{\max} (nujol) 1752 (CO), 1459 and 1377 (ArH) cm^{-1} ; ^1H NMR $\delta(\text{CDCl}_3)$ 1.27 (12H, t, $J = 7.8$ Hz, CH_3), 3.22 (4H, d, $J = 13.9$ Hz, ArCH_2Ar), 4.20 (8H, q, $J = 7.8$ Hz, CH_2), 4.73 (8H, s, OCH_2), 4.85 (4H, d, $J = 13.9$ Hz, ArCH_2Ar), 6.65 (12H, m, ArH); MS (FAB) m/z 769 ($[\text{M}+\text{H}]^+$), 656 (Found: C, 68.94; H, 6.09%. $\text{C}_{44}\text{H}_{48}\text{O}_{12}$ requires C, 68.75; H, 6.25%).

6.6.4 25, 26, 27, 28-Tetrakis[(*tert*--butoxycarbonyl)methoxy]calix[4]arene

(140)

Sodium hydride (2.0 g of 60% NaH dispersed in oil) was washed with petroleum ether (50 ml) and added slowly to a solution of 25, 26, 27, 28-tetrahydroxycalix[4]arene (2.0 g, 4.72 mmol) in dried THF (50 ml). After the reaction had subsided, the solution was treated with *tert*-butylbromoacetate (8.0 g, 41 mmol) and refluxed for 24 hours under a nitrogen atmosphere. The reaction mixture was then cooled, quenched with a few drops of ethanol, and the solvent was removed by evaporation on a Rotovapor. The residue was partitioned between water and dichloromethane. The organic phase was separated, washed with distilled water three times to give the crude solid product which was a mixture of cone and partial-cone conformations of the product. The mixture was separated by recrystallisation in dichloromethane/methanol. The cone conformation of the product crystallised from the solvent first as colourless needles (1.10 g, 24%) and the partial-cone conformation was obtained from the mother liquor by evaporation as a colourless solid (2.14 g, 52%). Analytical data for cone conformer: m.p. 256-258 °C; IR ν_{\max} (Nujol) 1748 (CO), 1461 and 1377 (Ar) cm^{-1} ; $^1\text{H NMR } \delta(\text{CDCl}_3)$ 6.61 (3H, s, ArH), 4.89 (1H, d, $J = 13.2$ Hz, ArCH₂Ar), 4.63 (2H, s, OCH₂CO), 3.22 (1H, d, $J = 13.2$ Hz, ArCH₂Ar), 1.46 (9H, s, C(CH₃)₃); MS (EI) m/z 880, 656, 57(100%) (Found: C, 70.95; H, 7.01 %. C₅₂H₆₄O₁₂ requires C, 70.89; H, 7.32 %). Analytical data for partial cone conformer: m.p. 163-165 °C; IR ν_{\max} (Nujol) 1750 (CO), 1460 and 1377 (Ar) cm^{-1} ; $^1\text{H NMR } \delta$ 7.55 (2H, d, $J = 7.53$ Hz, ArH), 7.11 (2H, dd, $J = 1.64$ Hz, $J = 7.58$ Hz, ArH), 7.06 (2H, d, $J = 7.43$ Hz, ArH), 6.96 (1H, t, $J = 7.53$ Hz, ArH), 6.88 (1H, t, $J = 7.43$ Hz, ArH), 6.46 (2H, t, $J = 7.58$ Hz, ArH), 6.17 (2H, dd, $J = 1.64$, $J = 7.58$ Hz, ArH), 4.45 (2H, d, $J = 15.16$ Hz, ArCH₂Ar), 4.39 (2H, d, $J = 13.9$ Hz, ArCH₂Ar), 4.36 (2H, s, OCH₂CO), 4.17 (2H, d, $J = 15.16$ Hz, ArCH₂Ar), 3.99 (2H, d, $J = 12.54$ Hz,

OCH₂CO), 3.86 (2H, s, OCH₂CO), 3.7 (2H, d, J= 12.54Hz, OCH₂CO), 3.10 (2H, d, J= 13.9 Hz, ArCH₂Ar), 1.60 (9H, s, C(CH₃)₃), 1.56 (6H, C(CH₃)₃), 1.53 (12H, C(CH₃)₃), 1.38 (9H, s, C(CH₃)₃); MS (FAB) m/z 881 ([M+1]⁺), 656 (100%) (Found: C, 70.83; H, 7.34 %. C₅₂H₆₄O₁₂ requires C, 70.89; H, 7.32 %).

6.6.5 25, 26, 27, 28-Tetrakis[(carboxy)methoxy]calix[4]arene (141)

25, 26, 27, 28-Tetrakis[(ethoxycarbonyl)methoxy]calix[4]arene (128) (1.5 g, 1.95 mmol) was suspended in trifluoroacetic acid (70% aqueous solution, 25 ml) and refluxed overnight. The solution was cooled and crystallised solid was obtained by filtration. The product was recrystallised from 70% aqueous trifluoroacetic acid (0.92 g, 72%), m.p. 265-267 °C; IR ν_{\max} (nujol) 1723 (CO), 1584 and 1461 (HAr) cm⁻¹; ¹H NMR δ (d₆-DMSO) 3.29 (4H, d, J= 12.6 Hz, ArCH₂Ar), 4.67 (8H, s, OCH₂), 4.89 (4H, d, J= 12.6 Hz, ArCH₂Ar), 6.69 (4H, t, J= 7.16 HZ, ArH), 6.95 (8H, d, J= 7.16 Hz, ArH), 12.35 (4H, s, br, OH); MS (FAB) m/z 657 ([M + H]⁺), 91, 77, 57 (Found: C, 65.74; H, 5.01%. C₄₄H₇₂O₁₂ requires C, 65.85; H, 4.91%).

6.6.6 25, 26, 27, 28-Tetrakis[(chlorocarbonyl)methoxy]calix[4]arene (139)

A suspension of 25,26,27,28-Tetrakis[(carboxy)methoxy]calix[4]arene (141) (0.1 g, 0.152 mmol) in dry dichloromethane (5 ml) was treated with excess of oxalyl chloride (5 ml) and the solution was stirred at room temperature under a nitrogen atmosphere overnight. The solvent was removed by evaporation and the residue was dried under vacuum. A white solid foam (0.10 g, 99%) was obtained which was used directly for the preparation of ionophore libraries without further purification. m.p. 256-258 °C; IR ν_{\max} (nujol) 1728 (CO), 1461 and 1377 (HAr) cm⁻¹; ¹H NMR δ (CDCl₃) 3.32 (4H, d, J= 13.7 Hz, ArCH₂Ar), 4.66 (4H, d, J= 13.7 Hz, ArCH₂Ar), 5.07 (8H, s, OCH₂), 6.68 (12H, s, ArH); MS (EI) m/z 730 (M⁺) (The peak

pattern of isotopes matches that of a compound containing 4 chlorine atoms with a strongest peak at 730).

6.6.7 Library of methyl-, ethyl-, propyl- and butyl-carbamoyl methoxycalix[4]arenes (142)

To a solution of a mixture of dimethylamine (0.191 ml of 2 M THF solution, 0.381 mmol), diethylamine (0.0278 g, 0.381 mmol), dipropylamine (0.0386 g, 0.381 mmol), di-n-butylamine (0.0493 g, 0.381 mmol) and triethylamine (0.15 g, 1.22 mmol) in dried dichloromethane (5 ml), a solution of 25, 26, 27, 28-tetrakis[(chlorocarbonyl)methoxy]calix[4]arene (0.20 g, 0.304 mmol) in dry dichloromethane (5 ml) was added with stirring. The solution was stirred under a nitrogen atmosphere at room temperature overnight and then washed twice with dilute hydrochloric acid and three times with distilled water. The solvent was evaporated and the residue dried in vacuum to give a mixture of products as a white solid foam.

6.6.8 Library of methyl-, ethyl- and propyl-carbamoyl methoxycalix[4]arenes (143)

To a solution of a mixture of dimethylamine (0.127 ml of 2 M THF solution, 0.254 mmol), diethylamine (0.0186 g, 0.254 mmol), dipropylamine (0.0257 g, 0.254 mmol) and triethylamine (0.0771 g, 0.762 mmol) in dried dichloromethane (5 ml), a solution of 25, 26, 27, 28-tetrakis[(chlorocarbonyl)methoxy]calix[4]arene (0.10 g, 0.152 mmol) in dry dichloromethane (5 ml) was added with stirring. The solution was stirred under a nitrogen atmosphere at room temperature overnight and then washed twice with dilute hydrochloric acid and three times with distilled water. The solvent was evaporated and the residue dried in vacuum to give a mixture of products as a white solid.

6.6.9 Library of methyl-, ethyl- and n-butyl-carbamoyl methoxycalix[4]arenes (144)

To a solution of a mixture of dimethylamine (0.127 ml of 2 M THF solution, 0.254 mmol), diethylamine (0.0186 g, 0.254 mmol), dibutylamine (0.0328 g, 0.254 mmol) and triethylamine (0.0771 g, 0.762 mmol) in dry dichloromethane (5 ml), a solution of 25, 26, 27, 28-tetrakis[(chlorocarbonyl)methoxy]calix[4]arene (0.10 g, 0.152 mmol) in dry dichloromethane (5 ml) was added with stirring. The solution was stirred under a nitrogen atmosphere at room temperature overnight and washed twice with dilute hydrochloric acid and three times with distilled water. The solvent was evaporated and the residue dried in vacuum to give a mixture of products as a white solid.

6.6.10 Library of methyl-, propyl- and n-butyl-carbamoyl methoxycalix[4]arenes (145)

To a solution of a mixture of dimethylamine (0.127 ml of 2 M THF solution, 0.254 mmol), dipropylamine (0.0257 g, 0.254 mmol), diethylamine (0.0186 g, 0.254 mmol), dibutylamine (0.0328 g, 0.254 mmol) and triethylamine (0.0771 g, 0.762 mmol) in dry dichloromethane (5 ml), a solution of 25, 26, 27, 28-tetrakis[(chlorocarbonyl)methoxy]calix[4]arene (0.10 g, 0.152 mmol) in dry dichloromethane (5 ml) was added dropwise with stirring. The solution was stirred under a nitrogen atmosphere at room temperature overnight and then washed twice with dilute hydrochloric acid and three times with distilled water. The solvent was evaporated and the residue dried in vacuum to give a mixture of products as a white solid.

6.6.11 Library of ethyl-, propyl and n-butyl-carbamoyl methoxycalix[4]arenes (146)

To a solution of a mixture of diethylamine (0.0186 g, 0.254 mmol), dipropylamine (0.0257 g, 0.254 mmol), dibutylamine (0.0328 g, 0.254 mmol) and triethylamine (0.0771 g, 0.762 mmol) in dry dichloromethane (5 ml), a solution of 25, 26, 27, 28-tetrakis[(chlorocarbonyl)methoxy]calix[4]arene (0.10 g, 0.152 mmol) in dried dichloromethane (5 ml) was added dropwise with stirring. The solution was stirred under a nitrogen atmosphere at room temperature overnight and then washed twice with dilute hydrochloric acid and three times with distilled water. The solvent was evaporated and the residue dried in vacuum to give a mixture of products as a white solid.

6.6.12 Library of ethyl- and propyl-carbamoyl methoxycalix[4]arenes (147)

To a solution of a mixture of diethylamine (0.0278 g, 0.381 mmol), dipropylamine (0.0386 g, 0.381 mmol) and triethylamine (0.0771 g, 0.762 mmol) in dry dichloromethane (5 ml), a solution of 25, 26, 27, 28-tetrakis[(chlorocarbonyl)methoxy]calix[4]arene (0.10 g, 0.152 mmol) in dry dichloromethane (5 ml) was added dropwise with stirring. The solution was stirred under a nitrogen atmosphere at room temperature overnight and then washed twice with dilute hydrochloric acid and three times with distilled water. The solvent was evaporated and the residue dried in vacuum to give a mixture of products as a white solid.

6.6.13 25, 26, 27, 28-Tetrakis(dimethylcarbamoyl methoxy)calix[4]arene (148)

A solution of 25, 26, 27, 28-tetrakis[(chlorocarbonyl)methoxy]calix[4]arene (0.50 g, 0.76 mmol) in dried dichloromethane (10 ml) was

treated with a solution of dimethylamine (1.90 ml of 2 M THF solution, 3.81 mmol) in dry dichloromethane (10 ml) in the presence of triethylamine (0.31 g, 3.05 mmol) and stirred under a nitrogen atmosphere at room temperature overnight. The solution was washed twice with dilute hydrochloric acid and three times with distilled water. The solvent was removed and the residue was dried in vacuum. The product was recrystallised from ethanol to give a white crystalline solid (0.50 g, 85%), m.p. 106-108 °C; IR ν_{\max} (nujol) 1660 (CO), 1460 and 1337 (HAr) cm^{-1} ; ^1H NMR δ 2.89 (12H, s, CH_3), 3.09 (12H, s, CH_3), 3.44 (4H, d $J=13.2$ Hz, ArCH_2Ar), 5.02 (8H, s, OCH_2), 5.31 (4H, d $J=13.2$ Hz, ArCH_2Ar), 6.72 (12H, m, ArH); MS (FAB) m/z 765 ($[\text{M}+\text{H}]^+$), 692 (Found: C, 69.45; H, 6.98, N, 7.03%. $\text{C}_{44}\text{H}_{52}\text{N}_4\text{O}_8$ requires C, 69.09; H, 6.85; N, 7.32%).

6.6.14 25, 26, 27, 28-Tetrakis(diethylcarbamoyl methoxy)calix[4]arene (149)

A solution of 25, 26, 27, 28-tetrakis[(chlorocarbonyl)methoxy]-calix[4]arene (0.50 g, 0.76 mmol) in dry dichloromethane (10 ml) was treated with a solution of diethylamine (0.279 g, 3.81 mmol) in dry dichloromethane (10 ml) in the presence of triethylamine (0.31 g, 3.05 mmol) and stirred under a nitrogen atmosphere at room temperature overnight. The solution was then washed twice with dilute hydrochloric acid and three times with distilled water. The solvent was removed and the residue dried in vacuum. The residue was recrystallised from hexane to give the product as a white crystalline solid (0.60 g, 90%), m.p. 110-112 °C; IR ν_{\max} (nujol) 1653.0 (CO), 1460.0 and 1377 (HAr) cm^{-1} ; ^1H NMR δ 1.05-1.17 (24H, m, CH_3), 3.21-3.35 (20H, m, NCH_2 and ArCH_2Ar), 4.93 (8H, s, OCH_2), 5.22 (4H, d $J=13.5$ Hz, ArCH_2Ar), 6.59-6.65 (12H, m, ArH); MS (FAB) m/z , $[\text{M}+\text{H}]^+$ 878, 777, 72 (100%) (Found: C, 69.60; H, 7.66; N, 6.25%. $\text{C}_{52}\text{H}_{68}\text{N}_4\text{O}_8$ requires C, 69.39; H, 7.61; N, 6.22%).

6.6.15 25, 26, 27, 28-Tetrakis(dipropylcarbamoyl methoxy)calix[4]arene (150)

A solution of 25, 26, 27, 28-tetrakis[(chlorocarbonyl)methoxy]-calix[4]arene (0.50 g, 0.76 mmol) in dry dichloromethane (10 ml) was treated with a solution of dipropylamine (0.39 g, 3.81 mmol) in dry dichloromethane (10 ml) in the presence of triethylamine (0.31 g, 3.05 mmol) and stirred under a nitrogen atmosphere at room temperature overnight. The solution was then washed twice with dilute hydrochloric acid and three times with distilled water. The solvent was removed and the residue dried in vacuum. The residue was recrystallised from hexane to give the product as a white crystalline solid (0.60 g, 82%), m.p. 122-124 °C; IR ν_{\max} (nujol) 1650 (CO), 1459 and 1377 (HAr) cm^{-1} ; $^1\text{H NMR}$ δ 0.83-0.95 (24H, m, CH_3), 1.54^f-1.61 (16H, m, CH_2), 3.19-3.33 (20H, m NCH_2 and ArCH_2Ar), 4.95 (8H, s, OCH_2), 5.28 (4H, d $J = 13.7$ Hz, ArCH_2Ar), 6.61 (12H, m, ArH); MS (FAB) m/z 990 ($[\text{M}+\text{H}]^+$) 861, 100 (100%) (Found: C, 73.05; H, 8.56; N, 5.73%. $\text{C}_{60}\text{H}_{84}\text{N}_4\text{O}_8$ requires C, 72.84; H, 8.56; N, 5.66%).

6.6.16 25, 26, 27, 28-Tetrakis(dibutylcarbamoyl methoxy)calix[4]arene (151)

A solution of 25, 26, 27, 28-tetrakis[(chlorocarbonyl)methoxy]-calix[4]arene (0.50 g, 0.76 mmol) in dry dichloromethane (10 ml) was treated with a solution of dibutylamine (0.49 g, 3.81 mmol) in dry dichloromethane (10 ml) in the presence of triethylamine (0.31 g, 3.05 mmol) and stirred under a nitrogen atmosphere at room temperature overnight. The solution was then washed twice with dilute hydrochloric acid and three times with distilled water. The solvent was then removed and the residue dried in vacuum. The residue was recrystallised from hexane to give the product as a white crystalline solid (0.65 g, 80%), m.p. 182 °C; IR ν_{\max} (nujol) 1664 (CO), 1460 and 1377 (HAr) cm^{-1} ; $^1\text{H NMR}$ δ 0.90-1.05 (24H, m, CH_3), 1.41-1.47 (16H, m, CH_2), 1.49-1.53 (16H, m, CH_2), 3.05-3.17 (20H, m NCH_2 and ArCH_2Ar), 5.00 (8H, s, OCH_2), 5.29 (4H, d $J = 13.7$

Hz, ArCH₂Ar), 6.57 (12H, m, ArH); MS (FAB) m/z 1102 ([M+H]⁺), 945, 128, 57 (Found: C, 74.41; H, 8.97; N, 4.93%. C₆₈H₁₀₀N₄O₈ requires C, 74.14; H, 9.15; N, 5.09%).

6.6.17 Library of ethyl- and morpholinyl-carbamoyl methoxycalix[4]arenes (153)

To a solution of a mixture of diethylamine (0.0278 g, 0.381 mmol), morpholine (0.0332 g, 0.381 mmol) and triethylamine (0.0771 g, 0.762 mmol) in dry dichloromethane (5 ml), a solution of 25, 26, 27, 28-tetrakis[(chlorocarbonyl)methoxy]calix[4]arene (0.10 g, 0.152 mmol) in dry dichloromethane (5 ml) was added dropwise with stirring. The solution was stirred under a nitrogen atmosphere at room temperature overnight and then washed twice with dilute hydrochloric acid and three times with distilled water. The solvent was evaporated and the residue dried in vacuum to give a mixture of products as a white solid.

6.6.18 Library of morpholinyl-, propyl- and pyrrolidyl-carbamoyl methoxycalix[4]arenes (152)

To a solution of a mixture of morpholine (0.0221 g, 0.254 mmol), dipropylamine (0.0257 g, 0.254 mmol), pyrrolidine (0.0181 g, 0.254 mmol) and triethylamine (0.0771 g, 0.762 mmol) in dry dichloromethane (5 ml), a solution of 25, 26, 27, 28-tetrakis[(chlorocarbonyl)methoxy]calix[4]arene (0.10 g, 0.152 mmol) in dry dichloromethane (5 ml) was added dropwise with stirring. The solution was stirred under a nitrogen atmosphere at room temperature overnight and then washed twice with dilute hydrochloric acid and three times with distilled water. The solvent was evaporated and the residue dried in vacuum to give a mixture of products as a white solid.

6.6.19 25, 26, 27, 28-Tetrakis(morpholinylcarbamoyl methoxy)calix[4]arene (157)

A solution of 25, 26, 27, 28-tetrakis[(chlorocarbonyl)methoxy]-calix[4]arene (0.50 g, 0.76 mmol) in dry dichloromethane (10 ml) was treated with a solution of morpholine (0.33 g, 3.81 mmol) in dry dichloromethane (10 ml) in the presence of triethylamine (0.31 g, 3.05 mmol) and stirred under a nitrogen atmosphere at room temperature overnight. The solution was then washed twice with dilute hydrochloric acid and three times with distilled water. The solvent was removed and the residue dried in vacuum. The residue was recrystallised from hexane/DCM to give the product as a white crystalline solid (0.56 g, 79%), m.p. 226 - 228 °C; IR $\nu_{\text{max}}^{\text{f}}$ (nujol) 1660 (CO), 1460 and 1377 (HAr) cm^{-1} ; ^1H NMR δ 3.25 (4H, d, $J=13.7$ Hz, ArCH_2Ar), 3.50 - 3.65 (32H, m, $\text{OCH}_2\text{CH}_2\text{N}$), 4.89 (8H, s, OCH_2), 4.97 (4H, d $J=13.7$ Hz, ArCH_2Ar), 6.63 (12H, m, ArH); MS (FAB) m/z 933 ($[\text{M}+\text{H}]^+$), 818, 86 (Found: C, 67.19; H, 6.33; N, 5.12%. $\text{C}_{52}\text{H}_{60}\text{N}_4\text{O}_{12}$ requires C, 66.94; H, 6.48; N, 5.00%).

6.6.20 25, 26, 27, 28-Tetrakis(pyrrolidinylcarbamoyl methoxy)calix[4]arene (156)

A solution of 25, 26, 27, 28-tetrakis[(chlorocarbonyl)methoxy]-calix[4]arene (0.50 g, 0.76 mmol) in dry dichloromethane (10 ml) was treated with a solution of pyrrolidine (0.27 g, 3.81 mmol) in dry dichloromethane (10 ml) in the presence of triethylamine (0.31 g, 3.05 mmol) and stirred under a nitrogen atmosphere at room temperature overnight. The solution was then washed twice with dilute hydrochloric acid and three times with distilled water. The solvent was removed and the residue dried in vacuum. The residue was recrystallised from hexane to give the product as a white crystalline solid (0.57 g, 86%), m.p. 108 -110 °C; IR ν_{max} (nujol) 1648 (CO), 1460 and 1377 (HAr) cm^{-1} ; ^1H NMR δ 1.80 -

1.94 (16H, m, CH₂CH₂), 3.24 (4H, d, J= 13.7 Hz, ArCH₂Ar), 3.40 - 3.45 (16H, m, CH₂N), 4.78 (8H, s, OCH₂), 5.17 (4H, d, J= 13.7 Hz, ArCH₂Ar), 6.60 (12H, m, ArH); MS (FAB) m/z 869 ([M+H]⁺), 770, 112 (Found: C, 71.61; H, 6.73; N, 6.32%. C₅₂H₆₀N₄O₈ requires C, 71.87; H, 6.96; N, 6.45%).

6.621 25, 26, 27, 28-Tetrakis(dipropargylcarbamoyl methoxy)calix[4]arene (155)

A solution of 25, 26, 27, 28-tetrakis[(chlorocarbonyl)methoxy]-calix[4]arene (0.50 g, 0.76 mmol) in dry dichloromethane (10 ml) was treated with a solution of dipropargylamine (0.35 g, 3.81 mmol) in dry dichloromethane (10 ml) in the presence of triethylamine (0.31 g, 3.05 mmol) and stirred under a nitrogen atmosphere at room temperature overnight. The solution was then washed twice with dilute hydrochloric acid and three times with distilled water. The solvent was removed and the residue dried in vacuum. The residue was recrystallised from hexane/DCM to give the product as a white crystalline solid (0.52 g, 72%), m.p., 90 - 92 °C; IR ν_{\max} (nujol) 3287 (HC≡), 2118 (C≡C), 1666 (CO), 1460 and 1377 (HAr) cm⁻¹; ¹H NMR δ 2.29 (8H, br, HC≡), 3.27 (4H, d J= 13.7 Hz, ArCH₂Ar), 4.34 - 4.35 (16H, d, J= 7.32 Hz, CH₂C≡), 5.02 - 4.96 (12H, m, ArCH₂Ar and OCH₂), 6.57 - 6.68 (12H, m, ArH); MS (FAB) m/z 967 ([M+H]⁺), 91, 77 (Found: C, 75.01; H, 5.60; N, 5.61%. C₆₀H₅₂N₄O₈ requires C, 75.30; H, 5.48; N, 5.85%).

6.6.22 25, 26, 27, 28-Tetrakis(diallylcarbamoyl methoxy)calix[4]arene (154)

A solution of 25, 26, 27, 28-tetrakis[(chlorocarbonyl)methoxy]-calix[4]arene (0.50 g, 0.76 mmol) in dry dichloromethane (10 ml) was treated with a solution of diallylamine (0.36 g, 3.81 mmol) in dry dichloromethane (10 ml) in the presence of triethylamine (0.31 g, 3.05 mmol) and stirred under a nitrogen atmosphere at room temperature

overnight. The solution was then washed twice with dilute hydrochloric acid and three times with distilled water. The solvent was removed and the residue dried in vacuum. The residue was recrystallised from hexane/DCM to give the product as a white crystalline solid (0.60 g, 81%), m.p., 62 - 65 °C; IR ν_{\max} (nujol) 1755 (C=C), 1665 (CO), 1462 and 1377 (HAr) cm^{-1} ; ^1H NMR δ 3.20 (4H, d, $J = 13.7$ Hz, ArCH₂Ar), 3.94 -3.97 (16H, m, H₂C=), 4.90 (8H, s, OCH₂), 5.06 - 5.15 (20H, m, ArCH₂Ar and CH₂C=), 5.67 - 5.83 (8H, m, CCH=), 6.52 - 6.65 (12H, m, ArH); MS (FAB) m/z 974 ([M+H]⁺), 91, 77, 55, 41(100%) (Found: C, 73.74; H, 7.10; N, 5.61%. C₆₀H₆₈N₄O₈ requires C, 74.05; H, 7.04; N, 5.76%).

6.6.23 25, 26, 27, 28-Tetrakis[bis(methoxyethyl)carbamoyl methoxy]calix[4]arene (158)

A solution of 25, 26, 27, 28-tetrakis[(chlorocarbonyl)methoxy]calix[4]arene (0.50 g, 0.76 mmol) in dry dichloromethane (10 ml) was treated with a solution of bis(methoxyethyl)amine (0.51g, 3.81 mmol) in dry dichloromethane (10 ml) in the presence of triethylamine (0.31 g, 3.05 mmol) and stirred under a nitrogen atmosphere at room temperature overnight. The solution was then washed twice with dilute hydrochloric acid and three times with distilled water. The solvent was removed and the residue dried in vacuum. The residue was recrystallised from hexane to give the product as a white crystalline solid (0.68g, 80%), m.p. 106 -107 °C; IR ν_{\max} (nujol) 1662 (CO), 1459 and 1377 (HAr) cm^{-1} ; ^1H NMR δ 3.23 (4H, d, $J = 13.7$ Hz, ArCH₂Ar), 3.29 (12H, s, OCH₃), 3.30 (12H, s OCH₃), 3.48 - 3.58 (32H, m, NCH₂CH₂O), 4.93 (8H, s, OCH₂), 5.04 (4H, d, $J = 13.7$ Hz ArCH₂Ar), 6.57 - 6.61 (12H, m, HAr); MS (FAB) m/z 1118 ([M + H]⁺), 956, 59, 45 (100%) (Found: C, 64.24; H, 7.68; N, 5.20%. C₆₀H₈₄N₄O₁₆ requires C, 64.50; H, 7.58; N, 5.01%).

6.7 Two Phase Extraction Experiment to Assess Complexation of Sodium by Calix[4]arene Ionophores

2.5×10^{-2} M aqueous sodium picrate in distilled water was prepared in volumetric flasks (100 ml). Solutions of the hosts (2.5×10^{-2} M) were also prepared in 10 ml plastic volumetric flasks using Analar dichloromethane. 5 ml of host solution and 5 ml of the sodium picrate solution were added to a 20ml separating funnel *via* volumetric pipettes and the two phase system was shaken 20 times and left still for 10 minutes. The UV absorbance of the aqueous phase was measured using a Hewlett Packard Diode array Spectrophotometer. The extraction percentage of each host solution was calculated by comparing the absorbance of the aqueous phase at 356 nm before and after extraction. An experiments with a blank sample (dichloromethane solvent without host compound) showed no extraction at all.

6.8 FAB MS Studies of Combinatorial Libraries

The last purification step for all libraries of mixtures (see synthesis procedures for each material in this chapter) was carried out in plastic containers and samples were stored in plastic sample tubes to keep the level of background metal ions as low as possible. Solvents and the matrix sample (3-nitrobenzyl alcohol) were treated in the same way and sodium free spectra for all samples were obtained. Sample solutions of calix[4]arene libraries (typically 0.02 M by using an average molecular weight for the mixtures) in dichloromethane were made in sterile Eppendorf tubes immediately before doing the MS. The sodium nitrate was the highest grade commercially available and was prepared as a methanolic solution (0.02 M) in 10 ml volumetric flasks. The sodium

nitrate solutions were pre-mixed with the sample solutions quantitatively according to the sodium level required in the experiment. All mass spectrometric experiments were carried out on a VG Analytical 7070 E normal geometry double focussing mass spectrometer, fitted with an Ion-Tech saddle-field gun. The latter was operated at 6 kV, with the gun current monitored at 1.6 mA, using xenon as the bombarding gas. All data were recorded on an 11-250 data system and acquired at 8 kV accelerating voltage, at a scan time of 20 s/decade over a mass range of 1400 - 50 amu, with an inter-scan delay of 2 s. In a typical experiment 1 μl (1 μl = 1 mm³) of library solution with or without mixing with a solution of sodium nitrate was loaded onto the stainless steel tip of the FAB probe to which 1 μl of matrix (3-NOBA) had been added with a plastic pipette. The solvent was allowed to evaporate by standing the probe for a while at room temperature. 20 successive scans were then recorded and scans 5 - 15 averaged to afford the observed spectrum.

6.9 MALDI - TOF MS Studies of Libraries

The samples were treated in the same way as for the FAB MS studies. Because the samples were sent to Fisons Instruments company, the solvents and matrices could not be treated in the way described in the last section. The mass spectrometric experiments were carried out on a VG ToFSpec - SE of MALDI - TOF mass spectrometer, in which a laser beam of 337 nm UV was used with option path length 1.60 metres for linear and 3.50 metres for reflectron. The samples of the libraries and mixtures were prepared at a concentration of 1.0 pmol/ μl as dichloromethane solutions which were mixed with a UV absorbing matrix solution in dichloromethane. By trial, dithranol was chosen as the matrix for all of the samples and samples with no matrix were also examined. THF was

initially tried as the solvent but the spectrum obtained included three $[M + \text{Metal}]^+$ peaks identified as $[M+\text{Na}]^+$, $[M+ \text{K}]^+$ and $[M+ \text{Cu}]^+$ by comparing the isotope peaks with those of computer models, the use of THF was therefore abandoned. In a typical experiment, a microliter of solution of each of 20 different samples was mixed with 1 equivalent of matrix solution and spotted on 20 of the target positions on a stainless steel sample holder, on which up to 130 samples could be placed simultaneously. These sample solutions were allowed to dry. Then the sample holder was loaded into the machine and viewed by a CCD camera moved (X- Y) under data system control. The energy of the laser beam used to bombard the sample was controlled to 20% - 60% of 180 microjoules, a source voltage of 25 kV was used (for accelerating ions generated), a focus voltage of 2 kV, and a reflectron voltage of 29 kV, the frequency of measuring the time taken for the ions to drift a fixed distance before arriving at the detector was 500 MHz. The spectrometer control and spectrum data processing were performed by a VG Opus data system. The linear mode was also tried. But it gave poor resolution for the spectra and was eventually abandoned.

6.10 Electrospray Ionization (ESI) MS Studies of Libraries

Sample were treated in the same way as for FAB MS studies. Because samples were sent to the Department of Biochemistry the metal level in the solvent could not be controlled. All the samples were prepared in dichloromethane at a concentration of 2×10^{-4} M. Initially, a concentration of 2.0×10^{-5} M was tried but it did not give a good spectrum. For every run, 20 μl of sample solution was injected into the spectrometer inlet system. The solvent used in the pumping system was HPLC grade methanol which had been degassed by sonification and then filtered

through a membrane. Dichloromethane was tried as the pumping solvent but it did not produce good spectra. After injection of the sample, the solvent was pumped at a flow rate of 2 - 6 $\mu\text{l}/\text{min}$. The sampling cone voltage was 30 V for focusing and the capillary tip voltage was 3.5 kV for ionisation.

Bibliography

1. J. D. Watson and F. H. C. Crick, *Nature*, **171**, 737 (1953)
2. J. D. Watson and F. H. C. Crick, *Nature*, **171**, 964 (1953)
3. a. S. Altman, *Angew. Chem., Int. Ed. Engl.*, **29**, 749 – 758 (1990)
b. T. R. Cech, *Angew. Chem., Int. Ed. Engl.*, **29**, 759 – 768 (1990)
4. G. Schramm, H. Grotsch and Dipl.-Chem. W. Pollmann, *Angew. Chem., Int. Ed. Engl.*, **1**, 1 (1962)
5. R. Naylor and P. T. Gilham, *Biochemistry*, **5**, 2722 (1966)
6. a. L. E. Orgel and R. Lohrmann, *Acc. Chem. Res.*, **7**, 368 (1974)
b. R. Lohrmann and L. E. Orgel, *J. Mol. Biol.*, **142**, 555 (1980)
c. T. Inoue and L. E. Orgel, *Science*, **219**, 859 (1983)
d. C. B. Chen, T. Inoue and L. E. Orgel, *J. Mol. Biol.*, **181**, 271 (1985)
7. T. Inoue, G. F. Joyce, K. Grzeskowiak, L. E. Orgel, J. M. Brown, *J. Mol. Biol.*, **178**, 669 (1984)
8. G. von Kiedrowski, *Angew. Chem., Int. Ed. Engl.*, **25**, 932 (1986)
9. W. S. Zielinski and L. E. Orgel, *Nature*, **327**, 346 (1987)
10. a. G. von Kiedrowski, B. Wlotzka and J. Helbing, *Angew. Chem., Int. Ed. Engl.*, **28**, 1235 (1989)
b. G. von Kiedrowski, B. Wlotzka, J. Helbing, M. Matzen and S. Jordan, *Angew. Chem., Int. Ed. Engl.*, **30**, 423 (1991)
11. A. R. Todd, In *Perspectives in Organic Chemistry*; A. R. Todd, Ed.; Interscience Publishers Ltd.: London, 1956; p 263
12. C. J. Pedersen, *J. Am. Chem. Soc.*, **89**, 7017 (1967)
13. a. J-M. Lehn, J. Simon, and J. Wagner, *Angew. Chem., Int. Ed. Engl.*, **12**, 578 (1973)
b. J-M Lehn and J. Simon, *Helv. Chim. Acta*, **60**, 141 (1977)
14. a. E. P. Kyba, M. G. Siegel, L. R. Sousa, G. D. Y. Sogah, D. J. Cram, *J. Am. Chem. Soc.*, **95**, 2691 (1973)
b. E. P. Kyba, K. Koga, L. R. Sousa, M. G. Siegel, D. J. Cram, *J. Am. Chem. Soc.*, **95**, 2692 (1973)

15. a. S. Goswami, A. D. Hamilton, and D. Van. Engen, *J. Am. Chem. Soc.*, **111**, 3425 (1989)
b. A. D. Hamilton and N. Pant, *J. Chem. Soc., Chem. Commun.*, 765 (1988)
c. B. Feibush, M. Saha, K. Onan, B. Kargar, and R. Giese, *J. Am. Chem. Soc.*, **109**, 7531 (1987)
d. A. D. Hamilton and D. V. Engen, *J. Am. Chem. Soc.*, **109**, 5035 (1987)
16. A. D. Hamilton and D. Little, *J. Chem. Soc., Chem. Commun.*, 297 (1990)
17. a. J. Rebek, Jr., *J. Mol. Recogn.*, **1**, 1 (1988)
b. J. Rebek, Jr., *Science* (Washington, DC), **235**, 1437 (1987)
c. J. Rebek, Jr., *Top. Curr. Chem.*, **149**, 189 (1988)
18. a. K. S. Jeong and J. Rebek, Jr., *J. Am. Chem. Soc.*, **110**, 3327 (1988)
b. J. Rebek, Jr. and D. Nemeth, *J. Am. Chem. Soc.*, **107**, 6738 (1985)
c. J. Rebek, Jr., B. Askew, P. Ballester, C. Buhr, S. Jones, D. Nemeth, and K. Williams, *J. Am. Chem. Soc.*, **109**, 5033 (1987)
19. a. D. J. Cram and H. E. Katz, *J. Am. Chem. Soc.*, **105**, 135 (1983)
b. D. J. Cram and P. Y-S. Lam, *Tetrahedron*, **42**, 1607 (1986)
20. a. T. J. van Bergen and R. M. Kellogg, *J. Chem. Soc., Chem. Commun.*, 964 (1976)
b. O. Piepers and R. M. Kellogg, *J. Chem. Soc., Chem. Commun.*, 383-384 (1978)
c. J. P. Behr, & J. M. Lehn, *J. Chem. Soc., Chem. Commun.*, 143 (1978)
d. T. Matsui, & K. Koga, *Tetrahedron lett.*, 1115 (1978)
e. T. Matsui, and K. Koga, *Chem. Pharm. Bull.*, **27**, 2295-2303 (1979)
f. D. J. Cram, & G. D. Y. Sogah, *J. Chem. Soc., Chem. Commun.*, 625 (1981)
g. G. L. Trainor, R. Breslow, *J. Am. Chem. Soc.*, **103**, 154 (1981)

- h. R. Breslow, G. L. Trainor, A. Veno, *J. Am. Chem. Soc.*, **105**, 2739 (1983)
21. a. T. R. Kelly, C. Zhao and G. J. Bridger, *J. Am. Chem. Soc.*, **111**, 3744 (1989)
b. T. R. Kelly, G. J. Bridger and C. Zhao, *J. Am. Chem. Soc.*, **112**, 8024 (1990)
22. a. T. Tjivikua, P. Ballester, and J. Rebek, Jr., *J. Am. Chem. Soc.*, **112**, 1249 (1990)
b. J. S. Nowick, Q. Feng, T. Tjivikua, P. Ballester and J. Rebek, Jr., *J. Am. Chem. Soc.*, **113**, 8831 (1991)
c. V. Rotello, J-I. Hong, & J. Rebek, Jr., *J. Am. Chem. Soc.*, **113**, 9422 (1991)
23. A. Terfort and G. von Kiedrowski, *Angew. Chem., Int. Ed. Engl.*, **31**, 654 (1992)
24. a. W. P. Jencks, F. Barley, R. Barnett, and M. Gilchrist, *J. Am. Chem. Soc.*, **88**, 4464 (1966)
b. T. Higuchi, L. Ebersson, and J. D. McRae, *J. Am. Chem. Soc.*, **89**, 3001 (1967)
25. L. Ebersson and H. Welinder, *J. Am. Chem. Soc.*, **93**, 5821 (1971)
26. S. C. Hirst and A. D. Hamilton, *J. Am. Chem. Soc.*, **113**, 882 (1991)
27. a. C. H. Park, H. E. Simmons, *J. Am. Chem. Soc.*, **90**, 2431 (1968)
b. E. Kimura, A. Sakonaka, T. Yatsunami, and M. Kodama, *J. Am. Chem. Soc.*, **103**, 3041 (1981)
c. E. Kimura, M. Kodama, and T. Yatsunami, *J. Am. Chem. Soc.*, **104**, 3182 (1982)
28. B. Dietrich, M. W. Hosseini, J. M. Lehn, and R. B. Sessions, *J. Am. Chem. Soc.*, **103**, 1282 (1981)
29. a. F. P. Schmidtchen, *Angew. Chem., Int. Ed. Engl.*, **16**, 720 (1977)
b. F. P. Schmidtchen, *Chem Ber.*, **114**, 597 (1981)

- c. F. P. Schmidtchen, *J. Am. Chem. Soc.*, **108**, 8249 (1986)
30. J - L. Pierre and P. Baret, *Bull. Soc. Chim. France*, **II**, 367 (1982)
31. a. B. Dietrich, T. M. Fyles, J - M. Lehn, L. G. Pease, and D. L. Fyles, *J. Chem. Soc., Chem Commun.*, 934 (1978)
- b. B. Dietrich, D. L. Fyles, T. M. Fyles and J - M. Lehn, *Helv. Chim. Acta*, **62**, 2763 (1979)
- c. G. Muller, J. Riede, and F. P. Schmidtchen, *Angew. Chem., Int. Ed. Engl.*, **27**, 1516 (1988)
- d. A. Echavarren, A. Galan, J - M. Lehn, and J. de Mendoza, *J. Am. Chem. Soc.*, **111**, 4994 (1989)
32. a. G. M. Dubowchik, A. D. Hamilton, *J. Chem. Soc., Chem. Commun.*, 293 (1987)
- b. K. H. Neumann, F. J. Vogtle, *J. Chem. Soc., Chem. Commun.*, 520 (1988)
- c. C. A. Hunter, M. N. Meah, J. K. M. Sanders, *J. Chem. Soc., Chem. Commun.*, 692, 694 (1988)
- d. H. Ogoshi, H. Hatakeyama, J. Kotani, A. Kawashima, Y. Kuroda, *J. Am. Chem. Soc.*, **113**, 8181 (1991)
- e. R. P. Bonar Law and J. K. M. Sanders, *J. Chem. Soc., Chem. Commun.*, 574 (1991)
- f. Y. Aoyama, A. Yamagishi, Y. Tanaka, H. Toi and H. Ogoshi, *J. Am. Chem. Soc.*, **109**, 4735 (1987)
- g. Y. Aoyama, A. Yamagishi, M. Asagawa, H. Toi and H. Ogoshi, *J. Am. Chem. Soc.*, **110**, 4076 (1988)
- h. I. P. Danks, T. G. Lane, I. O. Sutherland and Maurice Yap, *Tetrahedron*, **48**, 7679 (1992)
33. a. C. J. Walter, H. L. Anderson and J. K. M. Sanders *J. Chem. Soc., Chem. Commun.*, 458 - 460 (1993)

- b. C. J. Walter and J. K. M. Sanders, *Angew. Chem., Int. Ed. Engl.*, **34**, 217 (1995)
- c. L. G. Mackay, R. S. Wylie, and J. K. M. Sanders, *J. Am. Chem. Soc.*, **116**, 3141 (1994)
34. a. W. L. Jorgensen and J. Pranata, *J. Am. Chem. Soc.*, **112**, 2008 (1990)
- b. J. Pranata, S. G. Wierschke, and W. L. Jorgenson, *J. Am. Chem. Soc.*, **113**, 2810 (1991)
35. a. M. I. Page, & W. P. Jencks, *Proc. Nat. Acad. Sci. USA*, **68**, 1678 (1971)
- b. M. I. Page, *Chem. Soc. Rev.*, **2**, 295 (1973)
- c. M. I. Page, *Angew. Chem., Int. Ed. Engl.*, **16**, 449 (1977)
36. Y. Chao, D. J. Cram, *J. Am. Chem. Soc.*, **98**, 1015 (1976)
37. a. A. G. Fallis, *Can. J. Chem.*, **62**, 183 (1984)
- b. G. Brieger and J. N. Bennett, *Chem. Rev.*, **80**, 63 (1980)
- c. W. Oppolzer, *Angew. Chem., Int. Ed. Engl.*, **16**, 10 (1977)
38. A. E. Chichibabin, *German Patent* 374,291; *Chem. Zentr.*, **IV**, 725 (1923); *Chemical Abstracts*, **18**, 2176 (1924)
39. a. H. J. Den Hertog and J. P. Wibaut, *Rec. Trav. Chim.*, **55**, 122 (1936)
- b. H. J. Den Hertog and C. Jouwersma, *Rec. Trav. Chim.*, **72**, 125 (1953)
40. a. E. T. Tusza and B. Joos, *U. S. patent* 1,863,676 (June 21, 1932); *Chemical Abstracts*, **26**, 4347 (1932)
- b. O. A. Zeide and A. I. Titov, *Ber. Chem.*, **69**, 1884 (1936)
- c. I. Titov and B. B. Levin, *J. Gen. Chem. U. S. S. R.*, **11**, 9 (1941)
41. a. M. Katada, *J. Pharm. Soc. Japan*, **67**, 51 (1947); *C. A.*, **45**, 9536^d (1951)
- b. M. P. Cava and B. Weinstein, *J. Org. Chem.*, **23**, 1616 (1958)
- c. E. C. Taylor and J. S. Driscoll, *J. Org. Chem.*, **25**, 1716 (1960)

42. J. H. Markgraf, H. B. Brown, Jr., and R. G. Peterson, *J. Am. Chem. Soc.*, **85**, 958 (1963)
43. a. E. Klingsberg, 'Pyridine and Its Derivatives' Part 3, Interscience Publishers (1962), pp 510 - 548
 b. R. A. Abramovitch, 'Pyridine and Its Derivatives', Supplement Part 3, Interscience Publishers (1974), pp 599 - 644
44. B. H. Chase and J. Walker, *J. Chem. Soc.*, 3548 (1953)
45. B. A. Fox and T. L. Threlfall, *J. Am. Chem. Soc.*, **77**, 3154 (1955)
46. K. M. Doxsee, M. Feigel, K. D. Stewart, J. W. Canary, C. B. Knobler and D. J. Cram, *J. Am. Chem. Soc.*, **109**, 3098 (1987)
47. A. I. Titov, *J. Gen. Chem. (U. S. S. R.)*, **8**, 1483 (1938); *Chem. Abstr.*, **33**, 4248
48. P. M. G. Bavin, *Can. J. Chem.*, **36**, 238 (1958)
49. R. Adams, and F. L. Cohen, *Org. Syn.*, Coll. **1**, 240 (1932)
50. M. P. Cava, A. A. Deana, K. Muth, and M. J. Mitchell, *Org. Syn.*, Coll. **5**, 944 (1973)
51. E. Klingsberg, 'Pyridine and Its Derivatives' Part Three, Interscience Publishers (1962), pp 40-55
52. B. A. Geller and L. S. Samosvat, *Zh. Obshch. Khim.*, **34**, 613 (1964)
Chem. Abstr., **60**, 13112 (1964); *J. Gen. Chem. USSR*, **2**, 614 (1964)
53. a. W. N. White and J. T. Golden, *Chem. Ind. (London)*, 138 (1962)
 b. W. N. White, D. Lazdins, and H. S. White, *J. Am. Chem. Soc.*, **86**, 1517 (1964)
54. R. A. Abramovitch and J. G. Saha, *Adv. in Heterocyc. Chem.*, **6**, 243 (1966)
55. a. A. Binz and H. Maier-Bode, *Angew. Chem.*, **49**, 486 (1936)
 b. A. H. Berrie, G. T. Newbold, and F. S. Spring, *J. Chem. Soc.* 2590 (1953)

- c. C. A. Salemeink and G. M. van der Want, *Rec. Trav. Chim.*, **68**, 1013 (1949)
56. W. A. Waters, *J. Chem. Soc.*, 727 (1948)
57. P. J. Brignell, A. R. Katritzky, and H. O. Tarhan, *J. Chem. Soc. B*, 114 (1968)
58. W. Peppe, and W. J. Schweckendiek, *Liebigs Ann. der. Chim.*, 104 (1948)
59. W. J. Bailey, R. Barclay, Jr, and R. A. Baylouny, *J. Org. Chem.*, **27**, 1851 (1962)
60. B. M. Trost, T. R. Verhoeven, and J. M. Frotunak, *Tetrahedron Lett.*, 2301 (1979)
61. a. R. Grewe, A. Heinke, and C. Sommer, *Chem. Ber.*, **89**, 1978 (1956)
b. M. Kato, M. Kageyama, R. Tanaka, K. Kuwahara, and A. Yoshikoshi, *J. Org. Chem.*, **40**, 1932 (1975)
c. T. L. Gresham, J. E. Jansen, F. W. shaver, J. T. Gregory and W. L. Bears, *J. Am. Chem. Soc.*, **70**, 1004 (1948)
d. G. Holf and W. Steglich, *Synthesis*, 619 (1972)
62. M. Mousseron and F. Winternitz, *Bull. Soc. Chim. France*, 604 (1946)
63. a. A. J. Pearson and T. Ray, *Tetrahedron*, **41**, 5765 (1985)
b. E. O. Fischer and R. D. Fischer, *Angew. Chem.*, **72**, 919 (1960)
c. A. J. Birch, and M. A. Haas, *J. Chem. Soc. C*, 2465 (1971)
d. A. J. Birch, P. E. Cross, J. Lewis, D. A. White and S. B. Wild, *J. Chem. Soc. A*, 332 (1968)
e. E. Y. Shov and E. Hazum, *J. Chem. Soc., Chem. Commum.* 336 (1974)
64. a. J-E. Backvall, J-E. Nystrom, and R. E. Nordberg, *J. Am. Chem. Soc.*, **107**, 3676 (1985)

- b. J-E. Backvall, J. O. Bagberg, C. Zercher, J. P. Genet, and A. Denis, *J. Org. Chem.*, **52**, 5430 (1987)
- c. J-E. Backvall, P. G. Andersson, and J. O. Vagberg, *Tetrahedron Lett.*, **30**, 137 (1989)
- d. J-E. Backvall, P. G. Andersson, G. B. Stone, and A. Gogoll, *J. Org. Chem.*, **56**, 2988 (1991)
- e. J-E. Backvall and J. O. Vagberg, *Org Syn.*, **69**, 38 (1990)
65. B. M. Trost and T. R. Verhoeven, *J. Am. Chem. Soc.*, **102**, 4730 (1980)
66. a. O. Seide, *Ber. Chem.*, 2465 (1926)
- b. G. R. Lappn, *J. Am. Chem. Soc.*, **70**, 3348 (1948)
- c. C. R. Hauser and M. J. Weiss, *J. Org. Chem.*, **4**, 453 (1949)
- d. E. V. Brown, *J. Org. Chem.*, **30**, 1607 (1965)
- e. E. M. Hawes, and D. G. Wibberley, *J. Chem. Soc. (C)*, 315 (1966)
- f. F. B. Barlin and W-L Tan, *Austral. J. Chem.*, **37**, 1065 (1984)
67. a. J. R. Vaughan, Jr. and J. A. Eichler, *J. Am. Chem. Soc.*, **75**, 5556 (1953)
- b. J. R. Vaughan, Jr. and J. A. Eichler, *J. Am. Chem. Soc.*, **76**, 2474 (1954)
68. P. W. Atkins, *Physical Chemistry*, 3rd, Oxford University Press, 1986, p 715
69. A. J. Sholl, Ph. D Thesis, The Liverpool University (1994)
70. a. T. J. Murray, & S. C. Zimmerman, *J. Am. Chem. Soc.*, **114**, 4010 (1992)
- b. E. Fan, S. A. Van Arman, S. Kincaid, & A. D. Hamilton, *J. Am. Chem. Soc.*, **115**, 369 (1993)
- c. D. A. Bell, & E. Anslyn, *J. Org. Chem.*, **59**, 512 (1994)
- d. Y. Kyogoku, R. C. Lord, & A. Rich, *Biochim. Biophys. Acta*, **179**, 10 (1969)

71. T. J. Murray, & S. C. Zimmerman, *Tetrahedron Lett.*, **36**, 7627 (1995)
72. R. B. Woodward and R. Hoffmann, *J. Am. Chem. Soc.*, **87**, 395 (1965)
73. H. M. Geysen, R. H. Melven, & S. J. Barteling, *Proc. Natl. Acad. Sci., USA*, **81**, 3998-4002 (1984)
74. R. A. Houghten, *Proc. Natl. Acad. Sci., USA*, **82**, 5131-5135 (1985)
75. a. S. F. Parmley, & G. P. Smith, *Gene*, **73**, 305-318 (1988)
 b. J. K. Scott, & G. P. Smith, *Science*, **249**, 386-390 (1990)
76. R. B. Merrifield, *J. Am. Chem. Soc.*, **85**, 2149-2154 (1963)
77. a. K. S. Lam, S. E. Salmon, E. M. Hersh, V. J. Hruby, W. M. Kazmierski, & R. J. Knapp, *Nature*, **354**, 82-84 (1991)
 b. R. A. Houghten, C. Pinilla, S. E. Blondelle, J. R. Appel, C. T. Dooley, & J. H. Cuervo, *Nature*, **354**, 84-86 (1991)
78. a. S. P. A. Fodor, J. L. Read, M. C. Pirrung, L. Stryer, A. T. Lu, & D. Solas, *Science*, **251**, 767 (1991)
 b. J. M. Ostresh, G. M. Husar, S. E. Blondelle, B. Dorner, P. A. Weber, & R. A. Houghten, *Proc. Natl. Acad. Sci. USA*, **91**, 11138 (1994)
 c. A. Borchardt & W. C. Still, *J. Am. Chem. Soc.*, **116**, 373 (1994)
 d. J. K. Chen, & S. L. Schreiber, *Angew. Chem. Int. Ed. Engl.*, **34**, 953 (1995)
 e. B. Deprez, X. Williard, L. Bourel, H. Coste, F. Hyafil, & A. Tartar, *J. Am. Chem. Soc.*, **117**, 5405 (1995)
79. a. A. C. Pease, D. Solas, E. J. Sullivan, M. T. Cronin, C. P. Holmes, & S. P. A. Fodor, *Proc. Natl. Acad. Sci., USA*, **91**, 5022 (1994)
 b. T. J. Meade, & J. F. Kayyem, *Angew. Chem., Int. Ed. Engl.*, **34**, 352 (1995)
80. a. Y. Carrell, E. A. Wintner, A. Bashir-Hashemi, & J. Rebek Jr., *Angew. Chem., Int. Ed. Engl.*, **33**, 2059 (1994)
 b. Y. Carrell, E. A. Wintner, & J. Rebek Jr., *Angew. Chem., Int. Ed. Engl.*, **33**, 2061 (1994)
81. For an extensive review of calixarenes, see

- a. C. D. Gutsche, *Calixarenes*, Vol 1, Monographs in Supramolecular Chemistry, ed., J. F. Stoddart, RSC, Cambridge (1989)
- b. V. Bohmer, *Calixarenes : A Versatile Class of Macrocyclic Compounds*, ed., J. Vincens, Kluwer Academic, Dordrecht (1991)
- 82 a. C. D. Gutsche, B. Dhawan, & M. Leonis, *Organic Synthesis*, 68, 238 (1986)
- b. C. D. Gutsche, B. Dhawan, K. H. No, & R. Muthukrishnan, *J. Am. Chem. Soc.*, 103, 3782 (1981)
83. R. M. Izatt, J. D. Lamb, R. T. Hawkins, P. R. Brown, S. R. Izatt, & J. J. Christensen, *J. Am. Chem. Soc.*, 105, 1782 (1983)
84. a. C. D. Gutsche, & I. Alam, *Tetrahedron*, 44, 4689 (1988)
- b. S. Shinkai, K. Araki, & O. Manabe, *J. Am. Chem. Soc.*, 110, 7214 (1988)
- c. S. Shinkai, K. Araki, & O. Manabe, *J. Chem. Soc., Chem. Commun.*, 187 (1988)
85. a. A. Arduini, A. Pochini, S. Reverebi, R. Ungaro, G. D. Andreetti, & F. Ugozzoli, *Tetrahedron*, 42, 2089 (1986)
- b. F. Arnaud-Neu, E. M. Collins, M. Deasy, G. Ferguson, S. J. Harris, B. Kaitner, A. J. Lough, M. A. McKervey, E. Marques, B. L. Ruhl, M. J. Schwing-Weill, & E. M. Seward, *J. Am. Chem. Soc.*, 111, 8681 (1989)
- c. S-K. Chang, & I. Cho, *J. Chem. Soc., Perkin Trans. 1*, 211 (1986)
- 86 a. R. Perrin, R. Lamartine, & M. Perrin, *Pure & Appl. Chem.*, 65, 1549 (1993)
- b. R. Assmus, V. Bohmer, J. M. Harrofield, M. I. Ogden, W. R. Richmond, B. W. Skelton, & A. H. White, *J. Chem. Soc., Dalton Trans.*, 2427 (1993)

- c. L. C. Groenen, J-D. van Loon, W. Verboom, S. Harkema, A. Casnati, R. Ungaro, A. Pochini, F. Ugozzoli, & D. N. Reinhoudt, *J. Am. Chem. Soc.*, **113**, 2385 (1991)
- d. F. Toda, K. Tanaka, Y. Wang, & G. H. Lee, *Chem. Lett.*, 109 (1986)
- e. E. Nomura, H. Taniguchi, & Y. Otsuji, *Bull. Chem. Soc. Jpn.*, **67**, 792 (1994)
- f. S. Shinki, S. Mori, H. Koreishi, T. Tsubaki, & O. Manabe, *J. Am. Chem. Soc.*, **108**, 2409 (1986)
- g. Y. Okada, Y. Sugitani, Y. Kasai, & Nishimura, J., *Bull. Chem. Soc. Jpn.*, **67**, 586 (1994)
- h. E. Nomura, H. Taniguchi, & Y. Otsuji, *Bull. Chem. Soc. Jpn.*, **67**, 309 (1994)
87. a. M. A. Mc Kervey, E. M. Seward, G. Ferguson, B. Ruhl, & S. J. Harris, *J. Chem. Soc., Chem. Commun.*, 388 (1985)
- b. E. M. Collins, M. A. Mc Kervey, & S. J. Harris, *J. Chem. Soc., Perkin Trans. 1*, 372 (1989)
88. a. G. Calestani, F. Ugozzoli, A. Arduini, E. Ghidini, & R. Ungaro, *J. Chem. Soc., Chem. Commun.*, 344 (1987)
- b. A. Arduini, E. Ghidini, A. Pochini, R. Ungaro, G. D. Andreetti, G. Calestani, & F. Ugozzoli, *J. of Incl. Phenom.*, **6**, 119 (1988)
89. a. C. D. Gutsche, & I. Alam, *J. Org. Chem.*, **55**, 4487 (1990)
- b. R. G. Janssen, W. Verboom, J. M. P. van Duynhoven, E. J. J. van Velzen, & D. N. Reinhoudt, *Tetrahedron Lett.*, **35**, 6555 (1994)
- c. A. Casnati, P. Minari, A. Pochini, & R. Ungaro, *J. Chem., Soc., Chem. Commun.*, 1413 (1991)
90. a. M. Coruzzi, G. D. Andreetti, V. Bocchi, A. Pochini, & R. Ungaro, *J. Chem. Soc., Perkin Trans. 2*, 1133 (1982)

- b. G. Barrett, M. A. Mc Kervey, J. F. Malone, A. Walker, F. Arnaud-Neu, L. Guerra, M-J. Schwing-Weill, C. D. Gutsche, & D. R. Stewart, *J. Chem. Soc. Perkin Trans. 2*, 1475 (1993)
91. a. S. Shinkai, K. Fujimoto, T. Otsuka, & H. L. Ammon, *J. Org. Chem.*, **57**, 1516 (1992)
- b. K. Iwamoto, & S. Shinkai, *J. Org. Chem.*, **57**, 7066 (1992)
- c. S. Shinkai, & A. Ikeda, *J. Am. Chem. Soc.*, **116**, 3102 (1994)
92. C. Gruttner, V. Bohmer, W. Vogt, I. Thondorf, S. E. Biali, & F. Grynszpan, *Tetrahedron Lett.*, **35**, 6267 (1994)
93. a. F. Arnaud-Neu, G. Barrett, S. Cremin, M. Deasy, G. Ferguson, S. J. Harris, A. J. Lough, L. Guerra, M. A. McKervey, M-J. Schwing-Weill, & P. Schwinte, *J. Chem. Soc. Perkin Trans. 2*, 1121 (1992)
- b. E. M. Collins, M. A. Mc Kervey, E. Madigan, M. B. Moran, M. Owens, G. Ferguson, & S. J. Harris, *J. Chem. Soc., Perkin Trans. 1*, 3137 (1991)
94. V. Bohmer, W. Vogt, S. J. Harris, R. G. Leonard, E. M. Collins, M. Deasy, M. A. Mc Kervey, & M. Owens, *J. Chem. Soc., Perkin Trans. 1*, 431 (1990)
95. a. M. Barber, R. S. Bordoli, R. D. Sedgwick, & A. N. Tyler, *J. Chem. Soc., Chem. Commun.*, 325 (1981)
- b. J. R. Chapman, *Practical Organic Mass Spectrometry*, Wiley, Chichester, 2nd edn., 1993
96. a. R. A. W. Johnstone, I. A. S. Lewis, & M. E. Rose, *Tetrahedron*, **39**, 1597 (1983)
- b. R. A. W. Johnstone, & I. A. S. Lewis, *Int. J. Mass Spec. Ion Phys.*, **46**, 451 (1983)
- c. R. A. W. Johnstone, & M. E. Rose, *J. Chem. Soc., Chem. Commun.*, 1268 (1983)
97. a. P. D. Beer, *J. Chem. Soc., Chem. Commun.*, 1115 (1985)

- b. P. D. Beer, C. G. Crane, A. D. Keefe, & A. R. Whyman, *J. Organomet. Chem.*, **314**, C9 (1986)
- c. B. Ganem, Y.-T. Li, & J. D. Henion, *J. Am. Chem. Soc.*, **113**, 6294 (1991)
- d. T. Takahashi, A. Uchiyana, K. Yamada, B. C. Lynn, & G. W. Gokel, *Tetrahedron Lett.*, **33**, 3825 (1992)
- e. J. C. Medina, T. T. Goodnow, M. T. Rojas, J. L. Atwood, B. C. Lynn, A. E. Kaifer, & G. W. Gokel, *J. Am. Chem. Soc.*, **114**, 10583 (1992)
- f. M. Sawada, Y. Okumara, M. Shizuma, Y. Takai, H. Yamada, T. Tamaka, T. Kaneda, K. Hirose, S. Misumi, & S. Takahashi, *J. Am. Chem. Soc.*, **115**, 7381 (1993)
98. W. V. Ligon, Jr., *Biological Mass Spectrometry*, A. L. Burlingame & J. A. McCloskey (Eds), Elsevier Science Publishers B. V., (Amsterdam)
99. a. M. Karas, D. Bachmann, U. Bahr, & F. Hillenkamp, *Int. J. Mass Spec. & Ion Proc.*, **78**, 53-68 (1987)
- b. M. Karas, U. Bahr, A. Ingendoh, & F. Hillenkamp, *Angew. Chem., Int. Ed. Engl.*, **28**, 760-761 (1989)
100. a. S. F. Wong, C. K. Meng, & J. B. Fenn, *J. Phyl. Chem.*, **92**, 546-550 (1988)
- b. J. B. Fenn, M. Mann, C. K. Meng, S. F. Wong, & C. M. Whitehouse, *Science*, **246**, 64-71 (1989)
- c. G. J. Langley, D. G. Hamilton, & M. C. Grossel, *J. Chem. Soc. Perkin Trans. 2*, 929 (1995)
101. S. Walker, 'Kinetics of Gas Phase Reactions, C³ Consortium', to be published by Houghton Mifflin, Boston USA, 1997

Appendix 1

The equations of rate law for all species in equations 6.6-6.17, which were used for numerical calculations in the computer programme. (see 6.5 in chapter 6)

$$d[A]/dt = k_2 [C] + k_9 [F] - k_1 [A][B] - k_3 [A][B] - k_8 [A][B][D]$$

$$d[B]/dt = k_2 [C] + k_9 [F] - k_1 [A][B] - k_3 [A][B] - k_8 [A][B][D]$$

$$d[C]/dt = k_1 [A][B] - k_2 [C] - k_4 [C] - k_7 [C]^2$$

$$d[D]/dt = k_3 [A][B] + k_5 [E] + k_9 [F] + 2k_{11} [G] - k_6 [D] - k_8 [A][B][D] - k_{12} [D]^2$$

$$d[E]/dt = k_4 [C] + k_6 [D] - k_5 [E]$$

$$d[F]/dt = k_7 [C]^2 + k_8 [A][B][D] - k_9 [F] - k_{10} [F]$$

$$d[G]/dt = k_{10} [F] + k_{12} [D]^2 - k_{11} [G]$$

Appendix 2

Raw Data of Kinetic Studies of the Diels-Alder Reaction at 40 °C

(For Figure 4.2)

Curve a		Curve b		Curve c	
Time(s)	Conc of 116 (M)	Time(s)	Conc of 116 (M)	Time (s)	Conc.of 116 (M)
0	0.0000	0	7.5000e-4	0	1.5000e-3
1800	0.0000	1800	1.4167e-3	1800	2.5345e-3
3600	2.5862e-4	3888	3.1500e-3	3600	3.7340e-3
6300	7.5000e-4	7488	4.2115e-3	6300	5.1735e-3
9900	2.0192e-3	11088	6.3432e-3	9900	7.0102e-3
13500	3.2500e-3	14688	7.5425e-3	13500	8.8469e-3
17100	4.5536e-3	18288	8.7857e-3	17100	9.9545e-3
20700	5.3076e-3	21888	1.0094e-2	20700	1.1596e-2
27900	8.4091e-3	27288	1.1530e-2	24300	1.2611e-2
31500	9.0440e-3	32688	1.2288e-2	27900	1.3166e-2
35100	1.0299e-2	44460	1.3426e-2	31500	1.3643e-2
38700	1.0758e-2	52380	1.4500e-2	37740	1.4074e-2
44388	1.1351e-2	71577	1.4790e-2	41220	1.4294e-2
47988	1.1959e-2	79657	1.4960e-2	44580	1.4885e-2
54612	1.2600e-2			49260	1.4978e-2
62100	1.3101e-2			59220	1.5413e-2
74988	1.3791e-2			69120	1.5667e-2

Appendix 3

Raw Data of Kinetic Studies of the Diels-Alder Reaction at 23 °C

(For Figure 4.3)

Curve a		Curve b		Curve c	
Time (s)	Conc of 113 (M)	Time (s)	Conc of 113 (M)	Time (s)	Conc of 113 (M)
0	0.0000	0	7.5000e-4	0	1.5000e-3
12960	0.0000	5340	1.1554e-3	5400	3.1667e-3
27660	1.6304e-3	14940	3.5878e-3	14700	4.7000e-3
39480	2.8125e-3	22080	5.0873e-3	22800	6.8846e-3
50280	5.1000e-3	29880	6.2378e-3	30600	8.7000e-3
75240	7.3728e-3	37860	7.8750e-3	38700	9.6250e-3
92340	9.9107e-3	45120	8.7732e-3	44940	1.0117e-2
103440	1.1111e-2	54000	1.0383e-3	54660	1.0704e-2
119760	1.1557e-2	66000	1.1044e-2	66600	1.2049e-2
137160	1.2142e-2	86520	1.2245e-2	87180	1.3627e-2
162060	1.3359e-2	103980	1.2489e-2	88680	1.3500e-2
183300	1.3555e-2	119580	1.3410e-2	104460	1.3891e-2
203520	1.3700e-2	130980	1.3691e-2	120060	1.4763e-2
222240	1.3953e-2	161040	1.3565e-2	131640	1.4357e-2
255840	1.3813e-2	176460	1.3856e-2	161400	1.4833e-2
272340	1.3897e-2	205560	1.4024e-2	176640	1.4519e-2
297420	1.4297e-2	255780	1.4171e-2	206100	1.4802e-2
				264300	1.4958e-2